A DIGITAL GROUNDWATER MODEL INVESTIGATION OF A PERMO-TRIASSIC AQUIFER IN THE WEST MIDLANDS OF ENGLAND

EDWARD JOHN SMITH B. Sc.

Submitted to the University of Aston in Birmingham for the degree of Doctor of Philosophy

APRIL 1975

RESUMÉ

Increase in demand for potable water has led to a critical re-appraisal of water resources. Resource planning requires a systematic approach to the development of aquifer systems and, in order to maximise output, conjunctive use with surface reservoirs and rivers has to be considered ultimately. Before this can be implemented a complete understanding of the dynamic response of the system must be acquired. Analogue and digital simulation models have been developed for this purpose.

A digital finite difference approximation technique which utilises a backward difference formulation is considered to represent the linear partial differential equations of groundwater flow. A two dimensional model is formulated in which space and time are represented as discrete elements. The resultant simultaneous equations are solved iteratively by a Gauss-Siedal relaxation technique.

A Permo-Triassic aquifer sited between the Coalbrookdale and South Staffordshire Coalfields of the West Midlands is studied. A considerable amount of data has to be processed and in order to secure maximum benefit several anaytical techniques are developed.

The extent and thickness of the aquifer is obtained from consideration of the depositional and sedimentological history of the associated sediments. This, together with field work exploration and an analysis of the tectonic history of the strata enables the geometrical configuration and hydrogeological boundaries of the aquifer to be depicted.

The hydraulic characteristics of the aquifer are determined from graphical and numerical analyses of in situ tests and from laboratory investigations. Additional information is obtained from least squares and linear programming solutions to groundwater flow equations compiled from historical records.

Groundwater recharge and discharge are evaluated initially from surface catchment water balance models and finally by utilising watershed modelling techniques in which watershed behaviour is simulated by known physical laws.

The overall groundwater regime is determined from spatial and temporal fluctuations of the water level surface. This information is used to calibrate and subsequently verify the groundwater model.

ACKNOWLEDGEMENTS

The author is grateful for the assistance and guidance directed to him from his supervisors, Dr. R.J. Johnson and Dr. T.R.E. Chidley and for the help in obtaining information from the Water Resources Board, Meteorological Office, Wolverhampton Water Undertaking, East Shropshire Water Board, Stafford Corporation Water Undertaking, South Staffordshire Water Works Company, Severn River Authority and Trent River Authority.

CONTENTS

CHAPTER THREE

FIGURES

FIGURES Cont.

Illustrations

FIGURES Cont.

Illustrations

TABLES

APPENDICES

A DIGITAL GROUNDWATER MODEL INVESTIGATION OF A PERMO-TRIASSIC AQUIFER IN THE WEST MIDLANDS OF ENGLAND.

INTRODUCTION

The South Staffordshire and Coalbrookdale coalfields of England are separated by a twenty kilometer wide tract of pleasant rural countryside underlain by Permo-Trias formations (Fig.1). The highly industrialised regions in the vicinity of the coalfields and their associated high population density have created a demand for vast quantities of water. The rural areas, although more sparsely populated in the past, have in recent time increased their demands on the available water supplies owing to the development of new towns and their associated light industries. The demand is met in part by abstraction from surface waters, but the majority of water used (150000 cubic metres per day) is drawn from deep wells in the New Red Sandstones that separate the coalfield outcrop.

The region investigated in this study extends northwards for thirty kilometers from Dudley in the east and Quatt in the west. The western and eastern boundaries are delineated by the Coalbrookdale and South Staffordshire Coalfields respectively. To the north a line joining Newport in the west to Stafford in the east defines the northern limit. The total area comprises approximately 850 square kilometers.

The topography ranges from 33 m.A.O.D. along reaches of the River Severn valley at Bridgnorth, to 210 m.A.O.D. around Wolverhampton and Cannock (Fig. 2). The Permo-Triassic sediments have a more subdued relief than the surrounding Carboniferous deposits, and although they are traversed by N.W. - S.E. escarpments in the south, they rarely rise above 150 m.A.O.D. (Fig. 2). Monotonous areas of low relief between 100 and 150 m.A.O.D. characterise the Keuper Marl deposits in the north. On the other hand, the Pebble Beds of Cannock Chase rise to 180 m.A.O.D. and constitutes the highest ground attained by the Permo-Triassic sediments in the area. The region is traversed by a major surface watershed which trends N.W. - S.E. to divide the Trent and Severn drainage systems. To the southwest the River Worfe and Smestow Brook (tributary of the River Stour) flow southwards.

Their catchments are separated by an escarpment of Lower Keuper Sandstone which stretches south from Codsall Wood through Pattingham to Bobbington. To the northeast of the watershed the drainage pattern is more irregular. The River Penk flows north through Penkridge to join the River Sow at Stafford. Further to the west, over Keuper Marl, small brooks and ditches drain northwards to join tributaries of the River Sow.

Geological formations of the region range from the marls and cemented sandstones of Upper Coal Measures age to the soft red sandstones, conglomerates and marls of the Permo-Trias. Over 400m of the younger permeable red sandstones are preserved in a broad syncline which separates the older, relatively impermeable, rocks of the South Staffordshire and Coalbrookdale coalfields.

The region as a whole is dominated by a cool westerly marine climate with rainfall spread evenly throughout the year. Frontal systems associated with depressions account for much of the widespread winter (October to March) rainfall. The summer months (April to September) are dominated by convectional showery activity and rainfall can be localised. Cool winters associated with few hours of sunshine reduce evapotranspiration to nearly zero. Warm summers induce high evapotranspiration rates which often exceed precipitation. Consequently, groundwater recharge occurs predominantly during winter months.

Since the industrial revolution, densely populated areas have been restricted to localities near or on the Upper Coal Measure deposits. The Permo-Triassic deposits support a rural type of environment dominated by small villages and farmsteads. Mixed farming is very much in evidence over the southern half of the area on the sandstones and conglomerates. The badly drained, glacially infilled valleys are predominantly rough pasture lands. Dip slope topography of the Permo-Trias, which separates the valleys, is characterised by well drained red soils which are used for arable farming.

In the northern central area the predominance of Keuper Marl mudstones and Pleistocene boulder clays restricts land use to woodland and rough pasture.

SCOPE OF INVESTIGATION

Within increasing demands on the water resources of this area owing to expansion of the surrounding industrial complexes, it became obvious that an investigation of the extent of the groundwater reserves would be advantageous and thus this study was initiated.

Hydrological studies recently initiated by the International Hydrological Decade (IHD) in 1965 have been involved in investigations which concern the total water balance of various land areas. This has led to investigations of groundwater systems not only as separate entities, but also as reservoirs linked in conjunctive use with surface water sources. In recent years a more rigorous hydrogeological approach to groundwater management has been made possible by the development of analytical techniques for determining aquifer characteristics. Monitoring of observation wells and the development of watershed models have been utilised to predict spatial and temporal variations of groundwater recharge and discharge. The resulting information has been used as a guide to the input and output of the groundwater systems. Geological and geophysical investigations have been conducted in order to determine the thicknesses and extent of water bearing formations. To assess the dynamic behaviour of groundwater systems the data acquired during these investigations are incorporated within simulation models. Electrical analogue models have been used successfully but in recent years the production of large computers has encouraged the use of digital models.

Initial investigations of the area (at present under study) showed that the quantity of hydrogeological data was limited. Recent awareness for its demand, and the time-consuming and costly business of setting up observation wells and pump test facilities are obvious limiting factors.

Information abstracted from the records of relevant River Authorities and Water Boards therefore consist of observations required to determine the necessary hydrogeological parameters. This was supplemented by field work and laboratory experiments designed to determine the fundamental and derived properties of the water bearing formations. The Meteorological Office was helpful in supplying rainfall and potential evapotranspiration figures for the area, and discharge rates for the Rivers Sow and Stour were abstracted from the Water Resources Board. All this information had to be analysed before it was incorporated within a digital groundwater model. It was necessary therefore to develop algorithms which would accept the basic hydrological data as input and produce results in a format suitable for the model.

The object of initial runs on the model was to check the viability of the results from the algorithms and the model. Subsequently, as more data became available, and was analysed, the model parameters were up-dated. In areas of insufficient data, estimated values were adjusted within the limits set by hydrogeological reasoning. The process of up-dating and adjustment of estimated parameters continued until calibration was obtained, that is computed water levels matched historical levels. The model was subsequently verified by simulating a longer historical period. As a result it was assumed to represent a correct digital simulation of the aquifer within the bounds set by present hydrogeological and hydrological knowledge. A schematic flow diagram which depicts the procedures involved in securing the verified model is illustrated in appendix 6.

CHAPTER ONE

GEOLOGY OF THE WATER BEARING FORMATIONS AND THE CONFINING STRATA

Introduction

The period of geological history concerned in this study extends from the Coal Measure deposits of the Upper Carboniferous to the glacial deposits of the Pleistocene.

Stratigraphy of the Water Bearing Formations and the Basal Confining Strata

Carboniferous/Permian Period

After the accumulation of the deltaic deposits of the Coal Measures, the southern parts of Great Britain and Northern Europe experienced substantial tectonic activity which culminated in the Hercynian Orogeny. These disturbances were responsible for folding late Palaeozoic sediments and initiating a series of marked unconformities. Consequently, there was a marked change in the environment which was heralded by the onset of continentally deposited sediments. The ensuing land masses resulted in the sea attaining a position further to the south than it was in early Carboniferous times. To the north stretched a large continent upon which detritus was deposited from the newly formed and uplifted mountain chains. The stratigraphy of this period of geological history is confused because continental conditions occurred sporadically as the land masses were formed. Consequently the Carboniferous/Permian boundary is difficult to determine and is still one of speculation and controversy.

Permo-Triassic Period

Particularly in the English Midlands sediments of the Permo-Triassic period consist of red marls, sandstones, breccias and conglomerates of "red bed" facies. First evidence for "red beds" in the Midlands Upper Coal Measures is found in the Keele Group. These deposits consist of red marls

with subordinate sandstones which rest conformably on the older Coal Measures below. The ensuing Enville Beds are characterised by breccia fans which are evidence of uplift of the Mercian highlands in the south-east (Wills 1948). These are called locally either the Calcareous Conglomerates Group or Bowhills Group. Northwards, away from the highlands, the conglomerates pass laterally into sandstones and mudstones. The apparent absence of the Enville Beds around Newport and Stafford may be in part due to the difficulty in recognising these facies changes.

The calcareous conglomerates are succeeded, generally unconformably, by the Breccia Group (also called the Clent Group, Wells and Kirkaldy 1966). Repeated uplift of the Mercian Highlands gave rise to a series of stratified breccias and sandstones. Away from the highlands the coarser sediments pass laterally into mudstones similar to those of the Enville Beds. In time continuous denudation of the highlands lowered the relief to a peneplain, and this landscape was in turn buried by aeolean sands which heralded the onset of arid conditions. The strong unconformity which resulted was assumed to represent the Permian-Triassic boundary, Richardson (1929), and the aeolean dune deposits found above were referred to as the Lower Mottled Sandstone of the Lower Bunter. More locally and particularly around Bridgnorth, they are known as the Dune Sandstones (Shotton 1937 and Whitehead et al. 1947). The extent of their development further north is uncertain but outcrop pattern and borehole data suggests a thinning to the north and east of Bridgnorth. Near Newport, Stafford and Cannock these beds are absent altogether (Whitehead 1947 and Audley-Charles 1970b).

Renewed uplift of the Mercian and Welsh Highlands increased the relief of the hinterland surrounding the Midlands. This initiated seasonal rainfall which terminated the desert environment and caused the deposition of coarse shingle beds. Wills (1970) proposed that at this time the main drainage into the Midland cuvette was off highlands to the south-west, south

and south-east. The highland to the south was a klippe of an exotic nappe of older rocks across which the main Budleighenis river flowed south from France. This development could have been responsible for the removal of the Lower Mottled Sandstone deposits in areas where the Bunter Pebble Bed deposits now rest on the Carboniferous. The resulting unconformity is now recognised by most Permo-Triassic stratigraphers to represent the onset of the Triassic period (Wills 1948). Subsequent cyclic periods of deposition were responsible for a series of sandstones and conglomerates that are typical of Bunter Pebble Bed deposits. Cyclic deposition continued with the gradual degradation of the land surface as indicated by the sequence of sandstones and subordinate mudstones. These later deposits characterise the Upper Mottled Sandstone Formation which follows the Bunter Pebble Bed Formation conformably. However, difficulty in distinguishing between the sandstones of these formations leads to problems of correlation.

The upper division of the Trias, namely the Keuper, follows the Bunter, often unconformably. In the Midlands this is depicted by a change of facies from the typical soft red sandstone of the Upper Mottled Sandstone Formation to coarser, brown sandstones, mudstones and calcareous conglomerates of the Lower Keuper Sandstone Formation. No change in the attitude of the beds occurs across the boundary although evidence of an erosional surface, and the occurrence of coarser material, suggests some uplift of the hinterland. In the West Midlands, the base of the Keuper is known locally as the Basement Beds, and is characterised by sandstones, breccias and mudstones. They are succeeded by a series of alternating sandstones and mudstones which are known locally as the Buildingstones Group. These deposits in turn young into flaggy brown sandstones and interbedded mudstones of the Waterstones Group. The occurrence of cyclic periods of sedimentation within this group records episodes when the Murschelkalk Sea extended into the North Sea basin and terminated the

period continental deposition.

The final infilling of the Midland cuvette was accomplished during Keuper Marl times by the cyclic deposition of mudstones and evaporites. Sandstone lenses ("skerries") occur particularly in lower horizons but the Arden Sandstone, an important fossiliferous bed elsewhere, is absent from the study area.

By the close of the Trias period, the mudstones of the Keuper Marl had completely filled the Midland cuvette and the peneplained topography allowed the area to be invaded by the Rhaetic Seas.

Stratigraphical Nomenclature

The stratigraphical nomenclature which stems the period of geological history discussed above is still in a confused and primitive state. Inappropriate terminology, including the use of lithostratigraphical terms in a chronostratigraphical or chronological sense results in a misrepresentation of the concepts of time and space. However, now this aspect has been recognised, some stratigraphers believe that sediments of a particular horizon may be broadly the same age over large areas. The terminology is based predominantly on lithology and as a result is very misleading. For example, within the Bunter Pebble Beds can be found mudstones, sandstones and conglomerates. Indeed each division within the Permo-Trias can be recognised as a formation represented by a particular set of clastic sediments. As such in this study it is proposed to designate each division in the Permo-Trias as a Formation, i.e. the Bunter Pebble Bed Formation.

Summary

The Permo-Trias period is characterised by successive episodes of tectonic activity, upland denudation and intermontain deposition.

The predominance of a contintental depositional environment has resulted in an inadequate fossil record. Correlation is also hampered by successive lateral facies changes and numerous unconformities that occur

over an area lacking in surface exposures. However, recent work by Wills (1970) has included the implications of cyclic sedimentation for local and regional correlation. Where adequate borehole records and marker horizons exist this form of analysis could lead to a better understanding of the relationship between the facies and time. Consequently, this would allow for better correlations and improve estimates of the thicknesses and lateral extents of these important reservoir rocks.

Sedimentary Analysis of the Water Bearing Formations

Introduction

The predominant water bearing formations of the area under study occur between the well cemented and compact sediments of the Upper Coal Measures, and the mudstones of the Keuper Marl Formation. Consequently, the main bulk of the reservoir rocks consists of poorly cemented Permo-Triassic red sandstones and conglomerates. The sedimentary analysis was therefore conducted on the series of intercalated, continentally deposited, arenaceous and rudaceous sediments of the Midland cuvette.

Sampling Localities

Although sampling localities are restricted in some areas owing to the lack of outcrop, the occurrence of quarries and road cuttings enables an even distribution of sampling locations (Fig. 3). In any particular exposure the Lower Mottled Sandstone, Bunter Pebble Bed and Upper Mottled Sandstone Formations display a general uniformity of rock type. The Lower Keuper Sandstone Formation is more variable with rock types changing markedly in any particular exposure.

Fundamental Properties Analysis

Investigation into the fundamental properties of the water bearing formations results in a set of unique figures that are used as a quantitative guide to their lithological variations. This variation lends itself to interpretation with respect to the depositional environment and, consequently,

is a guide to correlation and variations in thickness. It is also responsible for changes in the derived properties of which porosity and permeability concern the hydrogeologist directly.

An infinite number of fundamental properties can be used to describe a sedimentary rock. Only those properties which are applicable to all sedimentary rock types and result in a complete and unique description are used. Thus the defining equation is:

$$Ki = f\ (Mp, Sv, Sh, Or, Pi)$$

where Ki = a characterising index;

Mp = the minerals present;

Sv = the size variation of each mineral;

Sh = the shapes of the minerals;

Or = the orientation of the minerals;

Pi = the packing of the minerals.

Standard methods of analysis are employed with the object of defining the sediments by a set of statistical figures. Simple interelationships are tested for, in order that the statistics may be used to interpret the depositional environment and explain variations in the derived properties.

Grain Size Analyses: Samples were collected from horizons between the base of the Lower Mottled Sandstone Formation and the base of the Keuper Marl Formation. Argillaceous sediments represent only a minor constituent of the aquifer and because they play no dynamic role in the groundwater cycle are not included in the analysis.

One hundred and thirty samples were collected of which between 400 and 500 grams of each are used in the analysis. The majority contain no humus and little cementing material and consequently required little pre-treatment. Fifteen samples from the Bunter Pebble Bed and Lower Keuper Sandstone Formations required soaking in dilute acetic acid to remove calcite cement.

Gentle crushing with pestle and mortar was sufficient to disintegrate the sediments into their individual grains. After drying, sample splitting and weighing, they were shaken for ten minutes in a nest of eight sieves. Samples containing over 3% of material finer than 53 microns (finest sieve) and greater than 2mm (coarsest sieve) were saved for further analysis. The fine material was analysed using the British Standard (BS 1377 1967) soil analysis method by hydrometer. This involved the use of sodium hexametaphosphate and sodium carbonate as a dispersing agent. Material larger than 2mm was sieved through a set of coarser sieves. Since the 'tails' of the distribution had been analysed thoroughly the resulting distributions are not too 'open ended' for statistical analysis.

Numerous methods of expressing grain size distribution exist but a lack of standardisation has resulted in much confusion and leads to difficulty in comparing the results of different workers.

A statistical analysis should summarise the characteristics of the frequency distribution curve. Since these distributions are continuous functions it is preferable to describe them in terms of the cumulative frequency curve, which is independent of class intervals. Interest in such curves and the percentile measurements derived have been expressed by Inman (1952), Folk and Ward (1957) and more recently, by McCammon (1962). Their methods of analysis have been adopted because of rigorous statistical concepts and popularity.

The program devised for analysis simulates the cumulative frequency curve by a series of straight lines plotted between points of observation (Fig.4). Differences experienced between this method and the generally accepted smooth curve technique are of the same order as those derived from different interpretations of a 'smooth' curve. All interpretations result in negligible differences in the final statistic.

The derived straight line equations are used to calculate the grain size diameters at a given set of percentiles on the cumulative frequency

curve. These percentiles are determined by the methods proposed by Inman (1952), Folk and Ward (1957) and McCammon (1962) for calculating the mean size, standard deviation, skewness and kurtosis. Little manipulation of the original data is required before input into the program. In fact the data can be prepared automatically on data sheets ready for punching onto computer cards or tape. The required percentile diameters are computed separately in subroutine (PERC). They are subsequently used in the master program to compute the required statistics (Appendix 1).

Grain Size Distribution in each Formation and Associated Lithological Variations:

1) Lower Mottled Sandstone Formation: The oldest formation is characterised at outcrop by dull red sandstone which exhibits conspicuous laminations and steeply dipping current bedding. Quartz grains, which range from $\frac{1}{4}$mm to $\frac{1}{2}$mm in diameter, and weathered feldspars constitute the dominant assemblage. More than 90% of the rock mass consists of quartz grains.

A thin pedicle of iron oxide coats and separates each grain, except occasionally at their contacts, and gives the rock its red colouration. This coating is the predominant cementing agent, and although the rock can be disintegrated by hand, the sandstone is sufficiently coherent to stand in vertical faces in areas around Bridgnorth.

These sandstones are remarkably uniform in texture and no horizons of argillaceous or rudaceous sediments have been reported.

The analyses of twenty five samples indicates that the dominant rock type is a well sorted, medium grain sized sandstone. Most laminations are the bi-product of the mixing of medium grain sized horizons with finer angular material; the remainder occur because of cementation by calcite cement. Current bedding represents the junction between two depositional phases across which there is a sudden change in grain size. Sediment finer than 64 microns (coarse silt) and coarser than 0.75mm (coarse sand) is a minor

constituent. Consequently, most samples possess over 90% of their grains between these limits.

Over 75% have a positive skewness, i.e. the tails of the distribution are skewed towards the finer size fractions. The remaining samples have a negative skewness.

The fourth statistic, kurtosis, reveals that excessively peaked distributions are indicative of 75% of the samples, that is the grains around the 'central portion' of the frequency curve are better sorted than those of the 'tails'. The remaining samples are deficiently peaked.

2) Bunter Pebble Bed Formation: Where the Lower Mottled Sandstone Formation is overlain by the Bunter Pebble Bed Formation, the junction appears to be conformable. Along the margins of the South Staffordshire Coalfield, however, absence of the older formation has resulted in 'pebble beds', apparently of the Bunter Pebble Bed age, lying unconformably on Upper Carboniferous deposits.

Facies variation throughout this formation includes conglomerate, sandstone and mudstone. The conglomerate occurs on the edge of the basin and intercalates with sandstones towards the centre. Although the occurrence of mudstone is uncommon at outcrop, it is encountered as thin lenses, interbedded with conglomerate and sandstone, during drilling (Fig.5).

Polygenetic pebble beds dominate the region around Cannock Chase. Hard calcite cemented horizons are interbedded with loose gravel throughout the formation and from gravel pit exposures appear to be lensoid in form (Fig.6). Elsewhere dull red sandstone predominates and pebble horizons are restricted to basal breccia and conglomeratic lenses several metres in thickness. The sandstone is often current bedded and cemented by an iron oxide coating on the grains. The laminated sandstone consists of well sorted, medium grain sized horizons that alternate with similar horizons mixed with fine quartz grains. Quartz, weathered feldspars and occasional flakes of muscovite comprise the dominant mineral assemblage.

The analyses of twenty nine samples indicate that, whereas the rock types range from very fine sandstones to medium sized pebble beds, the mean rock type is a moderately well sorted, coarse sandstone. Material finer than 64 microns occurs predominantly in the fine to very fine sandstones and coarser sized sandstones and conglomerates are characterised by less than 2% by weight of this material.

Skewed distributions are normally distributed and range from very positively to very negatively skewed. Over 90% of the samples have excessively peaked distributions; the remainder have only a slight deficiency in peakedness.

3) Upper Mottled Sandstone Formation: Bright red, fine grained sandstone which displays current bedding predominates. Thin marl partings (<1m) occur and, in general, deviation from arenaceous sediment includes argillaceous rather than rudaceous types.

Although the sandstone is current bedded, the planes of erosion and deposition are less steeply inclined than those of the Lower Mottled Sandstone Formation. Intermittent micaceous horizons produce a flaggy appearance and the associated bedding planes are accompanied by bottom structures and occasionally by mudstone pellets.

Apart from the iron oxide coating on grains, cementation is limited in that isolated horizons may be poorly cemented by calcite and/or quartz. Otherwise the rocks are soft but coherent.

Of the sixty samples analysed the average rock type is fine grained and well sorted. Most samples have over 90% of their grains between 64 microns and 0.75 mm in diameter; the remainder have grain size distributions that include material finer than 64 microns. The loamy character of some horizons and the absence of coarse material (>0.75 mm) is a dominant feature throughout this formation.

Positively skewed samples dominate; the remainder describe a near symmetric distribution. Normal to excessive peakedness is characteristic

of all samples.

4) Lower Keuper Sandstone Formation: The current bedded, poorly cemented, red sandstone that has dominated the previous formations is followed conformably by calcite cemented brown and red sandstones and mudstones of the Lower Keuper Sandstone Formation. The basal beds, which consist of pebbly sandstone with occasional mudstone pellets, are poorly sorted and often lenticular in shape. Intraformational erosion surfaces are abundant and the rock mass yields readily along these planes. Mudstone increases in abundance towards the top of this formation until, at the base of the Keuper Marl Formation, it is the dominant lithology.

The formation as a whole is characterised by alternations of sandstone, sandy marl and mudstone. The mudstone is generally purple, but the sandstones can be buff, brown, purple or red. Calcite cement is more widespread than in the older formations, and the rocks vary from poorly cemented friable sands to well cemented and compact sandstone. Bottom structures, current bedding and graded bedding are preserved in many horizons.

Of the twenty seven samples analysed the mean grain size diameter varies from fine to coarse grained sandstone. The mean rock type is a moderately sorted, medium grained sandstone. Grain size distribution which ranges from 64 microns to 0.75mm is characteristic of 70% of the samples. The remainder are excluded because of the inclusion of material larger than 0.75mm.

Although the skewness is evenly distributed, kurtosis is biased towards excessively peaked distributions. Approximately 25% have a slight deficiency in peakedness.

Conclusions: The water bearing formations, as a whole, can be considered as a series of moderately to well sorted sandstones of a fine to coarse grained texture (Fig.7). Skewness and kurtosis vary considerably throughout the formations (Table 1).

Quartz grains predominate and are accompanied by weathered feldspars,

micas and a variety of heavy minerals. Cementation is poor apart from occasional horizons in the Bunter Pebble Bed Formation, and in the Lower Keuper Sandstone Formation, where it is most abundant. Current bedding and laminations, together with the red iron staining, are obvious features at outcrop.

Shape, Roundness and Packing of the Grains: To observe the packing, two techniques were used. Firstly, poorly cemented sediments that could be dissected manually and without disturbing the packing were observed by binocular microscope. Secondly, more coherent samples were impregnated with araldite to allow the preparation of thin sections.

Sphericity and roundness variations were studied by disintegrating samples into their individual components and analysing a representative sample of 100 to 200 grains.

The techniques used in this analysis involved comparative figure tables. Although they are subjective in their approach, methods which utilise rigorous mathematical concepts were thought to be unnecessary and indeed were found to be too time consuming.

Variations Within Each Formation: The Lower Mottled Sandstone Formation is dominated by spherically shaped grains and, although they occur sporadically in younger formations, they are less spherical and more roller shaped. This loss of sphericity is accompanied not only by a loss of roundness but by a change in packing, from an open tangential type to a more compact longitudinal variety. Many horizons give the appearance of random packing and no pattern was discernible.

Laminations have developed from the periodic mixing of medium grain sized horizons with finer sediment. This has increased the number of contacts per grain and produced a more compact sandstone. Rocks of this type are in part responsible for the near vertical cliffs of sandstone found in some localities. Other laminations, particularly those of the Lower Mottled

Sandstone Formation, are characterised by medium grained sandstones with well rounded grains which alternate with finer grained sandstones with less well rounded grains.

There is no evidence for substantial compaction of the post-diagnetic rock structure. Contacts per grain range from 1.8 to 2.5. The oldest formation has a very open matrix which is characterised by the occurrence of floating grains and dominant tangential contacts. Occasional micas parallel to bedding planes are ruptured and bent in a manner to indicate slight over-burden compaction which probably occurred soon after deposition when rearrangement of the grains was most active. Sutured and complete contacts of the quartz grains are absent; reduction of pore spaces is the result of simple pore filling by calcite and red iron oxides.

The dominant red colouration, attributed to the breakdown of iron rich minerals during diagenesis, coats every grain separately. Only at the contacts of grains is the coating absent.

It is apparent that the reduction of pore space in all formations is a product of simple pore filling that is more acute in the younger horizons. The oldest formation still exhibits a remarkably open matrix.

Interpretation of Results from the Fundamental Properties Analysis

Investigations concerning the fundamental properties and overall structural configuration of sedimentary rocks is a guide to the interpretation of their depositional environments (Folk and Ward 1957, Wills 1970 and Buller and McManus 1971). In turn, this is a guide to the lateral facies changes to be expected. As a result, better stratigraphical correlations are achieved which lead to improved estimates of the thicknesses and lateral extent of the water bearing formations (Audley - Charles 1970a).

Depositional Environment: The Permo-Triassic sediments of the United Kingdom are of continental origin, deposited during and after the Hercynian Orogeny. Dominant red clastic sediments with numerous erosion surfaces dispersed

amongst current bedding, graded bedding and bottom structures, suggest at the most, periods of shallow water deposition. Although they have an extensive subsurface development, the lack of surface outcrops and stratigraphically useful fauna and flora, has resulted in regional correlation of a lithostratigraphical nature only.

1) Lower Mottled Sandstone Formation: The occurrence of fossil dunes, dreikanters and millet seeds in the Lower Mottled Sandstone Formation has been interpreted as aeolean in origin. Grain size distributions, and the absence of argillaceous sediments and micas, are similar to sediments of known desert environments. The current bedding dips at an angle that infers aeolean deposition. The forset slopes dip at 33° and the topsets at 11° (Shotton 1937). The sharp contrast in grain size across the bedding and the well sorted layers are the product of natural dune formation. Laminations which have resulted from the mixing of fine angular sand and well sorted coarse grained sand are interpreted as the product of sheet wash across a dune field.

2) Bunter Pebble Bed Formation: The change from desert sands to fluviatile pebble beds records a major change in geography, with the introduction of considerable areas of relief. Uplift of the hinterland was in part responsible for the change in climate from arid to semi-arid. Huge braided rivers deposited fan conglomerates and were probably responsible for the removal of the desert sands in the vicinity of the South Staffordshire Coalfield. The well rounded quartzite pebbles suggest that they have travelled far - probably northwards from Northern France.

The existence of the Midland cuvette as a basin of deposition during this period is suggested by Wills (1948). Subsequent interpretations, Audley - Charles (1970b), infer that the Worcester graben connected the Midlands to southern and south-western England and was responsible for changes in the depositional environment of the surrounding areas. The

presence of the Worcestershire Graben at the time of deposition of the basal pebble beds of the Bunter Pebble Bed Formation is well supported, and the resulting unconformity is now accepted as the Permo-Trias boundary (Audley - Charles 1970b). Arenaceous deposits are generally cross-bedded and arkosic. Each unit is separated by erosion surfaces which are accompanied by abundant mica. The less well rounded, more roller shaped, grains contrast with the well rounded spherical grains of the desert environment. Micaceous sandstones are interpreted as the lateral equivalents of the fan conglomerates. Their depositional environment suggests quiet water situated well away from the graben walls. The variations of lithology throughout this formation have been interpreted as desert cyclotherms by Wills (1970). Periods of uplift caused by movement along faults of the Worcester graben and subsequent erosion resulted in a series of intercalated conglomerates and sandstones. These 'flood' sequences alternate with periods of still water in which mudstones were deposited. Interbedded 'millet seed' horizons, that characterise the lower formation, occur sporadically throughout the formation and indicate a temporary change to aeolean deposition before the return of flood conditions.

3) Upper Mottled Sandstone Formation: The sandstones of the Upper Mottled Sandstone Formation are difficult to separate lithologically from the underlying sandstones of the Bunter Pebble Bed Formation. Cyclotherms are represented by current bedded sandstones alternating with evenly bedded, fine sandstones. The absence of rudaceous material and the inclusion of argillaceous sediments infer a reduction in elevation of the hinterland and the formation of temporary lakes along the basin.

4) Lower Keuper Sandstone Formation: The alternating sandstones and mudstones of the Lower Keuper Sandstone Formation are accompanied by abundant detrital micas and felspars. Numerous examples of small scale cross stratification, sole structures and graded bedding occur, e.g. 0.5 km north of Upper Ludstone (SO 803958). The reappearance of pebbly sandstones and conglomerates in the

Basement Beds is an important lithological horizon which represents a major palaeogeographical change. Above this horizon are found alternating current bedded sandstones and marls which are the remains of flood plain and estuarine deposits. They record an irregular distribution of rainfall, typical of semi-arid climates. Flood deposits are recognised by brown and grey sandstones with scattered pellets of marl, and the drought sequence by impersistent marls which are the remains of numerous channels.

The Waterstone Group was influenced by fluctuations in the level of the Muschelkalk Sea which introduced shales typical of shallow estuarine conditions.

By the onset of the Keuper Marl a shallow sea existed in the area, connected to oceanic waters by sills and channels. Complete infilling of the Worcestershire Graben during this time allowed a marine transgression to herald the onset of the Rhaetic.

Additional Analyses: Different depositional environments have been interpreted using double logarithmic plots of Trask's arithmetic Median diameter, Md, Quartile deviation, Qd, and Skewness, Sk (Buller and McManus 1971). By plotting Qd against Md, linear trends were observed and also a decrease in the gradients of the curves in the sequence aeolean - fluviatile - beach - quiet water. Similarly linear trends were indicated with a plot of Qd and Sk; however, the gradients of the curves were found to decrease in the reverse order. Using similar analyses and plots for the Permo-Triassic arenaceous and rudaceous sediments, two linear trends were evident. The resulting gradients indicated a basically aeolean type of deposition for the Lower Mottled Sandstone Formation and a basically fluviatile environment for the younger sediments above (Figs. 8 and 9). The shallow gradient which occurs early on in the Qd versus Sk plot for the younger sediments probably represents samples which are associated with several depositional environments.

Derived Properties of the Water Bearing Formations

Introduction

Those properties of direct interest to the hydrogeologist include absolute porosity, effective porosity and permeability. The following analysis involves the assessment of these properties in the laboratory and their relationships, if any, to the fundamental properties. The merits and problems of laboratory tests are well documented and the application of any results is known to be limited (Heath and Trainer 1968). However, if they are interpreted with the experimental errors and limits in mind, they can be a useful guide to the variations throughout the formations.

The samples used in this analysis were collected from identical localities to those used in the fundamental properties analysis. Two, suitably sized specimens were cut in order to conduct tests on their derived properties. These included a square of sides 60 cm to 70 cm, for the porosity tests, and a core, 70 cm in diameter by 140 cm long, for the permeability tests.

Absolute porosity was determined by soaking, with de-aired water, a sample of known dimensions and dry weight. The sample was then placed in a vacuum chamber until saturated.

Variation in Absolute Porosities

The Lower Mottled Sandstone Formation has consistently high porosities in the order of 30 to 40% (Fig. 10). A porosity of 43% was recorded as the maximum value for all four formations. The Bunter Pebble Bed Formation has two obvious populations. Porosities which range from 6 to 17% are representative of rocks cemented by calcite, whereas poorly cemented samples are characterised by porosities between 27 and 34%. A uniform distribution was found in the Upper Mottled Sandstone Formation. Values in the range of 25 to 35% account for 85% of the population. The wide range of porosities, 6 to 42%, encountered in the Lower Keuper Sandstone Formation, is caused by variations in the degree of cementation. Occasional high values, (40 to 42%)

are associated with 'red beds' that are in general more characteristic of the older formations.

Effective porosity determination simulated field conditions by allowing an orientated saturated sample to drain naturally under gravity. As such any laminations that were included had a horizontal to subhorizontal attitude. An air-tight perspex container was fitted with a wide meshed cradle upon which the sample was allowed to drain. Porous filters at the base allowed the drained water to pass through, while a 100% humid atmosphere was maintained in the closed system around the sample. The optimum drainage time was determined experimentally on a representative selection of samples. Each sample was weighed every three days and the optimum time period was chosen on the basis that at least 95% of the gravity water had been drained. This period occurs between 15 and 18 days.

Variation in Effective Porosities

Each formation has a high frequency of values between 6 and 8% (Fig. 11). Values ranging from 2.3 to 11.4% were recorded from the Lower Mottled Sandstone Formation and the latter value represents the highest effective porosity recorded from all four formations. The Bunter Pebble Bed Formation and the Lower Keuper Sandstone Formation have a similar range in values from 1.3 to 8.8% and 0.07 to 8.5% respectively. Both are skewed towards the lower values and this is more acute in the case of the Lower Keuper Sandstone Formation. The Upper Mottled Sandstone Formation, although skewed towards the lower values, shows a fairly even distribution between 2.2 and 7.7%.

Laboratory determination of permeability values was effective on all samples, except the 'pebble beds' of the Bunter Pebble Bed Formation. Quartzite pebbles and poor cementation made it difficult to cut suitable cores.

The laboratory technique used is based on the simple four point test devised by Cook and Howell (1970). The disadvantages of other methods,

including air permeameters and constant head devices, are that they either take too long, or involve the use of media other than water. The four point test involves the measurement of the time for four different sized pools of water to drain through a core. By substituting the specimens dimensions and mean flow rate into Darcy's Law, a value for the permeability can be obtained.

Permeability Anisotropy

Although difficulty was experienced in coring incoherent samples perpendicular to the laminations successful attempts reveal an average ratio of 3:2 between horizontal and vertical permeabilities respectively. All future discussion relates to the horizontal components only since this is the main component of groundwater flow. In all horizons this is parallel or subparallel to the laminations. Characteristically, permeabilities range from 4.0 to 10.0 m/d in most sandstones (Fig.12). Lower values, 0.04 to 4.0 m/d are associated primarily with the Bunter Pebble Bed and Lower Keuper Sandstone Formations. Higher values, 10.0 to 16.0 m/d, are associated with the Lower Mottled Sandstone Formation in particular.

Relationship Between the Derived and Fundamental Properties.

Introduction

The results obtained indicate few relationships that would be useful for general application. In the light of previous studies, by sedimentologists on other assemblages, this subject was not pursued further than to describe unique and obvious relationships. Conflicting statements have been quoted on occasions regarding these relationships. For example, Slichter (1899) inferred that porosity was independent of the constituent grain sizes whereas Trask (1931) and Cloud (1941) have postulated that porosity increases from coarse to fine grained assemblages. It is to be expected that erroneous results can occur when trying to relate two variables that are part of a

multivariate system. As already stated, only a rigorous petrological analysis that considers all the fundamental properties is meaningful.

Method of Analysis

Multiple linear regression techniques which involve variables with high correlation coefficients were chosen as one approach, with an assumption of independence of the fundamental properties. However, associated correlation coefficients were often significant. For example, finer grained samples are generally better sorted, with grains that are less well rounded. Indeed, it is difficult to isolate one fundamental property from the accompanying properties. Even if independence is assumed, correlation coefficients between derived and fundamental properties are not significant. If relationships are to be determined they will obviously include more complex relationships; such as analysis is outside the scope of this report.

Conclusions

With the above remarks in mind the following conclusions are made. Variations in the degree of calcite cementation and lamination have greatly influenced the derived properties. Those sediments affected by cementation have low absolute and effective porosities. Permeability values reflect the occurrence of cementation because of its partial obstruction to the flow of water. However, no sample was analysed in which cementation was sufficient to render the sediment 'impervious'.

The occurrence of laminations is a common phenomenon throughout all rocks and their effect on groundwater flow and storage is important. The effective porosity and permeability of the sediment is reduced significantly when water is induced to flow perpendicular to these planar fabrics. There is difficulty in quanitifying this effect but, for comparison, massive samples have in the order of 25% higher effective porosities and up to one order of magnitude higher permeabilities than their laminated counterparts.

The majority of samples are either laminated or cemented and their

influence on the derived properties masks the effect of the other fundamental properties. Only the obvious relationships are discussed.

Laminated but poorly cemented horizons, characteristic of the Lower Mottled Sandstone and Upper Mottled Sandstone Formations, show an increase in absolute porosity when accompanied by an increase in fine material. However, this increase in absolute porosity is not always accompanied by an increase in the effective porosity. High absolute and effective porosities characterise the very well sorted 'millet seeded' horizons of the Lower Mottled Sandstone Formation. An increase in finer sandy material in some horizons, results in reduced absolute and effective porosities. This finer material upsets the open tangential packing, and a denser matrix results in reduced porosities.

In conclusion, it is obvious that variations in cementation and laminations are important factors in influencing the derived properties. Involved to a smaller extent is the distribution of the grain sizes which appears to have more significance than the absolute grain sizes.

The Geological History of the Formations Above the Permo-Triassic Aquifer

Introduction

Rocks of the Keuper Marl Formation and the Pleistocene period are involved only to a limited degree in the groundwater resources of the study area. However, they perform an important role in influencing recharge to the groundwater system. As such, it is necessary to include a resumé of their geological history, lithology and surface distribution.

The Keuper Marl Formation

Geological History: The environment in which the Keuper Marl Formation was deposited is one of considerable controversy. Three main schools of thought exist. The first was conceived by Bosworth (1912) from detailed observations on the lithological variations throughout the formation. Sporadic seasonal

flooding was assumed responsible for the deposition of mudstones in playa lakes on what was essentially a desert plain. Subsequent desiccation, due to high evaporation, gave rise to mineral salt deposits, and wind erosion re-worked the mud before the onset of the next flood.

The second hypothesis suggests that salt deposits originated from evaporation of saline-waters which sporadically flooded into the area. Shearman (1966) suggests that the salt was derived from the evaporation of saline groundwater, and Brunstom and Kent (1967) infer it was from the leaching of Zechstein salt that was emergent in the North Sea basin. The resultant shallow inland sea was affected by high evaporation rates which caused brine to concentrate and eventually precipitate.

The third explanation, forwarded by Wills (1970), incorporates the ideas of the previous hypotheses under the overall control of a cyclically changing geographical environment. Flooding occurred periodically by both the sea and the rivers, and periods of drought and restriction of the brine to deeper hollows led ultimately to precipitation of evaporite minerals. The predominance of argillaceous sediments infer that western Europe was a very flat peneplain. To explain the vast thickness of sediment preserved (150 m at the centre of the Staffordshire syncline) and the abrupt changes in thickness, fault zones parallel to the walls of the Worcester graben are assumed to have been active. The associated movements were responsible for the relative changes in altitude between the peneplain and the ocean. This resulted in a cyclic influx of saline water along channels and over sills into the graben. A hot tropical climate gave rise to sporadic torrential rainfall which eroded the lateritic soils of the surrounding peneplain, and deposited them as vast sheets of mud in the graben. The remains of stratified clays represent the periodic influx of sediment into playa lakes. Periods of desiccation resulted in the re-working of the dried mud and the lateritic soils by the wind, to form a structureless "loess" clay. The constantly changing

salinity of the aquatic environment and the effect of a persistently high rate of evaporation upon the terrestrial environment, were responsible for the absence of any signs of life.

Although a complete sequence of the Keuper Marl Formation is not present in the study area, there is evidence for the continuation of faulting along the western margin of the Worcester graben (Audley-Charles 1970b). However, by the onset of the Rhaetic, the faulting which had exerted a considerable influence on sedimentation ceased to be effective and the Worcester graben had been completely infilled.

Surface Distribution and Lithological Variation: The Keuper Marl Formation is restricted to the region adjacent to the axis of the Staffordshire syncline and between Newport and Acton Trussel it outcrops in a 15 km wide tract and exhibits a synclinal outcrop pattern (Fig.2.)

The lithology of this formation is remarkably uniform over the study area. The most important rock type is the so-called marl which is in fact a red calcareous mudstone. It is usually structureless and contains small dolomite crystals. Stratified varieties include fine silt layers which are mixed occasionally with well rounded wind blown quartz grains. Interbedded sandstones occur infrequently. They are predominantly greenish grey and well cemented and exhibit ripplemarks and current bedding. Desiccation surfaces and small dolomite rhombs are abundant throughout.

The Glacial Deposits

Geological History: The Pleistocene Glacial Period includes a series of climatic oscillations from cold glacial to warm interglacial conditions. In the Midlands, four such episodes can be recognised (Wills 1948). Only patchy and highly dissected deposits remain from the first two glacial periods. These 'Older Drifts' are situated at higher elevations than the more recent 'Newer Drifts'.

Evidence for the first glacial period has been removed in most places by

later glaciers and rivers. However, evidence for the advance of two great ice sheets still remains. In the north Midlands, the Welsh Ice-Sheet and glaciers flowing south from the Pennines spread into the mid-Severn catchment. From the east came the second ice-sheet, but it is uncertain whether it actually reached the study area. The only remnants are isolated exposures of boulder clay and large boulders.

The interglacial period that followed was responsible for covering boulder clay deposits with outwash sands and gravels. Other sediments relating to this period are no longer evident.

The second glacial period was influenced by an ice-sheet from Wales. Although it was less extensive than its predecessor the region was affected by its melt waters draining down the present Severn valley. The Eastern Ice-Sheet advanced to a similar position attained during the first glacial period. As a result most of the study area remained between the two impending ice-sheets. Outwash deposits were probably extensive, but morainic surface features are now rare. However, sands and gravels near Kingswinford probably record the waning of the Welsh Ice-Sheet from the Stour valley, Boulton (1916).

Increasing volumes of melt water heralded the onset of the second Interglacial. This activity deepened and widened existing valleys and resulted in the deposition of river gravels on their flood plains. In general, the valleys of today had their directions established during this period and old flood plains are represented by well dissected river terraces some 30 m above present river levels. As the ice retreated to the north, tundra conditions were replaced by steppes. Wind polished cliffs and wind etched stones are evident (Raw 1934).

Two 'Newer Drifts' are remnants of the third and fourth glacial episodes. Evidence for these deposits is more forthcoming.

The new ice-sheets approached from the Irish Sea and Wales, invading the

area by the new open valleys. The Irish Sea Ice-Sheet penetrated down the Middle Severn valley as far as Bridgnorth and Wolverhampton. With it came boulders from Scotland and the Lake District. The encroachment of the ice-sheet from the north led to impoundment of waters from drainage basins further south to form large glacial lakes. To the west, outflow of these lakes was prohibited by the advance of the Welsh Ice-Sheet. The formation of Lake Lapworth to the west of Newport was largely responsible for the diversion of the Upper Severn. Partial melting of ice caused this lake to increase in depth and area and subsequently overflow across the watershed near Ironbridge and form the present deep overflow channel of the Severn gorge. Melting of the ice-sheets caused larger portions of the study area to develop extra-glacial conditions, which in summer were characterised by spring floods. Many deposits of sand and gravel above the present day flood plain are remnants of the dwindling ice-sheets. The Third or Main Terrace of the River Severn dates to this period. Since then, rejuvenation and active erosion has left a terrace 30m above the present River Severn at Bridgnorth. Similar deposits can be traced along the River Worfe and Smestow Brook.

Little time has elapsed since the third Glaciation and large areas of thick drift (50m) remain, particularly in glacially filled valleys.

Large scale in situ melting of the ice-sheets resulted in an un-stratified, very badly sorted mixture of boulders and 'rock flour'. These deposits are broadly classified as boulder clays, the majority of which preserved today date back to this period. Although this is evidencefor the partial retreat and melting of the ice-sheets, there is no evidence for truly interglacial conditions before the onset of the Fourth Glacial Episode.

A re-advance of the Welsh Ice-Sheet sent glaciers down the Upper Severn, but only as far as Shrewsbury (Wills 1948). Its effect on the Severn valley was to introduce sands and gravels which were superseded by outwash sands and gravels as the ice-sheets finally retreated. This resulted in further river

terraces (1 and 2) which are evident today along reaches of the River Severn. This post-glacial period saw the final melting of the ice-sheets and rejuvenation of existing river systems. Subsequent erosion of the unconsolidated, irregularly distributed gravels, sands and clays has resulted in a patchwork veneer across the country rock. This has been broken down by weathering to form a variety of soils. The eroded sediment has been subsequently re-deposited as alluvium in the river valleys.

Although it is difficult to relate the glacial drift deposits in any convincing chronological sequence, three groups can be distinguished tenuously on chronolithological grounds. They are:

(a) sands and gravels (Older Drift);

(b) river terraces (Younger Drift);

(c) boulder clay (Younger Drift).

The following discussion is primarily concerned in outlining the surface distribution and lithological variation of these drift glacial deposits in the study area.

Surface Distribution and Lithological Variation: Sands and gravels of Smestow Brook catchment are represented by falsely bedded sands with intervening 'lens-shaped' deposits of gravel and small erratics. Contorted bedding is present not only in the glacial sands but in the Trias sandstones below. These drift remains are either the remnants of river terraces or moraines belonging to the 'Older Drift'.

North of Bridgnorth and Wolverhampton, all record of the retreat of the first Welsh Ice-Sheet has been lost by the later invasion of the Irish Ice-Sheet. The Worfe catchment, south of Worfield is virtually devoid of glacial sands and gravels but further north, in the Upper Worfe valley, ridges of sand and gravel are numerous (Fig.13). South of Lizard Hill, the greater part of the Upper Mottled Sandstone Formation is overlain by sands and gravels, with an associated featureless landscape. Sands and gravels extend southwards and to the east of the River Worfe. Around Patshull and

Beckbury mounds of sand and gravel are the remnants of fluvio-glacial flood plain deposits. Ridges north of Blymhill are part of the Newport esker chain that stretches south-east to Wolverhampton. This phenomenon records the retreat of the Irish Sea Ice-Sheet and the deposition of sands and gravels by rivers flowing alongside. The sand is reddish brown and some horizons are well sorted and of medium grain size, much like the soft red sandstone of the Permo-Trias. Imbricate pebbles, often reworked from the Trias, are interbedded with current bedded sandstones.

To the north-east of the Newport esker sands and gravels occur in small irregular mounds on the boulder clay. They show a great variability in lithology and are often interbedded with laminated clays. Deposits, however, are restricted and northeastwards from a line through Norbury and Cannock they are absent altogether.

All present day rivers have river terraces at various levels along their course. Rejuvenation has affected most river courses, particularly those in the Severn catchment. Old flood plain deposits have consequently been dissected and left standing proud as terraces on the valley sides. River terraces belonging to the 'Older Drift' are limited to the south of the area and in the main to the Stour catchment. The only example of any consequence is situated to the west of Smestow Brook and probably outlines an old course of the river. The main bulk of the river terraces were deposited by melt waters of the main Irish Sea Ice-Sheet. In the higher reaches, coarse gravels were deposited in large sheets across the valley. Further down valley, deposits become less coarse and the terraces more uniform and regular. On the whole they belong to the Main or Third Terrace but younger deposits do occur at lower elevations east of Trysull.

The Worfe catchment contains abundant fluvio-glacial deposits in its lower reaches between Worfield and Claverly. Exposures include fragments of granite, limestone and coal. The Main Terrace dominates at approximately 18m

above the present day flood plain, and the Second and First Terraces at 15m and 3m respectively. North of Worfield these deposits thin out quickly and are absent in the higher reaches.

On both banks of the River Severn and along its whole course, old flood plain deposits are represented by a series of river terraces. It is doubtful whether terraces older than the Main Terrace occur within the study area. Odd patches of terrace-like deposits do occur at higher elevations near Quatt and Holt and may represent part of the 'Older Drift' (Fourth or Fifth River Terrace). The predominant Severn river terrace is the Main Terrace which flanks both banks from Apley Park to Hampton Loade. In general, coarse gravels persist, characterised by a wide variety of pebble types including sandstones, conglomerates and limestones. Three further terraces can be recognised at lower elevations, the lowest only 3m above the present flood plain.

Along the River Penk, north from Tettenhall, river terraces are not extensive until the confluence with Church Eaton Brook. Then along both valleys they are situated well above the present day flood plain, and as such are considered fluvio-glacial in origin. Terrace features are irregular, and grade down to the present flood plain through slumping and soil creep. Horizontally bedded brown and red sandstones occur intermingled with pebble beds. Similar river terraces occur along the River Sow and Doxey Brook. Consequently near Stafford, at the confluence of the rivers Penk and Sow, fluvio-glacial gravels spread out over a three kilometer wide tract.

Boulder clay deposits are, on the whole, restricted to recent glacial advances in which the Irish Sea Ice-Sheet was dominant. A large area of boulder clay extends south-west from off the South Staffordshire Coalfield to Wolverhampton. It has generally a light brown sandy clay matrix with pebble inclusions characteristic of the Triassic pebble beds. Towards Bobbington, irregular patches form hummochy ground on which numerous erratics rest.

The Lower Keuper Sandstone Formation to the west of Claverly is overlain in parts by structureless sandy clay with pebbles. Further west, and to the south of Worfield, boulder clay is restricted to covering the dip slppe of the Bunter Pebble Bed Formation near Barnsley.

The western boundary of the study area is characterised by irregular mounds of boulder clay. Boulders of various rock types contained within a clay matrix are dominant in the few exposures that do occur. Similarly the eastern boundary is covered by boulder clay which extends west from off the South Staffordshire Coalfield across Triassic strata. It is restricted to an area east of the River Penk and covers much of the Triassic pebble beds between Shareshill and Cannock. Pebbles in a reddish clay matrix occur at outcrop, but in exposures close to Triassic pebble beds the clay matrix is replaced by loamy material. To the west of the River Penk and to the north of Penkridge, boulder clay is found in the Church Eaton Brook catchment. Then, as far as Newport and Stafford, stony red and brown boulder clay occurs in irregular mounds on the Keuper Marl. The spreads are generally irregular in their outcrop pattern although minor ridges and the occasional drumlin can be delineated.

Summary

The highly eroded and dissected form of the glacial deposits are difficult to map precisely, and acute variations of lithology hinder their correlation. However, it is apparent from the preceding account that the central region of the South Staffordshire syncline is dominated by impermeable bounder clays and a superficial cover derived from mudstones of the Keuper Marl Formation. Elsewhere within the area of study a variety of superficial deposits occur. The areal extent and thickness of each deposit cannot be evaluated precisely and it is therefore difficult to predict the watershed behaviour of the associated catchments.

The Structural History of the Permo-Triassic Aquifer and Associated Confining Strata

Introduction

The area is dominated by the Staffordshire syncline which is broken by the Longmynd-Wrekin anticline to the west and by the South Staffordshire Coalfield to the east (Fig. 14). The axial trend of these broad folds is N.N.E. by S.S.W. with the synclinal area plunging gently to the north. Shallow dips (up to 8°) are encountered in Permian and younger sediments, except in regions traversed by faults. Both the faulting and folding have a general Caledonoid trend but, particularly in the south, a Malvernian trend with N. - S. axes occurs.

Permo-Triassic Movements

Transformation from the deltaic environment of the Coal Measures, to the continental environment of the Permian, was accomplished by a succession of pre-Triassic movements. Periods of structural deformation throughout the Middle and Upper Carboniferous resulted in a number of unconformities. The introduction of 'red beds' heralded the onset of continental deposition which spans the Carboniferous-Permian Boundary. It is now clear from geophysical and lithostratigraphical analyses that faulting during this period initiated the formation of the Worcester Graben (Kent 1949, Falcon and Tarrant 1951 and Cook and Thirlaway 1952). The most significant lithological discontinuity to be formed is the unconformity between the Lower Mottled Sandstone Formation and older Permian sandstones and marls.

Permo-Triassic sedimentation was dominated by intermittent rejuvenation of faults flanking the Worcestershire Graben. Major changes in topography are indicated by the pebble beds of the Bunter Pebble Bed Formation, at the onset of the Trias, and by the Basement Beds of the Lower Keuper Sandstone Formation.

Post-Triassic Movements

Uplift of the horst-like South Staffordshire coalfield, and the folding

within, occurred during post-Triassic times. Included in these movements was rejuvenation of existing faults along the Worcester Graben, including the Western Boundary Fault. The preservation of large areas of Permo-Triassic strata, and the present day outcrop pattern, is attributed to the broad fold regime and faulting of this period.

The eastern limb of the Permo-Triassic syncline is associated with the unconformity between the Trias and Upper Coal Measures. Outcrops of the Bunter Pebble Bed Formation extend from Cannock Chase south to Upper Penn, where they are intersected by the Lloyd House, Stappenhill, and Western Boundary Faults. A westerly down-throw has resulted in Bunter Pebble Bed and Upper Mottled Sandstone Formations in juxtaposition with Upper Coal Measures. To the north-west of Cannock the Western Boundary fault reappears from the Coal Measures, between Acton Trussell and Newton, as the Hopton Fault. Here sediments of the Lower Keuper Sandstone and Keuper Marl Formations rest up against pebble beds of the Bunter Pebble Bed Formation. To the west of the fault, but only in the south, the Bushbury fault downthrows the Lower Keuper Sandstone and Upper Mottled Sandstone Formations, to rest on the Bunter Pebble Bed Formation to the east. Further south, the Stapenhill Fault - a probable continuation of the Bushbury Fault - causes repetition of the western limb of the main syncline. Consequently, the eastern limb is not present between Dudley and Bobbington.

Post-Triassic folding along the Trimpley Anticline, and later longitudinal normal faulting along the limbs, has resulted in a horst-like structure penetrating through the Permo-Trias strata between Bridgnorth and Wolverhampton. It is bounded to the west by the Pattingham Fault, and in the east by the Enville Fault. The resulting anticlinal structure plunges north disappearing under the Permo-Triassic cover, north of Bobbington. Further north, the Pattingham and Pattshall Faults, with downthrows to the west, cut across gently eastward dipping strata. This combination is responsible for repetition of the beds north of Bobbington.

The River Worfe catchment is dissected by several minor faults trending N.E. - S.W. which have downthrows to the north and south. These, together with subsidiary E. - W. faults, cause displacement of the N. - S. striking strata.

The western limb of the main syncline is clearly indicated between Bridgnorth and Newport by the unconformable overstep of the Lower Mottled Sandstone Formation on older beds. South of Newport, the Bunter Pebble Bed Formation wraps round the Coalbrookdale anticline, owing to the north-easterly plunge of the fold. From the nose of this major fold, several minor folds trend northwards. Although they are traversed by E. - W. faults with northerly downthrows, these disturbances can be recognised in the Trias around Newport. Trending north-eastwards is the shallow Aqualate Anticline with associated longitudinal normal faults on the southern limb. Trending due north is the Lonco Brook anticline with its associated longitudinal normal fault.

Evidence regarding the continuation of faulting across the Keuper Marl Formation cannot be gained from any surface features. Several small boreholes and one major construction at Ivetsy Bank have recorded highly contorted beds in the main aquifer below the Keuper Marl Formation. This suggests that the faulting regime apparent in the south trends northwards but only within the older formations. Otherwise the area beneath the Keuper Marl Formation remains poorly documented.

CHAPTER TWO

HYDROLOGY OF THE PERMO-TRIAS AQUIFER, THE CONFINING STRATA AND THE SUPERFICIAL DEPOSITS

Introduction

The dynamic behaviour of a groundwater system is dependent upon the hydraulic characteristics of the water bearing and confining formations and the watershed characteristics of the overlying superficial deposits. The characteristics of the groundwater and surface water systems have to be determined; the latter requirement permits an evaluation of the spatial and temporal variation of the net groundwater recharge component.

Hydrogeology of the Permo-Trias Aquifer and the Associated Confining Strata

Introduction

In any aquifer system, rocks can be classified into two groups according to their hydraulic properties. Those which comprise the aquifer itself are capable of transmitting and storing potable water in sufficient quantities for abstraction. There are also impermeable rocks which restrict the movement of water and, because of their geometrical relationship to the aquifer, confine most of the water to the pervious horizons.

Groundwater Sources

Within the study area, several formations are capable of yielding supplies of groundwater (Whitehead et al.1927, 1928 & 1947). Those deposited prior to the Lower Mottled Sandstone Formation yield limited supplies from sandstones which are interbedded with marls. Sandstones of the Enville and Keele Beds of the Upper Carboniferous are the most significant sources of this period. Their compacted and cemented grain matrix restricts the movement of water and abstraction is therefore limited. Between these horizons and the Lower Keuper Sandstone Formation, a sequence of intercalated sandstones and conglomerates with subordinate mudstones occur. Cementation and compaction in these horizons is limited and high storage capacities (10%) and permeabilities (10 m/d) prevail. Their wide lateral

extent (850 km^2), and substantial thicknesses (up to 400m), Kent (1949), are accompanied by a relative uniformity in aquifer characteristics. Consequently, they are a reliable source of supply and form the bulk of the 'main' aquifer within the study area.

The Lower Keuper Sandstone and Keuper Marl Formations sustain small supplies from sandstones which are interbedded with mudstone. However, this source depreciates in quality and quantity in the Buildingstone Group and younger horizons, where evaporites and mudstones predominate (Warrington 1970).

Small domestic supplies are obtained from shallow bores sunk in glacial sands and gravels. However, they are unreliable, both in quality and quantity, because of the limited thicknesses and areal extent of these deposits.

The Permo-Trias Aquifer: It follows from the above discussion that significant groundwater abstractions are from the Lower Mottled Sandstone, Bunter Pebble Bed and Upper Mottled Sandstone Formations. Their associated sediments are Upper Permian and Trias in age and are referred to as the main aquifer from now onwards in the text.

Strata which confine the base of the main aquifer are Upper Carboniferous and Lower Permian in age. Although some transfer of water may occur between these sediments and those of the main aquifer, the quantities involved are assumed to be negligible in this investigation.

Aquifer Types: Although the hydrogeological configurations which exist between the main aquifer and the overlying beds are sometimes obscure, several aquifer types can be distinguished. Mudstones of the Lower Keuper Sandstone and Keuper Marl Formations in contact with the main aquifer produce confined conditions over the central portion of the Staffordshire Syncline. For all practical purposes they are considered to behave as aquicludes. Where sandstones of the Lower Keuper Sandstone Formation rest directly upon

the main aquifer semi-confined states exist. As these sandstones are less permeable than those of the main aquifer they respond as aquitards when the watertable is lowered in their vicinity. Similar conditions prevail where intercalated thinly bedded mudstones occur within the main aquifer. Unconfined conditions pertain where the main aquifer crops out, or is overlain by superficial sands and gravels. Sands and gravels found skirting the Rivers Worfe and Stour, and the Basement Beds of the Lower Keuper Sandstone Formation are often in hydraulic continuity with the main aquifer, and thus unconfined conditions prevail (Fig. 15).

To assess the behaviour of this aquifer system it was necessary to determine the hydraulic relationship between the main aquifer and the overlying sediments. This information was obtained from driller's logs where pump tests had been conducted and from knowledge of the regional geology.

Aquifer Boundary Configurations: The South Staffordshire syncline is responsible for the occurrence of Permo-Triassic sediments between the Coalbrookdale and South Staffordshire coalfields, and together with the graben-like structure in which the sediments accumulated, is responsible for the extensive deposits preserved today (Fig. 2). A hydrogeological boundary of major importance is represented by the unconformable relationship between the permeable deposits of the main aquifer and the relatively impermeable strata of the Upper Carboniferous and Lower Permian. This boundary crops out along the western edge of the syncline, and appears to continue along the base of the aquifer as far as the South Staffordshire Coalfield. The only changes in facies along the boundary that can be determined with confidence involve the occurrence of the Bunter Pebble Bed Formation in the east in place of the Lower Mottled Sandstone Formation. As such, an unconformable relationship still exists between the main aquifer and the underlying confining strata on the edge of the South Staffordshire Coalfield. However, in the extreme south, the Western Boundary Fault brings down sediments of the main aquifer to

rest directly against rocks of Upper Carboniferous age. The horst-like structure associated with the Trimpley Anticline interrupts the ground-water regime in the south. Its western boundary terminates the main aquifer abruptly against Permian and Upper Carboniferous breccias, sandstones and mudstones. Along the eastern limb of the anticline the unconformable relationship is again evident. The northern limit of the main aquifer extends northwards beyond Stafford and Newport and subsequently joins the Cheshire basin.

Faulting Within the Aquifer: Apart from determining the boundaries to the main aquifer the influence of faults on the groundwater regime within the aquifer is not obvious. A lack of exposure over both the unconfined and confined areas of the aquifer did not allow the nature and degree of faulting to be determined with any confidence. As a result, the following remarks are restricted to isolated observations where faults and their influence on the ground-water regime can be determined with some confidence.

Normal faults throughout the main aquifer are apparently associated with tension joints. Consequently, when they are encountered in boreholes high yields of water have been obtained. The intersection of the Lilleshall and Brockton Faults explains the abundant flow of groundwater in wells situated in the vicinity of Church Aston. The association of springs and faults has also encouraged the siting of shallow wells along fault zones. The occurrence of well faulted zones and the resultant increase in permeabilities have been referred to in many borehole logs.

The quantity of geological data available on the confined portion of the main aquifer is very limited. Thus, the continuation of fault traces northwards from the unconfined area across the confined aquifer is speculative. The only observation of any significance was from a borehole situated at Ivetsy Bank. Documents related to this investigation record the occurrence of very disturbed bedding associated with faults within the main aquifer.

The disturbance is not evident at the surface and in fact the borehole log indicated that it became more acute at greater depths. The drilling programme was abandoned when it became apparent that only a limited supply of water could be obtained. The reason for the lack of water is not entirely clear, but may be in part the result of extensive faulting adjoining impermeable mudstones and permeable sandstones. This would lead to a lowering of the regional permeability and hinder the movement of groundwater from the surrounding recharge areas.

Groundwater Discharge: Springs which result from the cropping out of the junction of intercalated mudstones and sandstones occur sporadically in all formations and are particularly associated with the 'skerries' within the Keuper Marl Formation and sandstones of the Lower Keuper Sandstone Formation. Small seasonal seepages are restricted, on the whole, to these horizons, and are indicative of their limited storage capacities.

Most surface waters over the unconfined area of the main aquifer are associated with perennial springs and seepages which are often in hydraulic continuity with the regional watertable. The occurrence of these perennial water courses has encouraged the siting of the main abstraction wells along the valleys of the River Worfe and Smestow Brook.

Summary

Unlike many confined/unconfined aquifer systems, it is the unconfined sediments which constitute the main source of groundwater. The bulk of the abstraction is from the Lower Mottled Sandstone, Bunter Pebble Bed and Upper Mottled Sandstone Formations. When confined conditions prevail, supplies from these formations are restricted. The predominance of uncemented sandstones and conglomerates in the main aquifer indicates that intergranular flow is the main factor which influences groundwater movement, although fissuring in the vicinity of faults increases the overall permeability.

Evaluation of the Net Groundwater Recharge Component

Introduction

In order to study the temporal fluctuation of groundwater recharge and discharge associated with the main aquifer a thirteen year period (1960 to 1972 inc.) was considered.

Climatic Variations (1960 to 1972 inc.)

The evaluation of aquifer recharge is a necessary and important procedure in the development of water budget schemes and models devised for aquifer systems. The principal component of recharge to the Permo-Triassic aquifer is a fraction of the direct infiltration from precipitation over the unconfined area. It is determined by considering the spatial and temporal distribution of precipitation and evapotranspiration. Rainfall records from ten raingauge stations were utilised, together with estimates of local evapotranspiration rates supplied by the Meterorological Office (Figs. 16 to 20). In addition, a more profound understanding of the temporal distribution of groundwater recharge and the problems involved in the assessment of precipitation and evapotranspiration rates were obtained from consideration of seasonal climatic fluctuations (Glasspole 1949 and Lamb 1964).

Although on a daily basis the weather over the British Isles is susceptible to rapid change, it is usually confined to well defined limits. As a result, it is possible to recognise patterns on a monthly or seasonal basis which act as a guide to the evaluation of water resources (Manley 1962).

Precipitation: A cool westerly marine climate predominates, with precipitation spread fairly evenly throughout the year (Kendrew 1953 and Papadakis 1966). Mean monthly rainfall totals for the study area from 1916 - 1950, indicate a distribution of 55% during winter (October - March) and 45% during summer (April - September). Mean annual precipitation * varies from a minimum of 686mm in the south at Ashwood to 757 mm in the north at Stafford. This is due mainly

* 50 year average annual values

to differences in latitude rather than altitude and, in general, the small variation of topography (60 to 150 M.A.O.D.) is reflected by a fairly even areal distribution of rainfall throughout the area.

Winter precipitation is predominantly associated with frontal systems that accompany depressions which track eastward from the Atlantic Ocean (Taylor and Yates 1967). It is usually widespread and uniformly distributed, with a light to moderate intensity. Clearance of the cold front heralds the onset of showery activity with a resultant sporadic distribution of precipitation. Development of high pressure systems over the continent in winter can produce ridges that extend west across central and eastern England. They are stable systems and act as a barrier to depressions approaching from the Atlantic. Cold easterly winds prevail and precipitation is reduced significantly.

Frontal systems approach the British Isles during summer months, but they are often weakened over central and southern England by the extension of ridges of high pressure from the Bay of Biscay. A period of dry, warm weather is often followed by convectional precipitation when one of these ridges collapses. The rainfall is often heavy but of short duration and its limited areal distribution can lead to large variations in daily totals.

The thirteen year period commenced with an exceptionally wet year in which rainfall totals were 30% up on the mean annual average. In fact, 1960 was the wettest year recorded over the period. A reversal in this trend during 1961 heralded the onset of four consecutive very dry years. At most stations they were some of the driest years on record and, in particular, 1964 totals were down by 50% on the annual mean average. Winter precipitation was no exception and 1962/1963 totals were down by over 50% on the average. The reduced precipitation over the recharge period resulted in a regional fall in the watertable (Fig.58).

Although during the following three years precipitation was above the

mean annual average, it was not sufficient to remove the cumulative deficit (Fig. 20). Deficits remained between 180 and 330mm from 1968 to 1972 because annual precipitation totals corresponded closely to the average annual mean. However, groundwater recharge was sufficient to enable water levels to recover to pre-1961 values.

Evaporation and Effective Precipitation: Effective precipitation (the proportion of incident rainfall that is involved in surface watershed hydrology) is dependent upon evapotranspiration rates, which in turn are dependent upon wind speed, humidity and temperature variations, temperature being by far the most dominant factor.

Mean average daily temperatures of between 4°C and 6°C are associated with the months December, January and February, and as a result low evaporation rates occur (Fig. 18). Transpiration rates are also reduced, but a significant part is also played by agricultural policies that lay bare large areas of ploughed fields. This is particularly evident over the dip slopes of the Permo-Triassic outcrop areas in the Severn catchment where arable farming predominates. The overall effect is a surplus of precipitation, a part of which is available for percolation directly into the aquifer or superficial deposits directly above. With the onset of rising temperatures and the growing season in March and April, evapotranspiration increases and effective precipitation is reduced. Conditions in April/May are such that effective precipitation usually ceases altogether. By mid-summer, a daily mean average temperature of 16°C and long hours of sunshine (mean daily of 5 hours) encourages evapotranspiration to exceed rainfall over long periods. Potential soil moisture deficits in the order of 75 to 150mm exist by September/October (Green 1964). Consequently, although precipitation in October and November exceeds evapotranspiration, effective precipitation does not usually occur until December when these deficits are removed. Variations in the absolute values of effective precipitation are therefore seasonal, but long term annual

variations are dominated by fluctuations in precipitation, rather than evapotranspiration.

The groundwater model was calibrated by using recharge values estimated for 1969 and 1970. To verify this calibration, a thirteen year run from 1960 to 1972 was implemented. Details of the relevant climatological data are summarised in figures 16 to 20.

Evaluation of Potential and Actual Evapotranspiration: Evapotranspiration limits to a considerable degree the amount of precipitation available for infiltration and supplementation of groundwater storage. The factors involved in the assessment of evapotranspiration therefore play an important role in the evaluation of groundwater recharge. They are concerned with the nature and extent of the vegetation cover, soil moisture conditions and climatic variations (Takhar and Rudge 1970 and Grindley 1969).

Seasonal fluctuations of potential evaporation are related specifically to climatic fluctuations. All surface catchments within the area of study experience similar climatic changes because of the small areas involved and the fairly uniform relief. Temporal fluctuations of evaporation are therefore assumed to be similar. Spatial variations are related to the radiating surface. Land use is dominantly agricultural and approximately 80% of the area is under root crops, grasses and cereals. The distribution of woodland and riparian areas is very limited and only accounts for 7% and 4% respectively of the total area. In general, the area is devoid of large industrial complexes and urban development is restricted to the edge of the coalfields. Together with the numerous small towns and villages which occur throughout the rural areas, populated areas account for 8% of the total area (Table 2).

Initial determinations of evapotranspiration for the period of study were centred around a versatile computerised method by Chidley and Pike (1970) until estimates were obtained from the Meteorological Office at Bracknell. The climatic data required included daily readings of the maximum

and minimum temperature, humidity, wind speed and sunshine. This was subsequently abstracted from the Meteorological Observatory at Edgbaston and Bracknell. By consideration of the areas latitude, longitude and altitude together with the sun's declination the total daily incoming solar radiation was calculated. Potential evapotranspiration rates were subsequently computed for a range of albedos characteristic of grasses, root crops and cereals. Results for the calibration period (1969 to 1970) are depicted in figure 18. Subsequent potential evapotranspiration data received from the Meteorological Office for Edgbaston and the Central Midlands compared favourably with these results. Annual totals from 1960 - 1972 did not deviate by more than 15% from the mean annual average of 480 mm although the cumulative departure was in excess by 150 mm.

Actual evapotranspiration rates are restricted by the availability of moisture. Soil moisture is conducted to the surface by vegetation and subsequently transpired. Consequently the availability of soil moisture for evapotranspiration is related to the depth of penetration of root systems. Actual rates were assumed to diverge from the potential rate according to the current and maximum soil moisture deficits (Grindley 1969). The associated root constants are:

75 mm Cereals and grasses;

200 mm woodland;

75 mm for 75% of the urban area (the remaining 25% was assumed water-proof and evaporation is at the potential rate during rainfall events);

200 mm riparian areas (soil moisture is always available and evapotranspiration occurs at the potential rate).

Average actual evapotranspiration values for the study period are shown in figure 19. On an annual basis they are between 5 and 15% lower than the potential estimates. Seasonal fluctuations are such that 80% of the annual total occurs during the summer months (April to September).

PAGE 48

MISSING

Evaluation of Effective Infiltration (model 1): Initial estimates of effective infiltration over the recharge area were based on a monthly water budget scheme (recharge model 1). The defining equation is;

$$I = f(P - E) \qquad (2.1)$$

where I = infiltration rate; mm/unit area/month

P = precipitation rate; mm/unit area/month

E = evaporation rate; mm/unit area/month

f = function of the superficial cover.

Equation (2.1) is operative provided that;

$$S\,M\,Do = 0$$

and $P > E$

where $S\,M\,Do$ = existing soil moisture deficit.

When $P < E$

$$I = 0$$

and $S\,M\,D_N = S\,M\,Do + (E - P)$.

where $S\,M\,D_N$ = updated soil moisture deficit.

When $P > E$

and $S\,M\,Do > 0$

$$I = f(P - E) - S\,M\,Do.$$

If $I < 0$

$$S\,M\,D_N = S\,M\,Do + I$$

and I is reset to 0.

The spatial distribution of recharge is determined by 'f' and the following estimates based on Land (1966) were used initially. They are;

$f = 1.0$ for outcrop areas;

$f = 0.75$ for superficial cover of sands and gravels;

$f = 0.50$ for areas covered by clayey drift.

The recharge model outlined above has two obvious defects. Firstly, cumulative totals whether on a monthly or weekly basis, induce an over

simplification of the water budget balance, and secondly, the estimated parameters, f, are only average values and are not necessarily representative of the catchments under study.

The build up of soil moisture deficits during summer months and their subsequent depletion during winter has to be monitored correctly if the onset of winter recharge is to be determined with any exactitude. Cumulative total analyses tend to smooth out the effects of individual rainfalls, particularly during summer months. For example, over 40% of the total rainfall for May, 1968 (65 mm) fell in less than 24 hours. Consequently, the actual evapotranspiration rate was exceeded, the soil moisture deficit removed, and a portion of the excess moisture was responsible for groundwater recharge. Although this element of recharge was only a small proportion of the annual total, it was important in assessing the temporal distribution of groundwater recharge, and for the maintainance of a correct water balance within each hydrological unit. On a monthly cumulative system, no aquifer recharge was predicted. A vast proportion of the precipitation was involved in reducing the soil moisture deficit. Therefore, in order to compute the spatial and temporal distribution of effective precipitation more realistically, a detailed study of the hydrology of each catchment was conducted.

Surface Catchment Areas

Before the aquifer receives any recharge, either directly from percolation at outcrop, or indirectly from infiltration into superficial deposits, a fraction of the incident precipitation is involved in surface runoff. This apparent removal of potential recharge may only be temporary and it is therefore necessary to trace the movement of all surface waters while they remain within the area of study. Any interflow between ground and surface waters must be adequately monitored in order to evaluate the correct inputs and outputs to the groundwater model.

The surface watershed, which divides the Trent and Severn river systems,

is included within the modelled area (Fig. 21). Although it is one of the main watersheds in Central England, it is geo-graphically featureless within the area of study. From Wolverhampton it trends north-westwards through Perton and Codsall Wood, and across the Keuper Marl Formation. It passes by Bishops Wood and exits from the study area in the vicinity of High Offley. To the south-west of the watershed, the Rivers Worfe and Smestow Brook are the main tributaries of the River Severn. Their catchments are divided, approximately, along a line indicated by the outcrop of the Pattingham Fault. To the east of this fault, near Bobbington, a ridge of well cemented Upper Carboniferous sandstones, which constitutes the Bobbington Anticline, forms the divide. Further north, an escarpment of the Lower Keuper Sandstone Formation continues the divide to the west of the fault. The source of the River Worfe is on the southern edge of an inconspicuous watershed between Sherrif Hales and Weston upon Lizard. In its lower reaches the River Worfe flows through incised meanders and, around Worfield, is joined by small streams before eventually flowing westwards into the River Severn at Bridgnorth. The River Severn flows eastwards across the Coalbrookdale Anticline and, near Apley flows across the main aquifer. By Bridgnorth, it skirts the western edge of the unconfined aquifer as it flows south, and discharges across the southern boundary just west of Quatt. Northwards from the head waters of the River Worfe, and to the west of the Trent-Severn watershed, Back Brook flows northwards and, on entering Aqualate Mere, discharges from the modelled area.

The escarpment of the Lower Keuper Sandstone Formation that forms a watershed through Pattingham broadens northwards and extends towards Tettenhall to form the watershed between the Penk and Smestow Brook catchments. At the base of the escarpment, Smestow Brook emerges and flows southwards to cross the southern model boundary near Swindon. These waters join the River Stour three kilometres north-west of Stourbridge.

The Trent catchment is represented by the River Sow and its tributaries.

The River Penk rises near Tettenhall and flows northwards towards Penkridge. To the west, an irregular network of small brooks crosses the Keuper Marl Formations and they eventually merge to form Church Eaton Brook, which joins the River Penk near Penkridge. Further east, several small brooks, which rise between Wolverhampton and Cannock Chase, flow westwards and join the River Penk. Overall, the main tributaries of the River Penk emerge from within the modelled boundaries, and, by way of the River Penk, flow northwards into the River Sow at Stafford.

Doxey Brook rises due east of High Offley and flows eastwards to cross the northern boundary before its confluence with the River Sow two kilometers north-west of Stafford. The River Sow never crosses into the modelled area, but skirts its north-eastern boundary.

Five sub-catchments can be depicted overall. The Worfe, Smestow Brook and Back Brook sub-catchments are part of the Severn Catchment, and the Doxey Brook and Penk sub-catchments are part of the Sow catchment.

Surface Watershed Characteristics

The total runoff from a catchment is a product of direct surface runoff, interflow and groundwater seepage in the form of springs and baseflow to rivers (Smith 1966).

Surface Runoff Component: Surface runoff is dependent upon the distribution and intensity of precipitation, and the type and condition of the surface terrain. Any precipitation that remains after surface runoff and evapotranspiration has occurred, infiltrates through the surface to become potential groundwater recharge.

The physical characteristics of the five sub-catchments are divided into two groups according to their superficial cover and the underlying country rock. The three sub-catchments of the Severn Catchment are overlain by sands, gravels and permeable soils (Table 3). All these deposits result from the weathering and erosion of the underlying Permo-Trias soft sandstones and

poorly cemented conglomerates. The catchment soils are therefore very permeable and induce high infiltration rates and small surface runoff components (Fig.22).

A wide range of hydrological properties characterise the superficial deposits and country rocks found within the sub-catchments of the River Sow. Church Eaton Brook and Doxey Brook drain the boulder clay deposits and clay soils which overlie the Keuper Marl Formation. These impermeable, high surface runoff areas, occur predominantly to the west of the River Penk and contrast with permeable sands and gravels found further east between Tettenhall and Cannock Chase (Fig.22).

Groundwater Discharge Component: Springs, seepages and baseflow to rivers are natural outlets for any groundwater system. They account for a high proportion of the total groundwater discharge within the study area and therefore it is essential to determine their areal distribution.

In all sub-catchments where the Lower Mottled Sandstone and Bunter Pebble Bed Formations cropout or are near the surface, small perennial springs arise. In the Severn catchment, they are predominantly a reflection of the regional watertable that is associated with the main aquifer. Consequently, boreholes located in their vicinity are associated with water levels not far below ground level. In the Trent catchment, seepages from the Bunter Pebble Bed Formation on Cannock Chase occur above the regional watertable owing to the occurrence of impermeable calcite cemented strata. This phenomena has been encountered during the excavation of conglomerates in the area, although the quantities of water involved have not been sufficient to warrant dewatering of the strata.

Small seepages from the Upper Mottled Sandstone Formation occur parallel to bedding planes which are situated between sandstone and marl partings. They are evident in many sand quarries particularly during winter months although they are never profuse and readily infiltrate into strata at lower

elevations. In general they locate the presence of perched watertables and when the confining strata are penetrated, either during drilling or quarrying, the associated water drains away rapidly. To the east of Smestow Brook, at approximately 90 to 120m. A.O.D., small seepages give rise to streams which, in their lower courses, are perennial in nature. A similar configuration occurs within the Worfe sub-catchment from seepages located at 60 to 75m. A.O.D. When water levels in surrounding wells are considered, it is apparent that some springs are situated above the regional watertable. Few springs emerge from similar strata within the Penk sub-catchment, but they appear to be more profuse in the Back Brook sub-catchment. In both locations intricate land drainage schemes prevent assessment of the origin of most surface waters.

The Lower Keuper Sandstone Formation is responsible for seepages and springs, the majority of which occur above the regional watertable. The occurrence of interbedded argillaceous and arenaceous sediments, with variable amounts of calcite cement, has resulted in an intricate groundwater flow pattern in this formation. As a result, numerous small seepages occur, but they are not usually persistent nor of sufficient discharge to maintain a course of their own. The source of Back Brook is maintained from seepages from this formation and by surface drainage from the Keuper Marl Formation.

The Tettenhall scarp separates the source of the River Penk in the north, from that of Black Brook, a tributary of Smestow Brook. Although their source of origin and the resulting drainage pattern is not obvious around the urban area of Tettenhall and in the region of the Staffordshire and Worcestershire Canal, they are apparently associated with the Lower Keuper Sandstone Formation.

A thick veneer of boulder clay and mudstones hinders direct location of the source of seepages on the Keuper Marl Formation. However, there are only a limited number of horizons from which they can be derived, and these are assumed to be 'skerries' and other semi-permeable horizons. An impermeable

superficial cover is able to maintain the course of all surface waters, the majority of which result from direct surface runoff and land drainage rather than groundwater seepage. As a result, the upper reaches of Doxey Brook and Church Eaton Brook are maintained during winter but are reduced significantly in summer when water courses are dry or stagnant.

Influent and Effluent Conditions: Recharge to the main aquifer, from springs and seepages associated with the Lower Keuper Sandstone and Keuper Marl Formations, is insignificant. Influent conditions are not apparent in the streams when they cross onto horizons of the main aquifer and the superficial cover is sufficient to prevent any significant leakage. In their lower reaches they are in contact with the regional watertable, but effluent conditions prevail. Within the main aquifer, springs and seepages reflect natural discharges which are, in general, associated with the regional watertable. Only in the Upper Mottled Sandstone Formation are they associated with perched water table conditions. This phenomenon has also been encountered in drilling and records indicate the occurrence of water at a number of horizons before the regional water table is reached. This can be misleading during investigations relating to the positioning of the regional water table.

Surface waters that are in contact with the regional water table are, in part, maintained by a baseflow. Over the unconfined aquifer, permeable superficial deposits limit the surface runoff component and baseflow dominates in maintaining surface flows. This pattern is typical of the Severn Catchment, but across the watershed, in the Sow Catchment, it is more complex. Where the course of the River Penk is over the Lower Keuper Sandstone Formation, baseflow is operative but at a reduced rate compared with the tributaries of the River Severn. Along its course, between Penkridge and Stafford, the Keuper Marl Formation contributes little or no baseflow. However, along the course of the River Sow, east of Stafford, significant baseflow is derived from groundwater flowing north from Cannock Chase.

Surface Water Balance

In order to maintain a water budget balance within the model, it was necessary to monitor all surface flows that emerge within its boundaries. Historical Runoff Records: Ideally, recording stations were required on each of the five sub-catchments but, as this was not a feasible proposition, records from stations in the immediate vicinity had to be utilised. The regime of the River Stour, as recorded at Kidderminster, was assumed representative of the River Severn sub-catchments. Similarly, the regime of the River Sow, as recorded at Milford, was assumed typical of the River Sow sub-catchments. Runoff records for the study period, 1960 to 1972 were collected from both stations and analysed. Hydrograph separation indicates the importance of the baseflow components on the total discharge of both rivers (Fig. 22). This in turn reflects the substantial storage capacities of the reservoir rocks, particularly in the Severn catchment. Analyses of below average rainfall periods during 1961 to 1964 indicate that the baseflow contribution to the total flow of the River Stour and River Sow is 80% and 60% respectively.

Surface runoff in the Stour catchment, above Kidderminster, is restricted by the permeable nature of the superficial cover, and is generally smaller than the baseflow component. In the Sow catchment, above Milford, surface runoff responds readily to intense rainfall events. It therefore exhibits a marked temporal variation and often exceeds the baseflow component.

Prediction of Missing Hydrograph Components: A continuous historical runoff record is not available for the study period, and therefore the possibility of predicting the hydrograph components from precipitation and evapotranspiration records was assessed (Smith 1964 and Law 1953). Historical surface runoff estimates were compared with months in which precipitation, P, exceeded evapotranspiration, E, i.e. $(P - E) > 0$. For both catchments

linear relationships were inferred.

In the Sow catchment there is a gradual increase in the surface runoff component/unit of effective precipitation from September to March. This phenomenon is assumed to be related to antecedent soil moisture conditions. The physical characteristics of the catchment during the months December to April result in a more efficient conversion of precipitation to surface runoff, compared with the period September to November. As a result two linear trends were inferred (Fig.23). They were;

$$\text{Surface Runoff} = 0.43\ (P - E), \text{ December to April;} \quad (2.2)$$

$$\text{Surface Runoff} = 0.19\ (P - E), \text{ September to November.} \quad (2.3)$$

For all remaining months it was assumed that;

$$\text{Surface Runoff} = 0.30\ (P - E). \quad (2.4)$$

In comparison, no marked seasonal variation occurs within the Stour catchment and one linear trend sufficed for prediction purposes (Fig.23). This was;

$$\text{Surface Run-off} = 0.13\ (P - E). \quad (2.5)$$

Similar linear relationships were gained when the baseflow component was compared with effective precipitation. Within the Sow catchment two populations were evident again (Fig.24). The first was related to the months early in the groundwater recharge cycle (November to January) and predicts a smaller baseflow component/unit of effective precipitation than the second population which occurs later in the cycle (February to April). They were;

$$\text{Baseflow} = 0.20\ (P - E) + 4.8, \text{ November to January;} \quad (2.6)$$

$$\text{Baseflow} = 0.28\ (P - E) + 10.0, \text{ February to April.} \quad (2.7)$$

For all remaining months it was assumed that;

$$\text{Baseflow} = 5 \text{ to } 10 \text{ mm} \quad (2.8)$$

For the Stour catchment one linear relationship again sufficed (Fig.24). This was;

$$\text{Baseflow} = 0.18\ (P - E) + 7.2; \quad (2.9)$$

Where all units are in mm.

Evaluation of Effective Infiltration (Model 2); The initial infiltration factors as proposed by Land (1966) were subsequently revised and the above relationships utilised. The defining equation for the water budget model (model 2) is now considered as;

$$I = (P - E) - SR; \qquad (2.10)$$

where SR = surface runoff mm/unit area/month

The constraints which apply to model 1 are also relevant to model 2 and as such the predicted groundwater recharge component was re-evaluated along similar lines.

Initial test runs with the groundwater digital model utilised the coarse predictions that resulted from Land (1966) and the above linear relationships. However, as the hydrogeological parameters were refined it became necessary to simulate more precisely the groundwater recharge and discharge components on a finer time scale. It was therefore necessary to trace the disposition of precipitation into its various elements and, in particular, to monitor variations in soil moisture conditions and actual evapotranspiration. Consequently, temporal and spatial variation of the surface runoff, baseflow and groundwater recharge components could be evaluated.

Watershed Modelling Techniques

The integration of these complexly interacting components was accomplished by a computerised watershed model which simulates the movement of surface and sub-surface water by a number of known physical laws (Dawdy and O'Donnell 1965). The required physiographic and climatological data were evaluated from historical runoff records and from an analysis of the spatial and temporal variation of precipitation and evapotranspiration.

The Watershed Model: The model was restricted to three storage elements;

(a) surface storage;

(b) soil moisture storage;

(c) groundwater storage.

Each element is incorporated in one or more subroutines which are linked together in a water budget scheme (Fig.25 and Appendix2). Each subroutine requires the pre-evaluation of several hydrological parameters in order to simulate the watershed behaviour of the study area. These characteristics were determined, initially, by considering the catchment's physiographic characteristics and the hydrological effects of rainfall events. The 'best fit' parameters were subsequently determined during a calibration procedure. A brief resumé of each subroutine follows:-

Subroutine FINF: The potential rate of infiltration of moisture through the soil is calculated according to Horton's Infiltration Capacity Equation (Horton 1933 and 1940). The governing exponential equation requires estimates of the soil moisture content, the maximum and minimum infiltration rates and the exponential 'die away' component.

Subroutine SURST: The rate at which moisture infiltrates into the soil is limited by the potential rate of infiltration and the availability of effective precipitation. Any surplus effective precipitation is considered, by this subroutine, to be involved in surface runoff.

Subroutine EPOR: When evapotranspiration exceeds precipitation, moisture is withdrawn from the soil and a soil moisture deficit ensues (Penman 1948 and 1949). However, the rate at which it is removed is dependent upon land use and the prevailing soil moisture conditions (Grindley 1969). The rate of removal of soil moisture is determined from the potential evapotranspiration rate, the mean root constant and the maximum possible soil moisture deficit.

Subroutine SOIL: This subroutine calculates the water content of the soil by maintaining a balance between infiltration from the surface and the removal by evapotranspiration. If the moisture available to the soil exceeds the maximum soil moisture content, the excess moisture is considered to be involved in groundwater recharge.

Subroutine GW: A balance within the groundwater element is maintained by

recharge from percolation and discharge in the form of baseflow. The baseflow component is determined by assuming that the groundwater system behaves as a linear reservoir. It is therefore necessary to determine the linear groundwater constant.

Climatological Imput Data: The response of surface catchments to rainfall events is dependent upon antecedent soil moisture conditions, rainfall intensities and actual evapotranspiration rates. A complete record of precipitation and evaporation rates is therefore required for the study period.

Precipitation: The spatial and temporal distribution of precipitation was determined from the records of ten daily recording rain-gauge stations (Fig. 26). In order to handle the data more efficiently a computer data file was created.

Each months data, for each individual station, was transferred to a set of three data cards; each card contained a maximum of twelve daily rainfall figures. A check on continuity during transfer to the computer rainfall file was maintained by including a number of identification parameters on each card.

These parameters included:

(a) a rain-gauge number;

(b) a card sequence number;

(c) month and year of data.

In addition, metrication of the recording procedure at the rain-gauge stations necessitated the inclusion of a unit identification parameter.

When the preparation of data cards was complete, each set of three cards was checked for consistency within an input program before being transferred to the rainfall file. This involved checking that each card within a set possessed an identical month, year and rain-gauge parameter, and sequence numbers which progressed in the correct order.

The processes involved in the formation of the data file involved

handling and transferring a substantial number of figures. Errors were therefore inevitable and it was necessary to cross-check all data that were subsequently stored on the file. This was executed by comparing historically recorded monthly totals with those computed from daily values abstracted from the data file. In order to correct individual figures and replace missing values-(values missing from historical records)-it was necessary to have access to individual months of data for each rain-gauge. The most efficient way of implementing this was to utilise a direct access file as a means of data storage. Each record within the file was reserved for a particular month of data. To determine its position within the file, the appropriate record number was computed by a small algorithm based on the station's number and the year and month of the data. To complete the data file, all missing values had to be evaluated (Landsberg 1963). A multiple linear regression technique was used on a twelve month period over which a complete historical record was available for each rain-gauge. The initial procedure involved the computation of a correlation coefficient matrix from which a sub-group of stations was chosen for each of the 'missing value' stations. Each station within the sub-group was selected on the basis that it was highly correlated with its respective 'missing value' station (dependent variable) but not well correlated with its associates (independent variables) within the sub-group. Four such independent stations were used and the resulting linear equation was of the form:

$$R = a\bar{W} + b\bar{X} + c\bar{Y} + d\bar{Z} + \bar{k} \qquad (2.11)$$

where

R = the missing rainfall value to be derived;

a, b, c, d = the regression coefficients for the independent stations;

$\bar{k}$ = the regression constant;

$\bar{W}, \bar{X}, \bar{Y}, \bar{Z}$ = rainfall values recorded at the independent stations.

A linear regression analysis was used to obtain a solution for a,b,c,d

and $\bar{k}$, and by substitution into equation (2.11), the missing rainfall value was determined. This procedure was repeated until the rainfall file was complete. A feasibility and consistency check was performed on the file before it was considered satisfactory. Monthly totals were compiled for each station and compared with available historical records. A total mass plot analysis checked for consistency in the historically recorded data and for feasibility in the calculated values (Fig. 27).

The rainfall distribution within each sub-catchment was derived according to the method devised by Theissen (Theissen 1911). By constructing a polygon around each station it was possible to regionalise the 'point' observations. Weighting factors related to the contribution each polygon made to the total surface area of each sub-catchment were evaluated for each rain-gauge. A simple algorithm was then compiled to create a sub-catchment file from the rainfall data file. A direct access file was utilised again, with each record prefixed by coded identification parameters. As such, each individual month of data could be used separately and the overall sequential arrangement of the data checked within the watershed model before computations commenced.

Evaporation: Potential evapotranspiration rates were only available for the observatory of Edgbaston in Birmingham, and, as such, they had to suffice for each of the catchment areas in turn. A serial data file was prepared and each months data prefixed by a suitable code for identification purposes.

Catchment Characteristics: Initial evaluations of the physiographic and hydrological parameters, characteristic of the Severn and Sow Catchments, were derived from analyses of historical surface and groundwater records and from consideration of their soil and rock profiles.

The calibration procedure involved matching computed baseflow and surface runoff components with historically recorded flows from the Stour and Sow catchments. In order to achieve this, the catchments characteristics were adjusted until a suitable response was attained. Calibration was accomplished

by determining the effect each characteristic had on the evaluation of the surface runoff and baseflow components. For example, when particular climatic conditions prevail certain characteristics either attain upper or lower bound values or are not operative. Consequently, they were eliminated from the calibration procedure and those that remained were studied in partial isolation.

It was important to choose the calibration period such that no influence from initial starting conditions was experienced. Consequently, in both catchments, the calibration period was modelled over five consecutive years and the first twelve months ignored. The remaining four years were chosen to coincide with a period during which historical records were available for comparison. A brief resumé of the procedures involved in the initial evaluation of the catchments characteristics and their subsequent adjustment during calibration, is described below.

Maximum Soil Moisture Content: Initial evaluation of this parameter was based on the assumption that soils throughout both catchments could support at least a 75 to 150 mm soil moisture deficit (Green 1964). Adjustment of this parameter influenced the onset of groundwater recharge and was consequently indirectly responsible for variations of the baseflow component. In addition the soil moisture content at any time was affected by this parameter and consequently influenced the rate of soil moisture infiltration.

Groundwater Depletion Factor and Initial Groundwater Storage: Initial values were estimated from historical records by considering the change in the baseflow component after a period of groundwater recharge. Two equations were derived:

$$BF = GD \times GF \qquad (2.12)$$

$$BF' = GD \times (GF + RC) \qquad (2.13)$$

where

BF = baseflow component prior to groundwater recharge;

BF' = baseflow component after groundwater recharge;

RC = groundwater recharge component*;

GF = groundwater storage factor prior to groundwater recharge;

GD = groundwater depletion factor.

Initial estimates of GD were too large for both catchments, and consequently the predicted baseflow components commenced at too high a rate. As a result, the groundwater storage element was rapidly depleted and dry weather flows were very low. In particular, baseflows during dry summer months were very sensitive to variations in GD and this parameter was adjusted accordingly. After several calibration runs, it was apparent that the initial groundwater storage component had been underestimated for both catchments. Consequently, it was adjusted until initial baseflow components compared favourably with historical records.

Soil Infiltration Components: Initial soil infiltration rates were estimated from the known physical characteristics of the superficial deposits and soils associated with each catchment. In order to calibrate maximum and minimum infiltration rates, particular periods were studied during which one or other of the components was known to be dominant. During most winter months, soil moisture deficits were zero and infiltration occurred at the minimum rate. Therefore, the resulting surface runoff and groundwater recharge components were sensitive to its adjustment. Although the maximum infiltration rate was never operative, its influence on the catchments behaviour increased as the soil moisture content decreased. As such, it was systematically adjusted, and the exponential 'die away' component of Horton's infiltration equation varied, in order to produce a continuous, 'smooth' variation in the infiltration rates as the soil moisture content was reduced. When an acceptable response was achieved, the initial soil moisture content component was calibrated.

Interception Store: A small interception store was assumed characteristic of both catchments because of the predominance of agricultural and pasture land. Therefore its influence on the catchments overall response was masked by the

* estimated from historical effective precipitation evaluations.

other characteristics. After a dry spell, when the interception store was depleted, a small influence on the surface runoff component was detected. Only on these occasions was it assumed justified to adjust the capacity of this storage element.

The primary objective of the calibration procedure was to match computed surface runoff and baseflow components with historical records. This was assisted by monitoring intermediate processes, such as the accumulation and depletion of soil moisture deficits, and comparing them with historical records. Similarly, variations in groundwater storage and groundwater recharge were compared with historically recorded groundwater hydrographs.

A total of thirty five runs per catchment were necessary to achieve a satisfactory response over the calibration period (Figs.28 and 29). However, in the Sow catchment this was hindered by historical records that inferred the occurrence of unwarranted high surface runoffs during the summer of 1964. This was assumed to be in response to heavy rainfall outside the bounds of the study area and was ignored. Otherwise, no serious discrepancies occurred and calibration was assumed complete when the sum of squares difference between historical and computed values was not improved significantly from one run to the next. In relation to the groundwater recharge component variations of the order of 5% were observed at this juncture. Consequently, a simulation run for the total study period was implemented for both catchments by utilising the calibrated characteristics and by reassessing the initial starting conditions (Table 4). The missing surface runoff and baseflow components were predicted and the groundwater recharge components determined. Subsequent simulation runs were conducted to determine the spatial and temporal distribution of groundwater recharge by considering each of the sub-catchments separately. The characteristics of the Stour catchment were assumed representative of the Smestow Brook, Back Brook and Worfe sub-catchments and the characteristics of the Sow catchment were considered

representative of the Penk and Doxey Brook sub-catchments.

Groundwater Levels

Introduction

Prior to, and for the duration of any hydrogeological study, an adequate network of observation boreholes should exist to record the spatial and seasonal fluctuations in the regional water table. Unfortunately, only recently have observation boreholes been erected specifically for this purpose; this response was initiated by the International Hydrological Decade and the Water Act of 1963.

Historical water levels were required for calibrating the digital groundwater model and for initialising starting conditions. Although a dynamic equilibrium run was necessary before the calibration procedure, a balance was obtained more readily by predicting initial water levels from historical records. To determine the appropriate boundaries for the model, variations in the head and hydraulic gradients in their vicinity were derived from the observation network.

Water Level Observations

Five observation wells are presently monitored within the area of study, and other records exist from previous investigations on the extent of cones of depressions in the vicinity of large abstraction wells. * Numerous spot rest water levels recorded from privately and publicly owned wells have helped to fill in gaps where data were scarce. However, it was necessary to carefully scrutinise all water level observations to ensure they were related to the main aquifer, and that there was no significant interference from groundwater abstration in the vicinity. Some missing values in the observation network over the calibration period (1969 to 1970) were evaluated by linear regression techniques.

From the continuous and intermittent observations it was possible to depict the pattern of groundwater fluctuations over the unconfined aquifer.

* Water level observations were conducted by local water authorities in order to delineate areas where dewatering necessitated compensation.

In the region of the unconfined/confined boundary, only general trends could be determined. The central confined area has a sparse observation network and, to determine the existing trends, data had to be extrapolated from the surrounding regions and intuitively adjusted to conform with the hydrogeological characteristics of the area.

The Water Level Surface

In order to assess the overall groundwater regime, a series of water level contour maps were constructed. A manual approach was successful in outlining the general trends, but their appearance was complicated and confused by discontinuities and irregularly shaped contours. A surface fitting technique, which involved a second degree Fourier surface fit analysis, incorporated within an optimisation routine, was utilised to evaluate a more regular surface. Several such exercises were conducted when an adequate historical record allowed them to be statistically viable (Fig. 30). From analyses of the manually constructed and computed maps it was possible to delineate the recharge and discharge zones. The overall groundwater contour regime implied that it was feasible for a groundwater balance to be obtained within the modelled area.

The direction of groundwater flow in the unconfined areas is influenced predominantly by the surface drainage pattern and the overall water table reflects, in a subdued manner, the surface topography. Although the strata in the Severn Catchment have a very shallow easterly dip, they have no regional influence on the direction of groundwater movement. Indeed, from investigations conducted in the laboratory, it was inferred that current bedding had more influence, but this again was only on a localised scale.

Within the Trent catchment the overall pattern of groundwater flow is not so obvious, although in the unconfined areas flow is again towards the main rivers. With this general trend apparent in both catchments, there is little groundwater movement towards the confined horizons. The groundwater flow regime

within the confined area is apparently influenced by N.E. - S.W. trending faults (Fig. 13). The groundwater is therefore confined to more or less isolated blocks with no recharge or discharge areas apparent. It was therefore assumed that within the confined aquifer, and particularly towards the centre of the South Staffordshire Syncline, there is little movement of groundwater under natural conditions.

The dominant divide has a similar trend to the Severn - Trent watershed divide, but is situated further to the north-east. As such, it divides groundwater flow, which is predominantly to the south-west in the Severn catchment and to the north-east in the Trent catchment.

Groundwater flow across the southern model boundary is restricted to discharge from the Smestow Brook sub-catchment; otherwise the boundary is impermeable. The western boundary is impermeable as far north as Church Aston and flow across the northern boundary is restricted to discharge from unconfined areas of the Back Brook and Penk sub-catchments. The intervening confined area is assumed to contribute insignificantly to the total discharge across the northern boundary. A westward movement of groundwater from the Cannock Chase area signifies recharge across the north-eastern boundary. Further to the south, however, the boundary is impermeable and it remains so as far as the southern boundary.

Within the modelled boundaries two major discontinuities in the groundwater flow regime occur, and are evidently associated with N.E. - S.W. trending faults. The Pattingham Fault in the south is responsible for separating the groundwaters of the Worfe and Smestow Brook sub-catchments. To the north, the Bushbury and Hopton Faults restrict the movement of groundwater westwards from Cannock Chase into the confined area; the bulk of this groundwater is assumed to be diverted northwards and towards the River Sow.

Hydraulic gradients to the south and west of the main groundwater divide are in the range 1 : 200 to 1 : 350 and fairly uniformly distributed.

Steeper gradients are located in the Cannock Chase area where at 180 m.A.O.D. they are in the order of 1 : 100. However, they become more shallow at lower altitudes being approximately 1 : 200. The shallow hydraulic gradient associated with the confined area was assumed to reflect the occurrence of a stagnant body of water with restricted recharge and discharge zones.

Temporal Variations of Water Levels

The majority of observations are from wells on or near outcrops of Permo-Triassic sediments. Water level fluctuations in their vicinity are a function of recharge variations and annual hydrographs respond to the seasonal fluctuation of effective infiltration. Maximum water levels are generally attained in March/April after the winter recharge period and the following recession results in minimum levels by October/November (Fig.31). Minimum annual fluctuations are recorded in the unconfined areas of the Worfe, Smestow Brook and Back Brook sub-catchments; Roughton, for example, exhibits an annual variation of 0.6 to 1.0 m during average rainfall years. Unconfined areas to the east of the Penk catchment are characterised by average annual fluctuations of 1.3 to 1.6 m, for example at Milford. In general, large storage capacities prevail in all unconfined areas to a depth of at least 10 to 17 m below the surface where, in general, these fluctuations occur. Towards the unconfined/confined boundary, annual cyclic variations still occur, but overall fluctuations are in the order of 3 to 5 m, for example at Cowley. This is due to smaller storage capacities and reflects either the occurrence of well cemented sandstones of the Lower Keuper Sandstone Formation, or the onset of semi-confined/confined conditions.

The overall pattern that was discernible from the observation network is confused by boreholes that are sited on the edge of the Permo-Triassic sediments, for example at Goldthorn Hill. These boreholes have penetrated into Carboniferous sediments and the characteristic cyclic hydrograph is no-longer

depicted. The resulting water level fluctuations are probably influenced by mining in the Coal Measures below.

During the study period, the majority of annual hydrographs correspond closely to the norm. However, water levels recorded during the period of drought, 1961 to 1964, indicate that a significant reduction in the storage of the main aquifer occurred (Fig. 58). Although the annual cyclic pattern was still maintained, the winter recharge period was greatly attenuated, and for three consecutive years water levels did not recover to the previous year's maximum. During 1964, maximum water levels over the unconfined areas were in the region of 3 m below those recorded in 1961. Unfortunately, many shallow wells over the unconfined/confined boundary dried up, but records suggest that the fall in water levels would have exceeded 5 m. This general decline in water levels necessitated a cut back in abstraction rates at the main public supply wells in order to maintain the water level at a suitable distance above the pumps. With a return to slightly above average rainfall from 1965 onwards, water levels recovered and by 1969 had attained similar levels to those recorded during 1961.

Although the overall annual variation in water levels suggests that groundwater recharge is restricted to the winter months, October to March, closer analyses of individual hydrographs indicate that a more complex seasonal variation occurs. In particular, very wet periods during April and May are able to prolong the winter recharge period because evapotranspiration rates are small. Individual intense rainfall events during the period June to October are responsible for small increments of groundwater recharge; these are depicted either by secondary peaks superimposed on the groundwater recession curve or by a sudden reduction of the rate of recession.

The response of water levels to effective infiltration appears to be rapid (0 to 5 days) over the unconfined aquifer and is assumed to be a function of the infiltration rates through the superficial deposits.

A similar response is detected in the region of the unconfined/confined boundary. Within the confined aquifer, water level responses are dependent upon the flow of groundwater from the unconfined aquifer and its associated recharge areas. The hydraulic conductivity between the two aquifer systems is low and therefore recharge pulses are delayed and also attenuated.

Groundwater Abstraction

Introduction

The groundwater resources are within the Trent and Severn River Authorities control and the bulk of abstraction is implemented by local water boards (Table 5). Additional abstractions are made from privately owned sources and these are monitored by the River Authorities. Small supplies, in the region of 5 cu. m/d, are abstracted at a number of farmsteads, but, with the change over to mains supplies increasing, many wells have been abandoned. Similarly, privately owned industrial boreholes where over 5000 cu.m/d are abstracted have been replaced by guaranteed sources from the water boards. As a result, less than 10% of the present days total abstraction is from privately owned sources.

Borehole Distribution and Abstraction Rates

Pumping stations are concentrated on the unconfined portion of the aquifer and they account for approximately 85% of the areas total abstraction. They are particularly abundant along the valleys of the River Worfe and Smestow Brook (Fig. 32). Further north, abstraction points are restricted to the edge of the confined aquifer, where the confining strata have no substantial thickness. Exploratory wells sited towards the centre of the confined area have not been able to sustain adequate yields, and as a result this region has not been considered a viable source of supply.

The considerable thicknesses of Permo-Triassic sediments have not been fully penetrated by most abstraction wells and the construction of observation wells in their vicinity has been almost completely neglected. In the

unconfined regions, the abundance of groundwater supplies has always been assumed. In effect the process of abstraction has been basically an engineering problem and little hydrogeological knowledge has been gained. Consequently, the majority of 'pump tests' undertaken involved testing that the required supply could be obtained and the pump was working correctly. All tests were able to sustain between 5000 and 15000 cu.m/d under steady state conditions.

Confined areas are characterised by substantial thicknesses of Lower Keuper Sandstone and Keuper Marl Formations and average abstraction rates are in the order of 4000 cu.m/d, compared with an average of 6000 cu.m/d over the unconfined area. To increase the flow to wells in the confined area adits have been constructed.

Abstraction rates from individual sources have remained virtually constant during the study period. Increased demands have been supplemented by the construction of additional sources of supply, for example at Copley, Neachley and Roughton. Supplies have been plentiful except in the central confined areas, but restrictions on abstration rates have had to be imposed in some instances due to the encroachment of saline waters from evaporite deposits.

Total Water Balance

Introduction

Before the groundwater model was utilised it was necessary to ascertain whether the required water level responses could be obtained, by considering the inputs and outputs of the system. It was therefore required to determine whether the estimated recharge and discharge components, when considered on an annual basis, could maintain a balance within the groundwater system.

Total Water Balance Summary

The water balance equation considered was:

$$P = E + BF + SR + D + DS + SD + BL \qquad (2.14)$$

where

P = precipitation;

E = evapotranspiration;

BF = baseflow;

SR = surface runoff;

D = groundwater abstraction;

DS = change in groundwater storage;

SD = change in soil moisture;

BL = groundwater flow across model boundaries.

From consideration of the groundwater flow pattern in the region of the model boundaries, the net effect was for groundwater to discharge from the study area. The actual quantity could not be determined accurately but was estimated to be equivalent to 10 mm/unit area/annum; as such it was not considered in the water balance summary (Table 6).

To overcome the difficulties experienced in assessing the change in groundwater storage and soil moisture content, the time period chosen was such that initial and final heads were similar and soil moisture content was at maximum capacity (Ineson and Downing 1964). The remaining parameters were determined from historical records. Subsequently, a water budget analysis was formulated for the Severn and Sow catchments for the period January 1968 to January 1969. A satisfactory balance was found to exist in both catchments and the error in the total balance was in the order of 3%. This error was assumed to be related to the exclusion of boundary flow estimates from the analyses.

CHAPTER THREE

DIGITAL GROUNDWATER SIMULATION

Introduction

The dynamic behaviour of the Permo-Triassic aquifer was simulated by utilising digital modelling techniques. It is therefore relevant at this juncture to consider the theoretical background to digital models and the required spatial and temporal distribution of their input data. Subsequent hydrological investigations can therefore be conducted specifically to meet these requirements.

Theoretical Considerations

Introduction

The two most fundamental lawa which are used in hydrological investigations are:

(a) The Law of conservation of mass.
(continuity equation)

(b) The Law of conservation of energy.
(first law of thermodynamics)

The second law of thermodynamics is also relevant to the flow of groundwater because a loss of mechanical energy is involved.

The continuity equation is used to evaluate net changes in any volume due to fluid movement. In a differential formulation this principle stipulates that the rate of increase in volume in an infinitesimal element is equal to the net rate of inflow of fluid. A steady state exists when the rate of increase of volume with respect to time is zero. It follows that the net rate of increase is zero in these circumstances. An unsteady state exists when the rate of increase with respect to time varies with time. For all conditions there can be no loss or gain of fluid mass within the system as a whole.

The first law of thermodynamics states that in any closed system there is a fixed amount of energy which can neither increase nor decrease in amount, that is the total energy within the system is constant.

The second law of thermodynamics states that the flow of a viscous liquid is accompanied by an irreversible transfer of mechanical to thermal energy because, in this case, of frictional forces between the fluid and the rock.

Two approaches to the establishment of the laws governing the movement of groundwater flow have been pursued. Hubert (1956) deomonstrated that microscopic theory can lead to certain macroscopic laws, and, in doing so, accomplished the derivation of Darcy's Law from the Navier-Stokes equation. However, the most popular approach was by direct experimentation (Darcy 1856).

Darcy's Experimental Law

Generalisation of the fundamental physical law governing the flow of water in porous media is credited to Henri Darcy (1856). Darcy concluded that the flow of water was directly related to the slope of the hydraulic gradient by a constant of proportionality.

That is;

$$Q = K.A. \frac{(h_1 - h_2)}{L} \qquad (3.1)$$

where Q = flow (volume per unit time);

K = constant of proportionality;

A = cross-sectional area of flow;

h_1, h_2 = water level elevations as measured above datum;

L = distance between manometer tubes.

See figure 43 for explanation.

Darcy's Law is most often quoted as;

$$\frac{Q}{A} = q = K.i \qquad (3.2)$$

where i = hydraulic gradient;

q = flow per unit area.

Hubbert's Experimental Law

If the nature of the constant of proportionality is considered it can be shown to be a function of the medium and the fluid. Experimental investigations

by Hubbert (1940 and 1956) showed that by varying fluid density, viscosity, and the geometry of the medium the following relationship existed:

$$K = \frac{c \cdot \rho \cdot d^2}{\mu} \qquad (3.3)$$

where μ = viscosity;

ρ = fluid density;

$\bar{d}$ = mean grain diameter;

c = the new constant of proportionality.

Thus K is dependent upon both fluid properties ρ and μ and the medium property $\bar{d}$.

Hagen-Poisuille Relationship

Another approach to understanding the basic dependency of the Darcy constant K is by consideration of the laws governing flow in small diameter pipes as defined by Hagen and Poisuille (Curle and Davies 1968). The Hagen - Poisuille equation is stated as:

$$q = \frac{Q}{A} = \frac{N \cdot \rho \cdot g \cdot R^2 i}{\mu} \qquad (3.4)$$

where N = dimensionless shape factor related to the geometry of the flow passage;

R = diameter of the flow passage;

g = acceleration due to gravity;

i = hydraulic gradient.

Significance of the Constant of Proportionality and the Hydraulic Head

Comparing Darcy's Law, equation (3.1), with (3.4):

$$K = \frac{N \cdot \rho \cdot g \cdot R^2}{\mu} \qquad (3.5)$$

By assuming that the mean grain diameter $\bar{d}$ is equal to the mean passage diameter R the following identity is obtained:

$$c = N \cdot g. \qquad (3.6)$$

Thus c is a function of the geometry of the sand grains and the packing density.

Since ρ and μ are dependent upon temperature Darcy's Law only applies

where conditions are isothermic. In these conditions changes in conductivity are only a function of changes in the medium.

Significance of the hydraulic head is gained from the generalised Bernouilli equation for incompressible flow in a fluid. It states that the energy of flow is a sum of:

a) gravitational potential energy;

b) pressure energy;

c) kinetic energy.

In groundwater flow the velocity is small and therefore the kinetic energy is ignored. The potential energy of flow becomes:

$$\phi = g.z + \frac{p}{\rho} \qquad (3.7)$$

where z = vertical distance above an arbitrary plane;

p = pressure of the fluid.

As such, Darcy's empirical law can now be stated as:

$$Q = -K.A.\frac{dh}{dL} \qquad (3.8)$$

where h = the total head, consisting of elevation and pressure;

L = the distance over which flow takes place.

The minus sign indicates that flow is opposite in direction to the increase in head.

Regional Groundwater Flow Conditions

Introduction

One of the most fundamental assumptions related to the movement of groundwater is that flow is laminar; consequently, Darcy's Law is valid. Since the velocity head can be assumed to be small the slope of the water surface or piezometric surface is equivalent to the energy loss gradient. The total head at any point within the aquifer is equivalent to the water level attained in a piezometer tube or well at that point. In addition it is assumed that the pressure distribution in the aquifer is hydrostatic and as

a result the hydraulic gradient at any depth in the aquifer is constant. If isothermic conditions prevail, the flow through any unit within the aquifer is a function of the aquifer properties and the pressure head gradient.

If it is assumed that the transmitting properties of the aquifer do not change with depth and they are only a function of the saturated thickness, the three dimensional problem can be considered in two dimensions only. In the following section the problem is related to two planar co-ordinate directions x and y. Consequently, it is assumed that slopes of the aquifer and pressure surface are small and the resultant flow paths are horizontal.

Theoretical Considerations

The generalised Darcy equation for flow in two co-ordinate directions, in a heterogeneous medium can be expressed as:

$$\frac{Qx}{Ax} = -Kx.\frac{dh}{dx} \quad \text{and} \quad \frac{Qy}{Ay} = -Ky.\frac{dh}{dy} \qquad (3.9)$$

where Kx = hydraulic conductivity in the x direction;

Qx = volume of flow in time t in x direction;

Ax = cross sectional area of flow;

$\frac{dh}{dx}$ = hydraulic gradient in x direction.

Similarly for the y direction.

Substitution into the continuity equation, and assuming in incompressible fluid, results in the equation;

$$\frac{d}{dx}\left(-Kx\frac{dh}{dx}\right) + \frac{d}{dy}\left(-Ky.\frac{dh}{dy}\right) = 0 \qquad (3.10)$$

This assumes that the volume remains unchanged.

If Q is the net groundwater withdrawal and H is the average saturated thickness, then the resulting equation for two dimensional transient flow is:

$$\frac{d}{dx}\left(Kx.H.\frac{dh}{dx}\right) + \frac{d}{dy}\left(Ky.H.\frac{dh}{dy}\right) = S.\frac{dh}{dt} + \frac{Q}{dx\ dy} \qquad (3.11)$$

where S = storage coefficient;

t = time dimension;

Q = volume withdrawn in time dt;

$d\bar{x}.d\bar{y}$ = dimension of the surface area of a unit element.

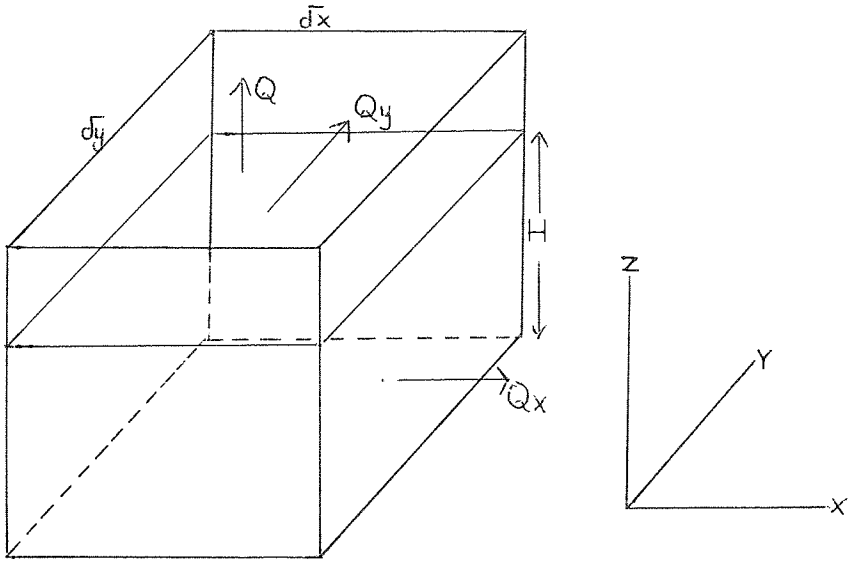

If Tx = Kx.H and Ty = Ky.H then:

$$\frac{d}{dx}\left(Tx.\frac{dh}{dx}\right) + \frac{d}{dy}\left(Ty.\frac{dh}{dy}\right) = S.\frac{dh}{dt} + \frac{Q}{d\bar{x}.d\bar{y}} \qquad (3.12)$$

Ir Tx and Ty are assumed constant and equal, the resulting equation is:

$$T\left(\frac{d^2h}{dx^2} + \frac{d^2h}{dy^2}\right) = S.\frac{dh}{dt} + \frac{Q}{d\bar{x}.d\bar{y}} \qquad (3.13)$$

Equation (3.13) has no general solution and therefore finite difference approximations are used to enable numerical solution on a digital computer. This results in a series of simultaneous equations which can be solved by using a number of strategies and algorithms. By using a number of nodal points, lying within the aquifer boundary, a set of equations can be derived to relate the pattern of groundwater flow between them. These equations can then be solved to evaluate the water levels at each node after a set period of time.

The surface area of the aquifer is divided into discrete units, and the differential equations are replaced by finite difference approximations. If a polygonal network is considered,equation (3.9) now becomes:

$$Q_{21} = -K_{12} \cdot A_{12} \frac{(H_1 - H_2)}{X_{12}} \qquad (3.14)$$

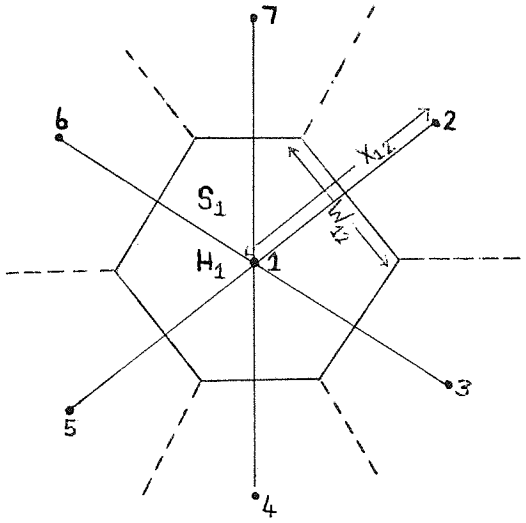

where Q_{21} = volume of flow from node 2 to 1 in time t;

K_{12} = hydraulic conductivity along the path between nodes 1 and 2;

W_{12} = width of flow path between nodes 1 and 2;

X_{12} = distance between nodes 1 and 2;

H_1 and H_2 = elevation of heads at nodes 1 and 2 respectively at time t + dt;

S_1 = storage coefficient of node 1.

It if is assumed that

HS_{12} = average saturated thickness between nodes 1 and 2;

T_{12} = transmissibility between nodes 1 and 2;

A_{12} = cross sectional area of flow between nodes 1 and 2;

then

$$A_{12} = W_{12} \cdot HS_{12} ;$$

$$T_{12} = K_{12} \cdot HS_{12}.$$

Contribution of groundwater flow from node 2 to 1 is:

$$Q_{21} = T_{12} \cdot W_{12} \cdot \frac{(H_2 - H_1)}{X_{12}} \qquad (3.15)$$

where

$$\frac{dh}{dx} = \frac{(H_2 - H_1)}{X_{12}}$$

The contribution from all the surrounding nodes to node 1 is

$$N = \sum_{1}^{M} \frac{T_{1N} \cdot W_{1N}}{X_{1N}} (H_N - H_1) \qquad (3.16)$$

where

M = the number of connecting nodes.

The change in storage in unit 1, of surface area A_1, from time t to t + dt is

$$A_1 \cdot S_1 (H_1 - H_1') \qquad (3.17)$$

where

S_1 = storage coefficient of node 1;

H_1' = head at node 1 at time t.

Finally, if the net flow of recharge and discharge at node 1 is $A_1 \cdot Q_1$, the resulting water balance equation for node 1 is

$$\sum_{N=1}^{M} \frac{T_{1N} \cdot W_{1N}}{X_{1N}} (H_N - H_1) = A_1 \cdot S_1 (H_1 - H_1') - A_1 \cdot Q_1 \qquad (3.18)$$

where Q_1 is now expressed as a depth/unit area.

A similar equation can be derived for each node in turn.

Equation (3.18) is a finite difference approximation to the general groundwater equation which is based upon a polygonal element. The equations in H_N are solved simultaneously by an iterative method.

Hydrogeological Models

Introduction

A model is a simplified representation of a complex system. Scaled down physical models, and analogue models such as the resistance capacitance type, have been utilised to simulate aquifer behaviour (Cole et al. 1973 and Rushton and Bannister 1970). Analogue models are discrete spatially, and time is represented by a continuous function.

Digital Models

Recently, digital solutions have been developed in which it is required to solve a series of simultaneous equations during the simulation period. These models are discrete both in space and time (Bittinger et al. 1967, Pinder et al. 1968 and Rushton and Tomlinson 1971). Digital models are generally preferred because they can deal with more complex problems than is practical with an analogue model.

The introduction of more sophisticated techniques for solving the large sets of simultaneous equations that result from digital simulations has been assisted by the development of computers with large storage capacities. Finite difference forms to the general groundwater equation, similar to equation (3.18), can be programmed for solution on these computers. It is the various techniques used in the construction of the finite difference approximations and in the solution of the resultant equations that account for the basic differences in digital models.

Initial attempts to utilise numerical techniques came in the early 1950's with the study of gas and oil flow through porous media (Bruce et al. 1953). Stallman (1956) first introduced numerical methods into groundwater hydrology with the aid of finite difference approximations to the head, at points on a finite difference grid. During the 1960's, development in the study of large scale groundwater reservoirs was initiated and sophisticated (Fayers and Sheldon 1962). Techniques also developed in other fields with the study of flow in petroleum reservoirs, infiltration rates in soils and drainage in ditches (Rubin 1968). Implicit and explicit iterative techniques and Gaussian elimination were developed during the 1960's for the solution of two dimensional flow problems. Subsequent refinement to these models has included versatility in their input and output options and the simulation of a number of different boundary conditions.

The sudden increase in recent years in the use and development of

digital models for groundwater problems has invoked numerous critical reviews. In particular, problems involved with finite difference approximations, and the optimum time and space steps they require, have been discussed in Rushton (1973) and Rushton (1974).

Construction of the Finite Difference Equations: Methods of solution can be classified into two groups. The first involves the use of explicit techniques in which the heads, at any time t, are computed directly from those at time t - dt. The second involves implicit solutions in which the heads, at time t, are a function of the heads at that time and, in some methods, at time t - dt also. The combination of these techniques has led to four basic methods of solution.

1) The Forward Difference Explicit Method: Computations are easily performed because only one unknown exists at any time, t, at each node. The solution is therefore dependent on the heads at time t - dt. However, this method of solution is susceptible to very bad instability if the ratio between the distance and time steps is not chosen carefully.

2) The Crank-Nicholson Implicit Method: Equal weight is given to the dependence of the solution on the heads at the particular time, t, and on those at the time, t - dt. Although it represents a sound approximation to the system, it requires the solution of a large matrix at any one time.

3) The Alternating Direction Implicit Method: In this approximation a rectangular gridded network is considered and the solution proceeds by formulating a set of equations for each row in the x - direction. Heads which contribute to the flow in the y - direction are held constant. The equations are solved by elimination and back substitution. The process is repeated for the y - direction using the latest estimates of heads from the previous step. The whole process is repeated until a suitable convergence is achieved. Difficulties can arise with this method if correct finite difference steps are not used.

4) The Backward Difference Implicit Method: All weight is placed on the heads at the time in question, t. Predicted heads are therefore obtained from solution of the simultaneous equations derived at that time. If a square grid is considered the notation for any node i, j is as follows:

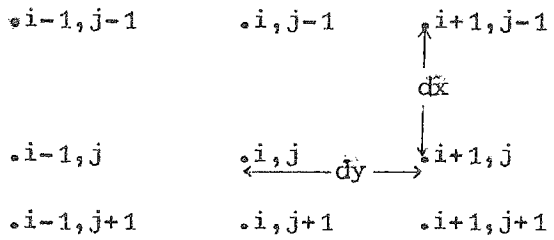

If it is assumed that dx=dy, from equation (3.18) Wij = Xij for all i and j. Therefore, by considering the node i, j at time t, the backward difference solution of the finite difference equation becomes;

$$
\begin{aligned}
& T_{i-\frac{1}{2},j}\left[Hi^{t}_{-1,j} - Hi^{t}_{j}\right] \\
+\ & T_{i+\frac{1}{2},j}\left[Hi^{t}_{+1,j} - Hi^{t}_{j}\right] \\
+\ & T_{i,j-\frac{1}{2}}\left[Hi^{t}_{,j-1} - Hi^{t}_{j}\right] \\
+\ & T_{i,j+\frac{1}{2}}\left[Hi,^{t}_{j+1} - Hi^{t}_{j}\right] \\
=\ & dx^{2}\left[S\ (Hij^{t} - Hij^{t-dt}) + Qij^{t-\frac{1}{2}}\right] \qquad (3.19)
\end{aligned}
$$

This method of solution is stable for all values of dx and dt (Rushton 1973) and, although instability problems may arise during the analysis of unsteady state flow in the vicinity of pumped wells, the solution is stable for regional groundwater analysis. Consequently, this technique was used in this study.

Solution to the Backward Difference Equations: This section outlines the finite difference approximations to the groundwater equations and the methods used in this study to solve the resultant equations. Iterative methods are generally used for solving linear algebraic equations, when the number of unknowns is large and each equation involves only a few of them. Consequently, they take advantage of the large number of zeros within the matrix of coefficients. Convergence towards a solution is achieved by systematically

adjusting the heads, so that the difference between the exact solution and successive approximations tends to zero as the number of iterations increases. The rate of convergence can be increased by utilising the most recent iterates as soon as they become available. This process is incorporated automatically into a computerised routine that is based on the method derived by Gauss-Siedel and Tyson and Weber (1963). As such, from equation (3.18) and for any node, I, at time t,

$$RES\ (I) = \sum_{N=1}^{M} C_{IN}\ (H_N^t - H_I^t) - A_I.S_I\ (H_I^t - H_I^{t-dt}) + A_I.Q_I \qquad (3.20)$$

where $\dfrac{T_{IN}.W_{IN}}{X_{IN}} = C_{IN}$

and RES (I) = residual in the water balance for node I.

After an initial estimate of H_I^t, it is adjusted so that the residual is minimised, that is RES (I) $\rightarrow$ 0. By differentiating the basic model equation (3.20) with respect to H_I, the technique to achieve this is derived:

$$\frac{d\ RES(I)}{d\ H_I} = \sum_{N=1}^{M} C_{I\,N} - A_I.S_I \qquad (3.21)$$

$$\text{however,} \quad \frac{\text{New Residual} - \text{Old Residual}}{\text{New } H_I - \text{Old } H_I} = \frac{d\ RES(I)}{d\ H_I} \qquad (3.22)$$

Since the new residual is required to be zero,

$$\text{New } H_I = \text{Old } H_I + \frac{RES(I)}{\sum_{N=1}^{M} C_{IN} - A_I.S_I} \qquad (3.23)$$

where RES(I) = residual derived at the previous iteration;

Old H_I = head derived at the previous iteration.

During the iterative procedure, better approximations to the new heads are achieved but, because an exact solution is not possible, certain criteria have to be defined to assess when an acceptable solution has been reached. A balance in the water budget is pursued for each node and the total error is

defined as the summation of all nodel errors. An acceptable solution is attained when this error is reduced below the required tolerance factor. In this study the tolerance factor was related to the annual water budget balance (Table 5), and was assessed to be approximately 5% of the average annual groundwater recharge.

The residuals at the end of each iteration were usually evenly distributed and, as such, the largest error in the predicted heads was associated with nodes characterised by the smallest storage coefficients. Therefore a check was maintained to ensure that their heads remained within an acceptable tolerance, which was estimated to be in the order of $\pm$ 15mm per month. As such, nodes associated with larger storage coefficients had smaller residuals. As a result an acceptable solution was reached when individual nodes, as well as the whole system, were balanced satisfactorily.

Although the Gauss-Siedel relaxation technique coverges towards a satisfactory solution for all time and space steps, a substantial amount of computation time is involved. It was therefore necessary to reduce the number of iterations per time step by including a relaxation factor to speed up the rate of convergence (Fig. 34a).

Since the predicted heads are incorporated into the iterative procedure as soon as they become available, the technique utilises a successive over-relaxation method of solution. The basic groundwater equation is, in matrix terms, $Fx = b$, where;

F = a symmetric positive definite matrix related to the hydraulic gradients;

x = function of the transmissibility;

b = groundwater flow component.

This type of equation, and the method of solution used, converges for $0 > V > 2$, where V is a relaxation factor (Carre 1961, Martin and Tee 1961 and Smith 1965). The new heads are therefore predicted by considering equation (3.23) in the form;

$$\text{New } H_I = \text{Old } H_I - \frac{V(RES(I))}{\left(\sum_{N=1}^{M} C_{IN} - A_I \cdot S_I\right)} \qquad (3.24)$$

In practice, the convergence rates were most rapid with V set between 0.8 and 1.2 and, in general, increased as dynamic equilibrium was approached (Fig. 34b).

Discretisation of Space: This procedure involves the distribution of the nodes and the construction of the intervening elements. Before it is implemented, several points have to be borne in mind.

Ideally, the parameters assigned to each node should be representative of the surrounding element and, where rapid variations occur over small distances, a close network should be used. In particular areas, where the elevations of the watertable or piezometric surface changes rapidly, a fine nodal spacing is required to model accurately the watertable's parabolic curvature.

Areas that are not well documented and have limited available data must be represented by intuitive estimates of the required parameters. If they cannot be designated in any detail, or indicate no rapid variation, a coarse grid is permissible until more information becomes available.

The desired accuracy and detail of the analysis must also be considered. Initial models, based on a coarse grid, can be used to test the overall response of the system with the minimum amount of calculation. However, if the grid is made too coarse, the finite difference approximations may be invalidated and the desired accuracy lost. Therefore, after initial test runs, it is necessary to construct a finer mesh if a more detailed analysis and a higher degree of accuracy is required. However, the fineness of the mesh is limited by the storage capacity and speed of the computer. Consequently, a balance must be maintained between the computational costs and the degree of accuracy and detail required.

The grid network should be constructed so that individual nodes are sited on hydrogeological phenomena that are involved in the groundwater

regime, for example rivers and lakes; these behave as constant head devices when they are in hydraulic continuity with the regional watertable.

Finally, where the extent of the study area is limited by the availability of data and no natural hydrogeological boundary exists, artificial boundaries have to be constructed. The nodal network should therefore allow for boundary nodes in order that the correct flow conditions are simulated across these boundaries.

From the foregoing discussion it is apparent that a versatile grid is required, that is one which allows close and wide spacing of nodes. Rectangular and square grids have the disadvantage that close spacing, in any one area, must extend along the co-ordinate directions to the model boundaries. As a result a high density nodal distribution is constructed in areas which do not warrant it. This becomes more exaggerated when several high density distributions are required and, as such, it is wasteful on computer storage and computation time. The method derived by Weber and Tyson (1963) allows for variability in the spacing of the nodes without this restriction. The only obvious disadvantage in the polygonal network is that it takes longer to construct than the more regularly shaped variety. This is outweighed, however, by its versatility and reduced costs during computation.

The lack of readily available information, particularly in respect to aquifer characteristic determinations and groundwater recharge estimates, necessitated the development of a coarsely gridded model to assist in the calibration procedure. From initial determinations of the required hydrogeological parameters, a fairly uniform spatial variation was found to exist. The grid network was also spaced uniformly with approximately an eight kilometer spacing. This resulted in eighteen internal nodes to monitor the aquifer behaviour, and eighteen external nodes to simulate the boundary flows.

After a comprehensive understanding of the groundwater regime had been

obtained from a detailed hydrogeological survey and the coarse model, a finer grid was prepared.

Successful simulations using the coarse model inferred that the finite difference approximations had been adhered to, and therefore the size of the finite difference grid was limited, ultimately, by the capacity and speed of the computer. The resulting model involved a hundred and forty five nodes of which a hundred and three were distributed internally to simulate the behaviour of the aquifer. A uniform variation of aquifer characteristics, and a smooth areal variation in the watertable over the unconfined aquifer, permitted an even distribution of nodes at approximately two kilometer intervals. The resulting uniform network was interrupted by nodes positioned on watercourses that were assumed in hydraulic continuity with the aquifer. Information regarding the aquifers characteristics under the Keuper Marl and Lower Keuper Sandstone Formations was not forthcoming in any detail and therefore a fine mesh grid was not required for the input or output of data. However, a substantial variation in the storage coefficients occurs across the unconfined/confined boundary, and significant seasonal water level fluctuations are recorded. The two kilometer grid was therefore extended across the unconfined/confined boundary and the confined area. The model occupied approximately thirty two thousand words of store and was able to compile satisfactorily without any additional storage requests. Consequently, the 'turn round' for results was not restricted.

Discretisation of Time: The effect of dividing time into discrete intervals is more complex and less well understood than the discretisation of space. However, the factors that are relevant to the discretisation of space apply here also. Where large temporal fluctuations in water levels occur, and are required to be monitored, small time steps are used. However this process can be very demanding on computational time and therefore an optimum time step must be used.

A recent critical review (Rushton 1973) on the response of digital water level simulations in the vicinity of pumped wells indicates that erroneous results occur when the time steps used are too large. This phenomenon occurs when there are large fluctuations in the discharge rates, that is when the wells are shut down or started up. There appears to be a satisfactory convergence towards the solution, yet the resultant water levels either oscillate or appear as smooth curves, but do not compare favourably with historical Theis drawdown curves. This problem was not encountered in the aquifer under study during the calibration period (1969 - 1970) because abstraction rates were fairly constant when averaged over each time increment. Also the eight kilometer network spacing was not fine enough to register marked water level fluctuations due to individual pumped wells. As a result, water level fluctuations at the majority of internal nodes were in response to natural variations in the groundwater regime. The optimum time step was selected by a trial and error process, and initial investigations commenced with a two week time step. This was systematically reduced during subsequent runs and, when a value of one week was utilised, convergence towards the solution was satisfactory. A comparative study using smaller time steps indicated that for the total calibration period a time step of three to four days utilised the least number of iterations. As such, it was considered to be the optimum time step.

A similar procedure was conducted on the finer meshed model and the optimum time step was evaluated to be between three and seven days. It was necessary, however, to consider the effect of new wells which commenced pumping during the study period 1960 to 1972. It has been proposed that, for successful simulation of the drawdown curves around wells, the necessary time step is formulated from;

$$\frac{dt\,T}{dx^2 S} < 0.1 \qquad (3.25)$$

(Rushton 1973)

where dt = time step;

dx = mesh spacing = 2 km;

T = transmissibility;

S = storage coefficient.

It was necessary, therefore, to consider the unconfined areas where the majority of abstraction wells occur. Since the transmissibility and storage coefficient are in the order of 300 m^2/d and 0.03 respectively, dt is approximately 40 days.

For wells situated on the unconfined/confined boundary T is of the order of 200 m^2/d and S in the range 0.012 to 0.003; as a result dt must be between 6 and 24 days.

It was apparent from equation (3.25) that the estimated optimum time step of 3 to 4 days was adequate to monitor any drawdown effects satisfactorily.

Initial Starting Conditions: Before proceeding with the analysis of results from a digital model it is essential to overcome the initial starting conditions. Problems arise in groundwater digital models because initial water levels are invariably incompatible with the proposed aquifer characteristic distribution. Although the water levels are derived from direct field observations, aquifer characteristic determinations are not usually associated with the same degree of precision, or frequency, in their spatial distribution. Consequently, the groundwater system is not in dynamic equilibrium initially and the resulting water level predictions are not a true reflection of the aquifer's response to its inputs and outputs.

Dynamic equilibrium is attained in electrical analogue models by re-cycling a period of recharge until successive cyclic responses in water levels are identical (Rushton and Wedderburn 1973). This is an expensive computational procedure when conducted on digital models, particularly if the necessary recycling time period is several tens of years. Therefore, to minimise computational costs the procedure was conducted on the coarse model

and interpolated to the finer mesh as required.

Initial water levels for the calibration period were derived by recycling an average year's recharge evaluated from the period 1960 to 1972. Initial water levels for the dynamic equilibrium run were derived from average water level conditions (Fig. 30). These conditions were assumed to represent a steady state within the aquifer and the period required to attain equilibrium was estimated from:

$$\frac{t\,T}{L^2 S} > 1.0 \qquad (3.26)$$

(Rushton and Wedderburn 1973)

where T = transmissibility;

S = storage coefficient;

L = length of maximum flow path;

t = time period.

If average aquifer characteristics are assumed in the order of T = 250 m^2/d, S = 0.01 and L = 15 km, t is approximately 24 years. In practice, predicted water levels attained dynamic equilibrium after a period of 15 to 18 years at all nodes.

A similar procedure was conducted before commencing the run on the study period 1960 to 1972. It was necessary to recycle an average year's recharge for a similar period before initialising the simulation period from 1960 to 1972.

Introducing Non-Linearity: Temporal variations in transmissibilities occur in unconfined aquifers because of changes in their saturated thickness. Thus, the governing groundwater equation is non-linear and the transmissibilities require to be updated according to fluctuations of the watertable.

Initial simulations on the coarse model assumed constant transmissibilities because variations in the saturated thickness were small compared with the total saturated thickness. However, to ensure a reduction in all possible errors, subsequent simulations, including those with the fine model, were conducted with permeabilities. Transmissibilities were subsequently re-

evaluated after each time interval according to the predicted saturated thicknesses.

Further non-linear conditions are imposed when the top level of the aquifer is intersected by the watertable. Where the aquifer is confined or semi-confined at the surface, it is necessary to monitor temporal variations in the storage capacity. This is implemented by introducing into the computations the appropriate storage coefficient. Where the aquifer is unconfined at the surface it is necessary to simulate the occurrence of surface flows. Therefore, if the watertable is predicted to be above ground level, the excess water is designated as spring or baseflow and the water-table is set to ground level.

The position of the watertable with respect to the aquifer's geometry is therefore important and, because each condition imposes unique and separate effects, they have to be tested for during each time interval.

The Computerised Digital Model

The digital model considered is based upon Chidley (1971) and Goodwill (1971). The model is programmed with thirteen subroutines, four of which are involved with the reading-in and transformation of the input data. The majority of the arithmetic computations involved in the iterative procedure are restricted to one subroutine and a check on the compatibility of the computed heads in relation to the aquifer's geometry is assessed separately. The vast quantity of results, required to check the models progress and for use in later computations, are reorganised in four subroutines. They utilise "scratch files" as temporary storage facilities and the line-printer as a visual display. The final output of results is controlled by three subroutines whose purpose is to depict the computed and historical water levels in graphical form.

A resumé of the procedures involved in each segment follows:

Master Segment; This segment creates the necessary array storage

facilities and initialises the required input and output peripheral devices and five scratch files for data storage. It is responsible for calling the main subroutines that are involved in the input of data, the iterative procedure and the output of results, that is, subroutines KRGW3, KRGWM and KRGWP respectively. After a successful run, control is returned to this segment and the computations terminated.

Subroutine KRGW3: Most of the data required to simulate the aquifer's behaviour over the test period are read in by this subroutine. A resumé of the data and their subsequent use follows:

Headings: In order to improve the appearance of the output display for subsequent filing purposes, a heading is printed out on each page of results. Data used for this purpose include:

(a) a run number;

(b) the simulation period;

(c) a description of the aquifer under study.

Time steps: Three groups have to be considered. They are related to the availability of the input data, the optimum iterative time step and the required output time interval. The individual time steps are controlled by:

(a) the availability of the recharge data;

(b) the availability of the boundary head data;

(c) the optimum iterative time step;

(d) the required time interval between the printing out of each water balance summary.

(This was set such that a monthly water budget analysis was performed and output format statements could be standardised to prevent any confusion in the interpretation of results).

The program was therefore designed with a unit time interval of one month and all the time steps are evaluated in terms of this. Finally, it

is necessary to determine the date of the commencement of the run and the time period, in months, of the simulation period.

Aquifer Geometry: The characteristics of the aquifer's geometry are described by reference to a series of nodes. Each node is associated with a discrete element and the characteristics chosen for it are assumed representative of that element. Each element is related to its immediate neighbours so that a three dimensional representation of the aquifer is formed and the model boundaries delineated. The following data are therefore required:

(a) the number of internal and external (boundary) nodes;

(b) an array to relate each node to its neighbour;

(c) the distance between each node and the width of the groundwater flow path between them;

(d) the elevation of the land surface;

(e) the elevation of the top and base levels of the aquifer;

(f) the position of any boundary that separates horizons of different storage capacities.

Aquifer Characteristics: Variations in the aquifer characteristics are related to the network of internal nodes. The data include:

(a) an assessment of the storage coefficient(s) at each node;

(b) an assessment of the permeability and/or transmissibility between each node.

Hydrogeological Parameters: These parameters are related to:

(a) the initial water level at each internal node;

(b) the type of aquifer represented at each internal node, for example confined or unconfined (See KRGW1);

(c) the type of model boundary between the internal nodes and external nodes surrounding the study area (See KRGW6);

(d) the minimum acceptable computed water level at each node (See KRGW1).

Aquifer Recharge: The data are prepared in equal time increments for the complete study period. It is assessed for each node as either a net value or as four separate components. The former method is utilised initially to test the response of the model and to evaluate the magnitude of the recharge component. Subsequently as more data become available the four component method is utilised.

Typically it is represented by:

(a) the effective precipitation component;

(b) the surface runoff component;

(c) the effluent discharge component;

(d) the artificial abstraction component.

The one component method is re-considered when a more precise determination of the net recharge is forthcoming from watershed modelling evaluations.

In order to minimise the amount of data preparation, each recharge component is associated with a conversion factor. A master conversion factor is also utilised specifically for metrication purposes.

Control Parameters for the Iterative Procedure: The parameters include:

(a) the relaxation coefficient;

(b) the tolerance factor per node and for the total model.

Arithmetic computations within this subroutine involve the transformation of the input data into a format suitable for the iterative procedure. Consequently, most of the data arrays are initialised and, in order to ensure easy access in subsequent subroutines, some are stored on scratch files.

A considerable amount of input data are required for the model and therefore consistency and compatibility checks are conducted wherever possible within the subroutine. Appropriate error messages are displayed when necessary and the run subsequently terminated to allow corrections to be made. Otherwise, a summary of the data is sent to the line-printer for cross checking with historical records.

Finally, before the iterative procedure is made operative the total surface area of the model is computed and displayed via the line-printer.

Subroutine KRGWM: The procedures involved in the formation of the backward difference equations and their solution by the Gauss-Siedel relaxation technique are incorporated in this subroutine. Their theoretical background has been discussed and therefore it suffices to present a summary of the algorithm used (Appendix 3).

In order to differentiate between a dynamic equilibrium run and a historical simulation run a master control parameter is utilised. If the former procedure is required, recharge data are recycled by rewinding the scratch file upon which it is stored. Otherwise data are abstracted from the file in chronological order.

Strategically placed optional output statements allow the convergence rate of the solution to be analysed in detail. This is particularly useful during initial runs when the model variation in residuals is not known.

Non-linear effects result from temporal variations in the saturated thickness and in the operative storage coefficient; as a result they are updated when necessary after each iterative loop. A check on surface flows and water levels approaching the base of the aquifer is maintained at the end of each time increment by calling subroutine KRGW1.

Boundary conditions are updated at the end of each unit time interval by reference to subroutine KRGW6.

After a series of test runs it was apparent that no more than twenty iterations per time increment were required if the solution was converging satisfactorily. Therefore, an upper limit was set and used as a method of terminating an apparently unsuccessful run.

An optional procedure is incorporated in this subroutine to print out the computed water levels at the end of each time increment. Although the results may be on too fine a time scale to compare with historical records, they permit

the progress of the run to be monitored and, in particular, badly responding nodes to be investigated.

A nodal water budget summary is maintained after each time increment until the end of a time interval is reached. A net water balance summary is then formulated in subroutine KRGW5 before control is returned to the iterative routine. At the end of the simulation period, program control is transferred to subroutines KRGWP, KRGWG and HPLOT and the results reorganised for output.

Subroutine KRGW6: Boundary flow conditions are updated at the end of each unit time interval by reference to either historically recorded heads or hydraulic gradients. During initial calibration runs it is not certain how the model will respond and therefore what predicted water levels will occur. It is probable that historical boundary heads will be incompatible with the predicted heads. In order to minimise this effect, historical boundary flow configurations are simulated as closely as possible. This is achieved by updating the heads of the boundary nodes such that the required hydraulic gradients are maintained between them and the predicted internal water levels. After reasonable water level responses are obtained at the internal nodes, boundary conditions are represented by historical heads to improve the simulation.

Subroutine KRGW1: During each time increment it is necessary to check that the predicted water levels are compatible with the geometry of the aquifer. If they are approaching the base of the aquifer appropriate action is taken to maintain them above it. Abstraction rates are systematically reduced and if this is not sufficient they are stopped altogether. Any further lowering of water levels causes termination of the run.

Historical water level fluctuations indicate that the base of the aquifer is well below the lowest attained level. As such, this fact is used as a control on the progress of the simulation procedure. When un-

realistically low levels are attained, appropriate outputs are displayed on the line-printer in order that the problem may be rectified during subsequent runs.

After a successful convergence a check is conducted on all the unconfined nodes to locate water levels predicted to be above ground level. Those found are reset to ground level and their associated relaxation coefficients are set to zero. Consequently, when a water balance is re-evaluated the appropriate water levels are not adjusted and their residuals are designated as surface flow. If the solution is still not acceptable the iterative procedure is repeated using the same constraints. If, at anytime during the proceeding time increments the residuals at the constrained nodes become negative the relaxation coefficients are reinstated and the water levels predicted as normal.

Subroutine KRGW5: This subroutine is used to formulate a monthly water budget summary for the model, from the nodal water balances achieved at the end of each time increment. The information includes the historical groundwater recharge and predicted surface flow components, and an overall evaluation of the change in groundwater storage and the net groundwater flow component. This information is systematically stored on scratch files together with the predicted water levels, ready for use in subroutine KRGWP.

Subroutine KRGW2: This optional output subroutine is used to print out the predicted water levels at the end of each time increment. It is particularly useful during initial calibration procedures when details of the water level responses are required.

Subroutine KRGWP: During initial test runs in particular, substantial volumes of output are required to study the progress of the simulation routine. Indeed, during the study of a 100 node model the volume of results necessitates the development of methodical output routines. Particular emphasis is made on the use of tables, graphs and contouring routines.

This subroutine reads the information from the appropriate scratch file and transforms it into a suitable format for output. Water balance summaries are tabulated with suitable headings and displayed via the line-printer. Water level results are rearranged, node by node, for the graphic display and, in preparation for a contour plotting routine, water level readings at a number of predetermined times are stored on a direct access file.

Subroutine KRGWG: A simple plotting routine is incorporated within the program to assist in the comparison of historical and predicted water levels during the calibration period. A high degree of precision is not required in the plotting and therefore the line-printer is employed. The overall computation time and cost is reduced because the graph plotter is not used nor required on standby.

Historical water levels are read from the data input device and with the appropriate predicted water levels are arranged in nodal order. The plotting routine is implemented by addressing the following subroutines for each node in turn.

(a) Subroutine HPLOT: This subroutine determines the maximum and minimum water levels in the plot. Subsequently, the most suitable scaling factor is evaluated (see subroutine HEADG) and the position of the points to be plotted is ascertained.

(b) Subroutine HEADG: A number of scaling factors are available for use, each taking maximum advantage of the width of the line-printer paper. The most suitable one is chosen and printed out along with the abscissa.

(c) Subroutine PRINT: In order to differentiate between historical and predicted water levels the appropriate symbol is selected in this subroutine. If the water level fluctuations are exceptionally large and outside the maximum available scale, the symbols A and B are used for those occurring above and below, respectively. When the appropriate symbols have been chosen they are printed out along with the ordinate.

At the end of the plotting routine control is returned to the master segment and the run is terminated (Appendix 4).

CHAPTER FOUR

AQUIFER CHARACTERISTIC DETERMINATIONS BY PUMP TEST ANALYSES

Introduction

In order to determine the dynamic behaviour of groundwater flow in an aquifer it is necessary to assess the hydraulic characteristics of the water bearing strata. Although laboratory determinations are an aid to the understanding of the fundamentals of the system, the resultant characteristics may not be representative of the aquifer as a whole. Particularly in fissured rocks, the dominant means of flow and storage are not considered. Similar disadvantages occur when aquifer characteristics are evaluated from well logs.

Pump test analyses are one of the most important techniques developed for determining the hydraulic characteristics of aquifers. In general their results are representative of a larger area than those of a single point observation. In addition they test the strata in their natural hydrogeological environment and overcome the problem of 'disturbed' samples which are encountered in laboratory analyses. The long term effect of groundwater abstraction can be monitored and the observations used to detect hydraulic boundaries, leakage from contiguous strata and changes in the aquifer characteristics.

Theoretical Considerations

Introduction

The first formula used to determine the transmissibility of water bearing strata in the vicinity of a pumped well was developed by Thiem (1906). Thiem's equilibrium equation was the only means of analysing drawdown data until the development of studies relating to unsteady state flow by Theis (1935). Since the derivation of the unsteady state equation it has been possible to determine both the transmissibility and storage coefficient of aquifer systems. The method analyses the development of the cone of depression with respect to

time from the commencement of pumping and distance from the pumped well. As such it overcomes the severe restriction of steady state conditions imposed by the Thiem equation. However, both analyses are restricted to pump tests for relatively simple aquifer conditions, as indicated by the following general assumptions:

(a) the aquifer behaves as if it is infinite in areal extent;

(b) over the area influenced by the test no hydraulic boundaries or other discontinuities exist;

(c) the aquifer is of uniform thickness;

(d) prior to pumping, the piezometric surface is nearly horizontal over the area influenced by the test;

(e) discharge is conducted at a constant rate;

(f) the pumped well fully penetrates the aquifer and horizontal flow predominates.

During the last few decades, new and refined methods of pump test analyses have been made possible by progress in the mathematical analysis and simulation of groundwater flow problems. Consequently, some of the restrictions imposed by the above assumptions have been relaxed and a wider variety of aquifer-well configurations can now be analysed. A resumé of the techniques utilised in the evaluation of the characteristics of the study area follows.

Steady State Flow in Confined and Unconfined Aquifers

The water table or piezometric surface in the vicinity of a pumped well is shaped as an inverted cone whose apex is centred on the well. The configuration of a typical confined aquifer-well system during a pump test is shown below.

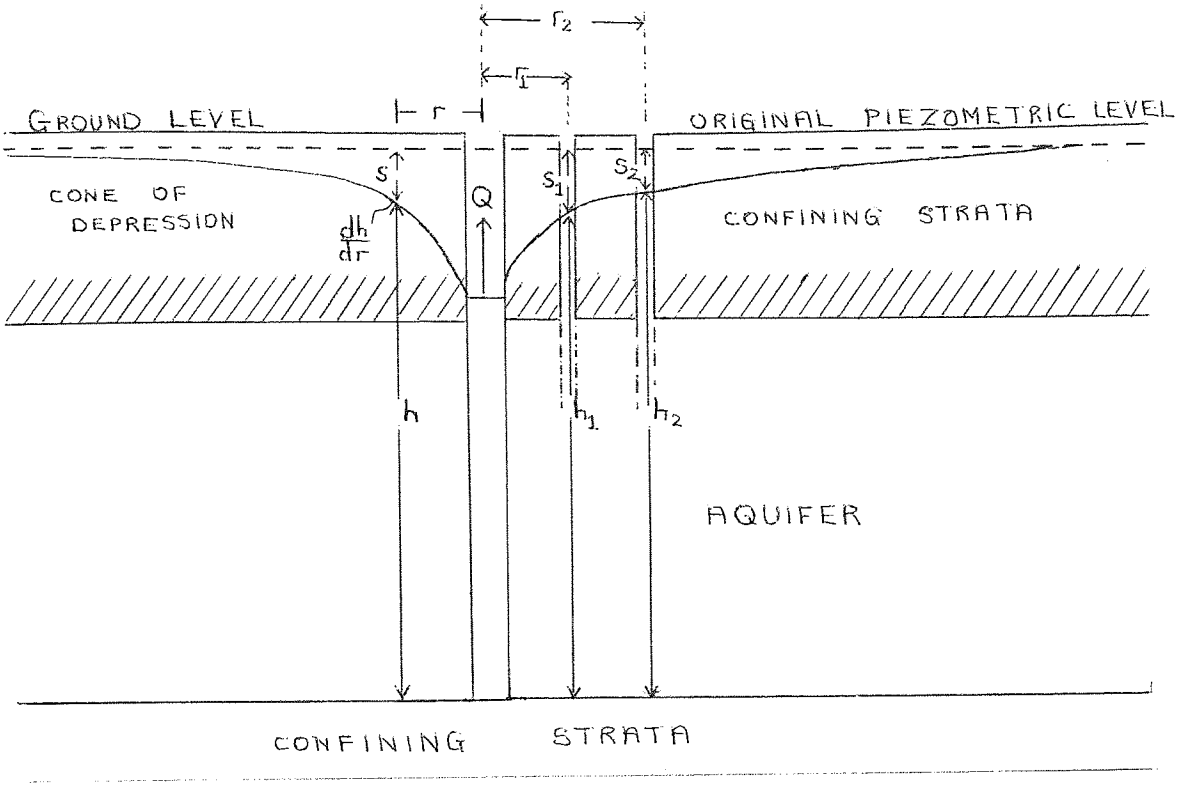

The shape of the cone of depression and hence the elevation of the piezometric surface at any distance r can be predicted from Darcy's Law. The equation for the quantity of water, Q, moving towards the discharge well at any radius, r, is:

$$Q = 2\pi r\, DK \frac{dh}{dr} \qquad (4.1)$$

where K is the permeability of the aquifer.

Integrating and rearranging equation (4.1) results in:

$$KD = \frac{Q \ln \frac{(r2)}{(r1)}}{2\pi (h2-h1)} \qquad (4.2)$$

This is more conveniently expressed as:

$$KD = \frac{Q \ln \frac{(r2)}{(r1)}}{2\pi (s1-s2)} \qquad (4.3)$$

Equation (4.2) was developed originally by Thiem (1906) and is generally known as the equilibrium or Thiem equation. Before it can be applied successfully additional assumptions to those already stipulated have to be satisfied. They are:

(a) the aquifer is confined;

(b) groundwater flow to the well is in a steady state, that is, the

drawdown with respect to time in the observation wells is negligible;

(c) water is derived only from the aquifer under test.

Methods for analysing steady state conditions in unconfined aquifers are based on Dupuit (1863). In order to arrive at a solution for the resulting differential equation which describes the motion of flow it is necessary to assume that:

(a) the velocity of flow is proportional to the tangent of the hydraulic gradient;

(b) flow is horizontal and uniform everywhere in a vertical section through the axis of the well.

In addition the saturated aquifer thickness does not remain constant, and at any distance, r, from the well is equal to D-s where:

D = the original saturated thickness;

s = the drawdown.

The modified Thiem equation for unconfined flow is therefore:

$$KD = \frac{Q \ln \frac{r2}{r1}}{2\pi(s1 - s2)} \qquad (4.4)$$

where

$$s = s - s^2/2D \qquad (4.5)$$

The expression (4.4) is similar to (4.3) and is known as Thiem - Dupuit's equation (Thiem 1906). Limitations to its use are identical to those of the confined aquifer analysis. Consequently, if the drawdown in relation to the saturated thickness is significant the assumption that the thickness of the aquifer is constant is invalidated. In addition the analysis is always associated with equation (4.5), the corrected drawdown equation.

Unsteady State Flow in Confined and Unconfined Aquifers

The first analysis to introduce the storage coefficient of the water bearing strata into the evaluation of pump test data was developed by Theis (1935). The resultant unsteady state formula was conceived from observations of the decline in head of confined aquifers pumped at a steady rate. The

decline in head multiplied by the storage coefficient, summed over the area of influence was found to be equivalent to the discharge measured at the abstraction well. If the water is derived only from the aquifer then a constant change in storage occurs; consequently, no steady state condition can ever exist in theory. In practice the cone of depression expands continuously and the rate of decline in head decreases.

The formula used to simulate the movement of groundwater during unsteady state conditions was derived from the analogy between heat flow in the vicinity of sinks and groundwater flow in the vicinity of pumped wells. The resulting equation is known as the Theis or nonequilibrium equation and is defined as:

$$s = \frac{Q}{4\pi KD} \int_{u}^{\infty} \frac{e^{-u}}{u} \, du \qquad (4.6)$$

It is also written as:

$$s = \frac{Q}{4\pi KD} W(u) \qquad (4.7)$$

where $$u = \frac{r^2 S}{4KDt}; \qquad (4.8)$$

S = storage coefficient;

t = time since pumping started;

$$W(u) = 0.5772 - \ln u - \frac{u^2}{2.2!} + \frac{u^3}{3.3!} - \frac{u^4}{4.4!} + \ldots\ldots \frac{u^N}{N.N!}$$

The exponential integral is the Theis well function.

In addition to the general limiting assumptions, equation (4.6) can only be utilised if:

(a) the aquifer is confined;

(b) flow to the well is in an unsteady state;

(c) the water removed from storage is discharged instantaneously with decline in head and is only derived from the aquifer under test;

(d) the diameter of the well is small enough for the storage

in the well to be neglected.

Jacob (1963) showed that the Theis equation can be adjusted to allow for dewatering in unconfined aquifers. In order to compensate for the decrease in transmissibility it is necessary to adjust the observed drawdowns such that,

$$s_1 = s - \frac{s^2}{2D} \qquad (4.9)$$

where

s_1 = the corrected drawdown.

This is identical to the correction applied in the Theim - Dupuit equation. Since the saturated thickness in unconfined aquifers is subject to variation during pump tests the observed drawdowns must always be corrected according to equation (4.9).

Similar assumptions to those applicable to the Theis equation are operative; the only necessary amendment is that the aquifer is unconfined.

The limitations imposed by the equilibrium and non-equilibrium equations are seldom satisfied in nature. Methods have been developed to analyse pump test data which have been compiled from more general well-aquifer systems. Derivation of some of the more popular methods utilised in the pump test analyses programme are outlined below.

Steady State and Unsteady State Flow in Semi-Confined Aquifers

De Glee (1930 and 1951) developed the theory for steady state flow in confined aquifers which are affected by leakage from overlying semi-pervious strata. As the piezometric head is lowered a vertical flow of water from the overlying strata moves towards the pumped aquifer. The volume involved is calculated from;

$$q = \frac{hw - hp}{c}$$

where q = the volume of water moving through the semi-pervious strata;

hw, hp = the height of the water table and the piezometric head respectively;

c = the hydraulic resistance of the saturated semi-pervious layer.

The formula which predicts the steady state drawdown, sm, at a distance, r, from the pumped well is:

$$sm = \frac{Q}{2\pi KD} \; Ko \; (\frac{r}{L}) \qquad (4.11)$$

where

Ko = modified Bessel Function of the 2nd kind and of zero order;

L = $\sqrt{KDc}$ (leakage factor);

c = D^1/K^1;

D^1 = the thickness of the saturated part of the semi-pervious strata;

K^1 = the hydraulic conductivity of the semi-pervious strata.

The assumption that the water is derived only from the pumped aquifer is relaxed and leakage from the overlying strata is permissible; otherwise similar restrictions to those imposed on the flow in confined aquifers exist. In relation to the semi-pervious strata two assumptions apply:

(a) the water table surface remains virtually constant therefore the leakage is proportional to the drawdown of the piezometric surface.

(b) The leakage factor is greater than three times the thickness of the aquifer.

For unsteady state flow Hantush and Jacob (1955) incorporated the effect of leakage into the Theis well function. The equation is therefore analogous to the Theis equation and is written symbolically as:

$$s = \frac{Q}{4\pi KD} \; W \; (u, \; r/L) \qquad (4.12)$$

The conditions restricting its application are similar to those associated with the Theis equation except that leakage is permitted from the overlying strata.

Unsteady State Flow in Semi-Unconfined Aquifers

Boulton (1963) introduced a method for the analysis of semi-unconfined aquifers, that is, unconfined aquifers which exhibit delayed yield due to slow gravity drainage. The resulting flow equation is usually expressed as:

$$s = \frac{Q}{4\pi KD} W(u_B, r/_B) \qquad (4.13)$$

where

$W(u_B, r/_B)$ = the well function of Boulton;

B = the leakage factor, L.

This is comparable with the equation derived by Hantush and Jacob (1955) and similar conditions must be satisfied before its application.

Image Well Theory

Image well theory is used in the analysis of aquifers limited by one or more boundaries. The types of boundaries considered are impermeable (barrier) and permeable (recharge) boundaries. The latter are represented by lakes, streams and rivers which are in hydraulic continuity with the groundwater system.

By assuming an imaginary well exists at an equal and opposite distance from the boundary as a real well, an aquifer of limited areal extent is transformed into one of apparent infinite extent. Although in the final analysis a multiple well system exists the net drawdown can be determined by the principle of superimposition.

The method developed by Stallman (Ferris et al. 1972) analyses unsteady state pumping test data from confined and unconfined aquifers which are influenced by one or more boundaries. If the distances between the piezometer and the real and imaginary well are r_r and r_i respectively, equation (4.8) can be written as:

$$ur = \frac{r_r^2 S}{4\,KDt}$$

and $$ui = \frac{r_i^2 S}{4KDt}$$

If $\beta = \frac{r_i}{r_r}$ equation (4.12) becomes:

$$s = \frac{Q}{4\pi KD} \quad W(ur) \pm W(\beta^2, ur) \pm \ldots\ldots W(\beta^2 n, ur)$$

where n = number of boundaries;

\+ = discharge well;

\- = recharge well.

The limiting conditions are similar to those for unsteady state flow in confined and unconfined aquifers. Additional assumptions apply to the configuration of the boundaries. They are:

(a) the aquifer is crossed by one or more straight fully penetrating boundaries which influence the development of the cone of depression;

(b) recharge boundaries have constant heads and their contacts with the aquifer are as permeable as the aquifer.

Variable Discharge Rates

Aquifers are sometimes pumped at variable discharge rates to test the response of the system and to determine the maximum yield. Cooper and Jacob (1946) developed a technique which utilises drawdown data from a system which is pumped in a step-wise fashion. The observed drawdown data have to be adjusted; this involves evaluating the times and distances at which the drawdown would have occurred if abstraction had been constant throughout the test at the rate when the observations were taken. If the drawdown is replaced by the specific drawdown, s/Q, the data can then be used in standard methods for analysing unsteady state flow in confined and unconfined aquifers. Consequently, the limiting assumptions to the use of the Cooper-Jacob method

are dependent upon these methods. The only exception is that the discharge is not at a constant rate.

Non-fully Penetrating Wells

It is sometimes necessary to analyse observations in the vicinity of a partially penetrating discharge well. However, within a radius r<2D around the pumped well the flowlines have a substantial vertical component, Anonymous (1964). Consequently drawdown data from wells sited within this prescribed area have to be corrected. Correction methods are available for most well-aquifer configurations (Hantush 1962 a, b and 1964 and Jacob 1963b).

Conclusion

With the development of sophisticated techniques for determining the geometry and lithological variations of water bearing strata, it has become apparent that the limiting assumptions inherent in the Thiem and Theis analyses are very rarely adhered to. In addition it is not always possible to conduct tests under the required conditions. Consequently, pump test analyse that are applicable to a wide variety of aquifer types and discharge configurations have been developed in recent years.

Evaluation of Aquifer Characteristics of the Permo-Triassic Aquifer from Pump Test Data

Introduction

In ideal circumstances the construction of pump test facilities and the supervision of tests are arranged to ensure that the limiting assumptions, previously described, are adhered to. However, the cost of construction of adequate boreholes and piezometers in the thick sandstone of the Permo-Triassic aquifer, and the time involved in conducting tests, prevented this approach from being fully implemented.

Availability of Data

In order to determine the aquifer's characteristics it was necessary to

analyse drawdown data which had been compiled by the River Authorities and the Water Boards. Additional analyses were conducted on information gained from tests performed in pumping stations where automatic water level recorders were available. The only available pump test data were therefore obtained from observation wells in the vicinity of the main public supply boreholes (Fig.32). Preliminary tests on most sites commenced with a trial borehole which was pumped to ascertain the quality and quantity of the source. In the majority of cases tests proved satisfactory and the main supply boreholes were constructed nearby. Pump tests were subsequently conducted and observation boreholes and disused wells in the vicinity were monitored. In particular, observations were maintained on privately owned wells in case their supplies were adversely affected. This often involved monitoring wells three or four kilometres from the test site. Tests usually lasted for several days by which time the rate of drawdown in the observation wells was negligible. The resultant drawdown data from these tests have been used in unsteady state analyses to determine the storage coefficient and transmissibility of the aquifer.

The development of a source of supply at each station has been implemented by construction of two or more production boreholes. In general abstraction from each station is constant and between 5000 and 15000 cu.m/d. Abstraction is continuous for long periods which are often in the order of several weeks and the supply is usually maintained from one borehole while the others are rested. Consequently, steady state conditions are attained in the vicinity of the pumping stations which enable a steady state method of analysis to be conducted on drawdowns measured in the observation boreholes.

Breakdowns and other unforeseen stoppages at the stations have allowed the water levels to recover. In most instances the cone of depression recovers by 90% in approximately 12 to 72 hours and therefore a stoppage of

a few days allows rest levels to be attained. The resultant water level trace, as recorded from the commencement of pumping, enables the Theis recovery method of analysis to be utilised. When pumping restarts the development of the cone of depression is depicted by water level hydrographs recorded in the vicinity and unsteady state methods are used to analyse the data.

Some production wells were pumped from rest in a step-wise fashion in order to assess the maximum yield and the characteristics of the pump. In circumstances where the resulting drawdown data were sufficiently detailed it was possible to use the Cooper-Jacob step-type pumping method of analysis.

The stations, Tom Hill and Stableford, are used to augment supplies when demand is high. They are therefore pumped intermittently and a succession of drawdown and recovery hydrographs are available.

Development of the groundwater resources in the vicinity of Roughton commenced with pump tests designed specifically to determine the aquifer's characteristics. Indeed this has been the only pump test on the study area designed specifically for this purpose.

Borehole Statistics

Although most abstraction wells are several hundreds of metres in depth not all of them completely penetrate the main aquifer. The base of the aquifer is represented by a transition zone consisting of soft red sandstone, well cemented sandstone and mudstone, some tens of metres in thickness. Consequently, the base of the main water bearing strata cannot be determined precisely. However, at most localities the associated well logs infer that either the base had been reached or that over 70% of the estimated aquifer thickness had been penetrated. Corrections to the drawdown data have been applied where over 30% of the aquifer thickness is unpenetrated.

The top 20 to 30 m of most production wells are cased off to prevent unconsolidated glacial sands and clays from encroaching into the borehole.

In addition it prevents surface pollutants that readily infiltrate into glacial sands and gravels from contaminating the source. Slotted tubes are utilised along the length of the intake portion of the well. In some old boreholes no screening below the top lining is evident, yet they all appear to be intact.

Additional lining is utilised where running sand and loose conglomerate are encountered. On the whole the lengths involved are small and less than 3m per 100m of lining. In general, therefore, the entire length of the borehole, below the top lining, contributes to the yield of the production wells.

Aquifer Types

Several different aquifer types can be distinquished within the groundwater flow system of the Permo-Triassic aquifer. Where the Lower Mottled Sandstone, Bunter Pebble Bed and Upper Mottled Sandstone Formations crop out or are overlain by superficial sands and gravels, unconfined conditions predominate. The majority of pump tests are associated with unconfined conditions which occur in the vicinity of the pumping stations along the River Worfe and Smestow Brook valleys (Fig. 32). It is apparent from groundwater level observations and surface runoff hydrographs in the Severn catchment that the aquifer is in hydraulic continuity with the surface waters and contributes substantially to their total runoff. It was therefore assumed that lowering the water table in the proximity of the streams and rivers would induce recharge to the groundwater system. This effect however was detected only at Neachley (Fig.46). At the remaining stations no obvious deviation from the Cooper-Jacob (1946) straight line method was depicted and no inflection point was apparent during the analyses of the drawdown data. In part this was due to tests of insufficient length for any significant drawdown to occur in the vicinity of the surface waters. At Cosford however, the pumping station is situated only a few metres from the River Worfe and, although the radius

of influence extends for several kilometres, the only noticeable effect upon the surface water has been the drying up of a few springs in the immediate vicinity. It is assumed, therefore, that the hydraulic conductivity between the river and the aquifer is small, and the apparent baseflow contribution to the river is from seepages situated above river level. The former deduction is substantiated by the occurrence of substantial thicknesses of glacial deposits in the infilled valleys. Where they are characterised by laminated clays and boulder clay the bed of the river is effectively sealed.

Although the formations which constitute the unconfined aquifer vary considerably in grain size and are characterised by current bedding, delayed yield phenomena were not detected in the available drawdown data. Delayed yield was expected, particularly in the Upper Mottled Sandstone Formation which is associated with intercalated fine grained laminated sandstones.

In general the unconfined aquifer behaves uniformly over wide areas, and although deviations from the type drawdown curve are depicted, they are not indicative of delayed yield or gravity drainage and are within experimental error.

Towards the centre of the South Staffordshire syncline the main aquifer is overlain by the Lower Keuper Sandstone Formation. At the base of the formation the Basement Beds are in hydraulic continuity with the main aquifer and laboratory tests indicate that their sandstone is characterised by similar hydraulic properties to that of the main aquifer. The inclusion of cemented sandstone and mudstone in the Buildingstone and Waterstone Groups give rise to semi-confined conditions particularly in the vicinity of the unconfined/confined boundary near Newport and Stafford. The only pump test conducted in this vicinity was at Gnosall, although it did not yield sufficient data for a semi-confined method of analysis because no leakage was detected during the test. This is assumed to be directly associated with horizontally bedded mudstone in the surrounding strata restricting vertical flow from the

semi-pervious horizon.

No pump test data are available from the central confined area which is overlain by the Keuper Marl Formation. Substantial thicknesses of the confining strata and the Lower Keuper Sandstone Formation have to be penetrated before the main aquifer is encountered. This has been an important limiting factor to the testing and development of the main aquifer in this region.

Conclusion

Although the quality of the pump test data was in some instances not ideal a considerable amount of information was suitable for processing. Consequently, a rapid method of analysis was required to evaluate the optimum aquifer characteristics, particularly in circumstances where the data were of poor quality. A numerical optimisation routine was developed which incorporates methods of analysis suitable for the well-aquifer configurations of the Permo-Triassic aquifer.

Numerical Analysis of Pump Test Data

Introduction

The computer program described is one which can be used to determine aquifer properties from pump test data. It is particularly suitable for use on a remote terminal computer system. The general program structure is simple and it can be used for a variety of problems which require the fitting of complex curves to different sets of data.

Method of Analysis

Conventionally, most methods of analysis of unsteady state drawdown data are graphical and this mode of approach can be used initially to evaluate the most appropriate formula to use. Alternatively, the user can try several numerical methods with the same set of data until a suitable 'fit' is obtained. The best 'fit' is determined by reference to the sum of squares fit which is the sum of squares difference between the observed and predicted drawdowns.

The optimum aquifer characteristics are evaluated numerically and within

an iterative optimisation routine. Consequently, if large sets of data are to be analysed within several routines it is essential to have access to a large computer, preferably via a small teletype. The input data require little pre-treatment apart from the correction of unconfined drawdowns, when they are associated with confined methods of analysis, and the conversion of units.

Additional time can now be spent on the interpretation of results since the graphical procedure is eliminated. For example, discontinuities in the pattern of drawdown caused by recharge, impermeable boundaries, leakage etc. are not always detected by curve matching techniques. The numerical method enables the drawdown data to be analysed in subsets and deviation from the type curve can be evaluated by reference to the sum of squares fit. Indeed, by analysing subsets of data it is possible to monitor any variations in the aquifer characteristics during the test.

In some circumstances the test data may not appear sufficiently accurate or detailed to warrant analysis by conventional methods. However, because the numerical optimisation routine is fast and the degree of fit is indicated, little time is wasted in analysing poor quality data. Indeed it ensures that the maximum amount of information is gained from the available data. Subsequent interpretation of results is obviously at the discretion of the analyst. To help in this respect, predicted and historical drawdowns are displayed with the results.

It is fortuitous for any pump test, however well prepared, to go completely to plan. As such it is possible to intuitively adjust the suspect data to determine their effect on the final solution. This procedure can be repeated with the minimum of effort. It is also feasible to evaluate the sensitivity of the solution to experimental errors in the observation data. Several tests can be implemented according to the analysts requirements, and the results used to assess the upper and lower bounds of the aquifer's characteristics. The latter evaluation is a particularly useful contribution

to the procedure involved in the calibration of groundwater simulation models.

The versatile operational procedure of this numerical form of analysis requires a computer in an interactive mode to ensure maximum benefit is gained. Indeed in a poorly documented aquifer it is often necessary to test a number of hypotheses related to the groundwater regime. The development of this approach is dependent upon results obtained from previous analyses. Consequently it is advantageous to be 'on-line' to a computer with an immediate 'feed-back' of results.

Although a variety of pump test analyses are available within the program it is virtually impossible to cover all the possible aquifer types and pumping regimes. Therefore, although a problem orientated language is more suited to handling a variety of methods a basic version of Fortran IV was used because it is easier to amend. As such additional routines may be incorporated with the minimum of effort. To ensure each routine is efficiently operated several I.C.L. scientific subroutines have been incorporated. They are available on most computer systems as standard functions which are stored in scientific library files.

The Optimisation Routine

The object of this routine is to select the set of aquifer characteristics which will best describe the observed drawdown. This is achieved by systematically adjusting both characteristics so that the sum of squares deviation between the predicted and observed drawdowns is continually reduced.

The most obvious strategy for adjusting the parameters is by a trial and error procedure in which the directions of search are re-evaluated at each iteration. However, once the initial search directions for both parameters have been determined, the probability that continuation in these directions will improve the fit is higher than in opposing directions. Consequently, the initial directions of search are given precedence in all future iterations

until the fit is worsened. At this juncture the directions of search are re-evaluated. Several optimisation routines based on these principles were tested and the method adopted is similar to that used by Flood and Leon (1964). The routine adjusts each parameter consecutively, and in a step-wise fashion moves towards the minimum sum of squares. The direction of search associated with each parameter is only changed when the fit is worsened.

Although more sophisticated search routines exist the algorithm devised is adequate for the solution of two unknowns. It is sufficiently independent of the numerical pump test analysis routines and can be utilised for a variety of problems.

The computation time required to reach a solution is proportional to the number of iterations utilised in the optimisation procedure. It is therefore a function of the efficiency of the routine and the degree of fit required.

The efficiency of the routine is related to the size of the search step employed and to the number of occasions the search has to be redirected. If no prior knowledge of the aquifer's characteristics exist each search step should be set as large as possible, somewhere in the order of 1 to 10% of the initial estimates of the parameters. In order to accomplish this, initial settings of both parameters should grossly over-estimate the expected field values. When necessary the size of each step is adjusted within the algorithm to ensure the resultant aquifer characteristics remain within the realms of physical reality. If prior knowledge of the characteristic exists the initial estimates and associated search steps are set accordingly.

Redirection of the search procedure is more frequent as the optimum solution is approached and it is often associated with a reduction in size of a search step. As a result the number of iterations per unit reduction in the sum of squares increases as the optimum solution is approached. Therefore, the number of iterations permitted should not be excessive or time may be wasted in redirecting the search in a region where the solution

is acceptable.

The criterion for best fit is when the sum of squares is minimised below an acceptable tolerence level and the difference between the historical and predicted water levels is within experimental error. The permitted tolerance factor is therefore variable and dependent upon the circumstances associated with each test. It is subject to interpretation, particularly when poor quality data are involved. The search routine is therefore terminated after a predetermined number of iterations and for most practical purposes 50 iterations suffice. If the resulting solution is not acceptable the search routine can be repeated with initial starting conditions set to the solution.

It is evident from this account that the initial starting conditions do not influence the final solution. Indeed nearly identical solutions are attained from widely different starting points.

Using the Numerical Routine

Initial Data Preparation: In order to use the system to analyse a typical set of pump test data the most suitable methods are selected and the data prepared accordingly. The latter procedure usually involves the conversion of units; the two basic units involved are metres and days. In all, three groups of data have to be prepared for all analyses which evaluate two aquifer characteristics. They are:

(a) The Drawdown Data: In general this consists of a series of drawdown observations taken at specific time periods after the commencement of pumping. The measurements are taken at observation boreholes situated at known distances from the discharge well. The resulting data are prepared in pairs as either time and drawdown or distance and drawdown (Table 7). When an unconfined aquifer is considered the drawdown must be corrected according to Jacob (1963b).

(b) The Data Constants: The parameters included in this group describe the geometry of the aquifer, the configuration of the pump test site and the rate of discharge from the pumped well. The size of the initial search steps for both aquifer characteristics are also included.

(c) The Initial Estimates of the Aquifer Characteristics: The parameters in this group are self explanatory. The format of input for each group is shown in table 7. In general a basic form of 'free' format is utilised.

Operating the Program: If it is assumed that the program has been incorporated into a computer system, the initial operation is to key into the computer and load the program from store. Once completed the program responds with a listing of the available pump test analysis routines. This is followed by a request to choose the required analytical method by typing in the appropriate method number.

The data requested by the computer depend on the method used, and in general three requests are made (Appendix 5). They are:

(a) Drawdown Data: The initial parameter is the number of pairs of data prepared. This is followed sequentially by each pair of drawdown statistics, which do not need to be in chronological order. If, in proceeding analyses, it is required to re-analyse these drawdown data the input procedure can be by-passed and the data called automatically from store. Otherwise, the procedure is repeated with a new set of data.

(b) Data Constants: The order of input and the required units are stipulated in the request for the data. The initial input parameter is the number of constants and this is followed in turn by each constant.

(c) Initial Aquifer Characteristics: The final input of data is the initial estimates of the aquifer characteristics.

The optimisation procedure commences when Ø.Ø is typed in.

The initial output of results is the sum of squares associated with the

initial estimates of the aquifer characteristics. The computational procedure then involves the optimisation routine which works independently of the operator and terminates after the predetermined number of iterations have been completed. A print out of the optimum solution and the associated sum of squares follows. In turn this is followed by a listing of the predicted and historical drawdowns.

The system then returns to the beginning of the program and waits for the next method of analysis to be chosen. In order to exit from the system the last method number, (15), is used and can only be selected after the completion of an analysis.

Although each routine requires a slightly different format of data the program is easy to use because each group of data is requested by the computer. In addition the system is ideally suited for repetitive analyses on one set of drawdown data.

Methods of Analysis Incorporated Within the Program

The theory and limiting assumptions applicable to the analysis of pump test data have been described. Before proceeding with any analysis it is essential that these facts are realised and not abused, in order that the most suitable method of analysis is chosen and the solution obtained is interpreted correctly.

The most popular methods of analysis involve the evaluation of the storage coefficient and transmissibility of confined and unconfined aquifers. Consequently, several unsteady state flow analysis routines are included. Other available options consider partially penetrating wells, variations in the discharge of pumped wells and the effects of recharge and barrier boundaries.

Steady state methods for confined and unconfined aquifers are incorporated within the program. The optimisation routine is automatically by-passed when they are used and the transmissibility evaluated explicitly.

Consequently, a cross-check between steady and unsteady state evaluations of transmissibility can be conducted.

In addition the analysis of steady state drawdowns in semi-confined aquifers results in the evaluation of the transmissibility of the aquifer and the permeability of the semi-confining strata. A resumé of all the numerical methods of analysis are shown in table 8.

Testing the Numerical Routine

Several tests were executed to ensure that the optimisation routine and the numerical analyses were simulating the drawdown equations correctly. Pump test data which had been previously analysed by traditional graphical techniques were re-analysed numerically and the solutions compared. One such test is described below and the results of the other tests are shown in table 9.

The Theis unsteady state drawdown formulation was tested on a set of data previously analysed by the Theis type curve technique and documented by Todd (1959). A good match was obtained by the graphical procedure and the solution obtained from the match point was:

Storage coefficient = 0.198×10^{-3}

Transmissibility = 1.03×10^{5} u.s. g/d/ft.

The drawdown data were subsequently analysed by the numerical routine and its progress monitored (Fig. 35). A number of initial starting conditions were utilised and the optimum results tabulated (Table 10). The solutions obtained were:

Storage coefficient = 0.181 to 0.183×10^{-3}

Transmissibility = 1.03×10^{5} u.s. g/d/ft.

This compares favourably with the results obtained from the graphical analysis. Indeed from consideration of the predicted drawdowns from both techniques it is apparent that the numerical routine has evaluated a better fit (Fig. 36).

Similar tests were conducted on the remaining numerical analyses. Most of the pump test data were abstracted from Kruseman and De Ridder (1970) and from the area under study. In all cases the nunerical solution compared favourably with previous solutions (Table 9). Some of the graphical solutions obtained from data on the Permo-Triassic aquifer are depicted in figures 44 to 50.

CHAPTER FIVE

EVALUATION OF AQUIFER CHARACTERISTICS BY A LEAST SQUARES FITTING TECHNIQUE AND LINEAR PROGRAMMING

Introduction

In recent years the use of groundwater simulation models has become an important technique in the development and management of groundwater basins. Most simulation models are calibrated by comparing predicted water level responses with historical records. This is achieved by a considerable amount of intuitive adjustment of the various hydrological parameters, and in general it is the aquifer characteristic distribution which is adjusted to secure the correct response. This is obviously subjective and dependent upon the availability of data. Current methods of evaluation of these parameters are by laboratory measurement and field work which involves pump tests. Consequently, the problem of reliably extrapolating the parameters throughout the area of study has to be overcome. It is therefore desirable to automate this procedure and to utilise the historical record in order to improve the spatial distribution of aquifer characteristic evaluations.

METHODS OF SOLUTION

Introduction

The techniques described are in effect the reverse of those used in simulation models. As such, hydrogeological parameters are evaluated at a number of nodes according to the historical record available. The evaluated parameters are therefore indicative of regional field values and the problem of extrapolation is overcome. Indeed, the techniques described make maximum use of available data in evaluating aquifer characteristics. However, the results must still be subjected to hydrogeological judgement before they are incorporated into simulation models.

Two techniques have been considered. The first is based on a least squares fitting procedure and the second involves linear programming solutions. Both

techniques were test-run on a hypothetical six node groundwater model and the evaluated parameters were cross-checked with the designated aquifer characteristics. The groundwater flow equations for the Permo-Triassic aquifer were derived from the eighteen node model and the historical period considered was the calibration period from 1969 to 1970.

Least Squares Evaluation

Theoretical Considerations: A multiple linear regression technique is used to solve a series of linear equations which result from the consideration of groundwater flow between adjacent nodes. A water balance is maintained separately at each node and the general equation for node, I, at time, t, is:

$$\sum_{N=1}^{M} \frac{T_{IN} W_{IN}}{Y_{IN}} (H_N^t - H_I^t) - A_I S_I (H_I') = A_I Q_I' \qquad (5.1)$$

where T_{IN} = transmissibility between node I and node N;

A_I = surface area of node I;

S_I = storage coefficient of node I;

Q_I' = recharge for node I between time t and t-dt;

H_I' = water level change at node I from time t-dt to t;

H_I^t = water level at node I at time t;

H_N^t = water level at node N at time t;

M = number of interconnected nodes;

dt = time interval.

Consider the following trivial six node system in which there are no boundary flows.

Diagram (1)

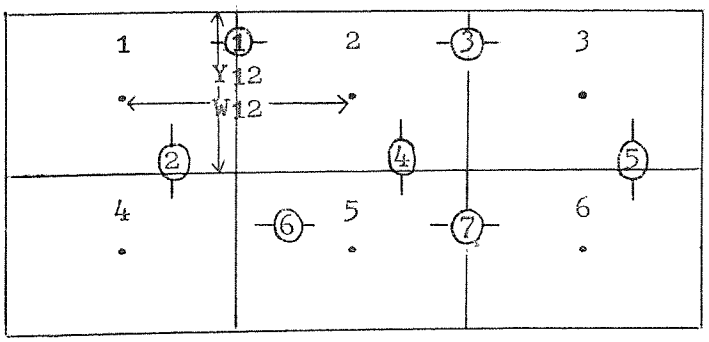

The matrix of water level differences (hydraulic gradients) present at time, t, is derived as follows:

Each nodal interconnection is numbered in order, starting from node 1, and a one dimensional array, L, is formed.

Therefore, L = 1 to NP

where NP = the number of nodal connections. (see Diagram 1)

Let, $H_I - H_N = G_{I,L}$

For example

$$H_2 - H_5 = H_{2,5} = G_{24} \quad \text{and so on.}$$

Consequently, for the six node configuration, as shown in diagram 1, the matrix of hydraulic gradients [G] is:

$$\begin{bmatrix} H12 & H14 & 0 & 0 & 0 & 0 & 0 \\ H21 & 0 & H23 & H25 & 0 & 0 & 0 \\ 0 & 0 & H32 & 0 & H36 & 0 & 0 \\ 0 & H41 & 0 & 0 & 0 & H45 & 0 \\ 0 & 0 & 0 & H52 & 0 & H54 & H56 \\ 0 & 0 & 0 & 0 & H63 & 0 & H65 \end{bmatrix}$$

Water level changes between times t - dt and t at each node are related to variations in storage. They are subsequently incorporated into the matrix as follows:

$$H_I' = G_{I,NP+I}$$

The resulting water level difference matrix [G] is depicted as:

$$\begin{bmatrix} H12 & H14 & 0 & 0 & 0 & 0 & 0 & H1' & 0 & 0 & 0 & 0 & 0 \\ H21 & 0 & H23 & H25 & 0 & 0 & 0 & 0 & H2' & 0 & 0 & 0 & 0 \\ 0 & 0 & H32 & 0 & H36 & 0 & 0 & 0 & 0 & H3' & 0 & 0 & 0 \\ 0 & H41 & 0 & 0 & 0 & H45 & 0 & 0 & 0 & 0 & H4' & 0 & 0 \\ 0 & 0 & 0 & H52 & 0 & H54 & H56 & 0 & 0 & 0 & 0 & H5' & 0 \\ 0 & 0 & 0 & 0 & H63 & 0 & H65 & 0 & 0 & 0 & 0 & 0 & H6' \end{bmatrix}$$

The matrix [X] which contains the aquifer characteristics is constructed as follows:-

$$\begin{bmatrix} X(1) \\ \vdots \\ X(NP) \\ X(NP+1) \\ \vdots \\ X(NP+NN) \end{bmatrix}$$

where NN = the number of internal nodes;

X(1)toX(NP) contain the transmissibility relationships between adjacent nodes;

X(NP+1) to X(NP+NN) contain the coefficients of storage for each internal node.

If the matrix of recharge elements between time t-dt and t is represented by $[R]$ and is depicted by:

$$\begin{bmatrix} R(1) \\ \cdot \\ \cdot \\ \cdot \\ R(NN) \end{bmatrix}$$

the groundwater equation (5.1) can be written as $[G]\,[X] = [R]$. The objective is to determine the elements of the matrix $[X]$ which will minimise the residuals in the water balance. When the water balance is considered for a number of time intervals the resultant matrix configuration is:

$$\begin{bmatrix} \text{Water level differences at time } t & \text{Water level differences between time t-dt and time t} \\ \text{Water level differences at time } t+dt & \text{Water level differences between time t and time t+dt} \\ \cdot & \cdot \\ \cdot & \cdot \\ \cdot & \cdot \\ \cdot & \cdot \end{bmatrix} \begin{bmatrix} X(1) \\ \cdot \\ \cdot \\ \cdot \\ X(NP) \\ X(NP+1) \\ \cdot \\ \cdot \\ \cdot \\ \cdot \\ X(NP+NN) \end{bmatrix} \quad \begin{bmatrix} \text{Net nodal recharge between time t-dt and time t.} \\ \text{Net nodal recharge between time t and time t+dt} \\ \cdot \\ \cdot \\ \cdot \\ \cdot \end{bmatrix}$$

The linear multiple regression solution for $[X]$ can be evaluated by the matrix formulation:

$$[X] = [G^T G]^{-1} \cdot [G^T R] \qquad (5.2)$$

The Algorithm Used: In theory 'n' variables can be determined from 'n'

independent equations. However, the system of equations represented above are not truly independent. Consequently, it is necessary to overdetermine the system if a meaningful solution is to be obtained. The six node problem required the solution of 13 variables and thus by considering 24 monthly water balances at each node, 144 equations were formed. The system was therefore overdetermined by a factor of 11. Similarly the eighteen node problem required the solution of 63 variables from 24 monthly periods and was overdetermined by a factor of 7. The resultant matrix of water level differences tended to be very large, particularly when the eighteen node model was considered, and was of the order of (400 x 63). Although a considerable amount of redundancy occurs between the equations this could not be eliminated and matrices of this size were inevitable if the best solutions were to be obtained.

An algorithm was written to perform the necessary matrix manipulations with the minimum amount of storage allocation. This process is helped by the fact that a considerable proportion of the elements in matrix $[G]$ are zero and the position of the non-zero elements can be determined from the nodal arrangement. In addition it is only necessary to store half of the hydraulic gradient elements since $H_{IN} = -H_{NI}$. Consequently, although the matrix $[G]$ is (18 x 63) for one time interval on the eighteen node model it is only necessary to store 63 elements. It is therefore possible to store $[G]$ and $[G^T]$ with the minimum amount of storage allocation. The product of $[G^T G]$ is a symmetrical matrix and storage is again reduced by only storing the upper diagonal. In turn inversion of $[G\ G^T]$ forms a symmetrical matrix and a similar storage arrangement can be devised. The final matrix multiplication of $[G^T G]^{-1}$ by $[G^T R]$ is the last step in the matrix arithmetic and therefore it is possible to overlay the storage facilities. The resultant matrix $[X]$ contains the desired aquifer characteristics. To ensure that each transmissibility and storage coefficient is positive, each

element of the water level difference matrix is associated with the appropriate sign.

If $W_L = W_{IN}$

and $Y_L = Y_{IN}$

then $$X(L) = \frac{T_L \, W_L}{Y_L} \qquad (5.4)$$

where $L = 1$ to NP

Similarly $$X(K) = A(K - NP) \cdot S(K - NP) \qquad (5.5)$$

where $K = NP + 1$ to $NP + NN$

Consequently, from equations (5.4) and (5.5) the transmissibility between adjacent nodes and the storage coefficient at each node can be evaluated.

Data Evaluation for the Six Node Model: Water level data were determined by the backward difference groundwater simulation model. The aquifer characteristics chosen to represent the system were of the same order as those of the unconfined aquifer of the study area. Recharge data were derived from the historical record for the associated outcrop area. In order to maintain a hydrological balance within the system net groundwater abstraction during the historical period was made approximately equal to the net recharge. The areas associated with nodes 1, 2,4 and 5 were designated as the predominant recharge zones and nodes 3 and 6 were the centres of steady groundwater abstraction.

Initial starting conditions for the simulation run were arrived at after a dynamic equilibrium run of approximately 10 years, which involved recycling the first 12 months of recharge data. Subsequently, water levels were predicted for the historical period and together with the historical recharge data were systematically dumped onto computer files. These files formed the basis of the data for the least squares analysis.

Boundary flows are not considered by the hypothetical six node

configuration and therefore they are only 13 variables to be solved. They consist of 7 transmissibilities and 6 storage coefficients (Diagram 1).

Sensitivity Analysis: Initial computer runs proved that this method of analysis was very sensitive to minor adjustments in the historical record. For instance, when apparently minor adjustments to the water level records for the eighteen node model were made, due to re-levelling of observation wells, significant changes in the solutions occurred. Indeed, errors of the order of $\pm$ 0.1 m in the water level record and $\pm$ 10% in the recharge data were sufficient to alter some parameters in both models by several orders of magnitude. The most significant changes to occur were related to individual transmissibility estimates. However, where the eighteen node model was concerned the overall regional estimates of the aquifer characteristics were always relatively constant. In this respect the analysis showed most promise and the following discussion is related to the results obtained from what was assumed to be the best set of historical data.

Significance of the Solutions: Several unrealistic values were obtained for the six node model; they were represented by 2 negative transmissibilities and 3 negative storage coefficients. Otherwise the positive solutions predicted aquifer characteristics of a similar magnitude to those utilised during the simulation run (Table 11). Since reasonable solutions were obtained it was assumed feasible to consider the Permo-Triassic system in the form of the equations from the eighteen node model. Boundary flows were included in this analysis and consequently it was required to solve 63 variables (Fig.59). Of the predicted variables 28 were negative; this total included 7 storage coefficients and 21 transmissibilities. The realistic results inferred that the smallest storage coefficients occur over the central confined and semi-confined areas and are of the order of 3×10^{-2} to 6×10^{-6}. The lowest transmissibilities are predominantly associated with the same

areas and are of the order of 8 to 200 m^2/d. The largest storage coefficient, 3.8×10^{-1}, and highest transmissibility, $2002 m^2/d$, were associated with nodes on the unconfined aquifer in the Severn catchment. All remaining solutions were associated with either unconfined or semi-confined nodes and were represented by storage coefficients between 9.0×10^{-1} and 8.0×10^{-4} and transmissibilities between 167 and $1750 m^2/d$.

The distribution of nodal water balance residuals indicated that the largest errors occurred over the confined area. This was evidently related to the unreliable nature of the historical water level records in the vicinity. The effect of this region of low quality data on the evaluation of the aquifer characteristic distribution could not be quantified; however, it was evident from the sensitivity analysis that it could be very significant. The historical record, as it is presently determined, is not adequate to define more than 50% of the aquifer characteristics. Although it was possible to increase the length of the historical record the quality of the data could not be improved. Consequently, this method of analysis was not considered further.

Linear Programming Solutions

Theoretical Considerations: In order to produce a linear problem from the water balance equations previously described, the absolute values of the errors are considered instead of the sum of squares errors. Linear programming solutions can be applied provided that the objective function is linear and the constraints are statements of linear equalities or inequalities. Several quantities can be chosen to be minimised and therefore several linear problems can be formulated (Kleindeke 1971). In this study three linear problems are considered. They are:

(a) to minimise the maximum absolute value of error in the water balance. The appropriate equations for each node, I, at the end of each time period are derived as follows:

If X is the maximum absolute value of error then from equation (5.1)

$$-X \leq \sum_{I=1}^{NN} \sum_{N=1}^{M} \frac{T_{IN} W_{IN}}{Y_{IN}} (H_N^t - H_I^t) + A_I Q_I' - A_I S_I H_I' \leq X \qquad (5.6)$$

If U_I^t and V_I^t are defined as non-negative slack variables the inequalities above can be written as:

$$\sum_{I=1}^{NN} \sum_{N=1}^{M} B_{IN} (H_N^t - H_I^t) - Z_I (H_I') + U_I^t - X = R_I' \qquad (5.7)$$

and

$$\sum_{I=1}^{NN} \sum_{N=1}^{M} B_{IN} (H_N^t - H_I^t) - Z_I (H_I') - V_I^t + X = R_I' \qquad (5.8)$$

where

$$B_{IN} = \frac{T_{IN} W_{IN}}{Y_{IN}} ; \qquad (5.9)$$

$$Z_I = A_I S_I ; \qquad (5.10)$$

$$R_I = A_I Q_I' . \qquad (5.11)$$

The linear objective is obtained by minimising X.

(b) to minimise the sum of the absolute values of error in the water balance. Consequently, the absolute value of the error at each node is required for each time period considered. This is achieved by again introducing non-negative slack variables into the general water balance equation. The resultant equation is expressed as:

$$\sum_{I=1}^{NN} \sum_{N=1}^{M} B_{IN} (H_N^t - H_I^t) - Z_I (H_I') + U_I^t - V_I^t = R_I' \qquad (5.12)$$

It is now required to minimise $U_I^t + V_I^t$. This is achieved when one variable is zero and the other variable is the absolute value of the error. Therefore, by minimising the sum of all U_I^t and V_I^t the sum of the absolute values of error is minimised.

(c) to minimise the sum of the maximum absolute values of error at each node for all time periods. The equations involved are of the form:

$$\sum_{I=1}^{NN} \sum_{N=1}^{M} B_{IN} (H_N^t - H_I^t) - Z_I (H_I') + U_I^t - X_I = -R_I' \qquad (5.13)$$

$$\sum_{I=1}^{NN} \sum_{N=1}^{M} B_{IN} (H_N^t - H_I^t) - Z_I (H_I') - V_I^t + X_I = -R_I' \qquad (5.14)$$

In this case X_I is the maximum nodal error attained and the object is to minimise the sum of all X_I.

The equations described for each method define typical linear programming problems in which it is required to find a solution for B_{IN} and Z_I. Hence the aquifer characteristic distribution can be evaluated.

Method of Solution: One of the chief advantages of linear programming is the relatively simple formulation of the computer program. This has resulted in the development of numerous standard packages, the majority of which are available on most computer systems. The only disadvantage in their use is the highly specialised and apparently complex nature of their programming codes. Typical problems are orientated towards cost-benefit applications where it is desired to optimise the allocation of resources according to certain constraints (Dracup 1966). Therefore, the primary objective is to produce algorithms which will transform the raw historical groundwater data into a form suitable for input into a linear programming package. Algorithms were devised according to the requirements of the I.C.L. linear programming package. The optimisation models developed were tested on the six node model and subsequently used on the eighteen node Permo-Triassic model. The results for each optimisation model are discussed below, and summarised in tables 12 and 13.

Method a: The constraints used in this method restrict the solution to those nodes with the largest errors. Consequently, for the majority of nodes no solution is obtained. For the six node model some solutions were obtained

for nodes 1, 2 and 5 and for the eighteen node model for nodes 2, 3, 9, 11 and 15.

Method b: Again the nodes with the largest errors dominated the final solutions. For the six node model some solutions were obtained for nodes 2, 3 and 5. For the eighteen node model solutions for nodes 2,3,9,11 and 15 were obtained again and, in addition, information was gained on node 10.

Method c: Although the constraints used in this method ensure that each node is considered, solutions for several transmissibility links were missing for the six node model. No feasible solution was obtained for any of the aquifer characteristics for the eighteen node model.

In order to improve the nodal distribution of aquifer characteristic determinations and the estimates of those already obtained, techniques were employed to introduce more variables into the final solution. It was assumed that the variables not evaluated were dropped from the final solution because they were negative and therefore in effect physically meaningless. Each node is influenced by its neighbour and therefore each set of equations is not truly independent, consequently any negative values will influence the final solutions. Additional constraints were consequently imposed on the water balance equations by defining upper and lower bounds for each aquifer characteristic. An error factor of $\pm$ 25% was assumed for the six node model and the constraints evaluated accordingly. Constraints for the eighteen node model were derived from the pump test analysis program, the results of which are summarised in table 14.

Solutions for the six node model only showed a slight improvement and the majority of variables attained lower bound values. Additional aquifer characteristics were solved for the eighteen node model but some variables which had been previously involved in the final solution were outside the range set by the constraints. Consequently, they were set at either upper or lower bound values.

With the addition of several more equations into the linear programming models, difficulties arose because of the size of the problem. Although the storage facilities required were not excessive the computer time required to reach a solution had increased substantially. In this respect although the third method worked satisfactorily for the six node model the computation time available was not sufficient for a solution to be obtained for the eighteen node model.

Sensitivity Analysis: The sensitivity of each of the unconstrained and constrained linear programming models to adjustment of the historical record was investigated with the six and eighteen node models. The water level data were adjusted by $\pm$ 0.1 m and the recharge data by $\pm$ 10%. Several combinations were investigated and on all occasions significantly different solutions were obtained. This was particularly apparent for some transmissibility links which, in each unconstrained model, varied by several orders of magnitude. Storage coefficient estimates were generally more consistent and apparently less sensitive to errors in the historical record.

In all the linear programs considered solutions were obtained for aquifer characteristics not previously evaluated. The majority were associated with the unconstrained models but they were not consistent with known aquifer characteristics in the six node model nor with the assumed characteristics in the eighteen node model.

The distribution of aquifer characteristics for which solutions were obtained remained essentially the same for both aquifer models. As such for the eighteen node model solutions for the confined aquifer were still dominant.

Significance of the Solutions: The solutions obtained for the six node model from each linear programming method were fairly consistent although only 3 variables were predicted with an error of less than 25%. All the remaining solutions have errors in excess of 50% and indeed no solutions

were obtained for 4 of the variables.

Consistency between solutions was also apparent for the eighteen node model although transmissibility estimates were sometimes several orders of magnitude different from those predicted by more conventional means. Most promise was indicated by storage coefficient estimates which were not only more consistent but also comparable with those obtained from pump tests and laboratory analysis. In all the solutions obtained, some estimates of the aquifer characteristics in the confined aquifer were included. This was particularly evident from the results of the analyses which involved method a. Consequently, it was assumed that the largest errors in the nodal water balances were associated with the confined aquifer.

Solutions for only 21 out of the 63 variables were obtained for the eighteen node model. This total includes the additional solutions acquired from the imposition of constraints on the variables. Transmissibility estimates were sparse and only 50% of them were within the range determined from pump test analyses. On the whole, storage coefficient estimates appeared more realistic and solutions for a total of 8 nodes were obtained from the unconstrained and constrained analyses.

Conclusions

Only general trends in the areal variation of aquifer characteristics were depicted from the least squares solution, and from the linear programming models the majority of estimates were meaningless. It is therefore apparent from both methods that the historical records presented were not adequate for a unique definition of the aquifer characteristics at the majority of nodes. Although each system of equations is apparently overdetermined the historical record does not contain sufficient data for a meaningful evaluation of most characteristics. For example, if the hydraulic gradient between adjacent nodes is small any reasonable estimate of the transmissibility can be inferred without upsetting the water balance significantly. Only when this gradient is

increased, say by groundwater abstraction in the vicinity, will the erroneous transmissibility be evident.

The sensitivity analysis inferred that a precise historical record was required in order to obtain accurate evaluations of the aquifer characteristics. Consequently a high degree of precision is necessary in the measurement of water levels and in the evaluation of the net nodal recharge component to the groundwater system.

Throughout all the analyses estimates of storage coefficients appeared realistic but the majority of transmissibility values were either meaningless or inconsistent with historical estimates. The predominance of unrealistic and meaningless solutions questions the validity of the solutions that appear to be acceptable; the occurrence of realistic solutions through chance cannot be ruled out entirely. As a result of these uncertainties in the interpretation of the solutions and the apparent inadequacy of the available historical records the least squares and linear programming techniques were not developed further.

CHAPTER SIX

DATA PREPARATION FOR THE CALIBRATION OF THE GROUNDWATER DIGITAL MODEL

Introduction

The previous chapters involve the collection and analysis of hydrological and hydrogeological information from the Permo-Triassic aquifer. The text which follows presents a resumé of the results obtained in preparation for the calibration of a digital model of the groundwater system.

Aquifer Geometry

Introduction

Initial investigations of the water resources of water bearing strata commence with the evaluation of the lateral and vertical extent of the main aquifer systems. This information is obtained by delineating aquifer boundaries as they appear at outcrop and by utilising geophysical and borehole logging techniques to help construct a three dimensional picture of the groundwater system. Levels at which discontinuities in aquifer characteristics are expected can be formulated and the upper and lower limits of possible water levels can be determined for simulation purposes.

Model Boundaries

Model boundaries can be constructed anywhere in the field of flow if the information required to simulate the groundwater regime in their vicinity can be obtained. It is obviously more desirable to utilise natural hydrogeological boundaries wherever possible, and in this study artificial boundaries were only constructed to limit the extent of the study area.

The unconformity between the main aquifer and the underlying older strata is an important hydrogeological boundary and is the dominant impermeable model boundary (Fig.2). It crops out along the flanks of the Coalbrookdale and South Staffordshire Coalfields to form the western and eastern boundaries respectively. The Pattingham, Lloyd House and Western Boundary Faults

terminate the main aquifer against older impermeable strata in the south and south-east of the area. These hydrogeological discontinuities were consequently modelled as no-flow boundaries.

All the remaining boundaries were constructed to limit the extent of the area of study (Fig. 37). To complete the boundary in the south, that is between the Enville and Western Boundary Faults, a head controlled boundary was simulated across the narrowest tract of the main aquifer. Groundwater flow in the vicinity of this boundary is southwards and towards the River Stour (Fig. 30).

The northern boundary was constructed approximately along a line between Newport and Stafford. It commenced at the northern limit of the outcrop of the Coalbrookdale Anticline and followed the north-easterly trend of the Aqualate Anticline towards Norbury. This structure was initially assumed to act as a groundwater divide but subsequent water level data did not support this supposition and groundwater flow in the vicinity is north-westwards. Between Norbury and Stafford the boundary intersects the confined portion of the aquifer. From the analyses of a limited number of boreholes, and on the assumption that a horizontal to shallow easterly dip is characteristic of the strata, the hydraulic gradient is subparallel to the boundary.

The positioning of the boundary between Stafford and Cannock was controlled primarily by the course of the River Sow. Groundwater flow is north-westwards from Cannock Chase towards the river which acts as a constant head controlled boundary. To complete the eastern boundary between the River Sow and Cannock a head controlled boundary was devised across Cannock Chase. This was positioned along the line of a groundwater divide which separates flow north-westwards towards the South Staffordshire Syncline and River Sow, from flow north-eastwards away from the area of study and towards the River Trent.

The modelled area enclosed by the boundaries described above is

approximately 850 square kilometres.

Aquifer Thickness

Ideally the thickness and lateral extent of each lithological unit which constitutes the aquifer is required in order to simulate precisely spatial and temporal changes in storage and transmissibility. The necessary evidence can be gained from cross-correlation of available borehole logging data, palaeontological evidence and geophysical investigations. However, a more precise understanding of the possible variations in lithology can be obtained by consideration of the depositional history of the sediments, as interpreted from sediment analyses and the principle of uniformitarianism, and their subsequent geological history, as interpreted from present outcrop patterns and microscope studies.

The strata of the main aquifer were deposited in a variety of continental environments. Lacustrine, aeolean and fluviatile conditions have been identified. Thus regionalisation by correlation of borehole logs is difficult because of extensive lateral facies changes and the lack of preservation of a suitable fossil record.

Periodic faulting throughout the Triassic period had an important influence on the thickness and nature of the sediments. The main water bearing formations were deposited within a fault controlled basin and periodic uplift of the hinterland resulted in a series of intercalated sediments of varying grain size. Consequently, rapid vertical changes in lithology occur, particularly on the edge of the basin. Towards the centre of the basin considerable thicknesses of sediment are preserved.

Although the activity and influence of graben faulting waned towards the end of the Triassic period, the thickness of the semi-confining strata also increases towards the centre of the basin. Periods of cyclic deposition are evident throughout the Lower Keuper Sandstone Formation and not until the Keuper Marl Formation is a continuous confining horizon apparent above the main aquifer.

Post-Triassic folding and faulting are responsible for the present outcrop pattern within the study area. In particular the broad fold regime of the South Staffordshire syncline has preserved considerable thicknesses of water bearing formations. The gentle dipping strata have been disturbed by strike faults which have caused repetition of the beds within the western limb of the syncline. In the south between the Enville and Western Boundary Faults the eastern limb is absent.

The area of study is characterised by a lack of outcrop and suitable surface features to map. Consequently, the areal extent of faulting, particularly across the Keuper Marl Formation, is speculative and the junctions between each formation cannot be depicted with certainty.

Much work has yet to be undertaken before a complete picture of the structure and extent of each formation is compiled (Wills 1970). However, tentative isopachyete maps have been prepared for each formation from available borehole logs and with assistance from Kent (1949), Cook, Hospers and Parasnic (1952) and Audley-Charles (1970b). It is therefore possible to determine levels at which major changes in the storage coefficient of the main aquifer occur (Figs. 38 to 43). Similarly, by monitoring variations in the saturated thickness it is possible to adjust regional transmissibilities during simulation runs.

Evaluation of Aquifer Characteristics

Introduction

The evaluation of aquifer characteristics is an important procedure in modelling the dynamic behaviour of groundwater systems. Ideally a dense network of aquifer characteristic evaluations is required but, because of the expense and time necessary to conduct pumping tests, the coverage is usually far from ideal. It is therefore essential that both a qualitative and quantitative analysis of the system is performed in order to help regionalise the available data and in some circumstances to estimate parameters in poorly

documented areas. All the relevant hydrogeological information has to be considered and the lower and upper bound values for each characteristic determined at a number of well distributed localities.

Laboratory Analyses

Although this type of analysis does not enable representative field values to be determined it does give insight into the variations to be expected. A necessary and complementary procedure to this analysis is a detailed field survey of the lithology of the water bearing formations and a sedimentary analysis of representative samples. This permits identification of the fundamental properties which are likely to have most influence on the derived properties. From these studies the regionalisation of aquifer characteristics becomes more objective and is related to a better understanding of the fundamentals of the groundwater system. A summary of the results and conclusions for each formation follows:

(a) Lower Mottled Sandstone Formation: This formation is dominated by well sorted, medium grain sized sandstones and is devoid of argillaceous and rudaceous strata. As a result uniformity of aquifer properties is to be expected.

Some of the largest storage capacities for the Permo-Triassic aquifer (0.11) are associated with sandstones of this formation and in particular with well sorted 'millet seed' horizons. High permeabilities (10 to 16 m/d) prevail, particularly in well sorted sediments. There is a tendency for low permeabilities and small storage capacities to occur in less well sorted sediments due to the inclusion of finer grained material.

(b) Bunter Pebble Bed Formation: Sedimentary rocks which range in grain size from fine sandstones to medium pebbles are characteristic of this formation. However, the derived property analysis had to be restricted on the whole to the sandstones because of the incoherent nature of the pebble beds.

Storage capacities range from 0.01 to 0.09 and permeabilities are of the

order of 1 to 4 m/d. Some sediments are affected by the presence of calcite cement which occupies the interstices and produces a relatively coherent and impervious sediment. General relationships between the derived and fundamental properties suggest that the largest storage capacities and highest permeabilities are associated with pebble beds, particularly where they are well sorted and uncemented. However, where calcite cemented horizons occur it is apparent that the capacity of the formation to transmit and store water is considerably reduced. Mudstone lenses are not abundant but where they do occur a lowering of the overall permeability and effective porosity of the formation is expected.

(c) Upper Mottled Sandstone Formation: Fine grained, well sorted and uncemented sandstones predominate and the relative homogeneity in lithology results in fairly uniform aquifer properties throughout this formation.

Storage capacities range from 0.02 to 0.08 and permeabilities from 4 to 10 m/d. Indeed these values are representative of average aquifer characteristics for the uncemented arenaceous and rudaceous strata of the Permo-Triassic aquifer. The formation is not affected to any large extent by cementation although the occurrence of marl partings at some horizons will reduce the overall permeability and effective porosity.

(d) Lower Keuper Sandstone Formation: This formation is represented by alternations of sandstone, sandy marl and mudstone. The sandstones are the main sources of groundwater and their sediments are generally moderately sorted and of medium grain size.

The storage capacity and permeability of the uncemented sandstones are of the order of 0.08 and 1 m/d respectively. However, calcite cemented strata are common in this formation and small storage capacities (0.0007) and low permeabilities (0.09 m/d) occur. In addition mudstone becomes a dominant rock type in younger horizons and consequently the overall permeability and effective porosity are significantly reduced.

It is evident from the above analysis that the strata of the main aquifer within and in the vicinity of the unconfined area are dominated by relatively uncemented fine to coarse grain sized sandstones which are moderately to well sorted. Their effective porosities and permeabilities are of the order of 0.01 to 0.1 and 0.1 to 10 m/d respectively. Variation of aquifer characteristics within these sediments is mainly attributed to changes in the quantity of fine grained material and to sub-horizontal current bedding and laminations. Calcite cementation occurs at a number of horizons and reduces the capacity of the strata to transmit and store water. This is exemplified by effective porosities of less than 0.01 and permeabilities of less than 0.1 m/d. In addition, the presence of mudstones, particularly in the Lower Keuper Sandstone Formation, reduces the regional values of the aquifer characteristics even further.

Pump Test Analyses

It is obvious from the previous account that the overall effect of grain size variations, sedimentary structures and marl partings upon the hydraulic characteristics of the aquifer has to be quantified. In addition the influence of secondary processes such as cementation, faulting and jointing has to be evaluated.

Pump test analyses are the most popular and useful means of evaluating field values of aquifer characteristics. However, the cost involved and time required to adequately investigate the study area restricted the degree to which this approach could be implemented. Analyses were therefore confined to pump tests conducted at existing sites, most of which were in the vicinity of the main abstraction boreholes (Fig. 32). Initially, conventional methods of analysis were utilised to determine the storage coefficient and transmissibility of the main aquifer. Some of the results and associated time-drawdown curves are illustrated in figures 44 to 47. In order to secure maximum benefit from the poor quality data a numerical optimisation routine

was devised and is described in chapter four. Consequently, it was possible to compute upper and lower bound values of the hydraulic characteristics at a number of localities (Table 14).

Steady state analyses and the Theis recovery method were also used to determine the spatial variation of transmissibility. Some of the recovery curves are illustrated in figures 48 to 50 and the range of values is shown in table 14.

The highest transmissibility values are associated with the unconfined areas of the Severn catchment and in particular with the Worfe and Smestow Brook sub-catchments. They are a function of consistently high permeabilities, and variations in aquifer thickness result in a range of values from 100 to 800 m^2/d. Further north unconfined transmissibilities are of the order of 200 m^2/d and this reflects a reduction of the aquifer thickness towards the edge of the basin and the occurrence of horizons of low permeability. On the edge of the confined aquifer and within the semi-confined region, transmissibilities are between 50 and 200 m^2/d. Although substantial thicknesses of the main aquifer are encountered (300 to 400m) this is obviously counterbalanced by low permeabilities.

Unconfined storage coefficients range from 0.10 to 0.03 within the Severn catchment and from 0.01 to 0.008 within the Sow catchment. Semi-confined storage coefficients are characterised by values of the order of 0.004 to 0.0009.

The variation of aquifer characteristics within the main aquifer underlying the Keuper Marl Formation had to be estimated from a limited amount of data. Attempts to exploit the confined aquifer have generally been unsuccessful because of insufficient quantities of water. In addition the source has been of poor quality and often of high chloride content. A substantial thickness of confining strata (100 - 200m) has been preserved towards the centre of the basin and contorted bedding within the main

aquifer has been encountered at Ivetsy Bank. It is therefore apparent that graben-type faulting parallel to the axis of the South Staffordshire Syncline has affected both the main aquifer and the confining strata (Fig. 13). This has resulted in the partial isolation of the confined aquifer from the movement of meteoric groundwater and, as such, calcite cementation and connate water are probably more abundant in this region than in the unconfined areas. Consequently, transmissibility estimates were assumed to be less than in the semi-confined area and of the order of 25 to 50 m^2/d. Storage coefficients were assumed typical of confined granular media and estimated to be between 0.001 and 0.00001.

Least Squares and Linear Programming Solutions

The problem of reliably extrapolating aquifer characteristic evaluations in order to produce a suitable distribution for the digital model was approached by utilising least squares and linear programming techniques (Chapter Five). Both methods predicted hydraulic characteristics at a series of nodal points from historical water level and recharge data. Although a considerable proportion of the evaluations were meaningless general trends did emerge which were compatible with hydrogeological reasoning. High transmissibilities (200 to 2000 m^2/d) and large storage coefficients (0.04 to 0.004) were characteristic of the unconfined aquifer, whereas semi-confined and confined conditions were associated with lower transmissibilities (10 to 1000 m^2/d) and smaller storage coefficients (0.03 to 0.000006).

Summary

From the analyses considered above it was possible to delineate upper and lower bound values of aquifer characteristics at eighteen localities within the unconfined and semi-confined aquifers. Interpolation between these sites and also across the confined aquifer was subject to hydrogeological reasoning as gained from laboratory investigations, and

restricted by the upper and lower bound values as predicted from the inverse solution techniques.

Groundwater Recharge and Discharge

Introduction

In order to simulate historical water level fluctuations it is necessary to delineate the main areas of recharge and discharge within the aquifer. In addition temporal variations of the recharge and discharge components have to be evaluated for the study period. Consequently, the response of surface catchments to climatological events during this period has to be monitored and subsequently analysed to determine the hydrological characteristics of each catchment. These studies lead to a more profound understanding of catchment behaviour and enable the components of the water balance to be quantified.

Groundwater Recharge

Precipitation and evapotranspiration are the two dominant factors involved in the evaluation of groundwater recharge. Temporal variations of the recharge component are dependent upon seasonal and long term variations of these climatic factors. In particular, monthly variations result from the seasonal fluctuation of evapotranspiration whereas long term trends, as considered over several years, are more dependent upon variations in rainfall.

Precipitation: Precipitation is fairly evenly distributed throughout the year and 55% of the mean annual total (1916 - 1950) occurs in winter and 45% in summer. During winter months it is usually widespread and of fairly uniform intensity whereas in summer it is more sporadic and variable in intensity. Mean annual rainfall totals range from a maximum of 757 mm in the north of the area to a minimum of 686 mm in the south. The areal distribution of rainfall for the period of study was evaluated on a daily basis from ten rainfall stations (Fig. 26).

Evapotranspiration: This was by far the most difficult factor of the two to evaluate. Initial studies commenced with the computation of potential evapotranspiration rates from climatological observations (Chidley and Pike 1970) and subsequently continued with estimates obtained from the Meteorological Office.

During winter months potential evapotranspiration rates are low and less than 25mm/month and during summer months are often in excess of 100mm/month (Fig. 18). As such over 80% of the mean annual total of 480mm occurs during the summer. Any areal variations were assumed to be related to differences in the radiating surfaces and not to variations in the climatic regime across the area. Consequently, potential rates were evaluated for a surface dominated by agricultural usage and areal variations were assumed to be negligible.

Actual evapotranspiration rates were subsequently found to deviate markedly from the potential rates particularly during summer months. Actual values were evaluated by the method proposed by Grindley (1969) and the root constant for shallow rooted vegetation was assumed to be dominant (Table 2).

Evaluation of Effective Infiltration: The principal means of recharge to the main aquifer is from infiltration of precipitation over the unconfined area. This occurs directly where strata of the main aquifer crop out and indirectly by percolation through overlying superficial deposits. Infiltration into the confining strata and their overlying superficial deposits recharges minor aquitards above the main aquifer. The initial determination of effective infiltration over the recharge area of the main aquifer was evaluated by a simple monthly water budget scheme (Land 1966).

The defining equation is;

$$I = f\,(P - Ep) \qquad (6.1)$$

where I = infiltration;

P = precipitation;

Ep= potential evapotranspiration;

f = function of the superficial cover.

Initial recharge estimates were derived from areal rainfall based on the ten rain-gauge Theissen network, potential evapotranspiration, as derived from Chidley and Pike (1970) and the Meteorological Office, and superficial cover factors as proposed by Land (1966). Equation (6.1) was incorporated into recharge model 1 (Chapter Two) and monthly recharge components were evaluated for each sub-catchment. The results for the Worfe and Penk sub-catchments are illustrated in figures 51 and 52 (see method 1).

Subsequent evaluations were based upon factors characteristic of the study area and the defining equation (6.1) was modified to;

$$I = (P - Ep) - SR \qquad (6.2)$$

where SR = surface runoff component.

The surface runoff component was derived from historical total runoff records of the Rivers Stour and Sow and predicted from inferred linear relationships between effective precipitation and surface runoff when the records were incomplete (Fig.23). Equation (6.2) was subsequently incorporated into recharge model 1 and monthly recharge estimates re-evaluated (Figs.51 and 52, see method 2).

It is evident from the results of both methods that no groundwater recharge is predicted during periods of below average rainfall, for example, the winter 1961/62. This is inconsistent with historical groundwater level fluctuations (Fig.58). The problem evidently appears to be related to an excessive build-up of soil moisture deficits during the summer months. As a result effective precipitation during proceeding winter months is involved in reducing this deficit and groundwater recharge is not predicted. However, periods of above average precipitation are apparently modelled successfully because moisture is available in sufficient quantities to limit the build-up of soil moisture deficits. During 1968, for example, the soil moisture content was never far below field capacity and evapotranspiration occurred at or near the potential rate.

The divergence of actual evapotranspiration from the potential rate during dry weather conditions is assumed to be significant and the method proposed by Grindley (1969) was utilised. Actual evapotranspiration rates, E_A, were derived from potential estimates and root constants based on land utilisation over the recharge area (Table 2). Therefore, E_A was used to replace Ep in equation (6.2) and recharge model 1 was used to re-calculate the recharge component (Figs. 53 and 54). Compared with the results from methods 1 and 2 there is a considerable reduction in maximum annual soil moisture deficits. Consequently, groundwater recharge is predicted to occur each winter when soils are at field capacity and the overall temporal variation of groundwater recharge is compatible with historical water level fluctuations.

To further improve the temporal distribution of groundwater recharge a watershed simulation model based on Dawdy and O'Donnell (1965) was employed (Chapter Two). The model was calibrated for the Severn and Sow catchments (Table 4) and the characteristics assumed representative of their associated sub-catchments. Rainfall data based on the Theissen rain-gauge network and potential evapotranspiration figures evaluated from Chidley and Pike (1970) and the Meteorological Office were used as input. Actual evapotranspiration was derived within the model according to Grindley (1969). The resultant effective precipitation component was distributed according to the hydrological characteristics of the sub-catchment and daily groundwater recharge and baseflow components were computed. Monthly totals for the Worfe and Penk sub-catchments are shown in figures 55 and 56.

Groundwater Discharge

Under normal conditions groundwater discharge from an aquifer occurs in the form of springs, effluent seepages to surface waters and leakage into contiguous beds. The net component of flow from the semi-confining and confining strata of the Permo-Triassic aquifer was assumed to be negligible

because, under natural conditions, the net change in the water level surface is small. Consequently, the predominant outlet was assumed to be in the form of springs and seepages which appear as the baseflow component of the rivers within the area. Indeed during years of below average precipitation the baseflow component of the total runoff from the Severn and Sow catchments is approximately 80% and 60% respectively.

The baseflow component was derived for each catchment from hydrograph separation of mean daily flows where historical records were available and from linear relationships depicted in figure 24. Monthly totals were derived for both catchments (Fig.57). Finally, the component was re-evaluated by the watershed model for each sub-catchment; the results for the Penk and Worfe sub-catchments are shown in figures 55 and 56.

Artificial groundwater discharge occurs in the form of abstraction from privately and publicly owned boreholes. During the study period total abstraction ranged from 125000 to 150000 cu. m/d. Approximately 90% is attributed to the Waterboards whose pumping stations are concentrated on the unconfined aquifer. Increased demands have been supplemented by additional sources of supply and abstraction rates at individual stations have remained virtually constant. For comparative purposes abstraction has been expressed as a depth per unit area and is illustrated in figures 55 and 56.

Historical Groundwater Levels

Introduction

Although historical groundwater level fluctuations are not considered during the simulation of the dynamic behaviour of the aquifer they are important to the calibration procedure. The spatial distribution of historical water levels is used to initialise heads at the start of dynamic equilibrium runs and to simulate hydraulic gradients across head controlled boundaries.

Initial Groundwater Levels

Initial nodal water levels for dynamic equilibrium runs were derived from average water level conditions for the study period (Fig.30). Initial water levels for simulation runs were evaluated by recycling an average year's net recharge until successive annual water level variations were identical (Rushton and Wedderburn 1973).

Historical Groundwater Level Fluctuations

Typical water level fluctuations for the unconfined and semi-confined areas indicate that maximum levels are attained in March/April and minimum levels in October/November (Fig.58). Although groundwater recharge occurs predominantly during the winter months (October to March) increments are detected during the summer period also. They are represented by either secondary maxima superimposed on the recession curve or by sudden reductions of the rate of recession.

Mean annual fluctuations in the unconfined aquifer range from 1 to 2m and in the semi-confined aquifer from 3 to 5m. A regional decline of the water table occurred between 1961 and 1964 and although recovery commenced during 1965 levels did not attain pre-1961 values until 1969. From 1969 onwards mean annual water levels were fairly consistent.

A lack of suitable observations in the confined region and the apparent complex interaction between the main aquifer and numerous aquitards within the Lower Keuper Sandstone Formation, prevented a suitable water level record being formulated for the confined aquifer.

CHAPTER SEVEN

CALIBRATION AND VERIFICATION OF THE GROUNDWATER MODEL

Introduction

The previous chapters are involved primarily with the collection and analysis of hydrological and hydrogeological data in preparation for the calibration of a groundwater digital model. The accuracy and therefore the value of the simulation model in aquifer management depends upon the quality and quantity of these data and upon a correct application of the finite difference techniques. Indeed, unsuccessful simulations are usually a function of poor quality data and a lack of insight into the dynamic behaviour of the groundwater regime and its associated recharge and discharge areas. Therefore, use was made of any sources of data that would allow the necessary hydrogeological constraints to be evaluated for the calibration procedure.

The objective of the calibration procedure is to match the predicted water level fluctuations with those recorded in the field. This involves a systematic adjustment of aquifer variables and parameters until the correct response is obtained. Success has been achieved by calibrating in an arbitrary manner (Lovell 1972) and therefore extreme caution was exercised to ensure that each parameter and variable remained within the realms of hydrological reasoning.

A polygonal network was used to divide the aquifer spatially and the characteristics associated with each node were average values for the surrounding element. Time was also considered as a discrete function and at the end of each time increment during the simulation a water balance was pursued for each node. This was achieved by a systematic adjustment of the water levels until each node and subsequently the total aquifer balanced within an acceptable tolerance.

The Digital Model

Introduction

The theoretical background to the development of the digital groundwater model and its associated data requirements are discussed in chapter three.

Model Construction

Once the model boundaries were defined and the area of study was outlined the nodal network and the associated polygonal elements were constructed. A coarse, eighteen node model was constructed initially because of a lack of readily available data (Fig.59). As more data were obtained, resulting in a better understanding of the hydrological regime, a finer meshed network of 103 nodes was considered (Fig.60).

External nodes are required to simulate boundary flow conditions. During initial simulation runs the response of the system was unpredictable and correct boundary flow conditions were maintained by imposing constant hydraulic gradients across head controlled boundaries. As such they were independent of internal water level fluctuations and realistic boundary configurations were maintained at all times. During subsequent simulations the model's calibration improved and it was possible to utilise historical water level fluctuations at the boundary nodes.

Each internal node has the ability to simulate a change in aquifer conditions between two states and as such two storage coefficients are required. The coefficient operative at any one time is dependent on the current water level and therefore the levels at which hydraulic discontinuities occur have also to be determined. In this study unconfined, semi-confined and confined aquifer types were recognised and the corresponding boundary horizons have been defined (Fig.15).

Groundwater movement between adjacent nodes is a function of the permeability and saturated thickness of the aquifer. Transmissibility evaluations have therefore to be evaluated for each link between the internal

nodes and, in the vicinity of head controlled boundaries, additional evaluations are required between the internal and external nodes. Each value is assumed to be representative of the intervening portion of the aquifer. Initial simulations assumed that each transmissibility remained constant throughout the period considered. Later, as the calibration procedure progressed, transmissibilities were re-evaluated at the end of each time increment according to the computed saturated thickness.

Groundwater recharge was evaluated initially from basic surface water budget models and subsequently from a watershed model; the principal recharge area is shown in figure 61. The required hydrological components were stored on computer files and a link program was written to relate the groundwater nodal network with the surface catchments. Subsequently recharge data files which were compatible with the groundwater model were created.

The dominant groundwater discharge component occurs in the form of baseflow to the river system. This component was evaluated from historical runoff records and from the watershed model. Within the groundwater model the assumed contributary areas can either be restricted to nodes along the river courses or associated with nodes which are more evenly distributed within the catchments. The latter method was adopted for two reasons. Firstly, the groundwater component of the river systems is not derived entirely from seepages through the river beds but also from springs and seepages above the river courses (Fig.62). Secondly, the groundwater model assumes that the horizontal groundwater flow component is dominant and it is not designed to simulate vertical flow components associated with rivers which partially penetrate aquifer systems.

The main public supply boreholes account for the majority of groundwater abstraction and each station is associated with the nodal network according to the element in which it occurs. However, it must be noted that the

predicted water levels will not represent the pumped water levels. Only when the element is equal to the size of the well is the well head simulated. Otherwise, the predicted levels represent the average level for the element and their overall response is related to variations of the net recharge component.

The geometrical configuration of the aquifer is formed from a set of parameters which are associated with each node. A three dimensional picture is simulated by interpolation between each nodal link.

Time Steps

The optimum time step used during simulation runs was chosen in order to minimise the computation costs without abusing the finite difference approximations (Rushton 1973). Consequently, the time steps considered were betwen three and seven days and it was therefore essential to ensure that the input (recharge) files remained compatible with the results format in which a time step of one month was utilised. When the monthly water budget models were considered and the optimum time step was seven to eight days the nodal recharge components were simply divided into four equal increments. However, the procedure involved in the organisation of the results from the daily watershed model was more complex. The fine meshed model was utilised with a time step of three to four days and consequently each months daily recharge statistics had to be re-arranged into suitable time units. To permit the evaluation of water balance summaries at the end of each month the variation in the number of days associated with each calendar month had to be taken into account. A link program was written to form eight groups of recharge data for each month; each group was either of three or four days duration. Consequently, the predicted water levels during each month resulted from actual fluctuations of the net recharge component as they occurred during that month. It was therefore possible to compare predicted and historical water levels on a finer time scale than previously considered.

Model Calibration (1969 to 1970 inc.)

Introduction

Initial stages in the verification of the model included the collection and analysis of hydrological data. The resultant information was subsequently incorporated into the coarse (eighteen node) model. This period of study enabled the response of the system to be examined and was an opportune time to check the computerised simulation procedures and to perform minor adjustments. In particular, the dynamic equilibrium procedure was incorporated into the model and the input procedures were adapted to ensure compatibility with the input (recharge) files. In addition the data output procedures were amended and water level data files were created for contour plotting routines.

The Coarse Model

The information obtained from the hydrological investigations was incorporated initially into the coarse (eighteen node) model.

Dynamic Equilibrium: Dynamic equilibrium was attained by recycling an average year's recharge (Rushton and Wedderburn 1973). The resultant configuration of the water level surface and its temporal fluctuation are a good guide to the plausibility of the model. Consequently, as the aquifer characteristic distribution is improved, initial water levels converge towards mean historical values and water level fluctuations associated with the dynamic equilibrium cycle correspond more closely to historical fluctuations.

The Calibration Procedure: To assist the calibration procedure initial historical water levels were reset equal to the initial water levels used in the simulation run and all succeeding historical levels were adjusted to the same degree. Consequently, it was easier to compare predicted and 'historical' levels and calibration was achieved when both sets coincided.

It was necessary to run the model several times before calibration was achieved and in all thirty-four runs were required. New information had to be assimilated and, particularly in poorly documented areas, a number of hypotheses related to the groundwater regime had to be tested. It became apparent that although a measure of the imbalance in any one area could be obtained from comparison of historical and computed levels and nodal water balance summaries, the degree of correction to be applied to each of the aquifer's parameters and variables was problematical. It was assumed that incorrect nodal responses were a function of the aquifer characteristic distribution and the net groundwater recharge component.

It was decided to concentrate initially on the evaluation of surface water budgets because precipitation, evapotranspiration and runoff records were available. As such it was possible to determine the temporal and spatial variation of the recharge and discharge components with more exactitude than the aquifer characteristic distribution for which there was little readily available information.

Initially four components were considered from the surface water budget models. They were:

Input (recharge)	=	effective precipitation;
Output (discharge)	=	baseflow, surface run-off, and groundwater abstraction.

Finally the watershed model was utilised and the net recharge component was evaluated for each node.

After the recharge component had been evaluated satisfactorily the calibration procedure concentrated on adjusting the aquifer characteristic distribution. A measure of the imbalance at each node was gained from comparison of historical and predicted water levels and from consideration of the storage coefficient and surface area of the surrounding element.

Since a monthly nodal water balance is performed and, in particular, nodal gross flows evaluated, the degree of correction required can be obtained. However, problems arise in determining which aquifer characteristics to adjust and the magnitude of the adjustment. The characteristics must always remain within the realms of physical reality and must correspond with the known hydrogeology or, where this is insufficient, with acceptable hydrogeological reasoning. In addition, it should be noted that nodal responses are not independent actions and the effect of aquifer characteristic adjustment at one node spreads out radially to all nodes.

In general, long term water level trends within an element are a function of the nodal transmissibility interconnections, whereas seasonal fluctuations are dependent upon the storage coefficient. Initial calibration runs were therefore concerned with adjusting the transmissibility network to obtain acceptable water balances at each node. Indeed it was the calibration of this characteristic which was responsible for the majority of the calibration time required. Transparent overlays were used to help depict regions where water levels showed continuous upward and downward trends in order that the appropriate transmissibility links were adjusted. Where possible, nodes with an excess of water were relieved in such a way as to compensate those with a deficiency. Otherwise, where adjustments were not obvious, a number of transmissibility networks had to be tested. Particularly in poorly documented areas values had to be estimated from the hydrogeological conditions that were assumed to be prevalent.

Within the Worfe and Smestow Brook sub-catchments transmissibilities in excess of 400 m^2/d could not support the regional hydraulic gradient. Water levels towards the centre of the sub-catchments showed a continuous upward trend while those on the catchment boundaries continuously declined. The high transmissibilities (500 to 1300 m^2/d) recorded in the vicinity of Roughton and Stableford were therefore apparently not representative of regional values

or indicate erroneous results. Hydraulic discontinuities apparent within the unconfined areas are associated with N.E. - S.W. striking faults which have brought strata of varying permeabilities into juxtaposition. In the vicinity of the Pattingham Fault a region of low transmissibility occurs (100 m^2/d) and this acts as a partial groundwater divide between the two sub-catchments.

Within the unconfined and semi-confined areas of the Penk and Back Brook sub-catchments transmissibilities of the order of 100 to 200 m^2/d secured satisfactory nodal balances. Only minor adjustments within this range were necessary to maintain a balance between groundwater recharge and groundwater flow across the northern boundary. In order to maintain a balance in the unconfined area of Cannock Chase and to prevent excessive water level rises in the confined aquifer, a low transmissibility unit was simulated in the vicinity of the Bushbury and Hopton Faults.

Transmissibilities in excess of 100 m^2/d within the confined aquifer resulted in a gradual but continuous decline in the piezometric surface until levels were similar to the surrounding semi-confining areas. The necessity for low transmissibilities supported the supposition that this portion of the aquifer is a low permeability unit which is partially isolated from the surrounding area.

The development of reasonable water balances was followed by the calibration of the storage coefficient network. Each coefficient was adjusted to secure correct temporal water level fluctuations. Storage coefficient factors were increased where the amplitude of water level fluctuations was too large. Similarly, values were decreased where it was required to increase the water level response. As a result unconfined values range from 0.05 in the Smestow Brook and Worfe sub-catchments to 0.03 in the Penk and Back Brook sub-catchments. Semi-confined values range from 0.03 in the south to 0.012 in the north, while in the confined aquifer values are of the order of 0.003.

In attempting to secure correct temporal fluctuations the hydraulic gradients between adjacent nodes were altered slightly. It was therefore necessary to finely re-adjust the transmissibility links to restore acceptable nodal water balances. Consequently, the calibration of both characteristics was repeated until the best match between historical and predicted water levels was obtained.

Boundary flows were simulated initially by fixing constant hydraulic gradients between the appropriate internal and external nodes but as calibration of the aquifer characteristics improved, historical boundary conditions were utilised. The original model boundary configuration proved to be satisfactory and did not have to be amended to secure calibration.

The Fine Model

A finer meshed model was constructed to ensure that simulation errors inherent in finite difference approximation models were minimised. This also enabled information to be assimilated in more detail and thus permitted a more precise simulation of the hydrological regime. Elements were strategically placed where possible to coincide with natural hydrological and hydrogeological units in order to minimise the necessity for rearrangement of the input data.

The resultant network consisted of 145 nodes of which 103 were distributed internally (Fig.60). To reduce the computation time required to reach dynamic equilibrium, starting levels were evaluated initially on the eighteen node model and subsequently transferred. The dynamic equilibrium procedure for the fine model commenced with these levels until a balance was attained. This ensured that errors due to interpolation between the coarse and fine model had been eliminated.

Only minor adjustments to the aquifer characteristic distribution were necessary to secure adequate nodal water level responses for the calibration period. The resultant distributions were in general agreement with the upper and lower bound values forwarded from previous hydrogeological investigations

(Figs. 63, 64 and 65). It was therefore assumed that the model calibration was complete.

Model Verification (1960 to 1972)

Introduction

To verify that the calibrated model could simulate regional groundwater flow conditions a thirteen year historical period (1960 to 1972 inc.) was considered on the fine meshed network. Dynamic equilibrium was attained in the usual manner and historical water levels were adjusted accordingly. The net groundwater recharge component was evaluated by the watershed model and subsequently rearranged into a suitable format.

Results

The resultant predicted hydrographs for the unconfined and semi-confined areas compare favourably with the historical record (Figs. 66, 67 and 68). Within the confined aquifer no historical record is available but predicted seasonal and long term water level responses were small.

Conclusions

The model is calibrated sufficiently to simulate regional groundwater flow conditions as they are presently conceived. The associated best fit parameters and variables are however restricted by the response of the system during the study period and are a function of the quality and quantity of the available data. Consequently, when more information becomes available it may be necessary to update the model.

CHAPTER EIGHT

CONCLUSIONS

During the primary phase of hydrogeological investigations maximum benefit must be gained from existing records. Analytical techniques were therefore developed to utilise the considerable volume of data which had been collected by the various Water Authorities and government scientific establishments. From the resultant information it was possible to formulate an understanding of the hydrological regime within the area of study. This process enabled the necessary parameters and variables to be defined for the groundwater model and, in poorly documented areas, enabled intuitive interpolation. During the calibration procedure the groundwater model itself acts as an analytical tool which can be utilised to test the feasibility of hypotheses related to the groundwater regime. In particular, several transmissibility distribution networks were considered and the 'feed back' of results allowed poorly documented areas to be outlined.

The validity of the calibrated model is dependent upon the 'best fit' parameters and variables which in turn are a function of the quality and quantity of the original data. Since the objective of this investigation was to secure regional groundwater responses by utilising the existing data it is proposed that further field work is required, particularly within the un-developed areas of the aquifer. This secondary phase of investigation should be conducted to obtain the necessary information for simulating particular aquifer development schemes. When this has been achieved the model can be used with confidence to assist management decisions in conjunction with other hydrological simulation models.

Several hydrometric investigations are proposed in order to qualify certain aspects of the hydrological cycle within the area. They are;

(1) A water level observation network is required to determine the spatial

and temporal variation of the water level surface with more exactitude. Water level recorders would help to determine rates of recharge and aquifer characteristics in their immediate vicinity.

2) In situ pump tests are required to evaluate;

   a) the aquifer characteristic distribution in more detail, particularly where semi-confined and confined conditions exist.

   b) the degree of hydraulic connection between the rivers and the main aquifer.

   c) the extent of any hydraulic continuity between the main aquifer and the semi-permeable strata of the Lower Keuper Sandstone Formation.

   d) aquifer boundary conditions, particularly in relationship to the dominant S.W. - N.E. striking faults which are apparently responsible for discontinuities in the groundwater flow pattern.

   e) the effectiveness of marl partings in dividing the aquifer into separate units.

   f) the degree of variation of aquifer properties with depth below ground level and in particular to determine whether the entire thickness of the aquifer contributes to groundwater flow in the vicinity of abstraction boreholes.

   g) the occurrence of discrete high permeability zones in the vicinity of faults.

3) A more precise evaluation of the temporal and spatial variation of groundwater recharge is required. This could be secured by;

   a) the installation of autographic rainfall measuring devices in order to determine the temporal and spatial variation of rainfall.

   b) improved actual evapotranspiration estimates. This could be achieved by the installation of automatic climate stations,

evaporation pans, lysimeters and a more comprehensive soil use survey.

c) an improved river gauging network devised to evaluate the total runoff from small study catchments within the area.

All additional information to that previously collated will have to be incorporated into the model and the calibrated components and variables may have to be adjusted accordingly. Consequently, it may be necessary to re-calibrate the model using the techniques previously described in this study.

FIGURE 1

PRINCIPAL FEATURES OF AREA OF STUDY

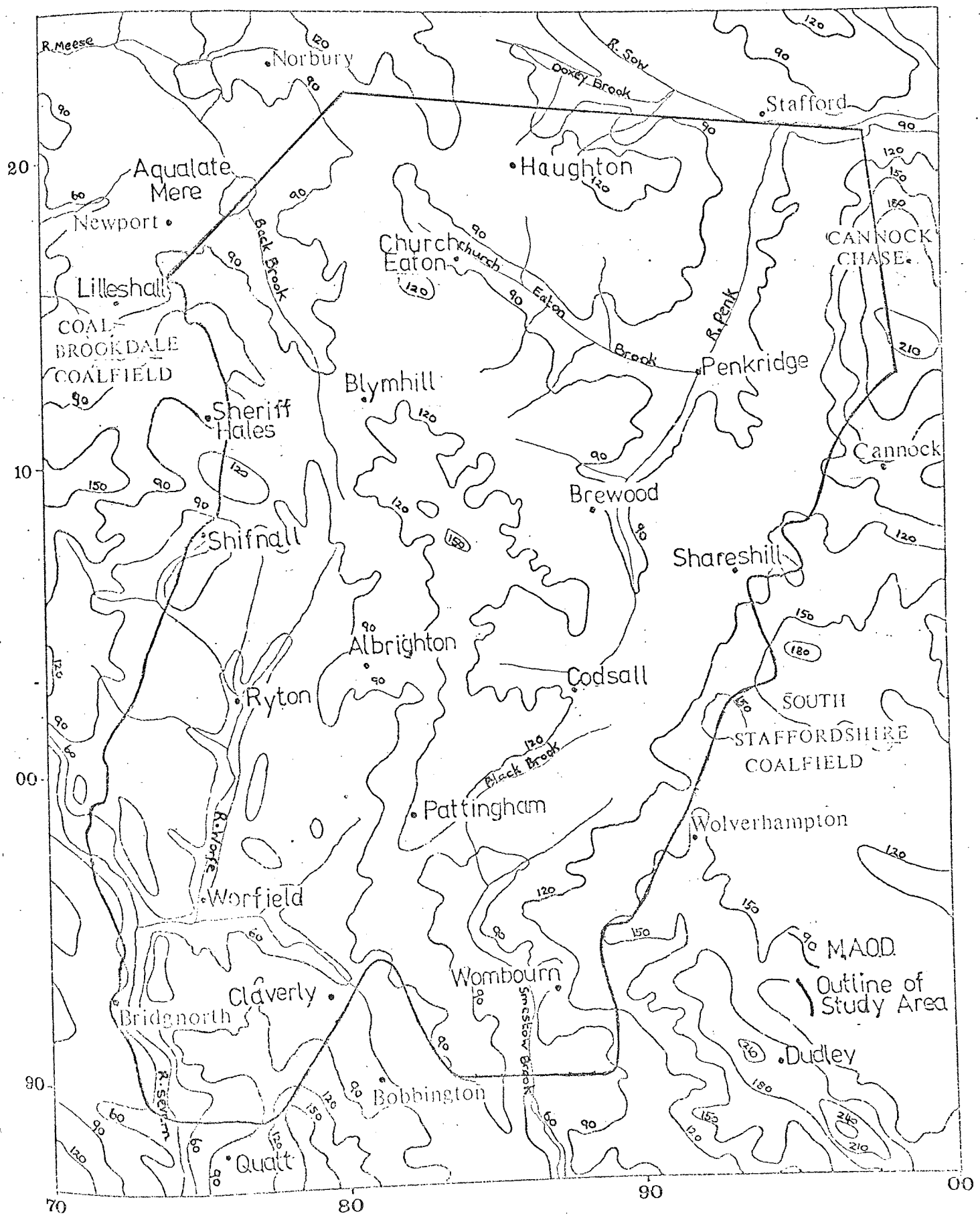

FIGURE 2

GEOLOGY OF STUDY AREA

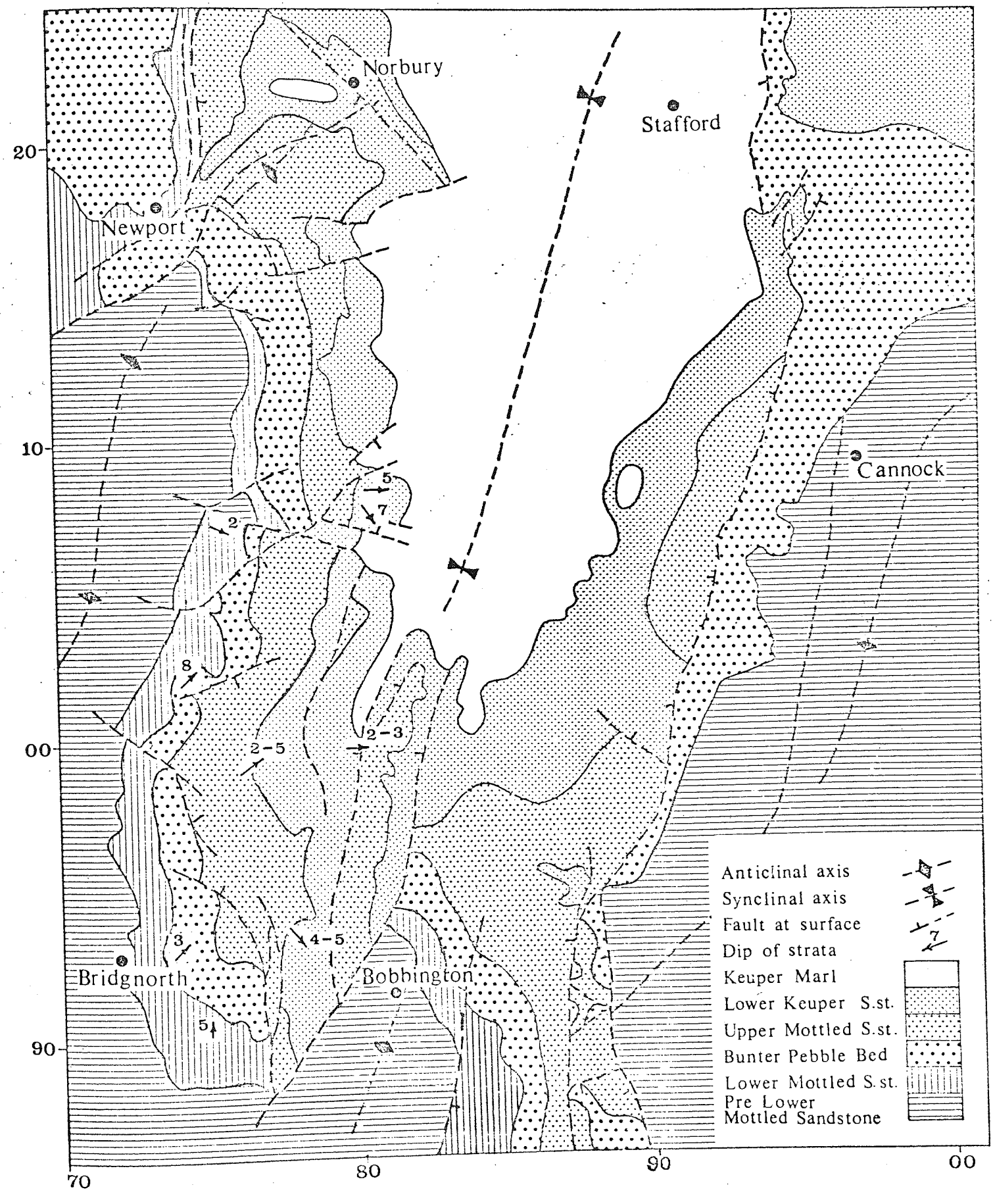

FIGURE 3

LOCATION OF SAMPLING SITES

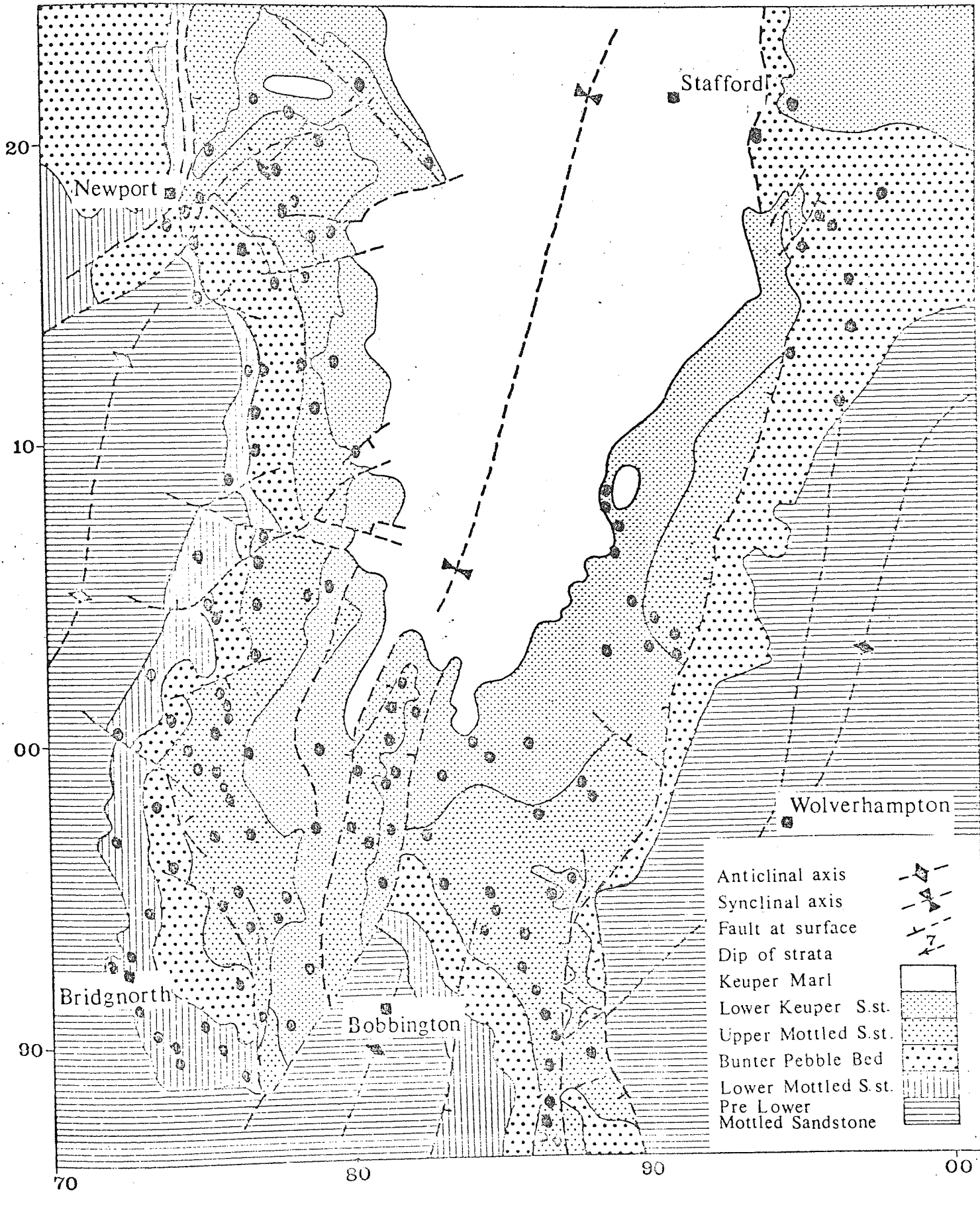

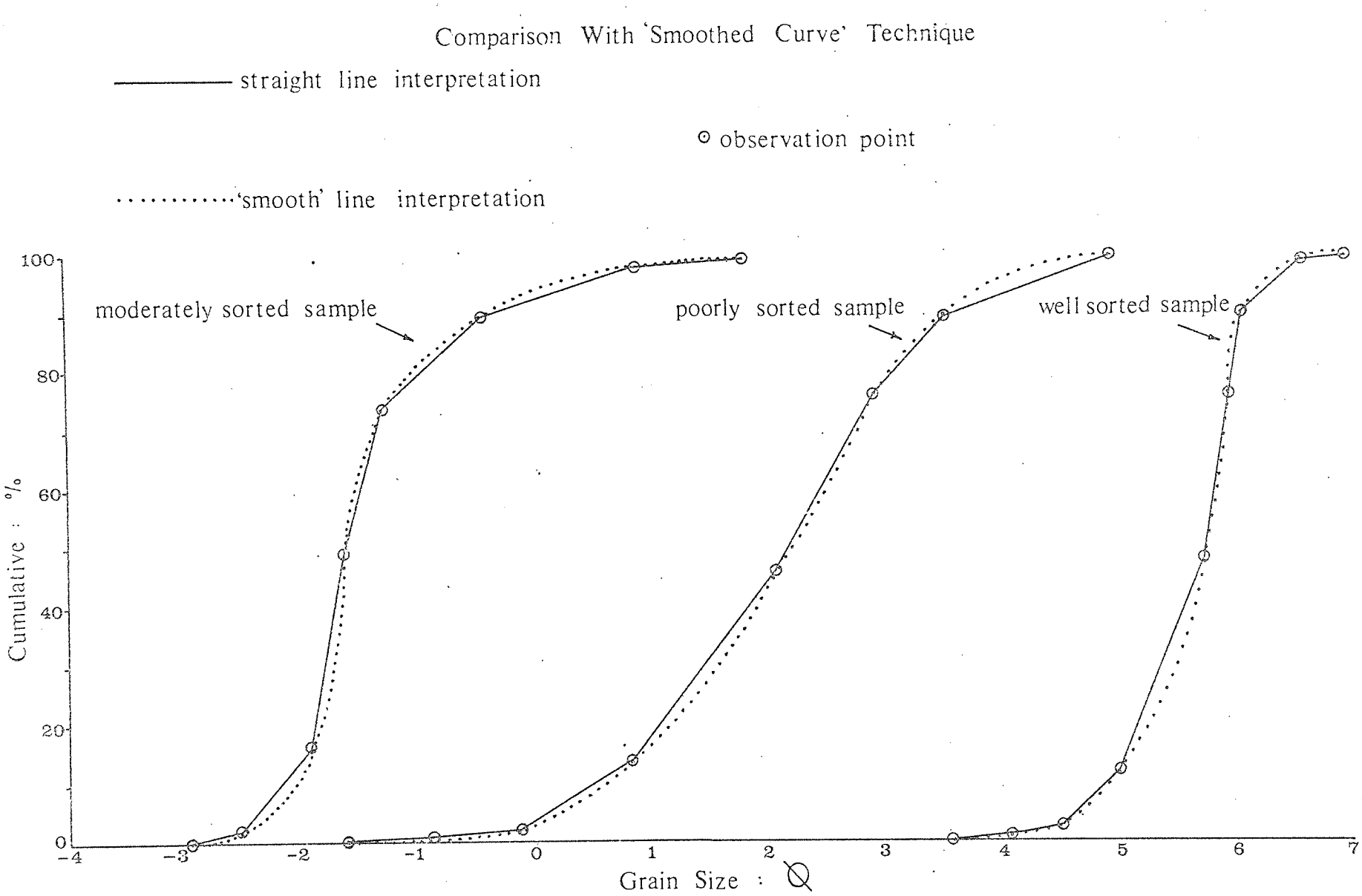

SIMULATION OF CUMULATIVE FREQUENCY CURVE BY STRAIGHT LINE METHOD

FIGURE 4

FIGURE 5

FACIES VARIATION WITHIN THE MAIN AQUIFER

Borehole Logs From Neachley Pumping Station SJ 783 067

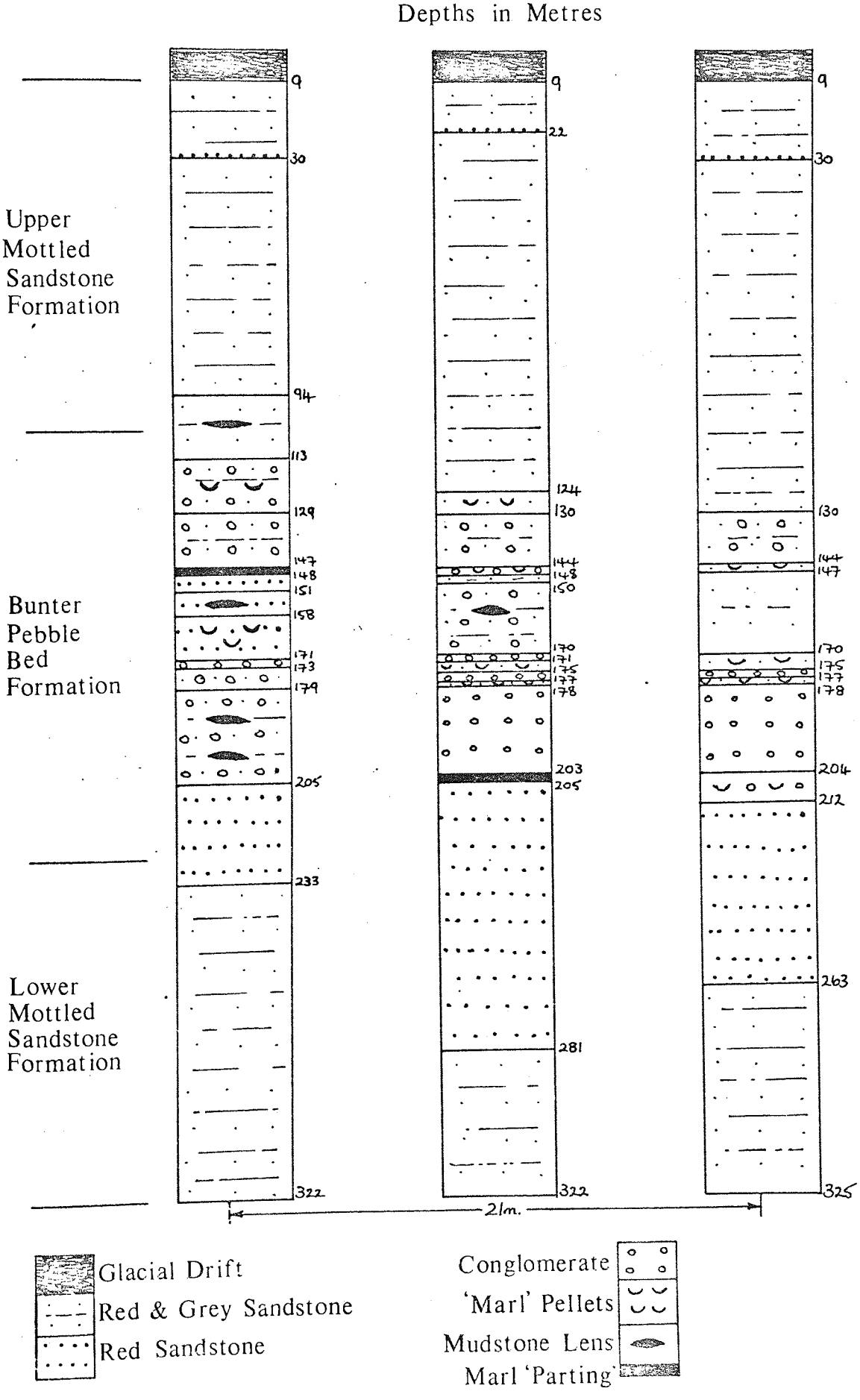

FIGURE 6

FACIES VARIATION WITHIN THE BUNTER PEBBLE BED FORMATION

Borehole log from Milford Pumping Station SJ 975 213

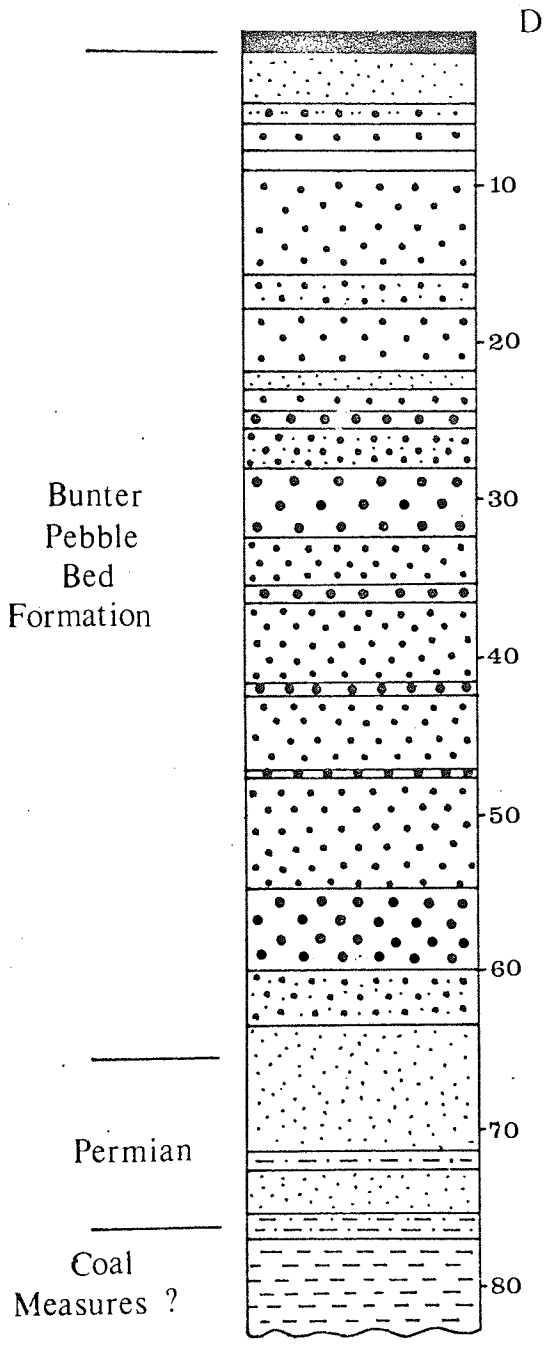

Top Soil
Sandstone
Loose Conglomerate
Cemented Conglomerate
Mudstone

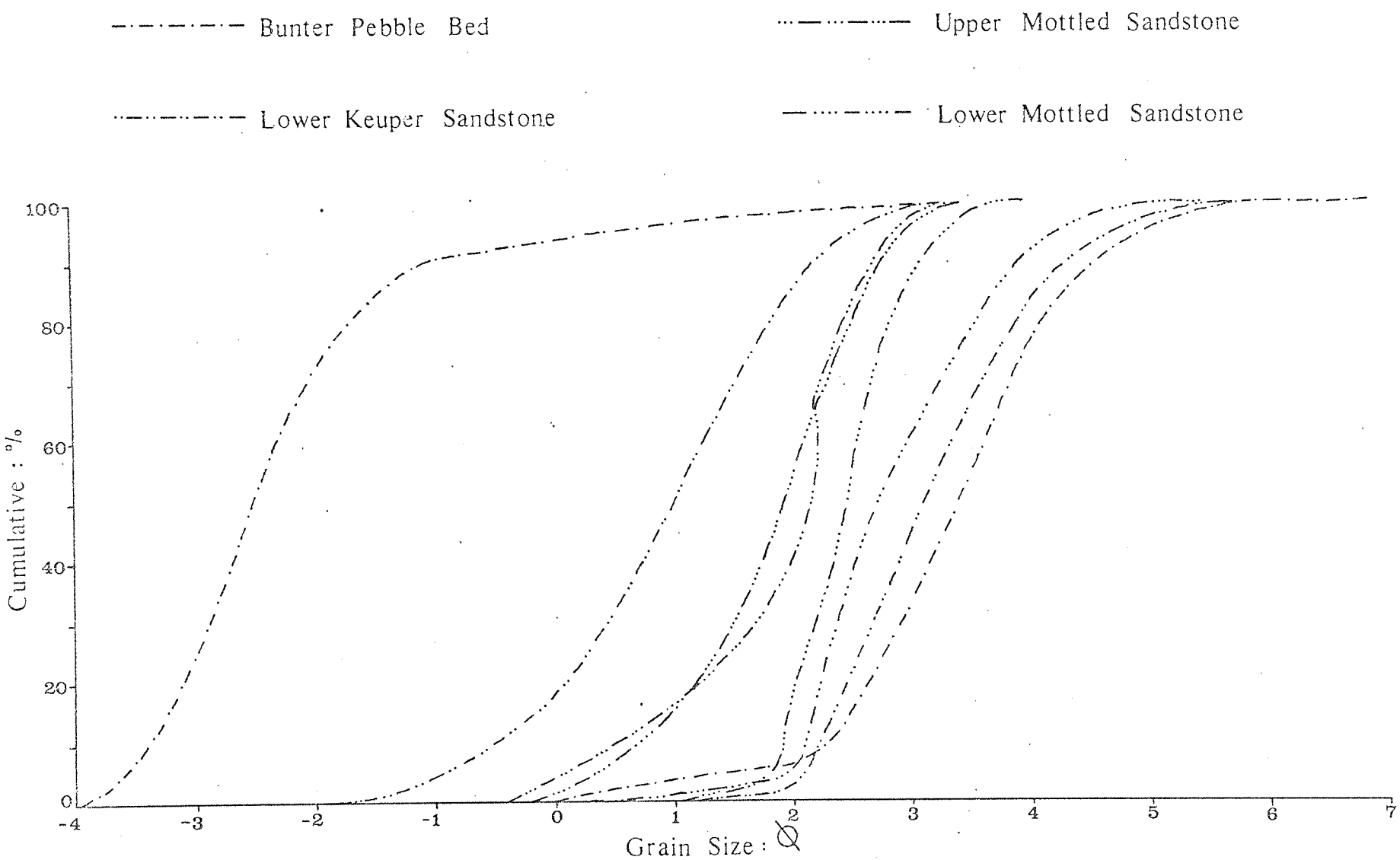

GRAIN SIZE : CUMULATIVE FREQUENCY RANGES FOUND IN EACH FORMATION

FIGURE 7

FIGURE 8

GRAIN SIZE STATISTICS

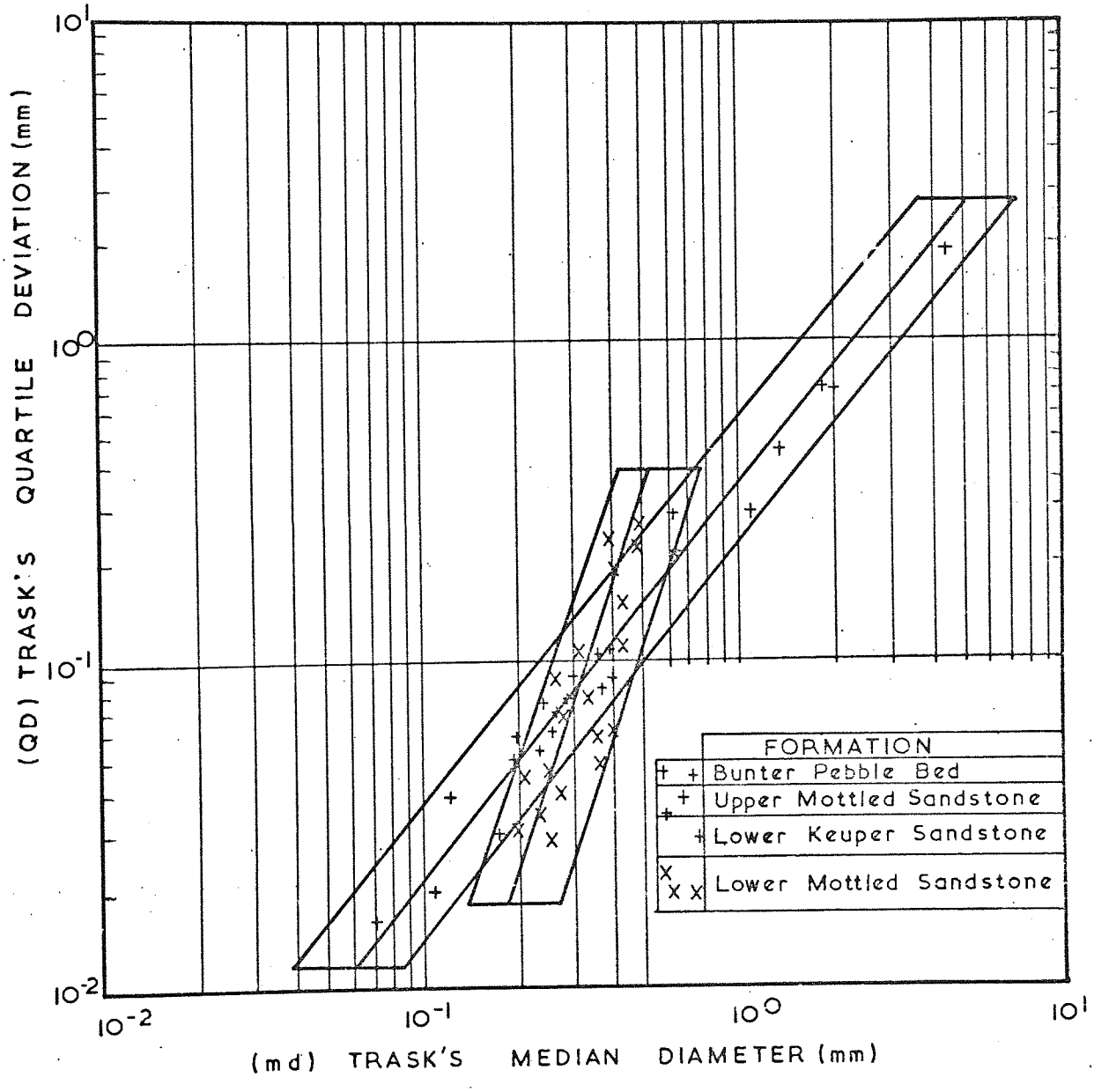

FIGURE 9

GRAIN SIZE STATISTICS

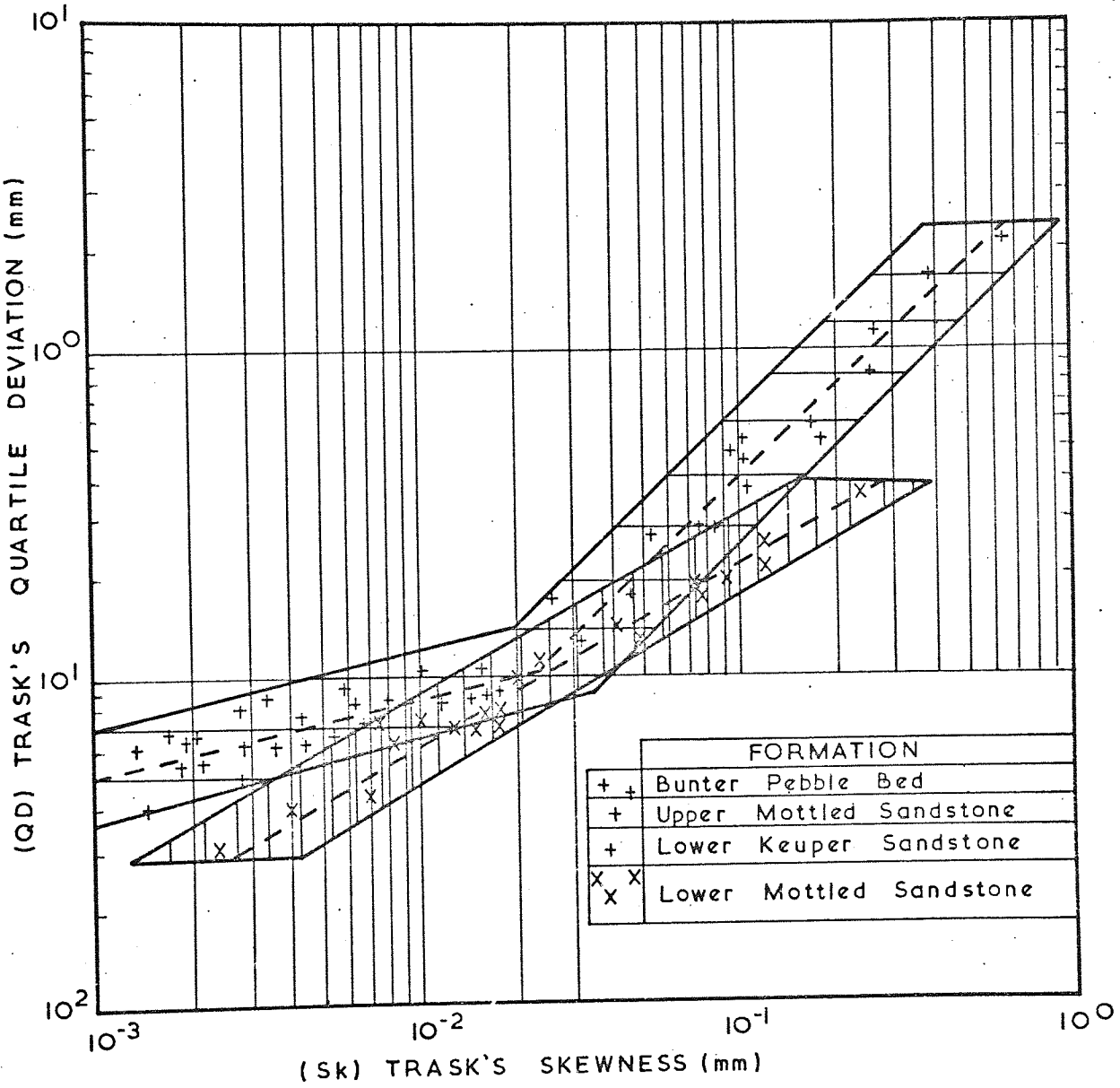

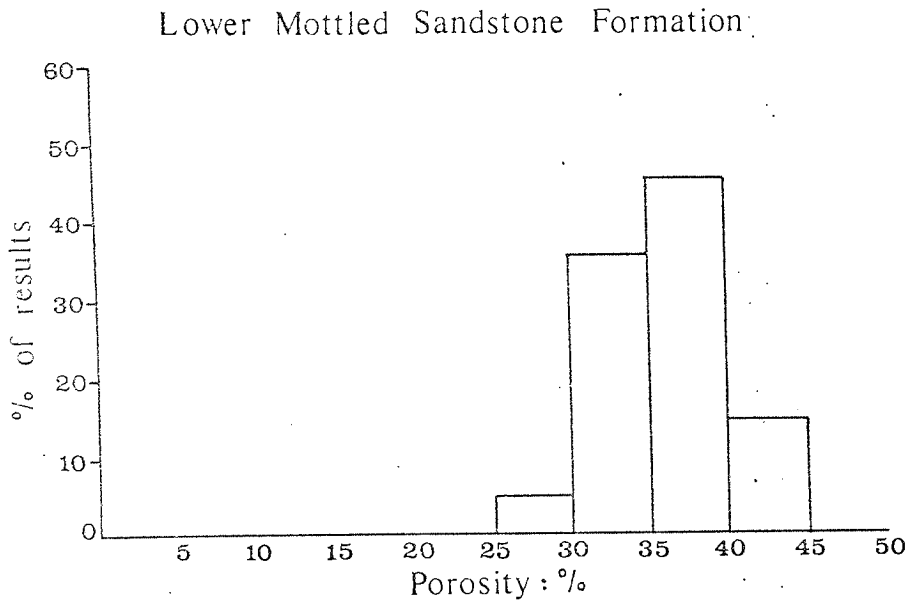

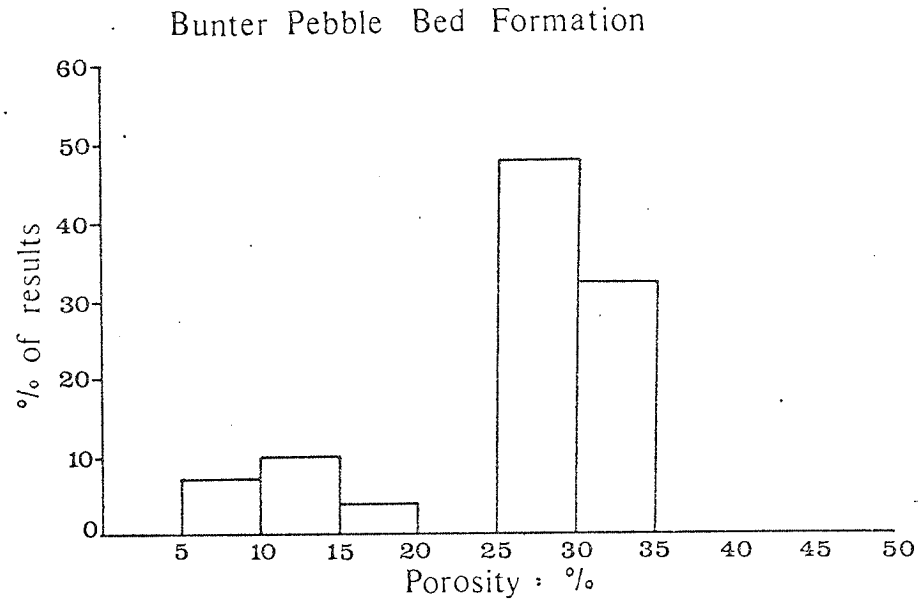

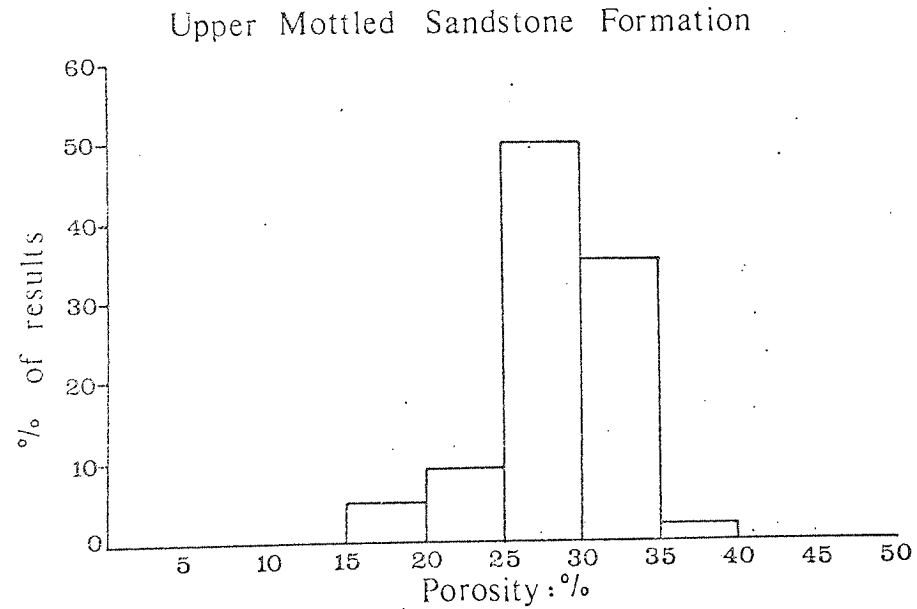

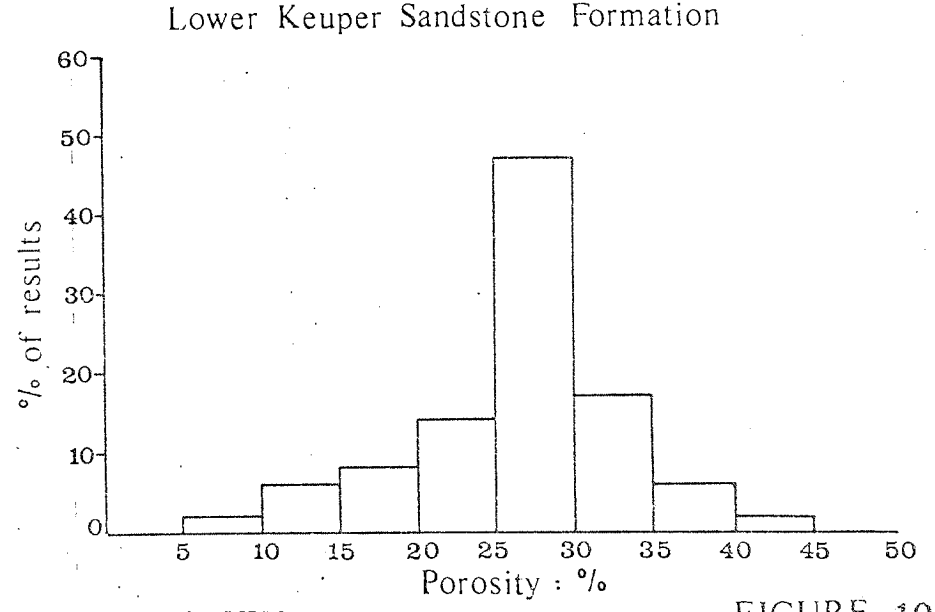

LABORATORY DETERMINATION OF POROSITY

FIGURE 10

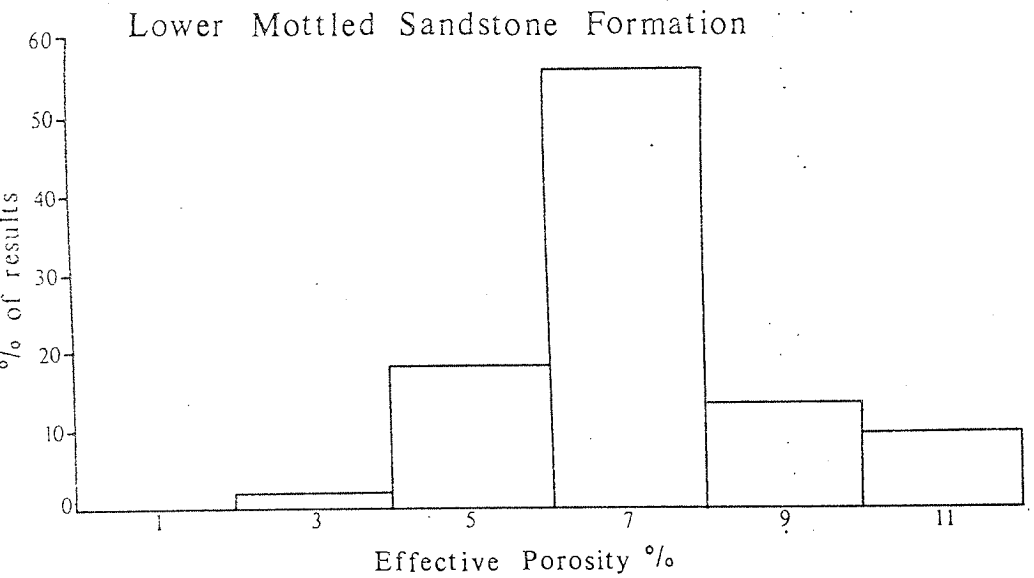

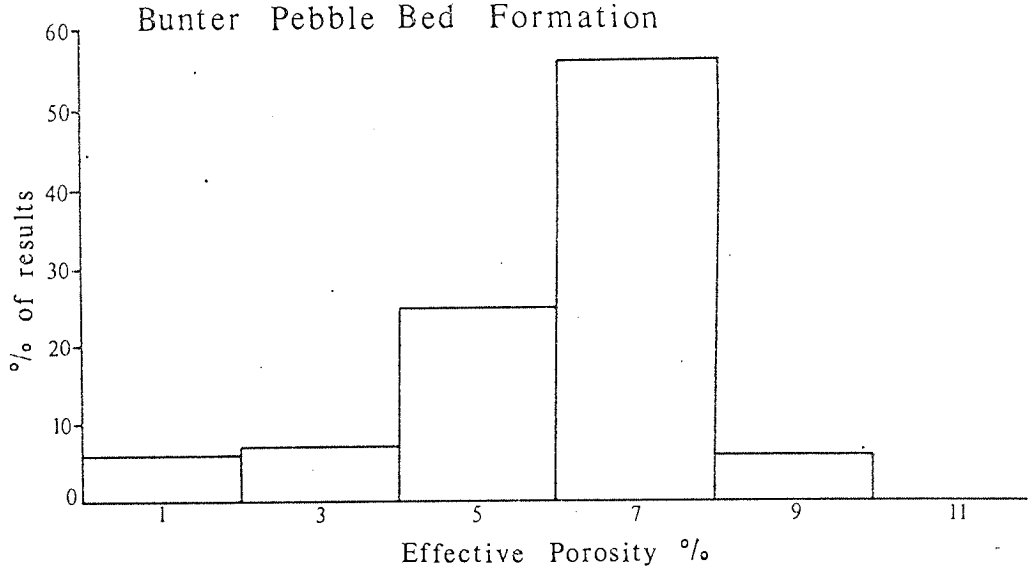

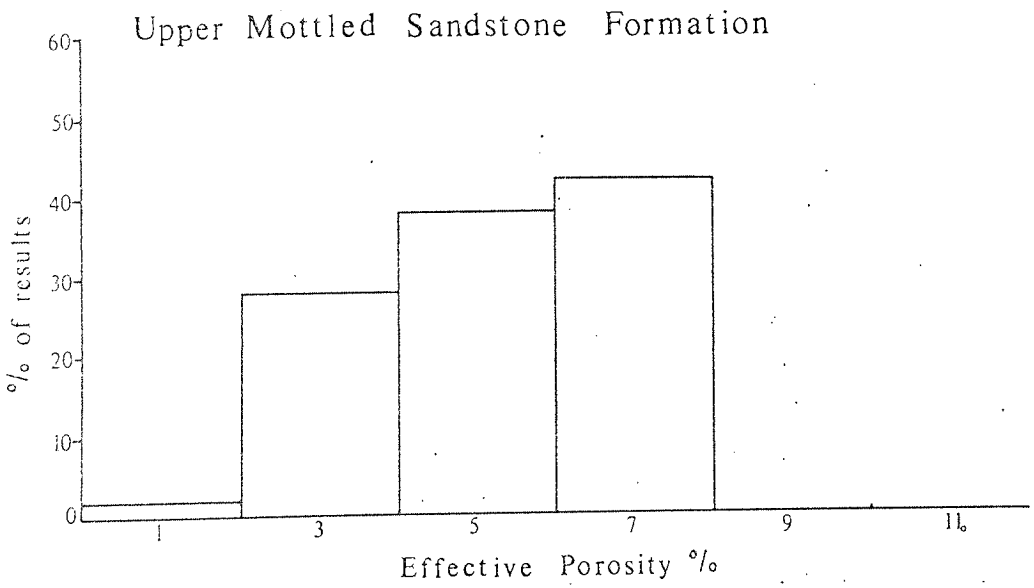

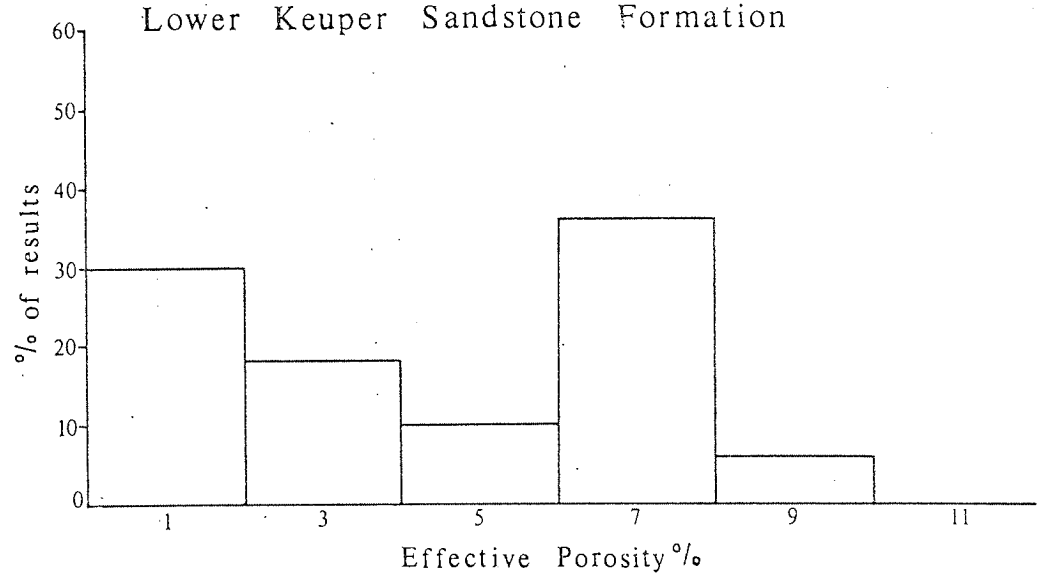

LABORATORY DETERMINATION OF EFFECTIVE POROSITY

FIGURE 11

Lower Mottled Sandstone Formation

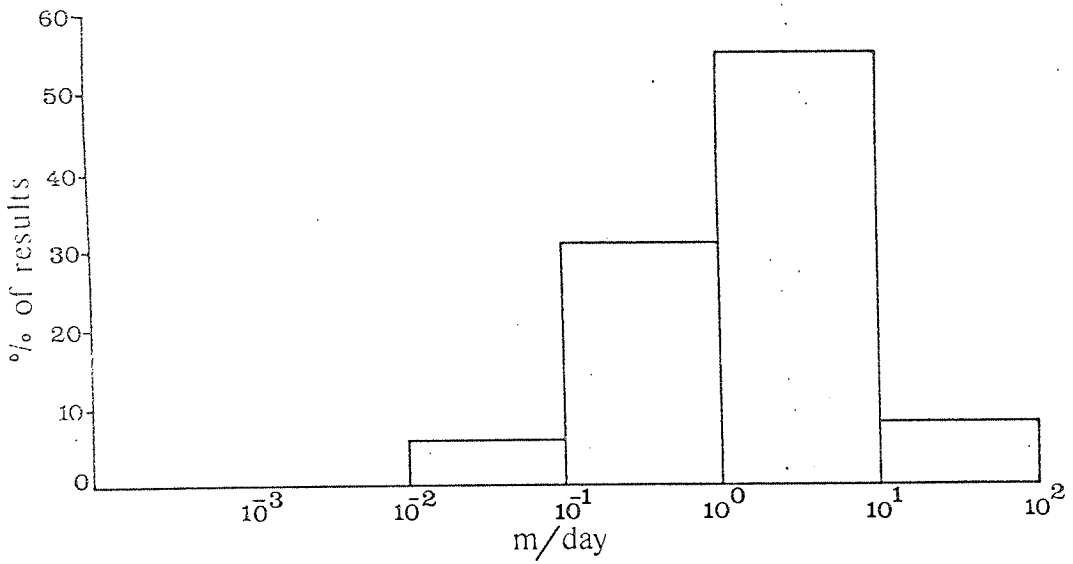

Bunter Pebble Bed Formation

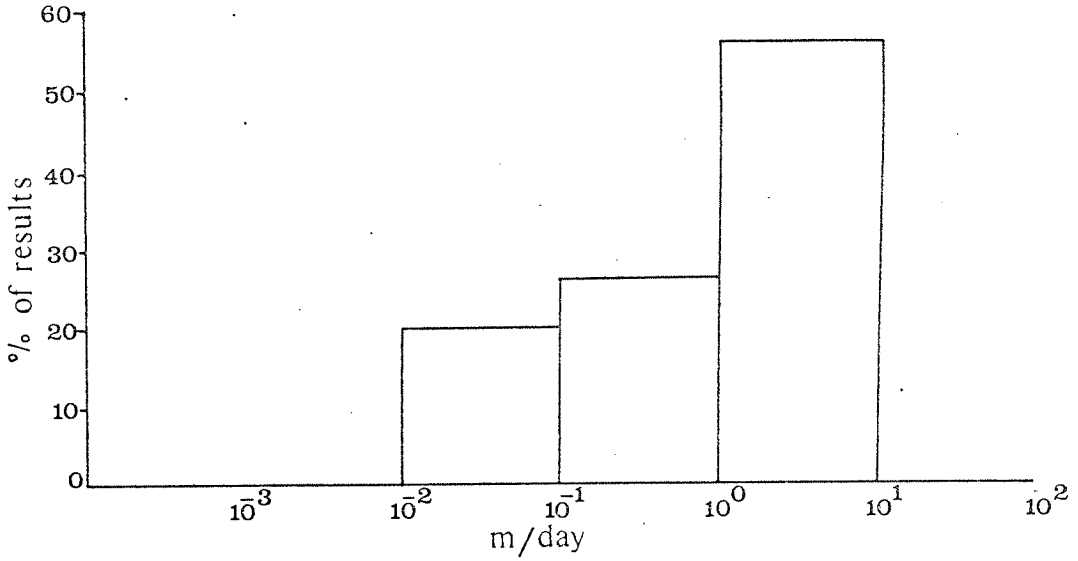

Upper Mottled Sandstone Formation

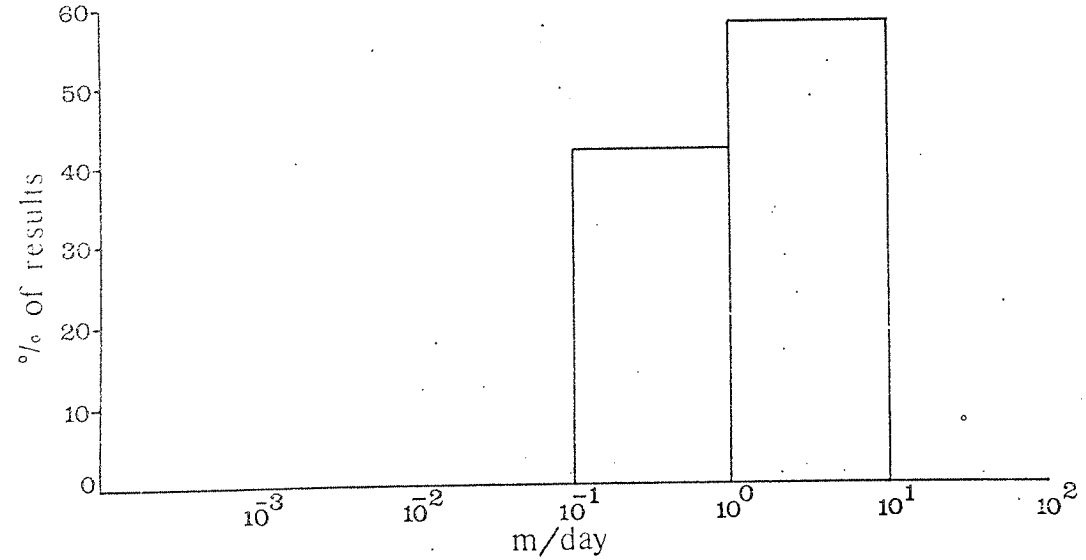

Lower Keuper Sandstone Formation

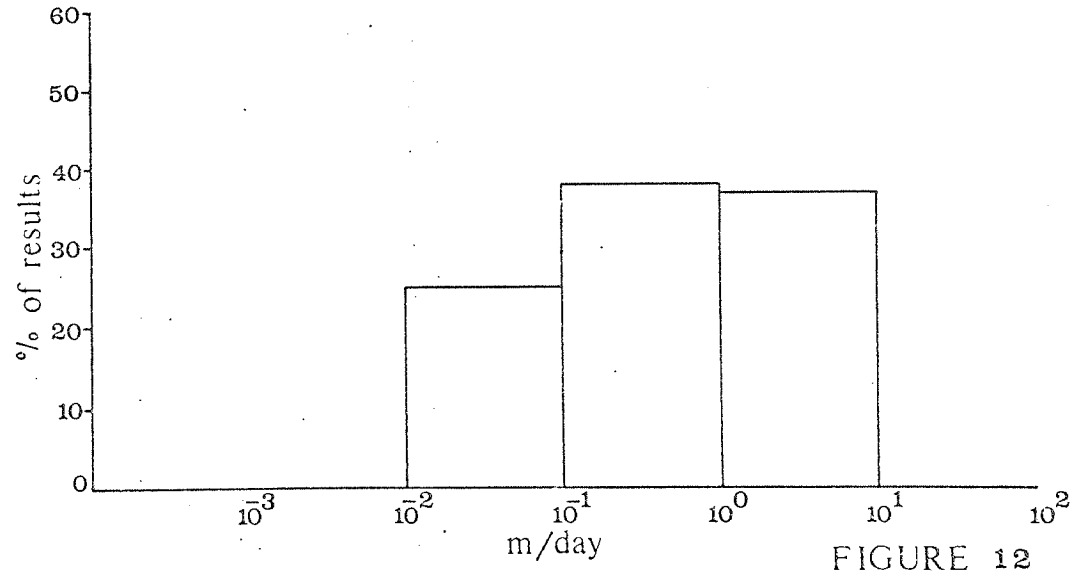

FIGURE 12

LABORATORY DETERMINATION OF PERMEABILITY

FIGURE 13

DISTRIBUTION OF SUPERFICIAL DEPOSITS

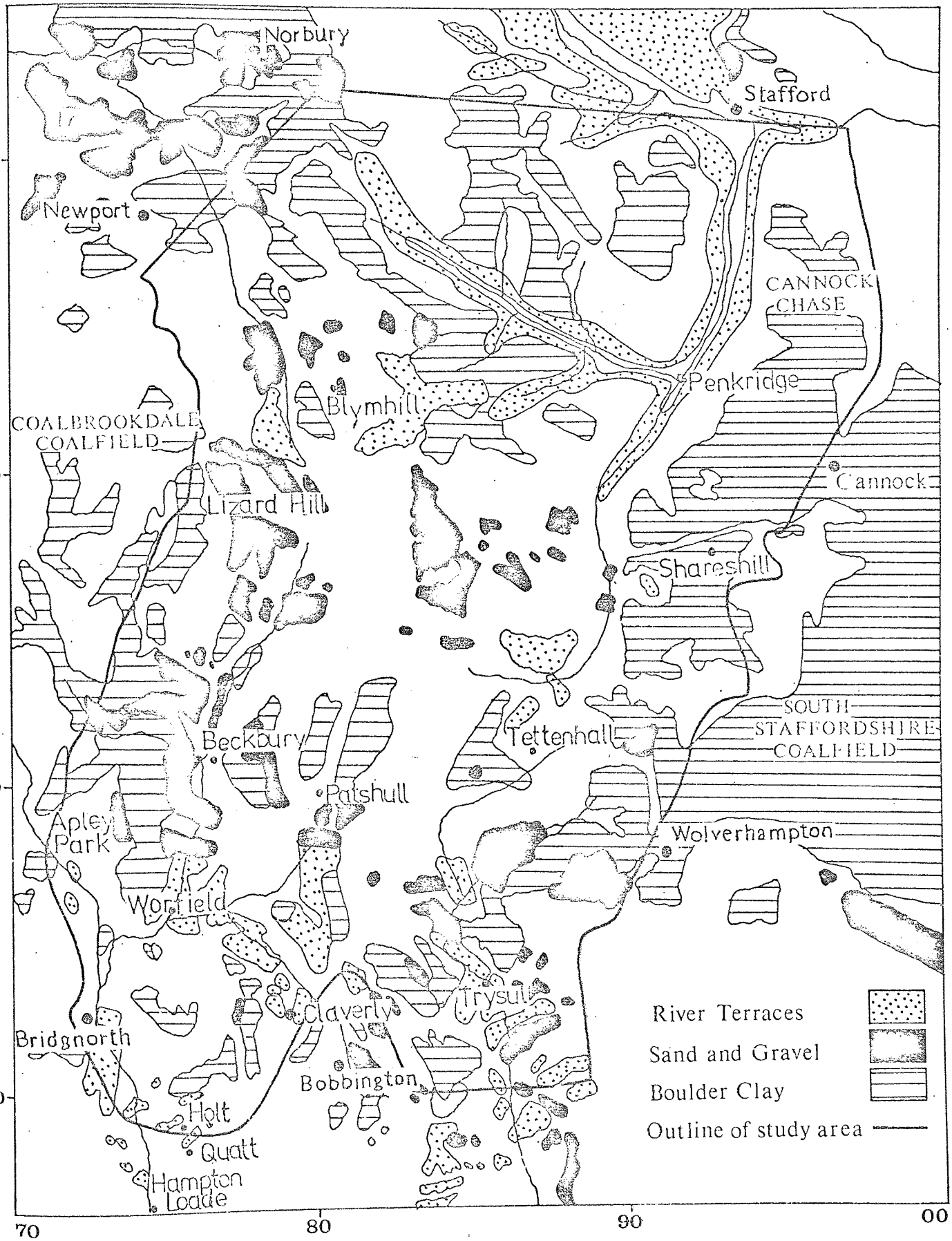

FIGURE 14

GEOLOGICAL STRUCTURE : FOLDS AND FAULTS

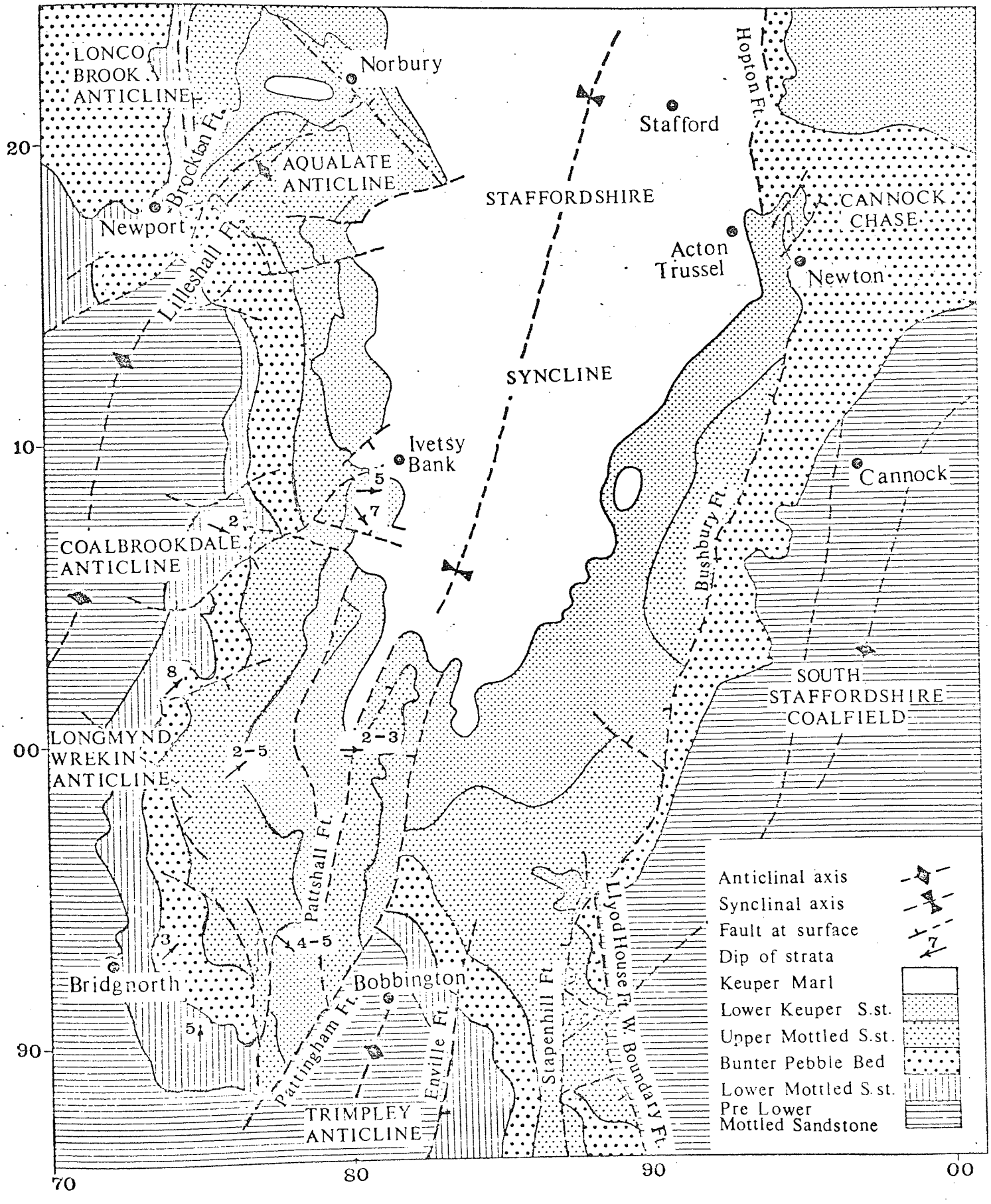

FIGURE 15

SCHEMATIC DIAGRAM OF MAIN AQUIFER CONFIGURATION

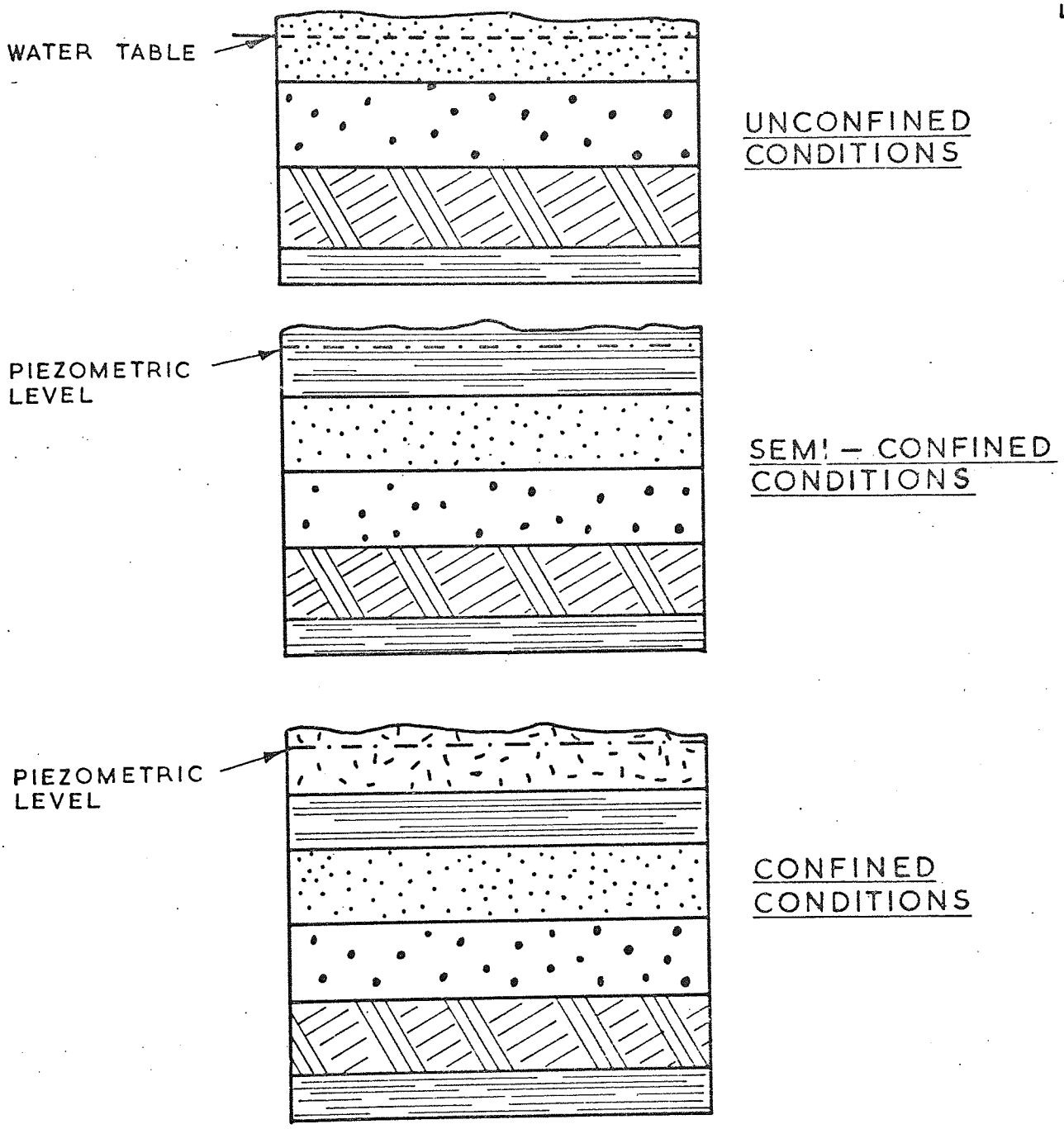

		FORMATIONS
CONFINING STRATA		KEUPER MARL
SEMI-CONFINING STRATA		LOWER KEUPER SANDSTONE
MAIN AQUIFER		UPPER MOTTLED SANDSTONE
		BUNTER PEBBLE BED
		LOWER MOTTLED SANDSTONE
CONFINING STRATA		PRE – LOWER MOTTLED SANDSTONE

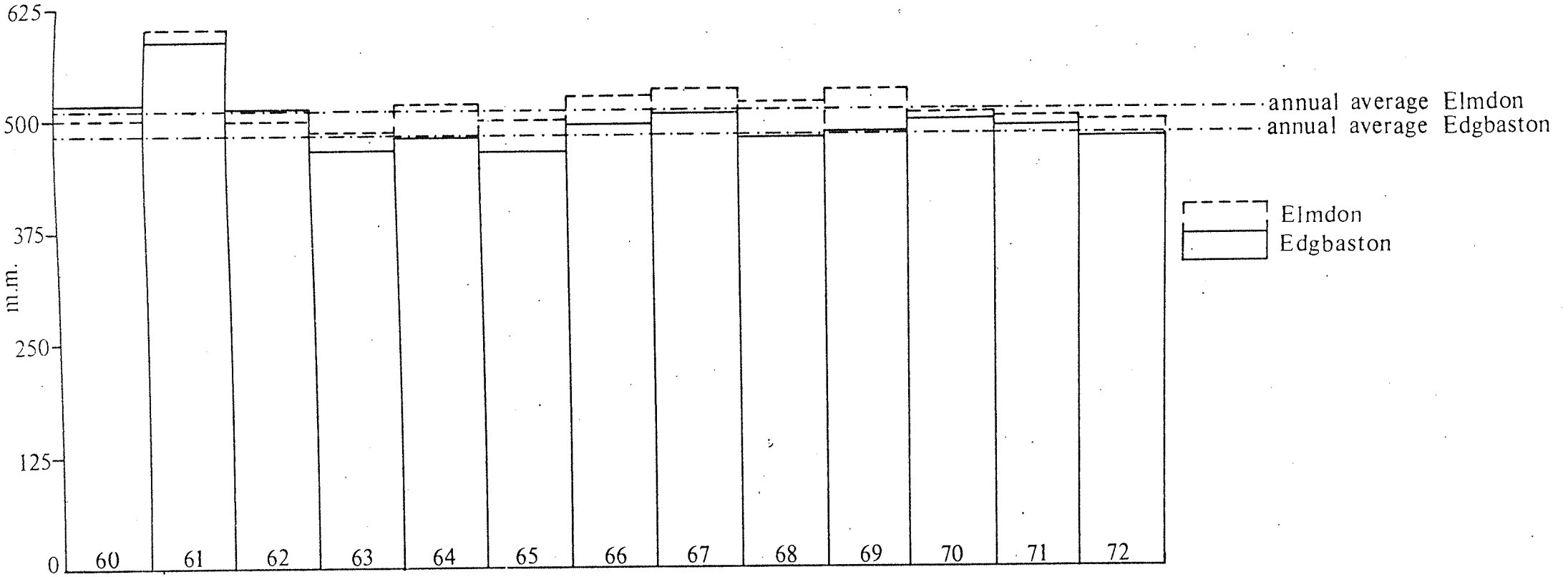

Potential Evapotranspiration : Annual Variation (1960 1972)

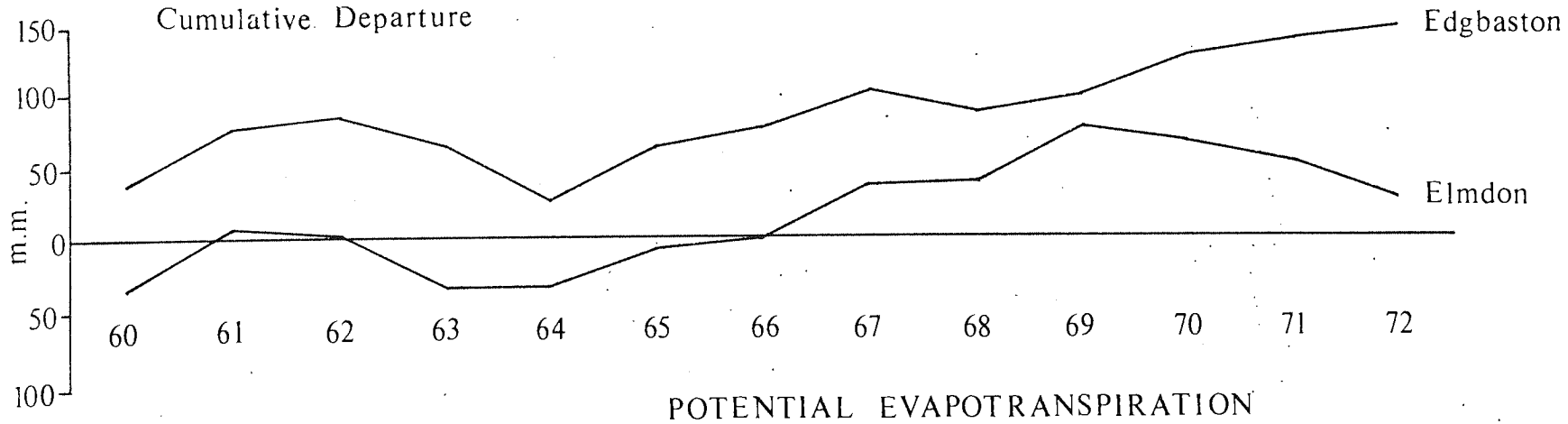

POTENTIAL EVAPOTRANSPIRATION

FIGURE 16

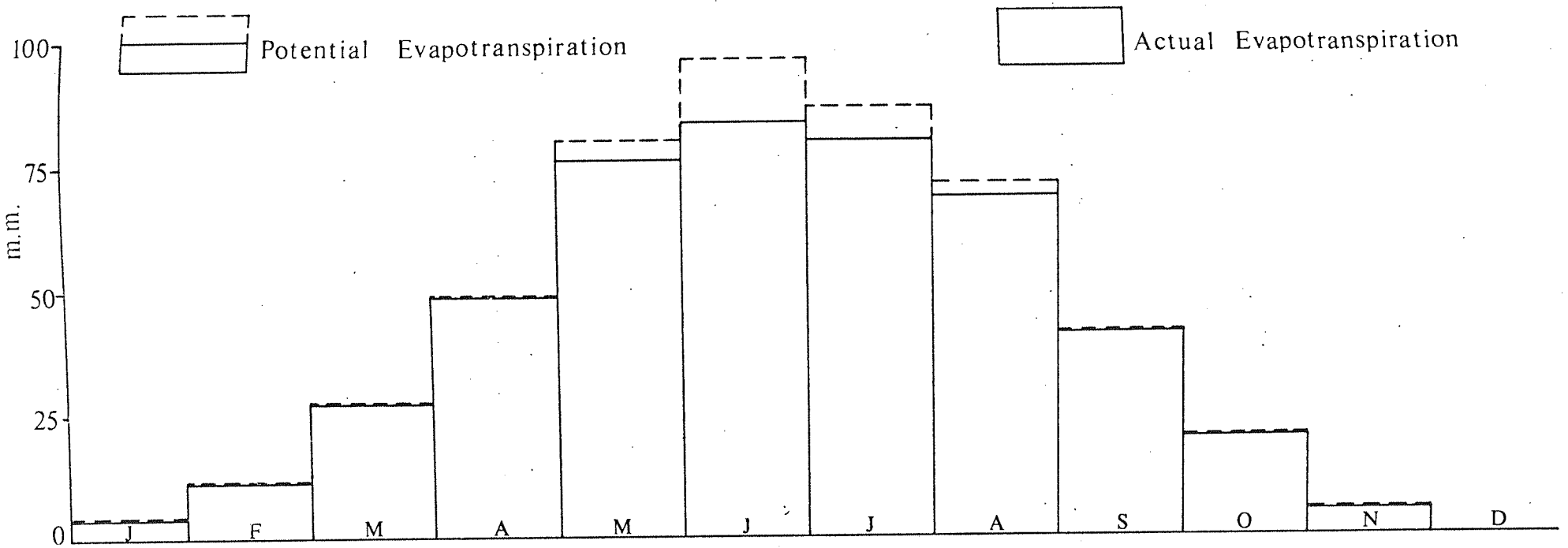

Average monthly actual and potential evapotranspiration at Edgbaston
(1960–1972)

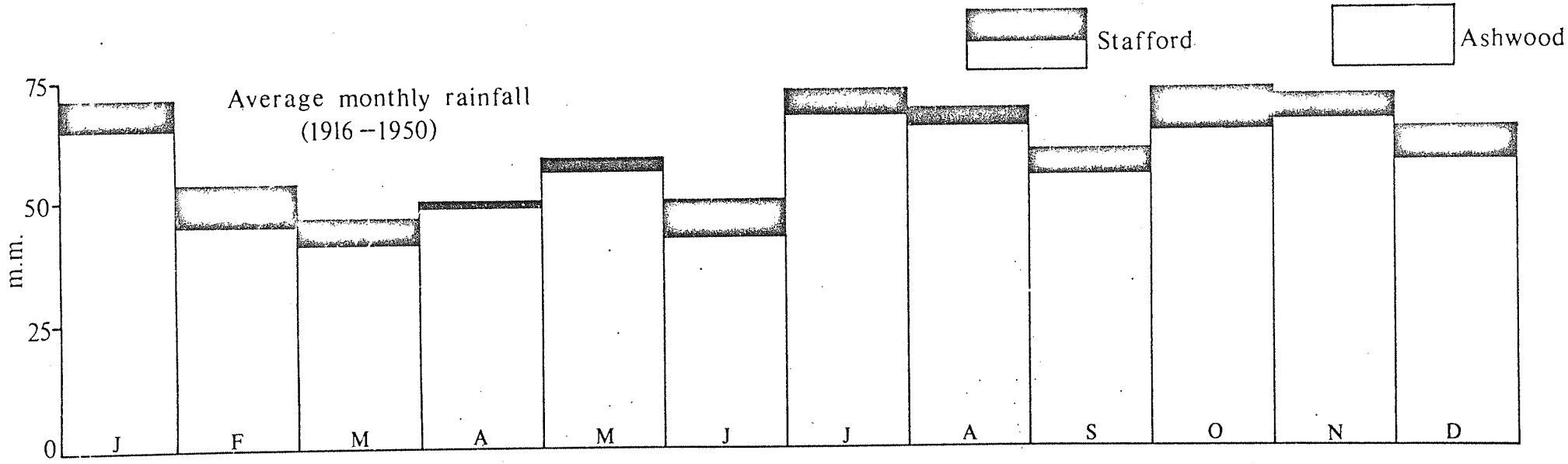

AVERAGE MONTHLY EVAPOTRANSPIRATION AND PRECIPITATION

FIGURE 17

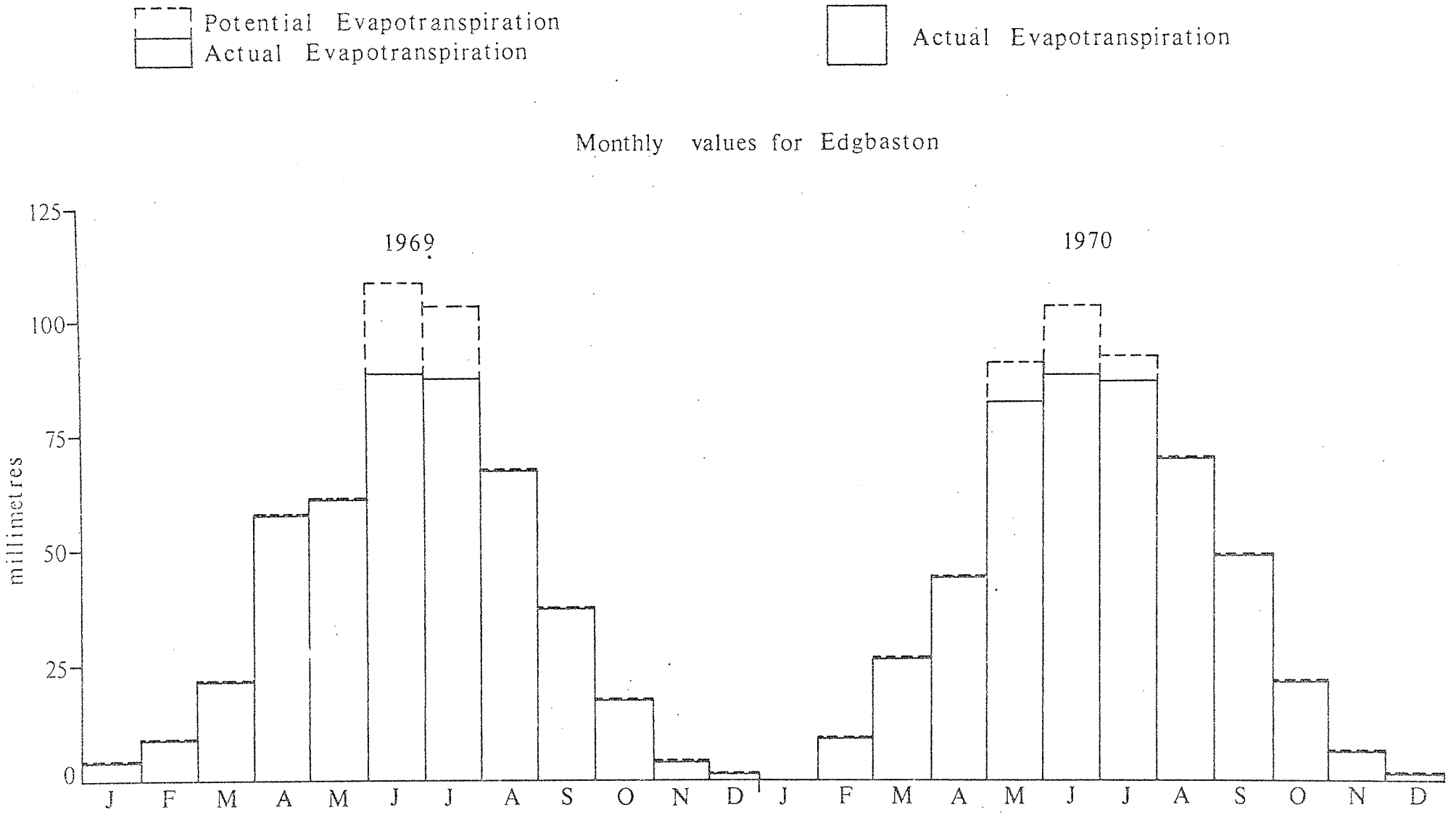

COMPARISON OF ACTUAL AND POTENTIAL EVAPOTRANSPIRATION

FIGURE 18

Monthly Figures 1960-1972 Edgbaston

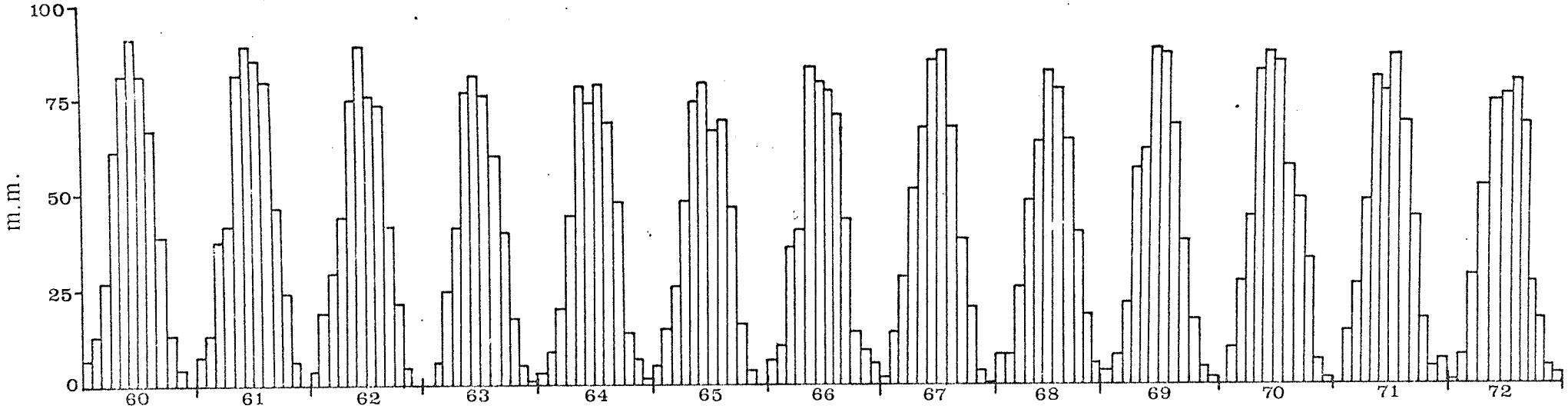

ACTUAL EVAPOTRANSPIRATION

FIGURE 19

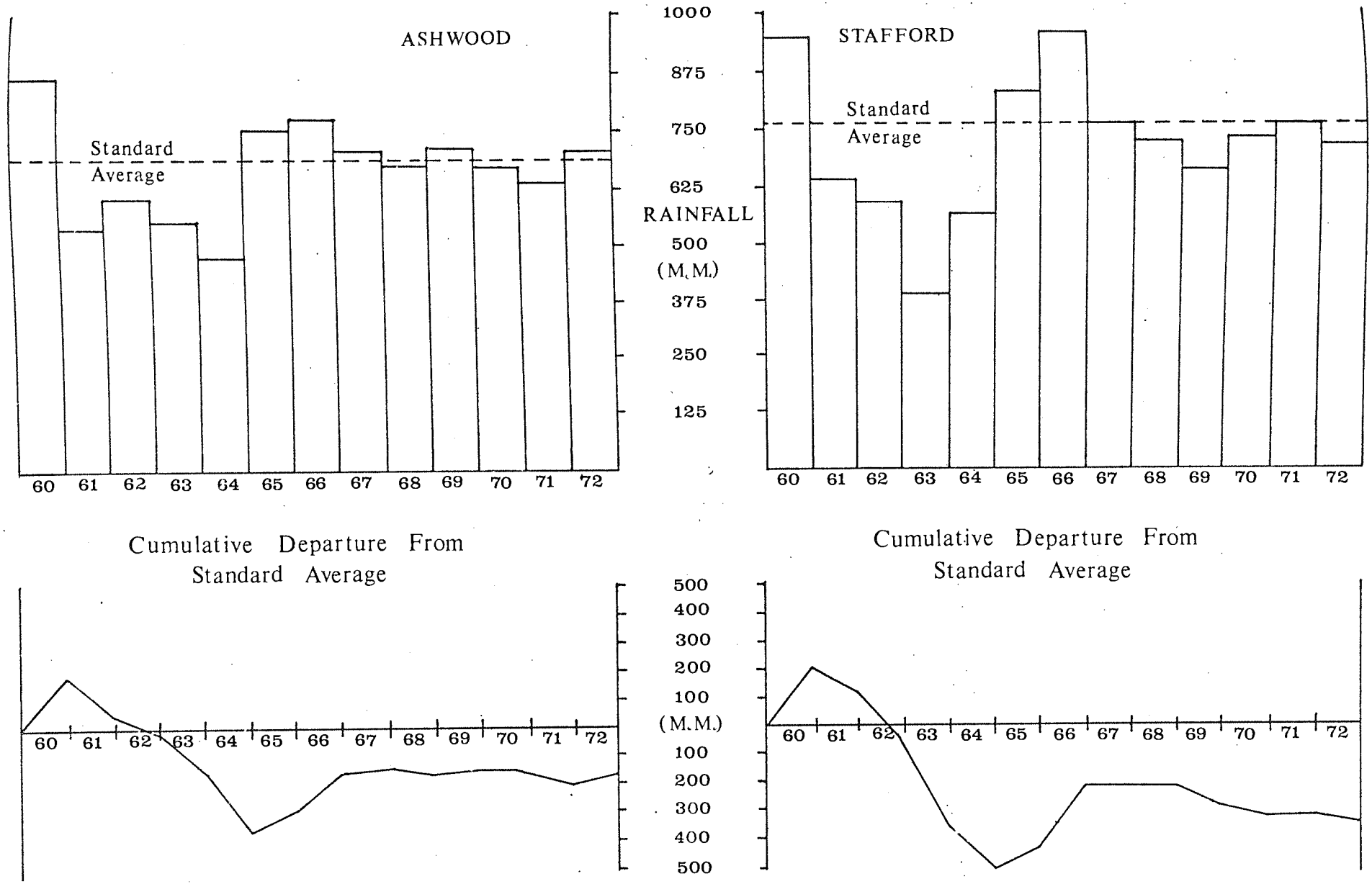

RAINFALL STATISTICS 1960-72

FIGURE 20

FIGURE 21

SUB-CATCHMENT AREAS

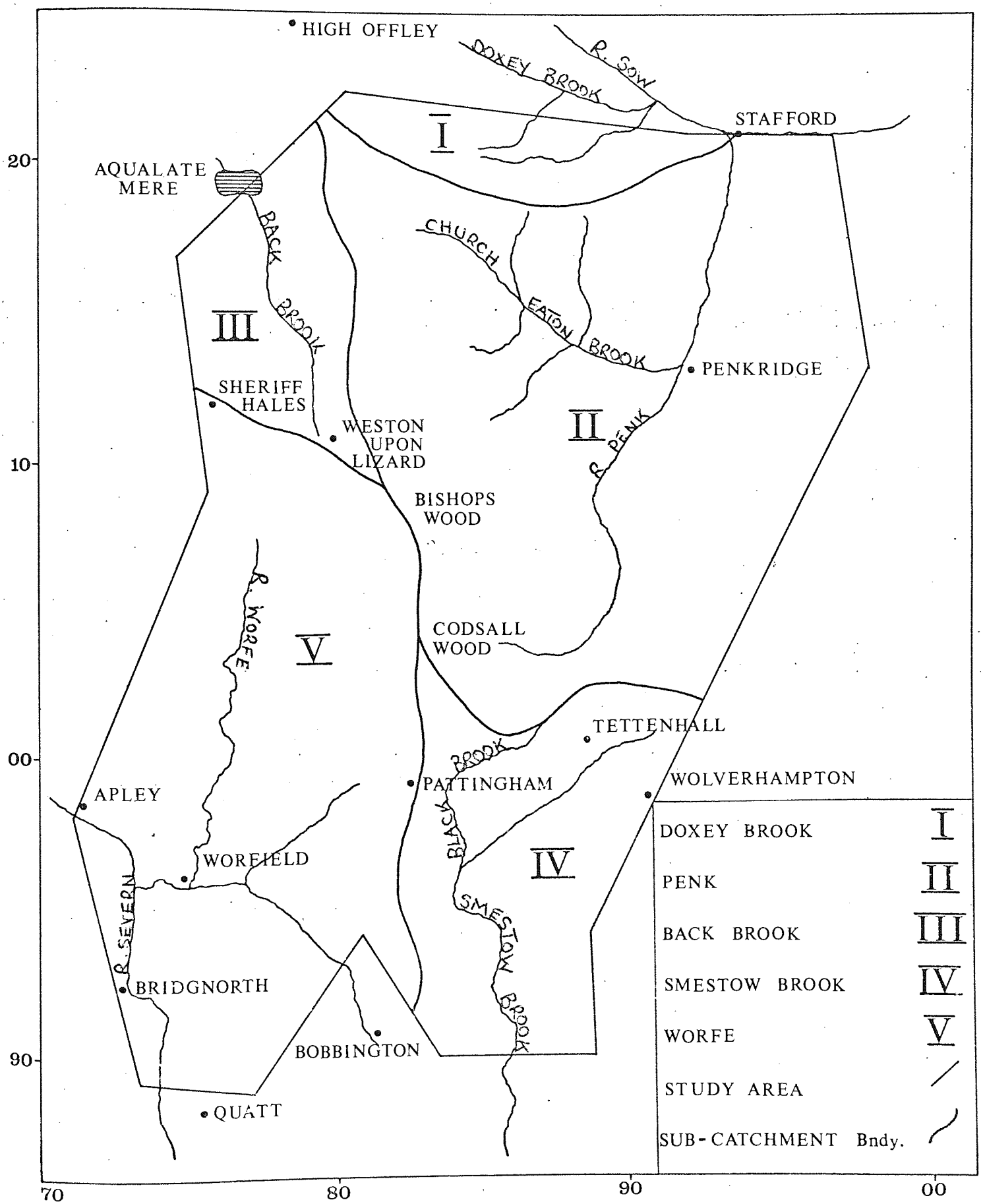

CHARACTERISTIC HYDROGRAPH COMPONENTS - SEVERN AND TRENT CATCHMENTS

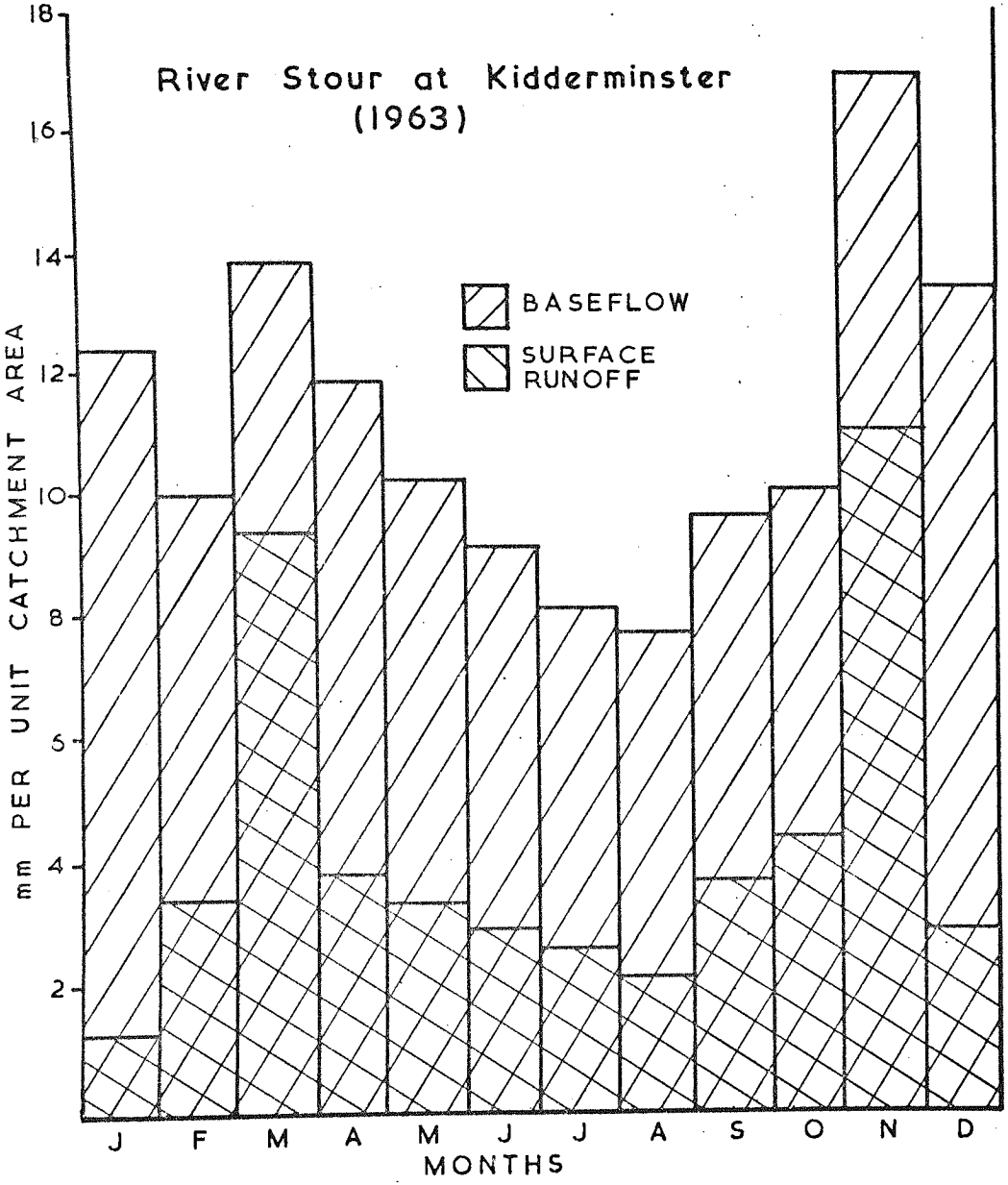

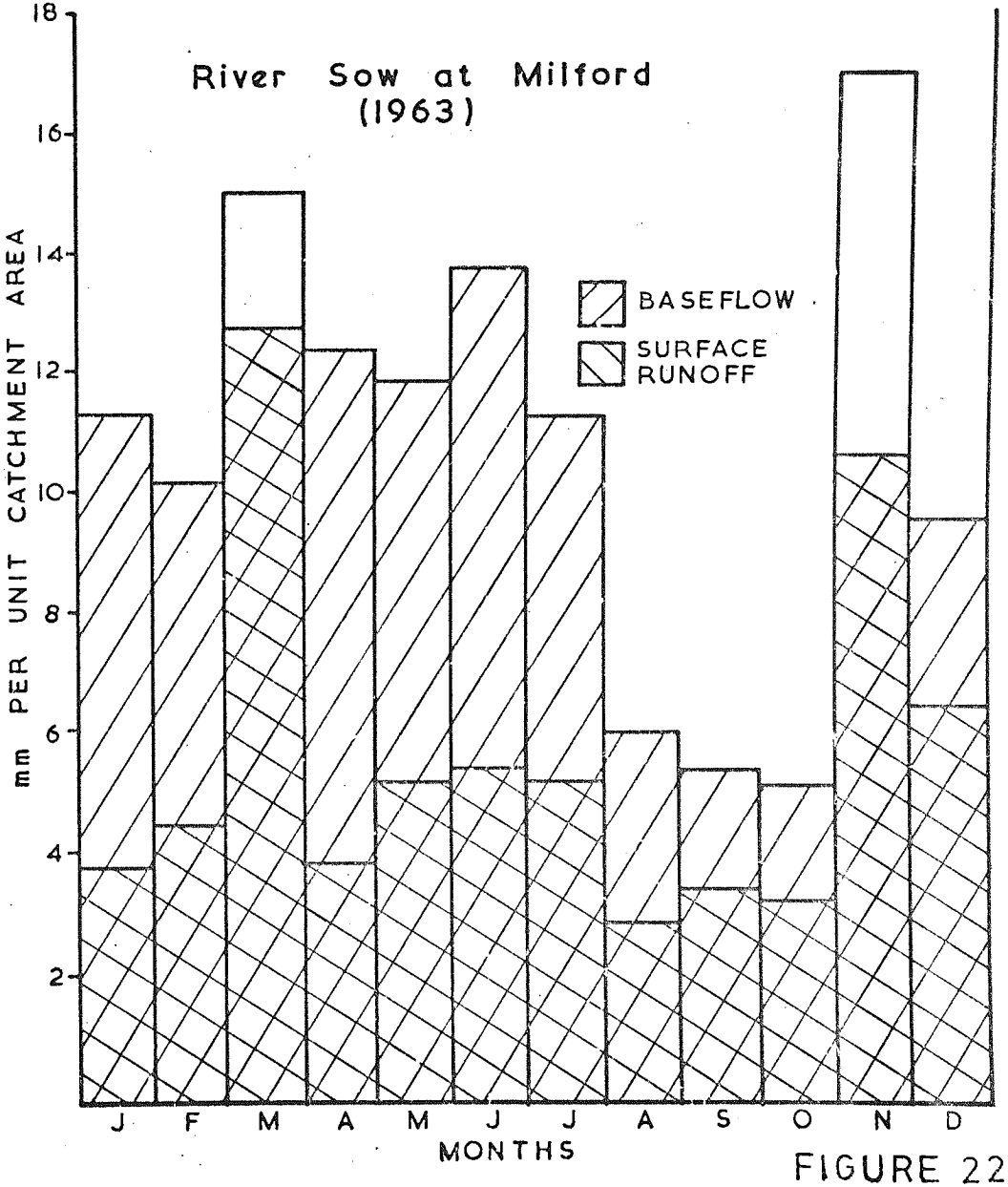

FIGURE 22

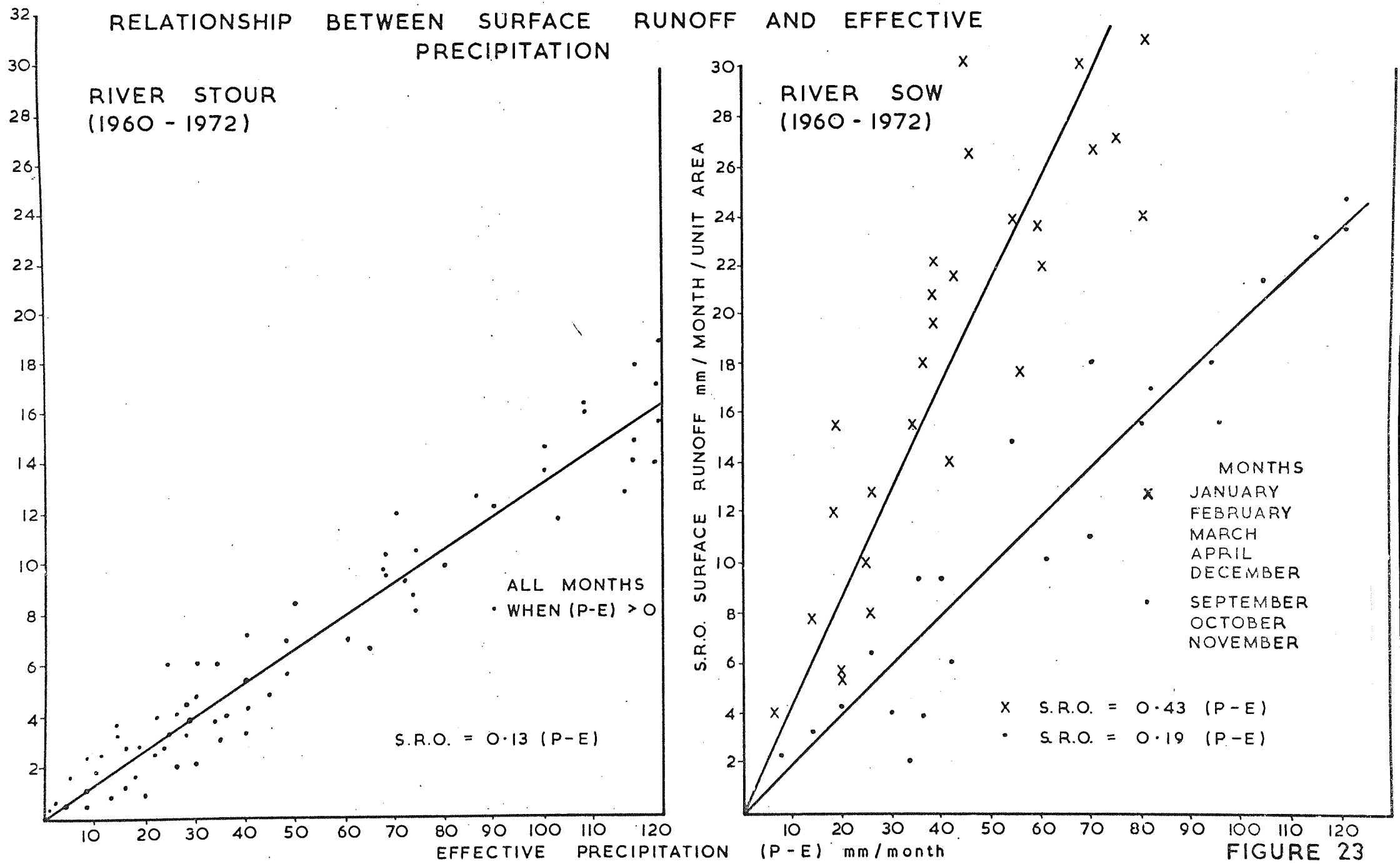
RELATIONSHIP BETWEEN SURFACE RUNOFF AND EFFECTIVE PRECIPITATION
RIVER STOUR
(1960 - 1972)
ALL MONTHS
• WHEN (P-E) > O
S.R.O. = 0·13 (P-E)
RIVER SOW
(1960 - 1972)
S.R.O. SURFACE RUNOFF mm / MONTH / UNIT AREA
MONTHS
JANUARY
FEBRUARY
MARCH
APRIL
DECEMBER
SEPTEMBER
OCTOBER
NOVEMBER
X S.R.O. = 0·43 (P-E)
• S.R.O. = 0·19 (P-E)
EFFECTIVE PRECIPITATION (P-E) mm / month

FIGURE 23

RELATIONSHIP BETWEEN BASEFLOW AND EFFECTIVE PRECIPITATION

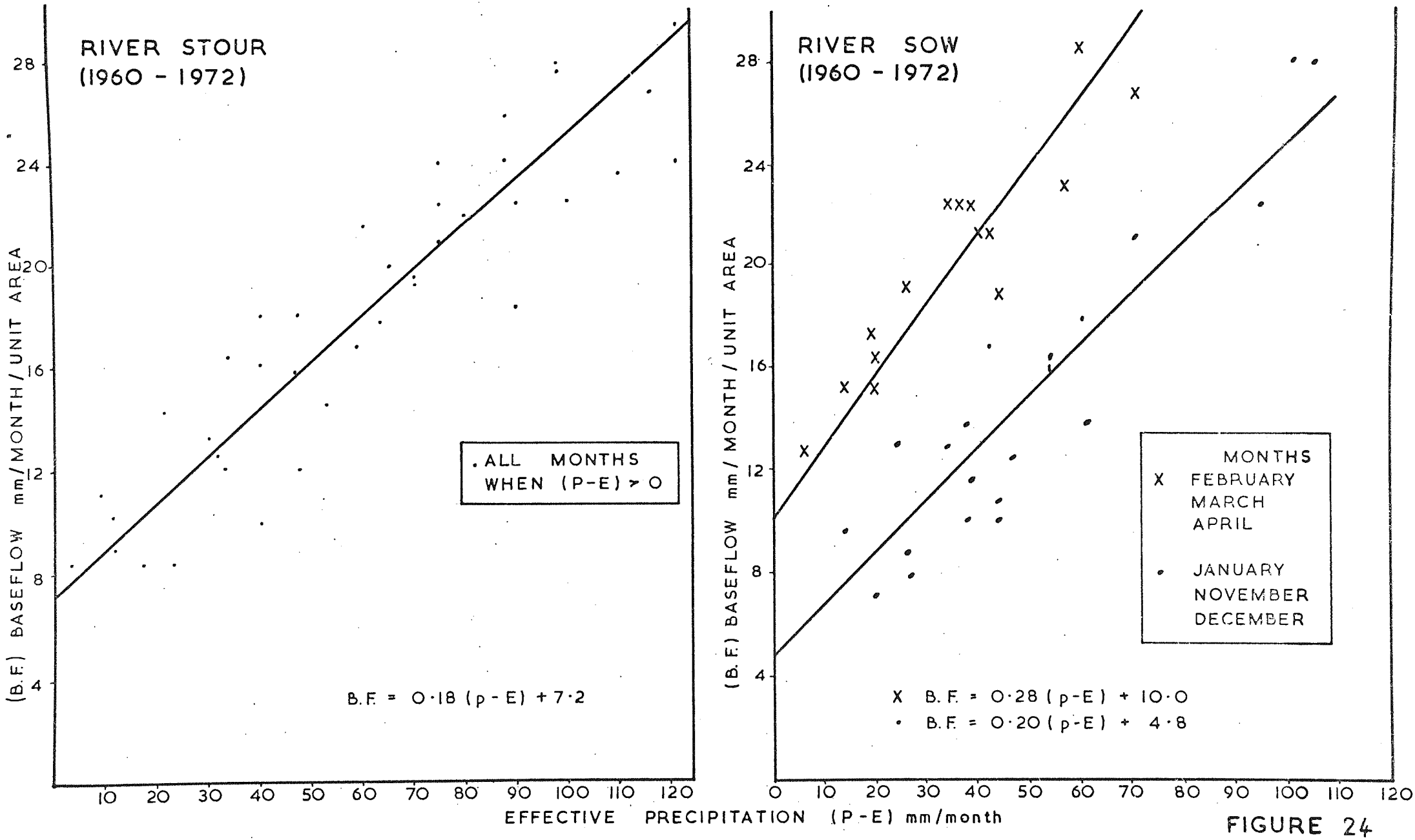

FIGURE 24

FIGURE 25

SCHEMATIC DIAGRAM OF MODELLED HYDROLOGICAL CYCLE

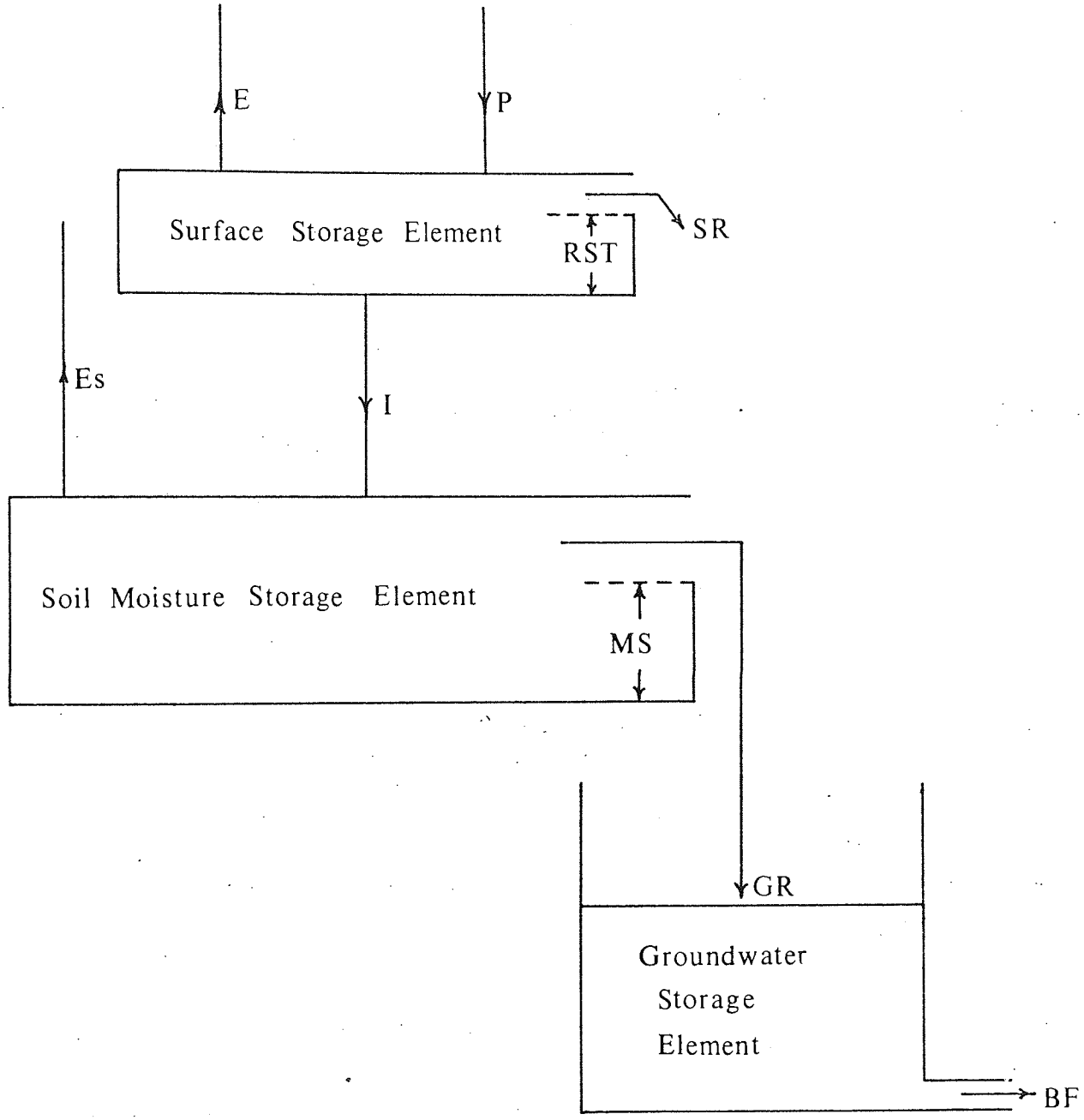

Precipitation	P
Potential Evaporation	E
Surface Retention	RST
Surface Runoff	SR
Infiltration	I
Soil Moisture Evapotranspiration	Es
Maximum Soil Moisture Content	MS
Groundwater Recharge	GR
Baseflow	BF

FIGURE 26

RAINGAUGE DISTRIBUTION NETWORK

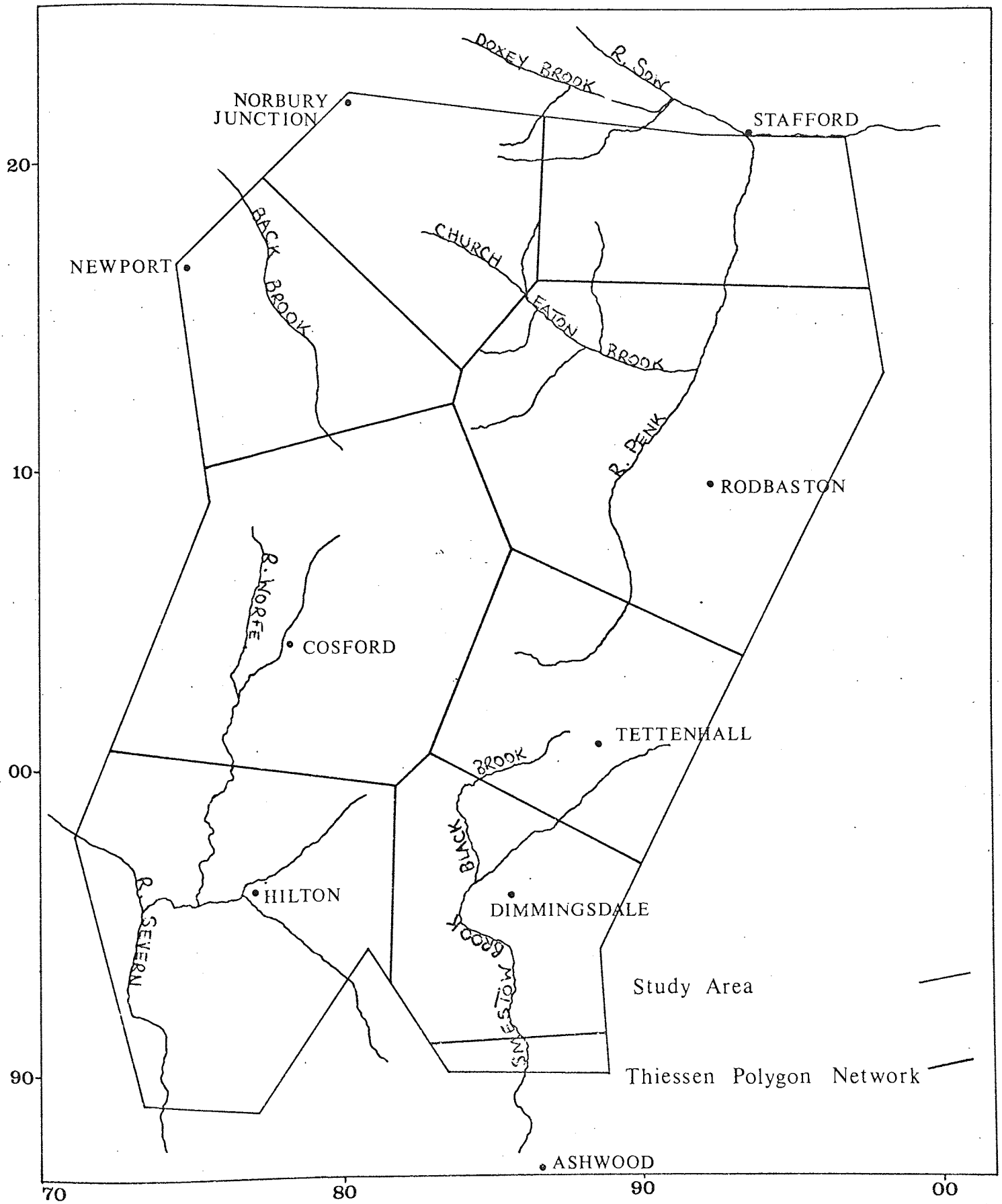

FIGURE 27

RAINFALL MASS PLOT ANALYSIS
1960 to 1972

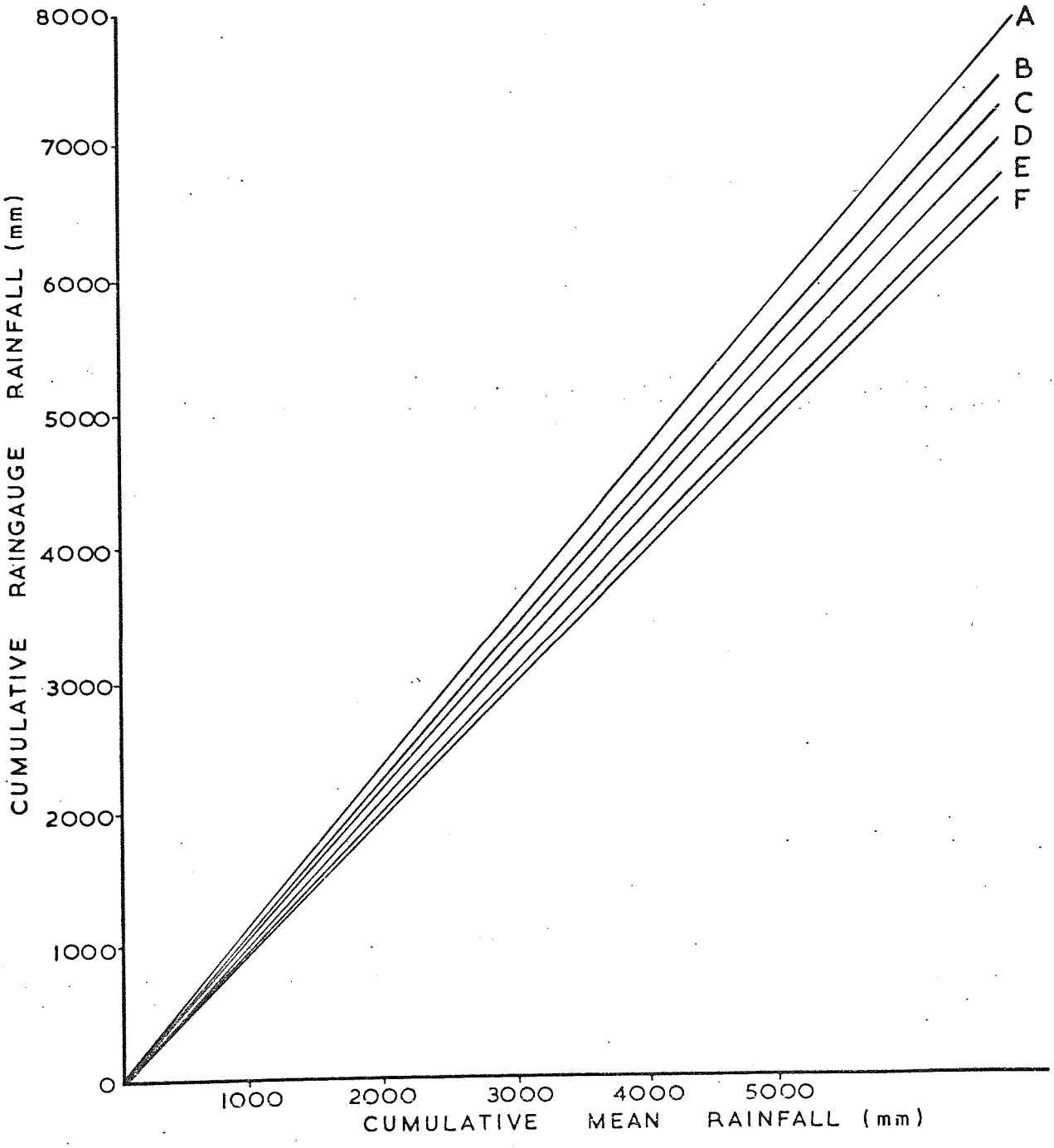

Representative Raingauges

A Shavers End
B Norbury Junction
C Tettenhall
D Cosford
E Hilton
F Dimmingsdale

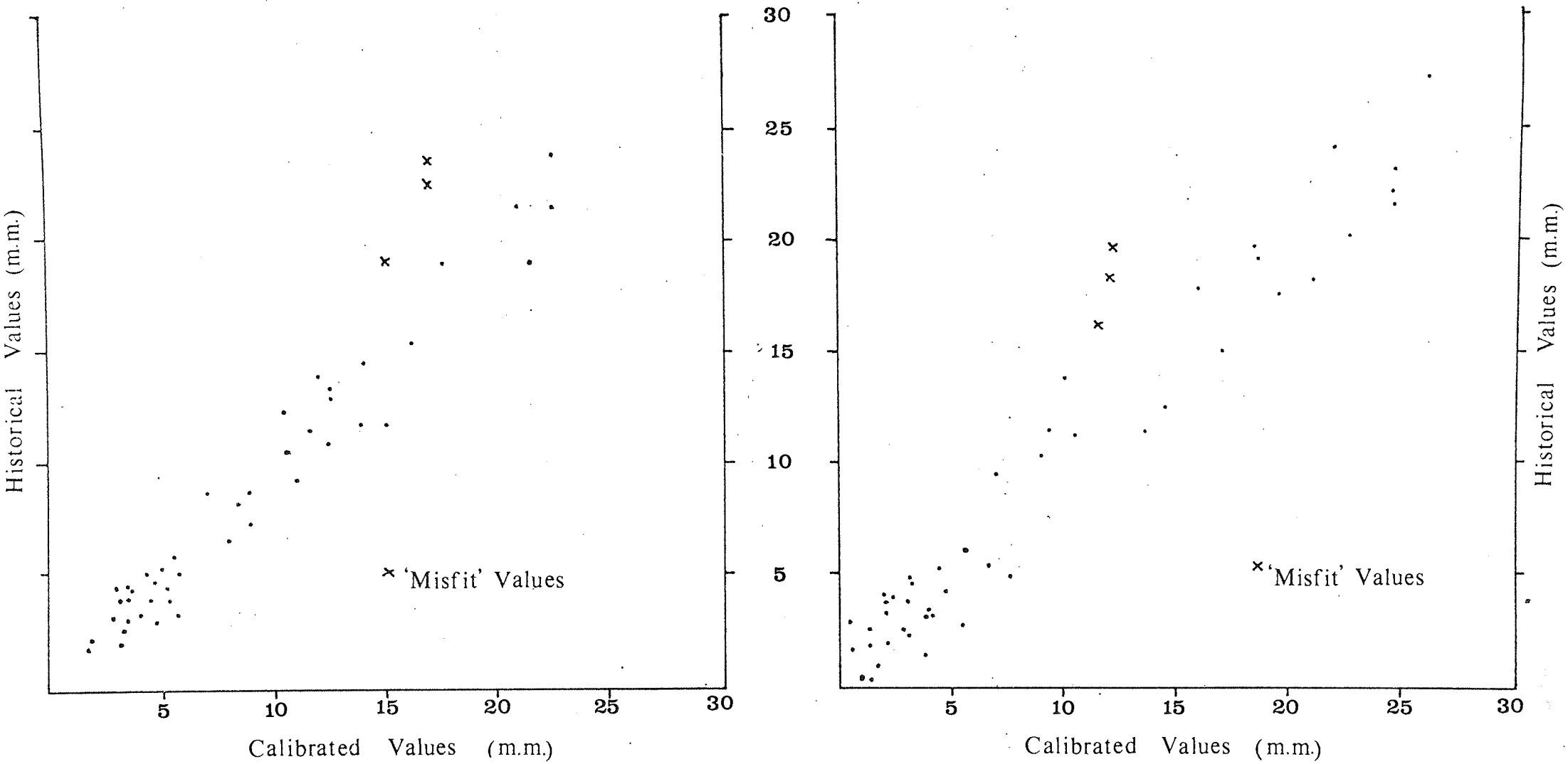

RIVER SOW – CALIBRATION 1961 to 1964

FIGURE 28

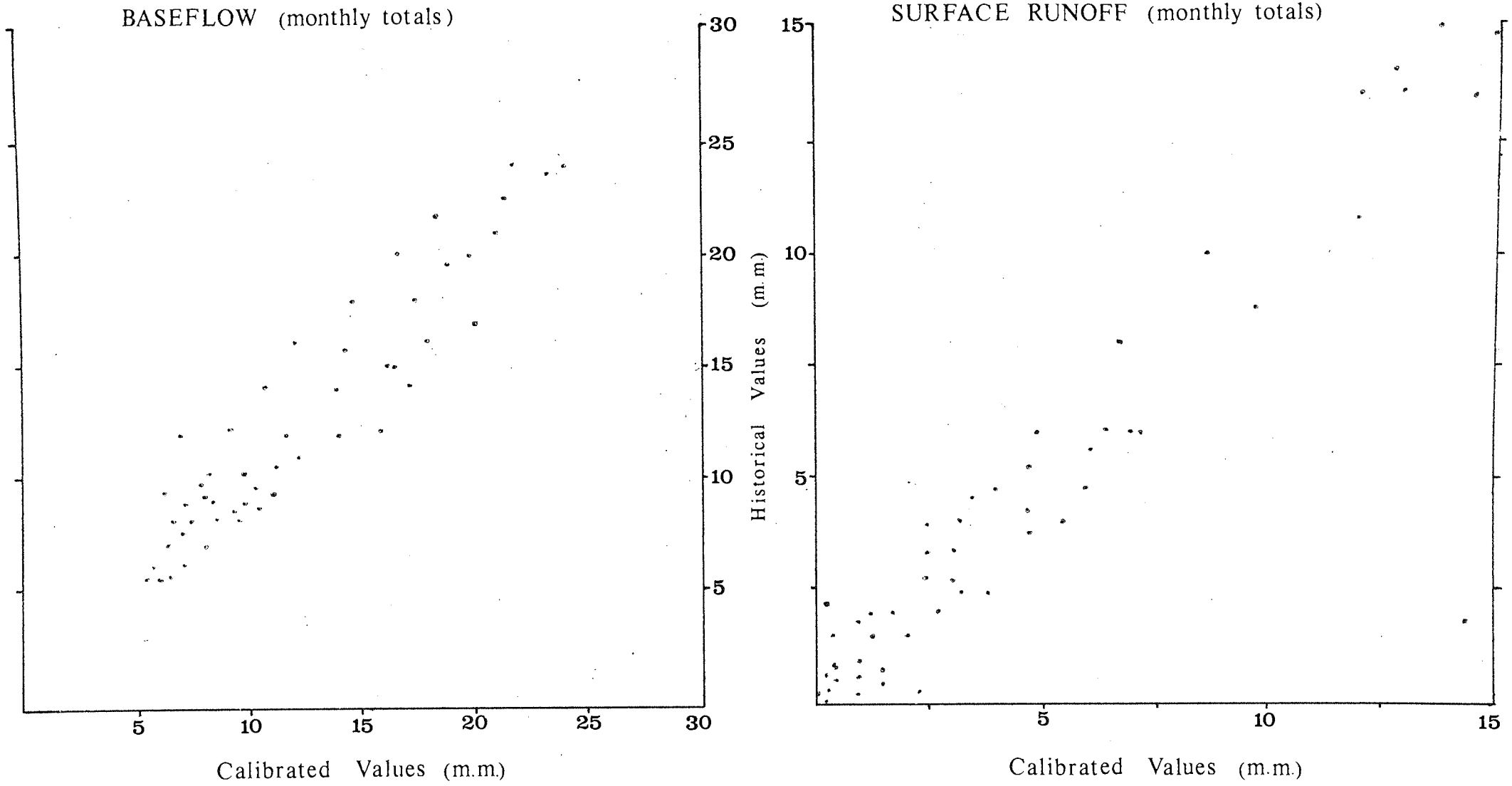

RIVER STOUR CALIBRATION 1960 to 1963

FIGURE 29

FIGURE 30

AVERAGE GROUNDWATER LEVEL CONDITIONS

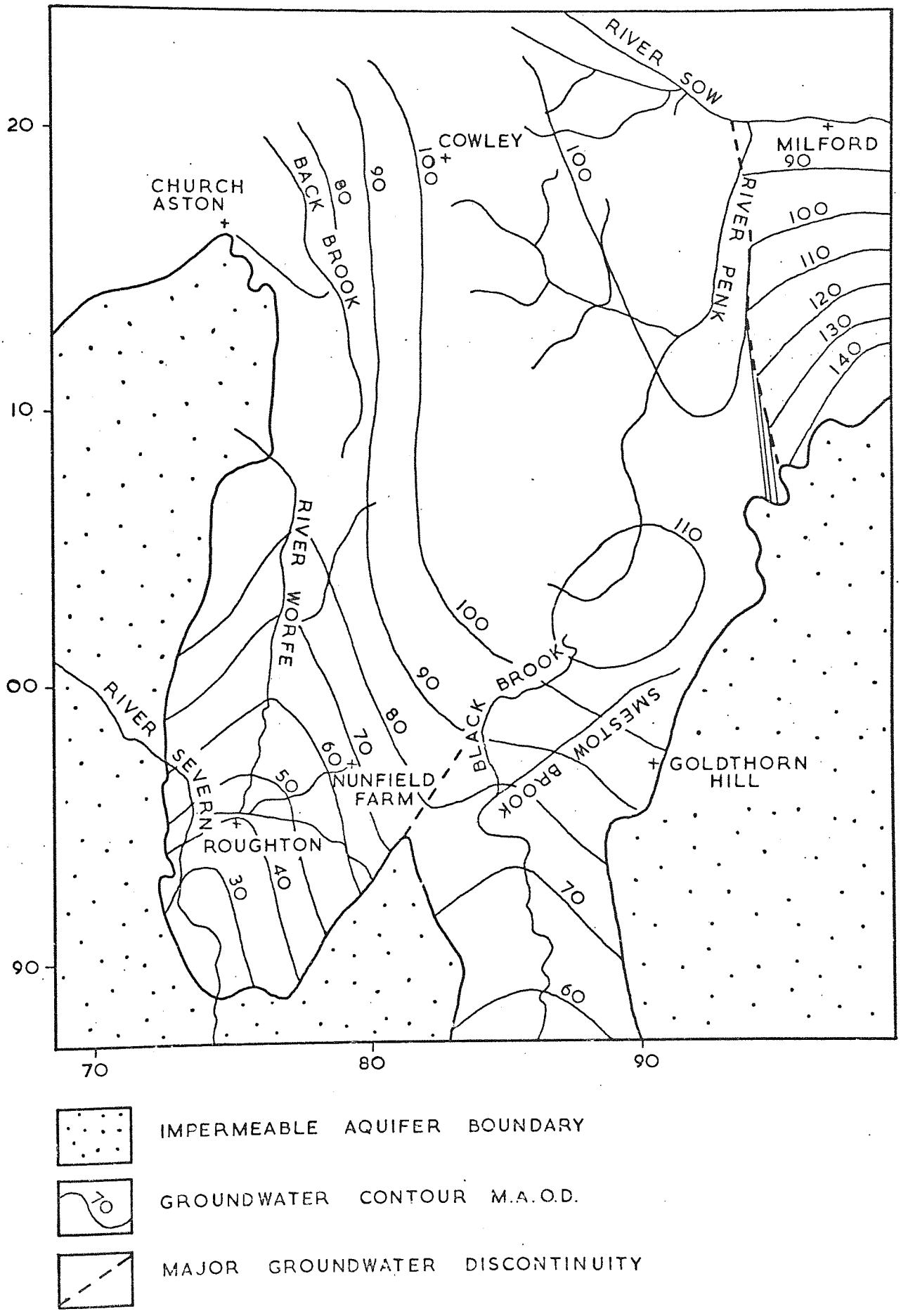

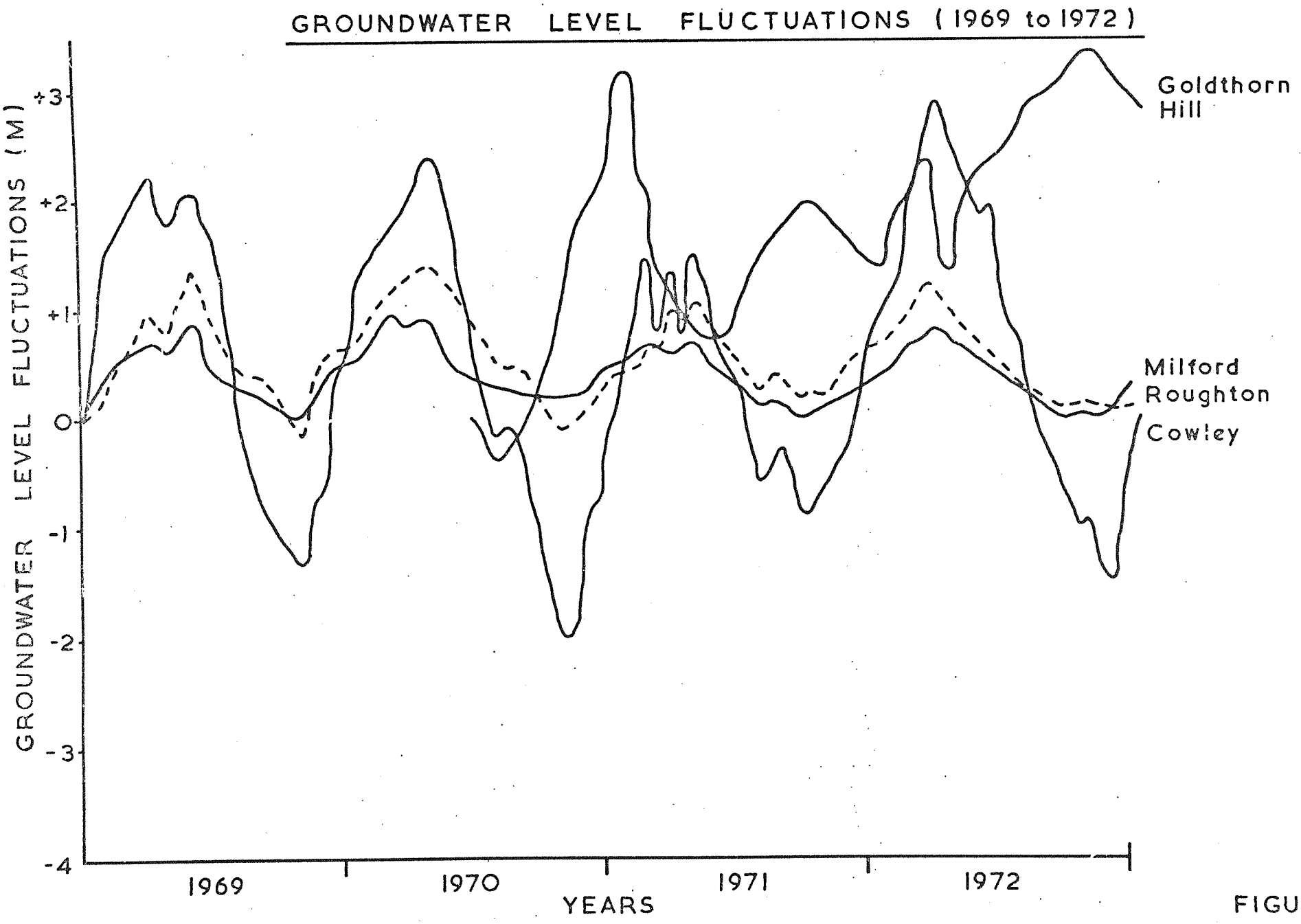
GROUNDWATER LEVEL FLUCTUATIONS (1969 to 1972)
GROUNDWATER LEVEL FLUCTUATIONS (M)
+3
+2
+1
0
-1
-2
-3
-4
1969
1970
1971
1972
YEARS
Goldthorn Hill
Milford
Roughton
Cowley

FIGURE 31

FIGURE 32

DISTRIBUTION OF MAIN ABSTRACTION BOREHOLES

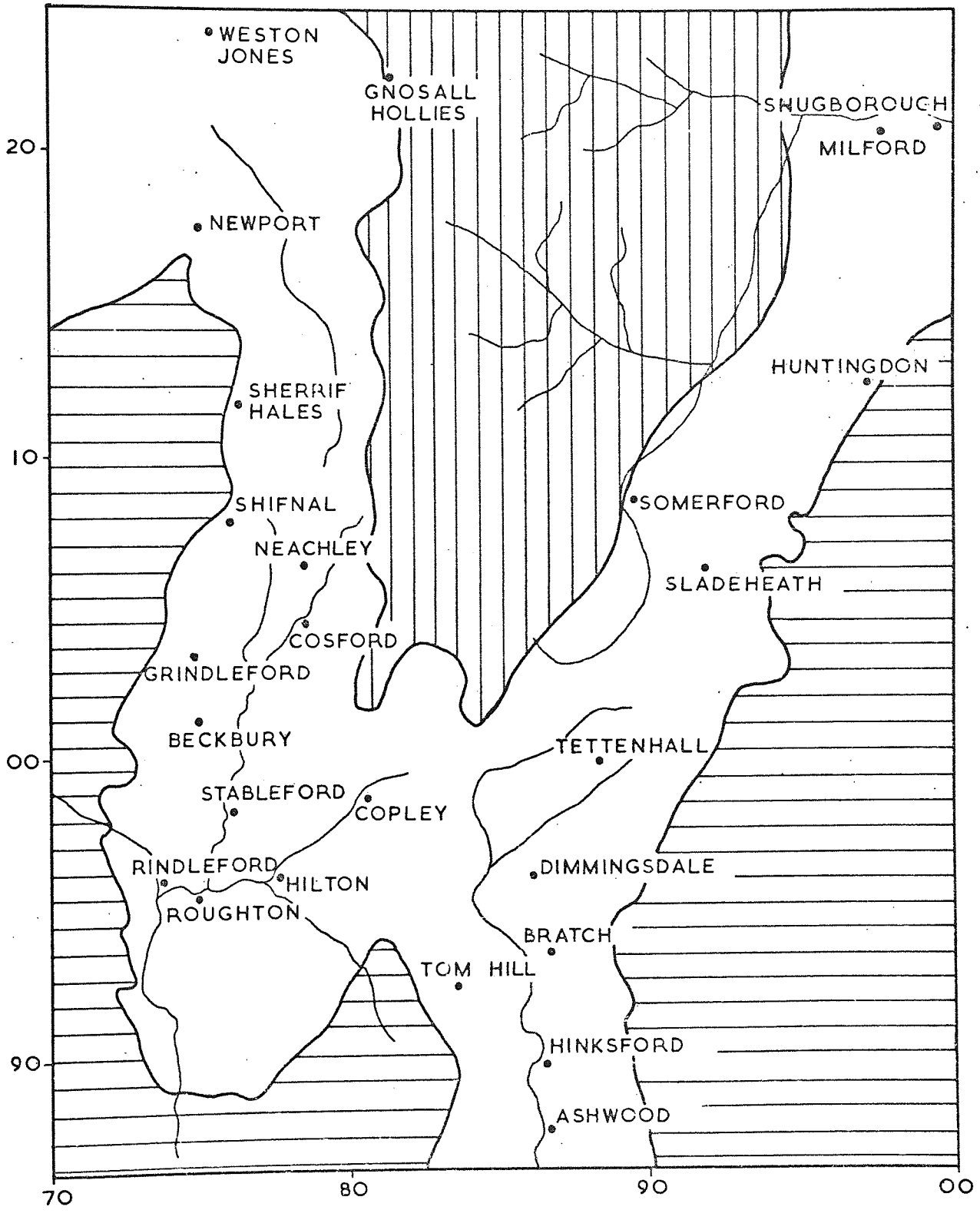

CARBONIFEROUS AND OLDER STRATA

UNCONFINED AQUIFER

SEMI-CONFINED "

CONFINED AQUIFER

FIGURE 33

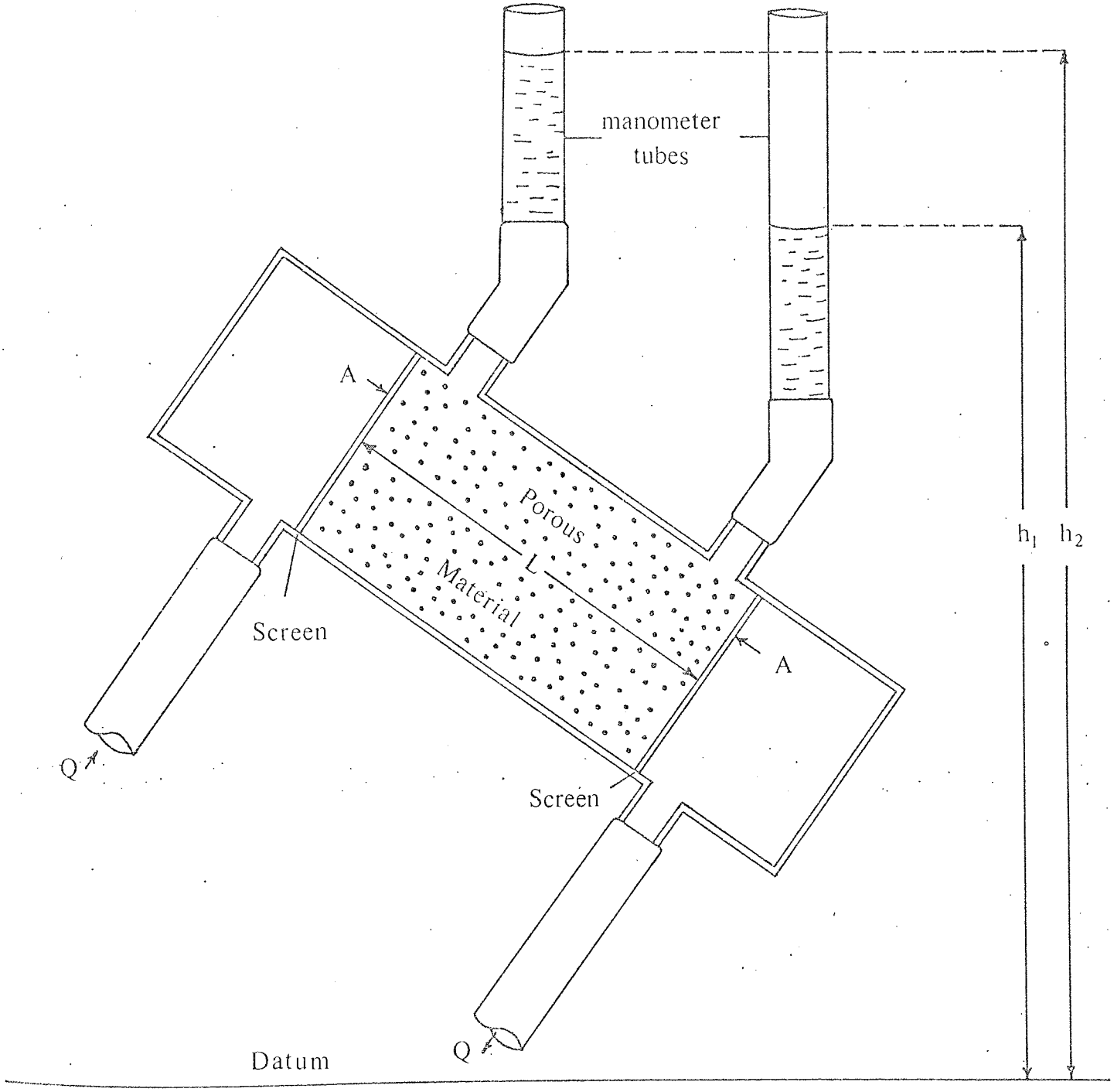

APPARATUS USED TO VERIFY DARCY'S LAW

FIGURE 34a

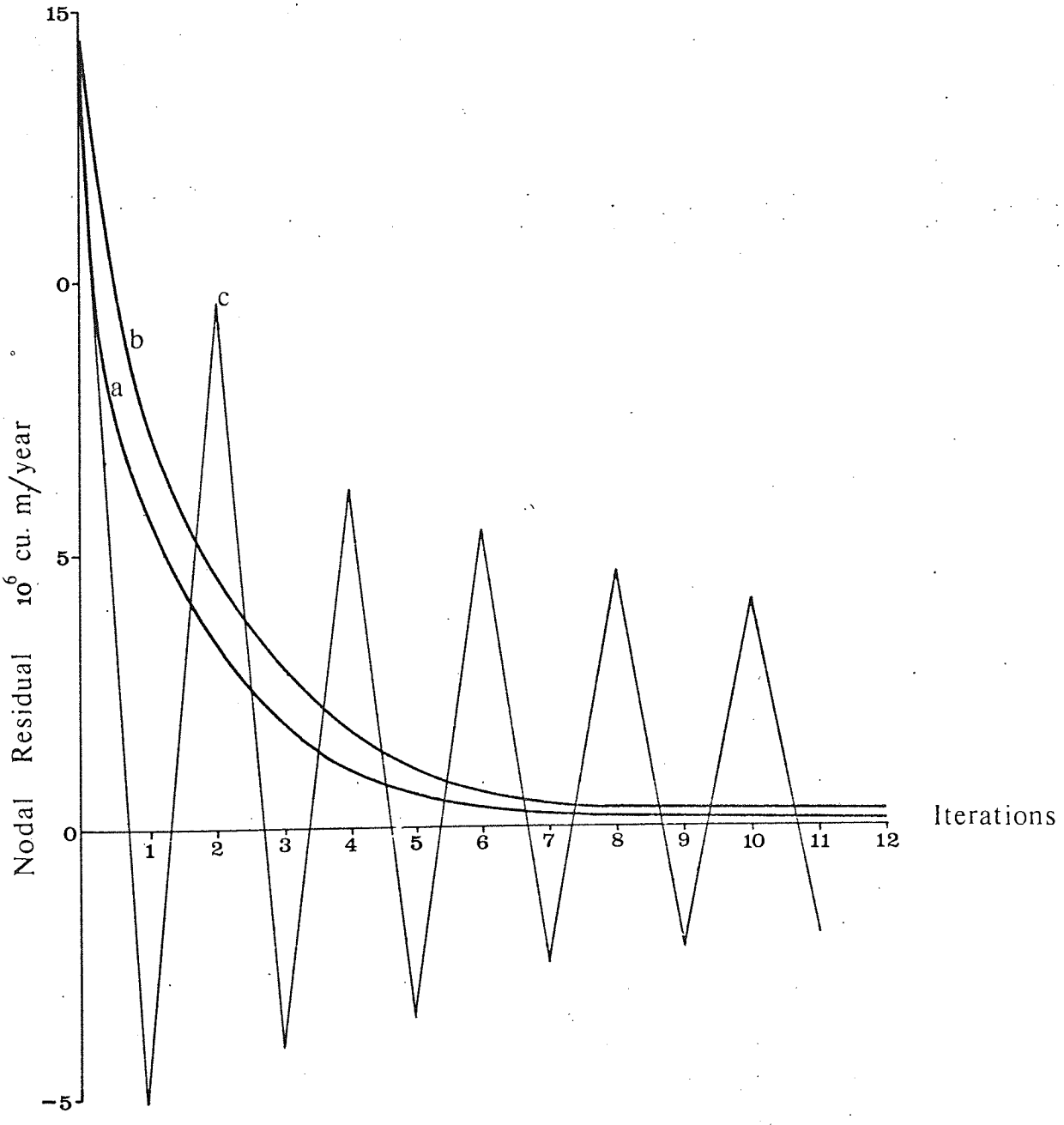

TYPICAL VARIATION OF THE CONVERGENCE RATE AT A NODE DUE TO ADJUSTMENT OF THE RELAXATION COEFFICIENT

FIGURE 34b

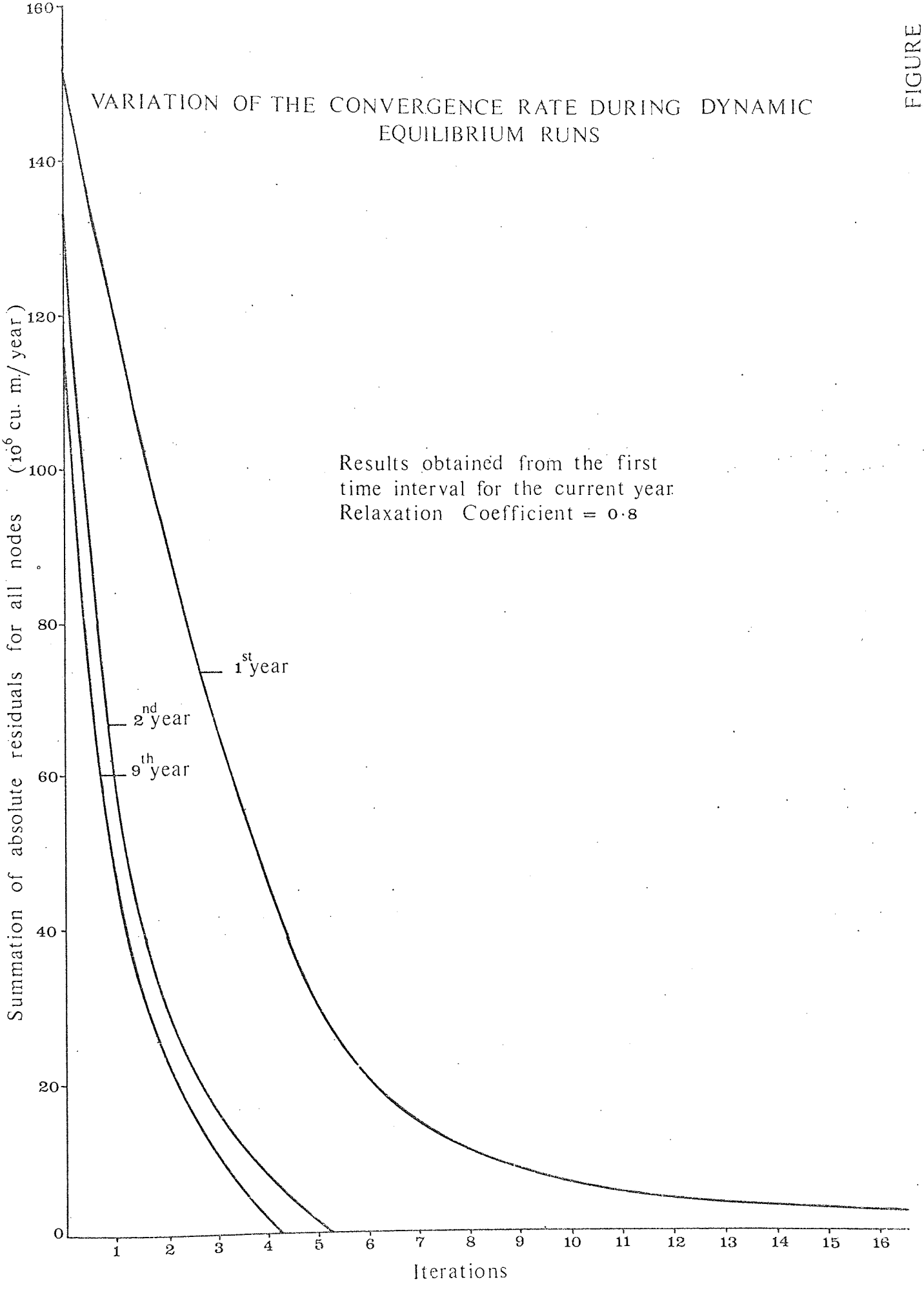
VARIATION OF THE CONVERGENCE RATE DURING DYNAMIC EQUILIBRIUM RUNS
Results obtained from the first time interval for the current year
Relaxation Coefficient = 0·8
1st year
2nd year
9th year
Summation of absolute residuals for all nodes (10^6 cu. m./year)
Iterations
0
20
40
60
80
100
120
140
160
1
2
3
4
5
6
7
8
9
10
11
12
13
14
15
16

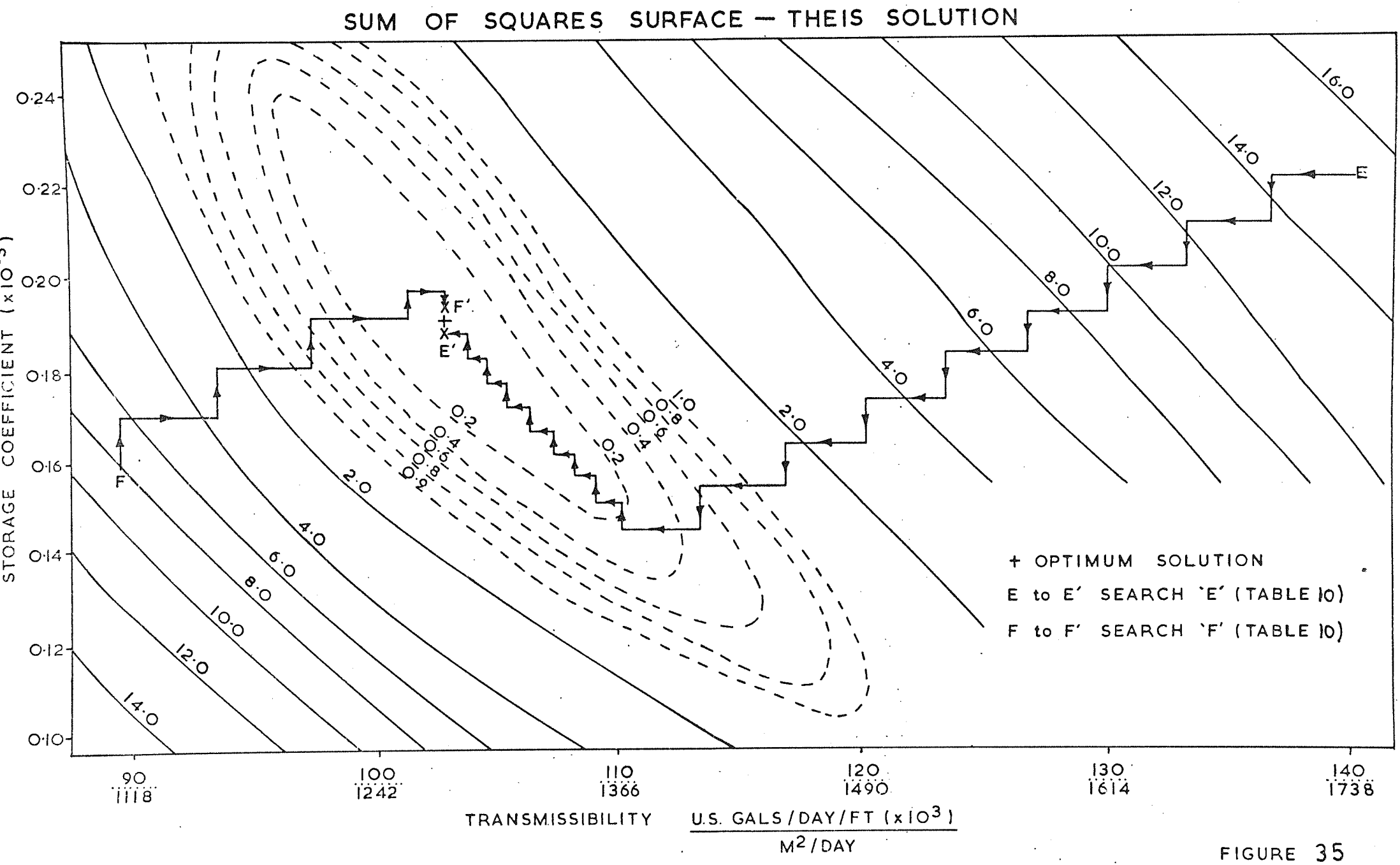
SUM OF SQUARES SURFACE — THEIS SOLUTION
STORAGE COEFFICIENT (x10⁻³)
0·24
0·22
0·20
0·18
0·16
0·14
0·12
0·10
16·0
14·0
12·0
10·0
8·0
6·0
4·0
2·0
1·0
0·2
F
F'
E'
E
+ OPTIMUM SOLUTION
E to E' SEARCH 'E' (TABLE 10)
F to F' SEARCH 'F' (TABLE 10)
90
1118
100
1242
110
1366
120
1490
130
1614
140
1738
TRANSMISSIBILITY U.S. GALS/DAY/FT (x10³) / M²/DAY

FIGURE 35

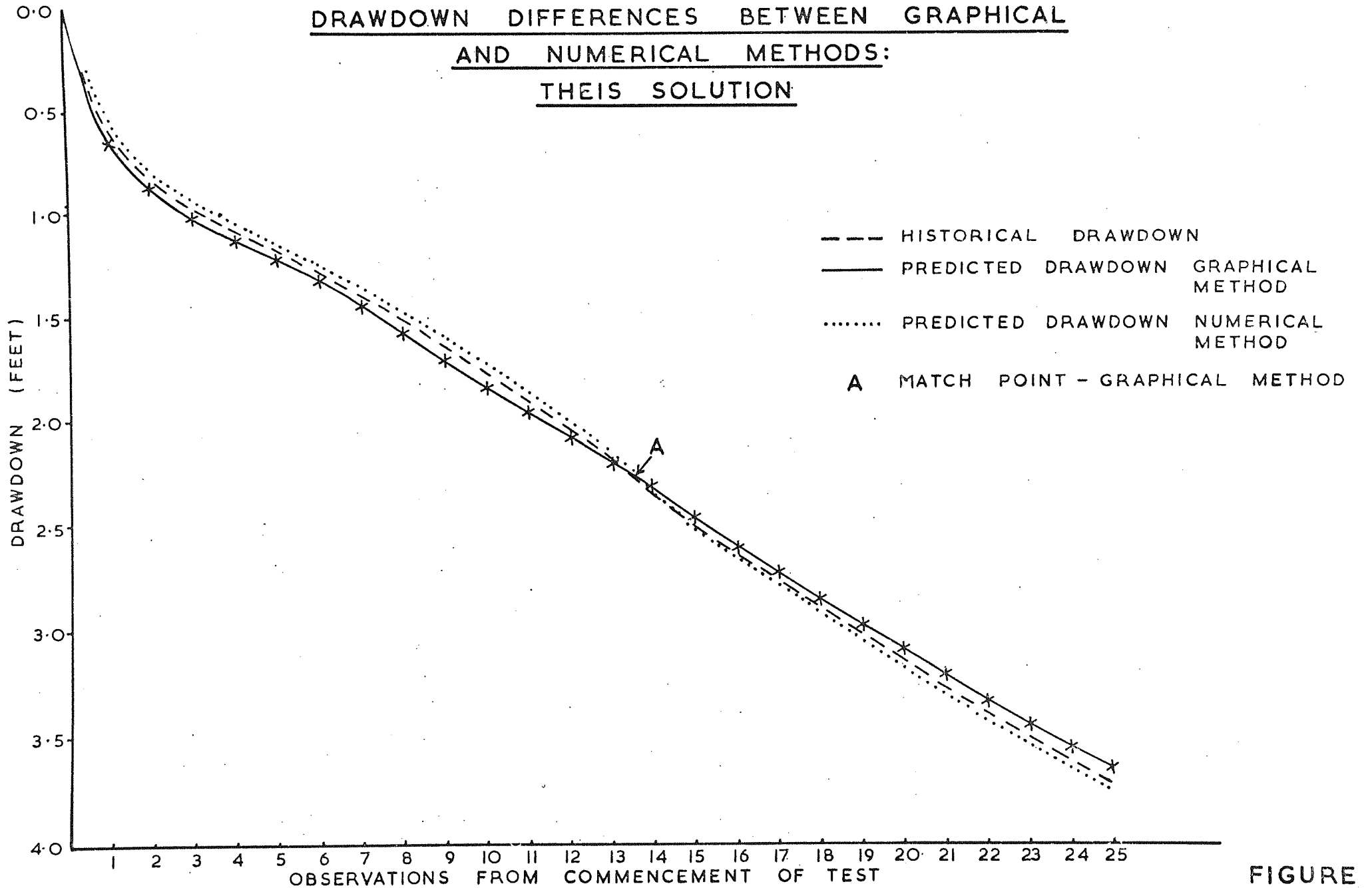
DRAWDOWN DIFFERENCES BETWEEN GRAPHICAL AND NUMERICAL METHODS: THEIS SOLUTION
HISTORICAL DRAWDOWN
PREDICTED DRAWDOWN GRAPHICAL METHOD
PREDICTED DRAWDOWN NUMERICAL METHOD
A MATCH POINT - GRAPHICAL METHOD
A
DRAWDOWN (FEET)
0·0
0·5
1·0
1·5
2·0
2·5
3·0
3·5
4·0
1 2 3 4 5 6 7 8 9 10 11 12 13 14 15 16 17 18 19 20 21 22 23 24 25
OBSERVATIONS FROM COMMENCEMENT OF TEST

FIGURE 3

FIGURE 37

MODEL BOUNDARY CONFIGURATION

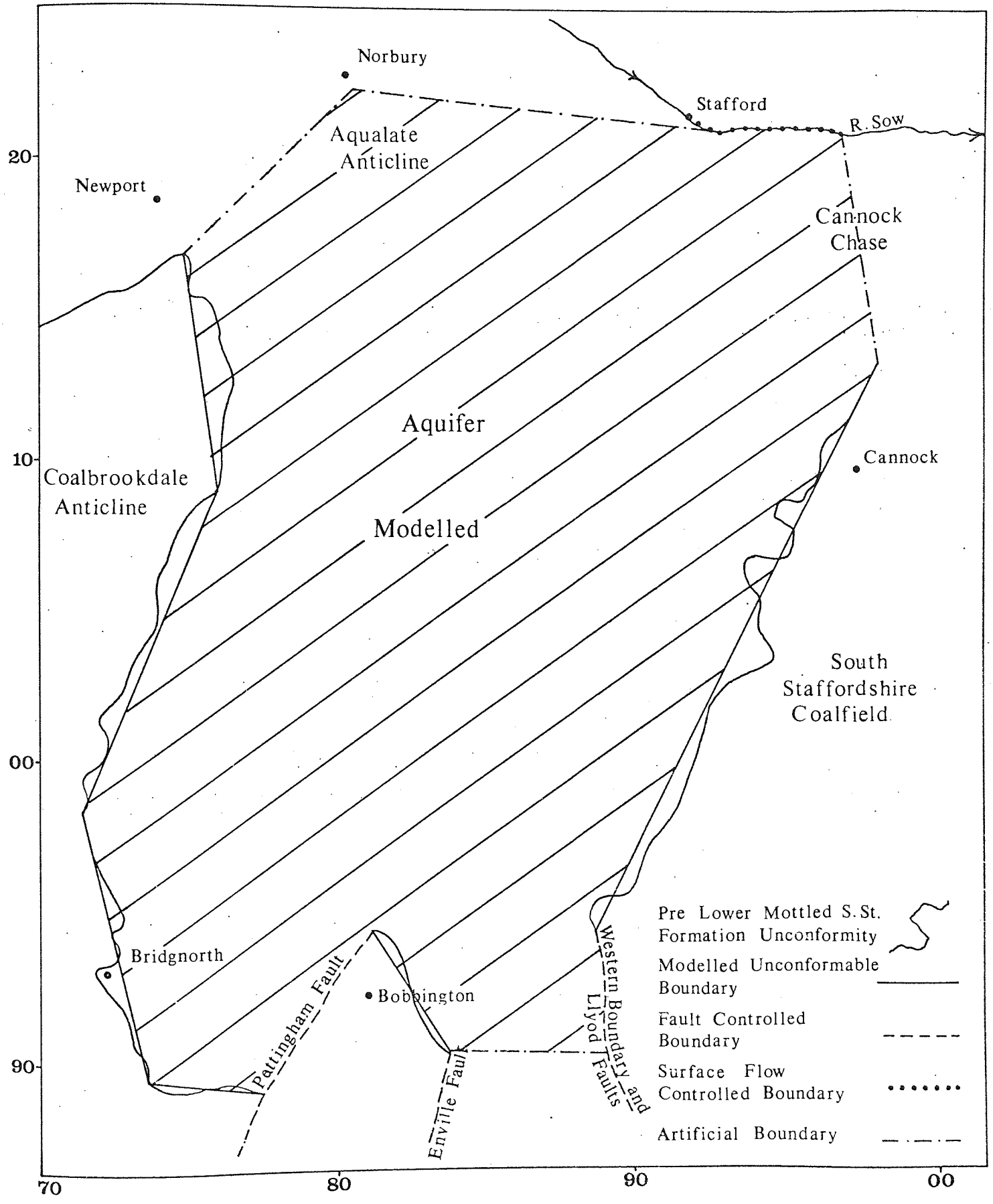

FIGURE 38

ISOPACHYTES OF THE

MAIN AQUIFER

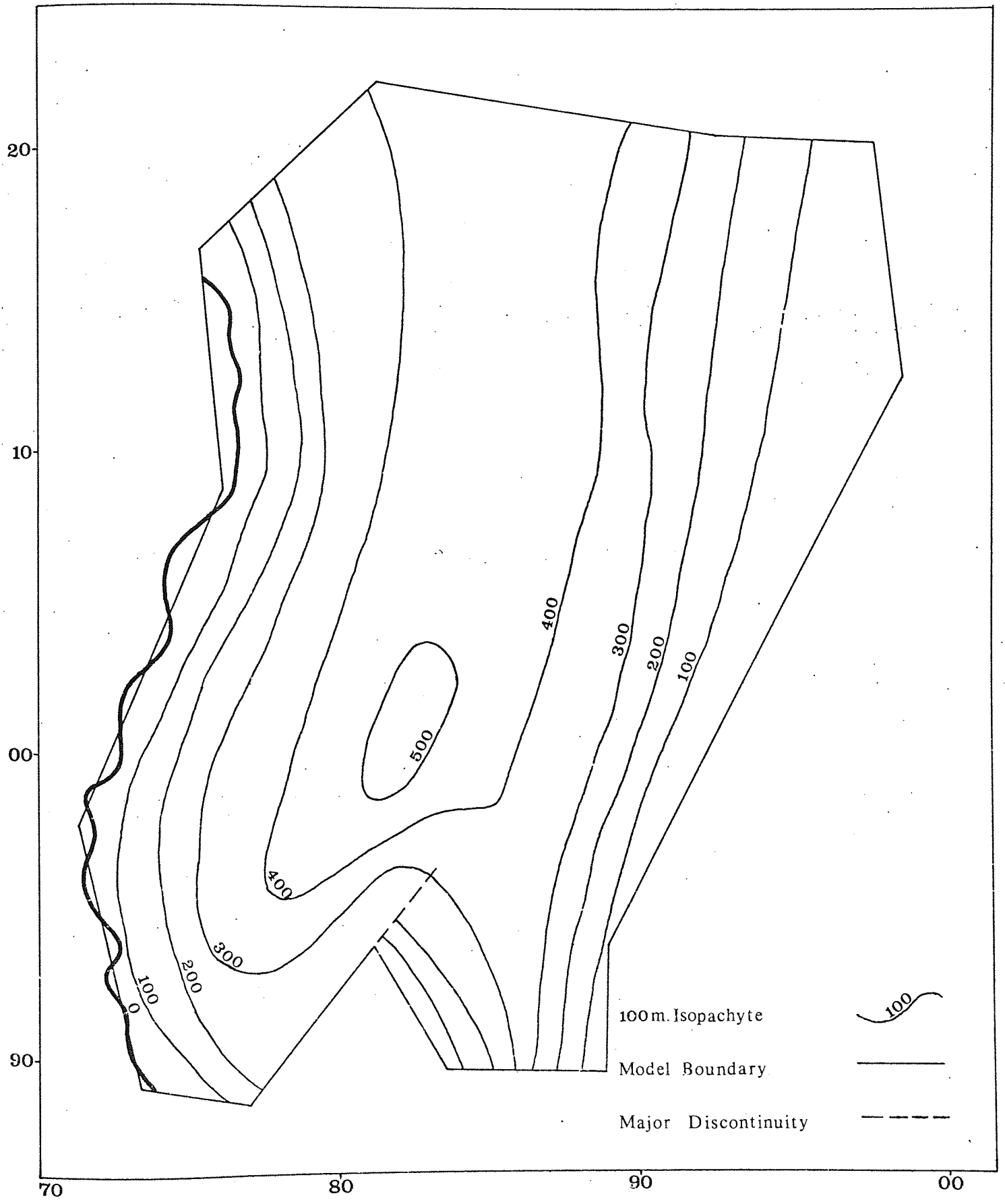

FIGURE 39

ISOPACHYTES OF THE LOWER

MOTTLED SANDSTONE FORMATION

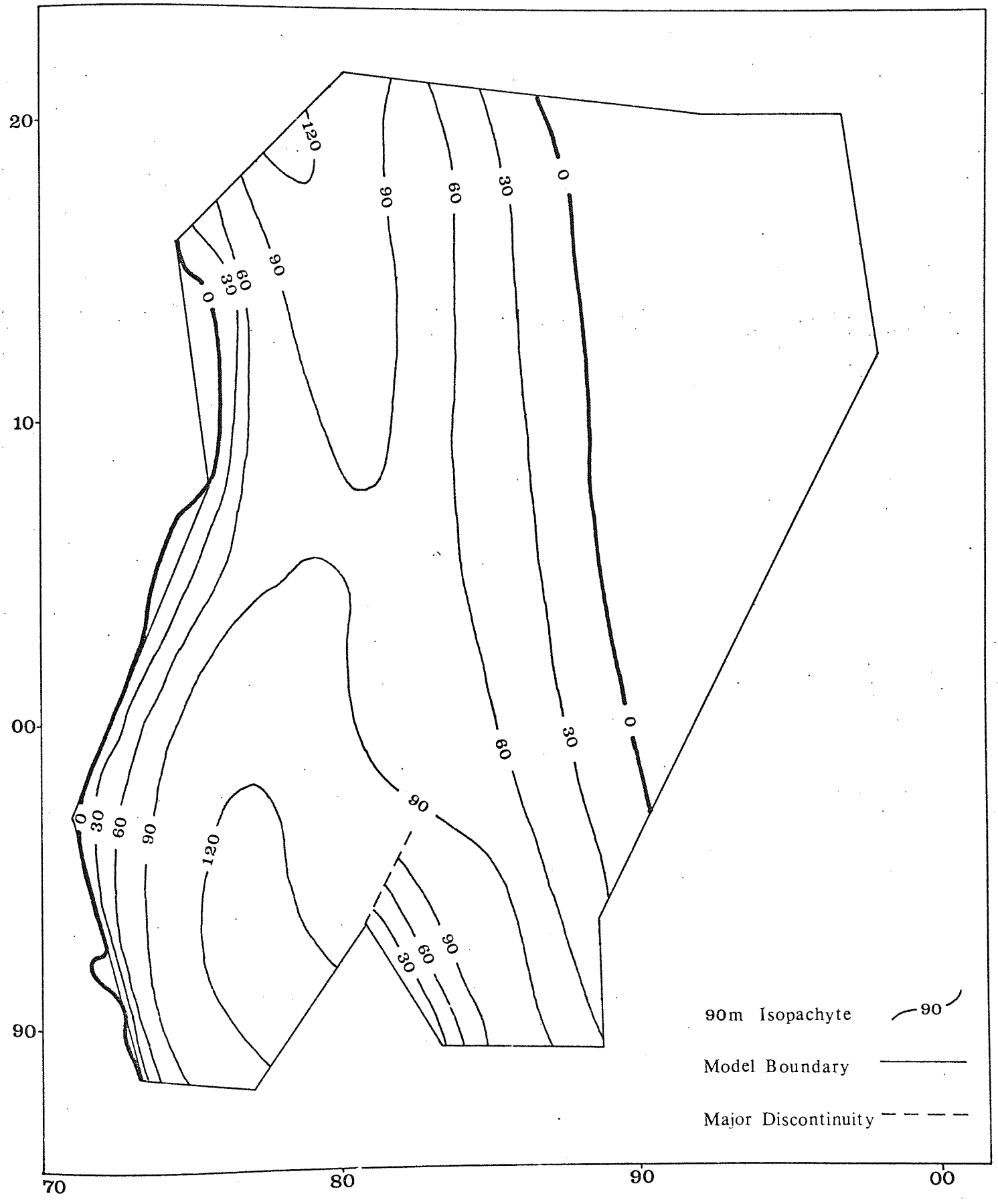

FIGURE 40

ISOPACHYTES OF THE BUNTER PEBBLE BED FORMATION

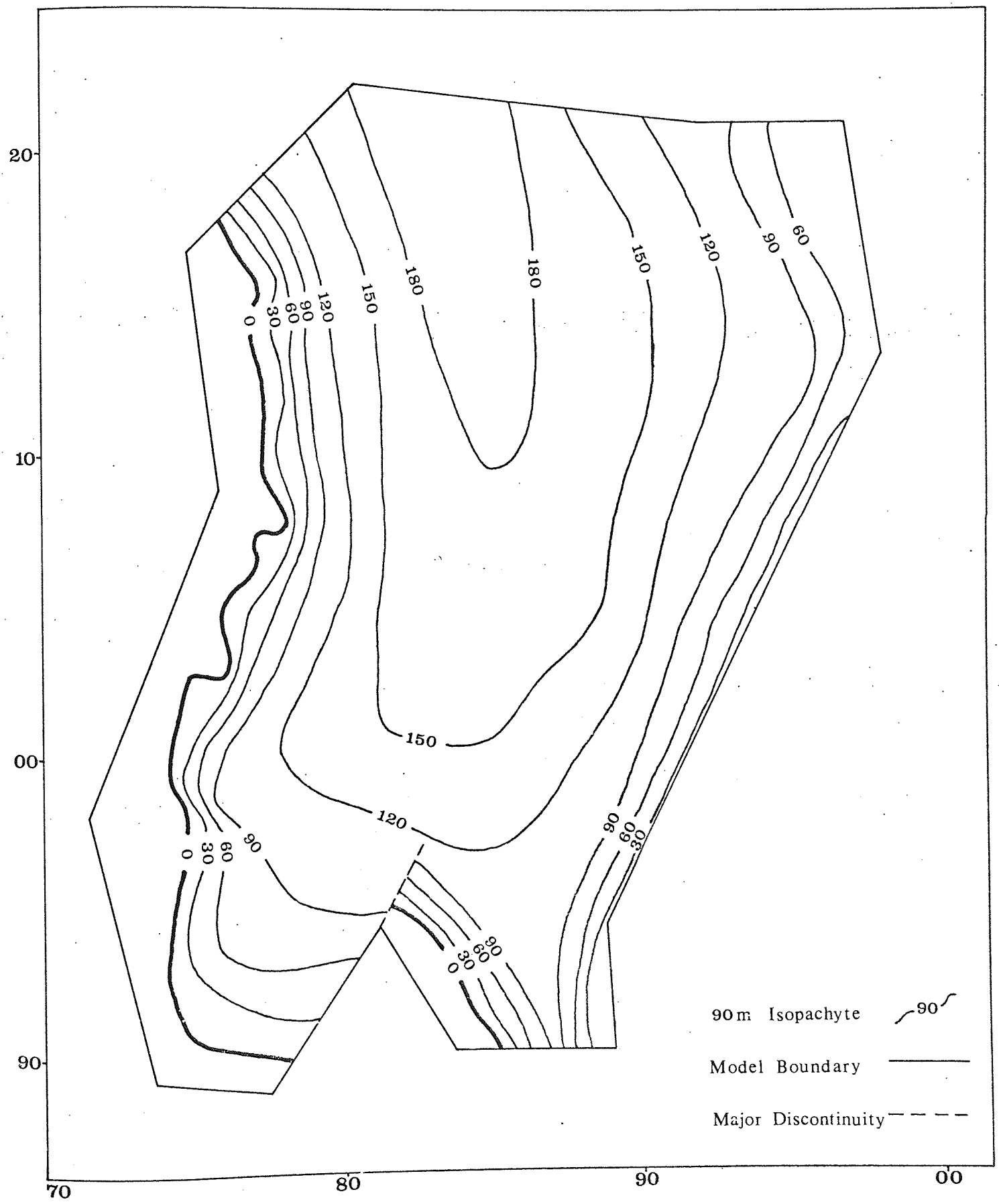

FIGURE 41

ISOPACHYTES OF THE UPPER MOTTLED SANDSTONE FORMATION

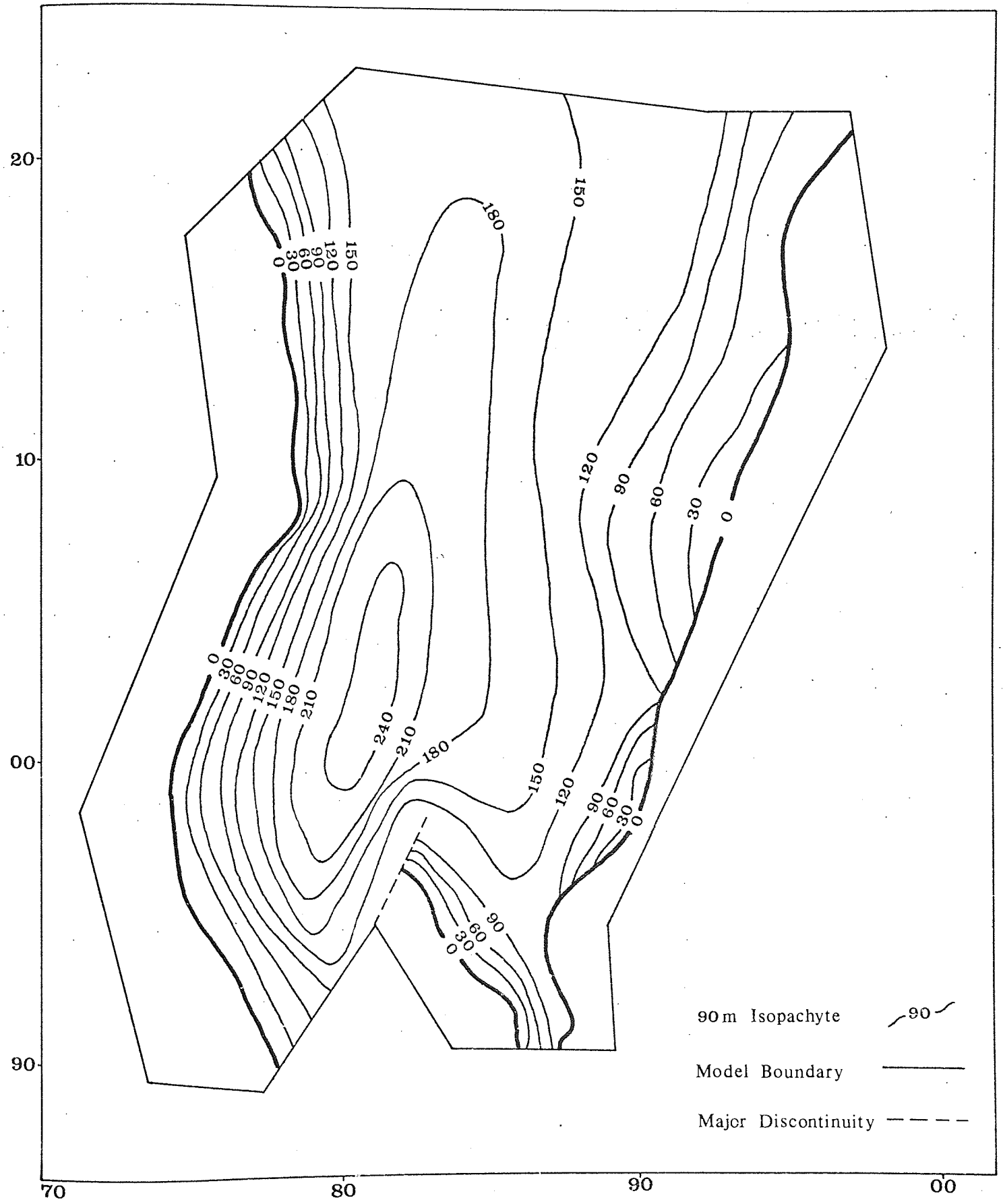

FIGURE 42

ISOPACHYTES OF THE LOWER KEUPER SANDSTONE FORMATION

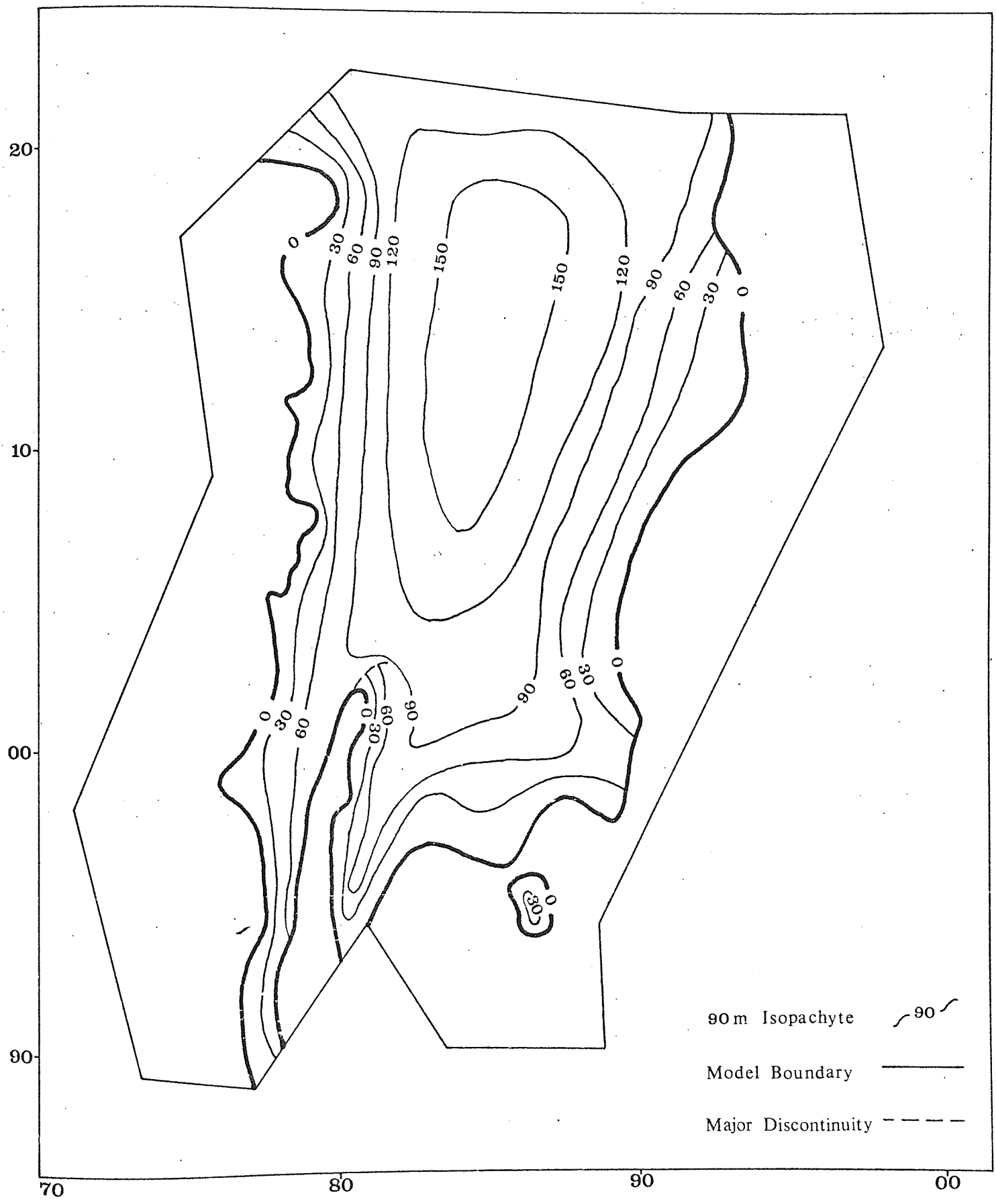

FIGURE 43

ISOPACHYTES OF THE KEUPER MARL FORMATION

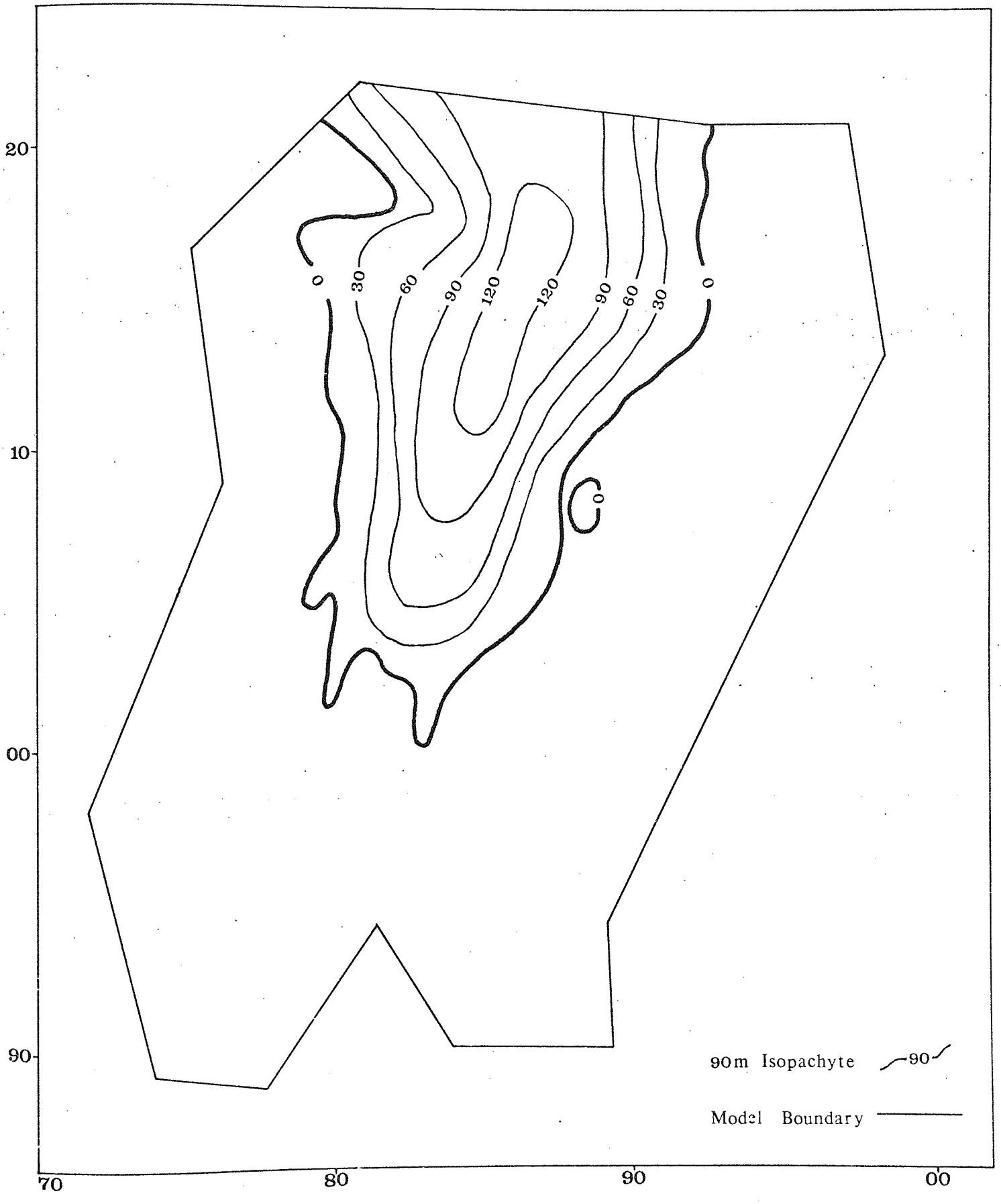

FIGURE 44

PUMP TEST ANALYSIS

TEST SITE	ROUGHTON
METHOD OF ANALYSIS	COOPER AND JACOB (1946)
TRANSMISSIBILITY	803 m^2/d
STORAGE COEFFICIENT	0·0128

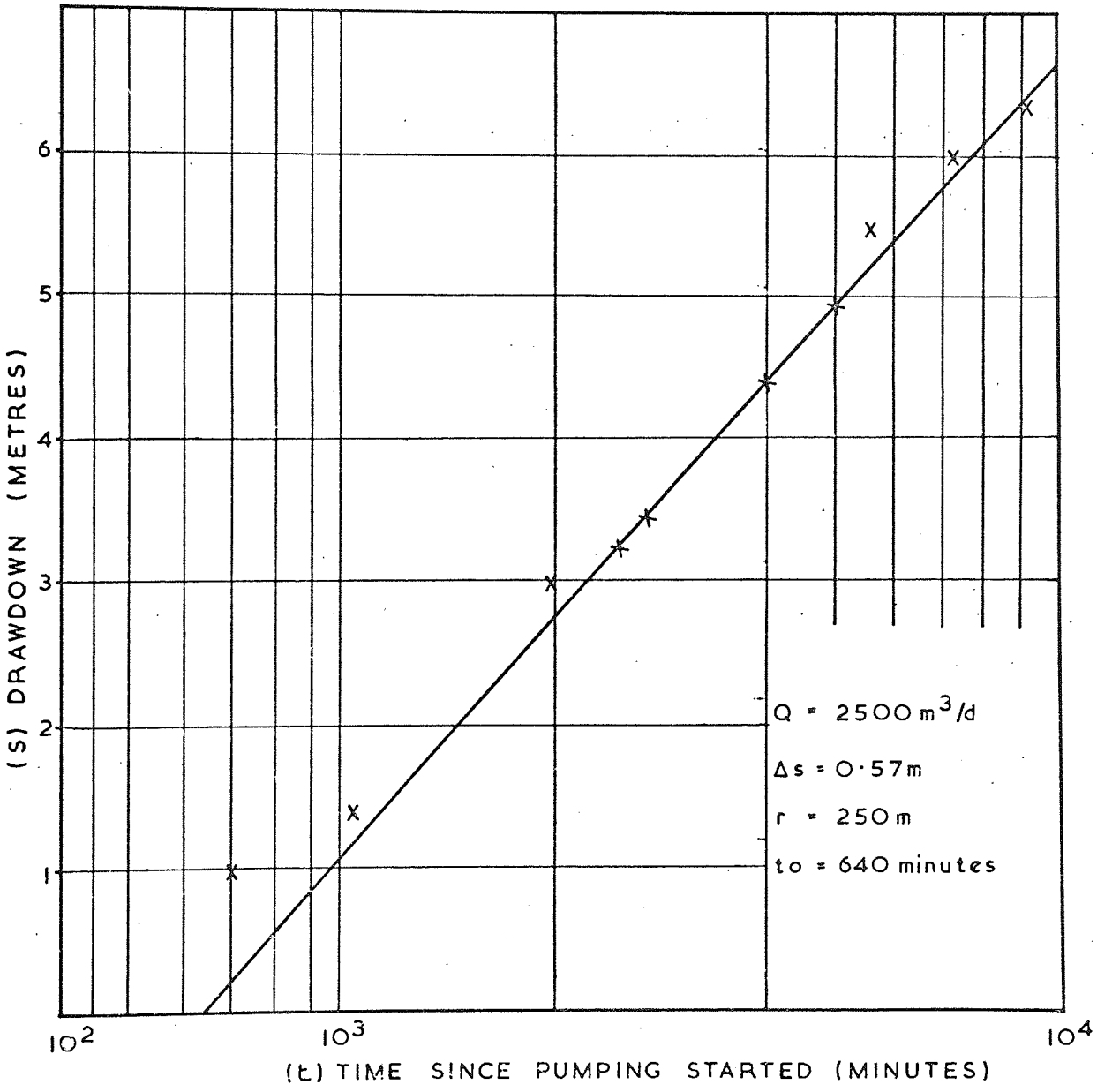

FIGURE 45

PUMP TEST ANALYSIS

TEST SITE	WESTON JONES
METHOD OF ANALYSIS	COOPER AND JACOB (1946)
TRANSMISSIBILITY	90 m^2/d
STORAGE COEFFICIENT	0·0043

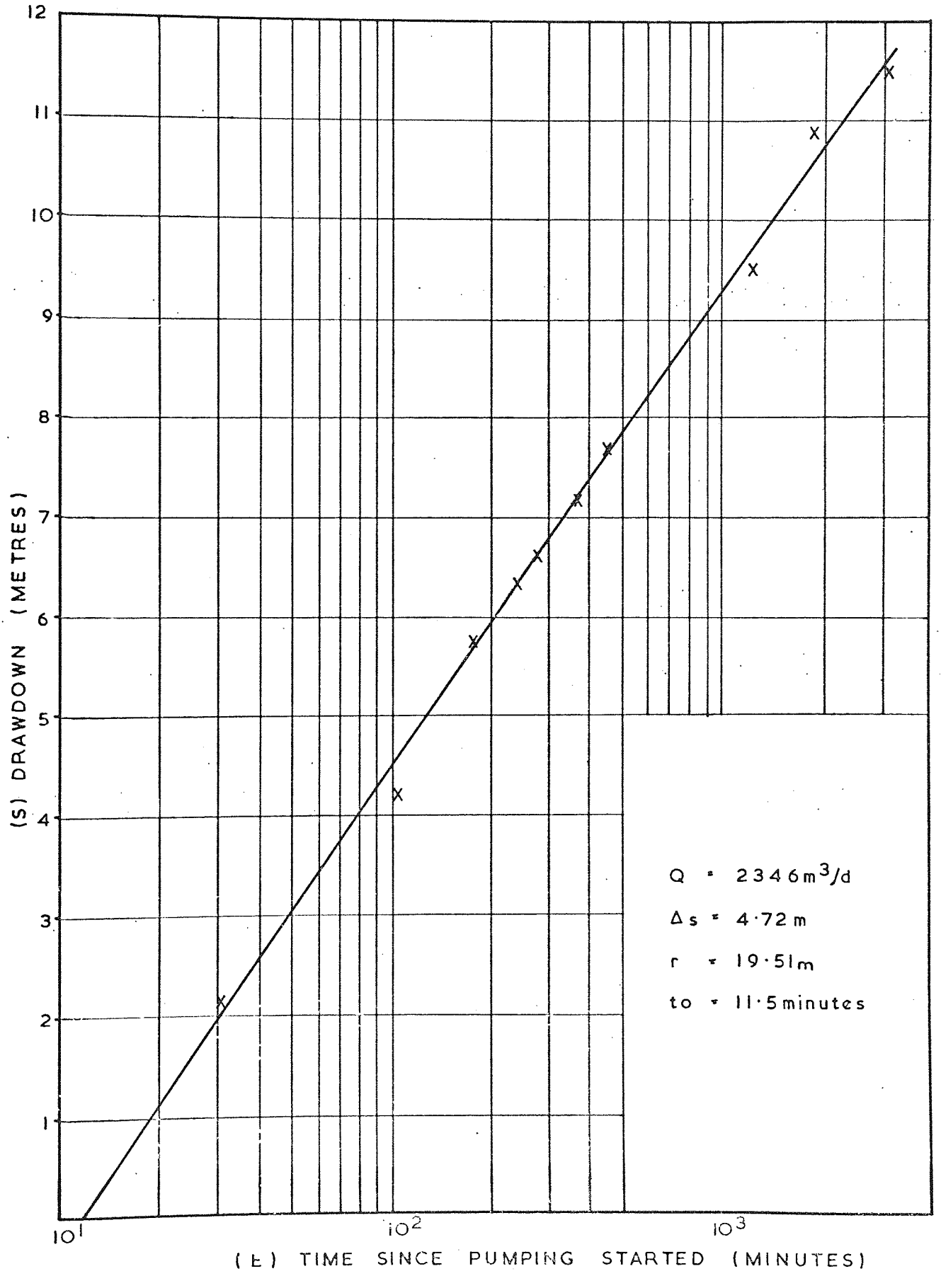

PUMP TEST ANALYSIS

FIGURE 46

TEST SITE	NEACHLEY
METHOD OF ANALYSIS	HANTUSH (1959)
TRANSMISSIBILITY	88 m^2/d
STORAGE COEFFICIENT	0·0069

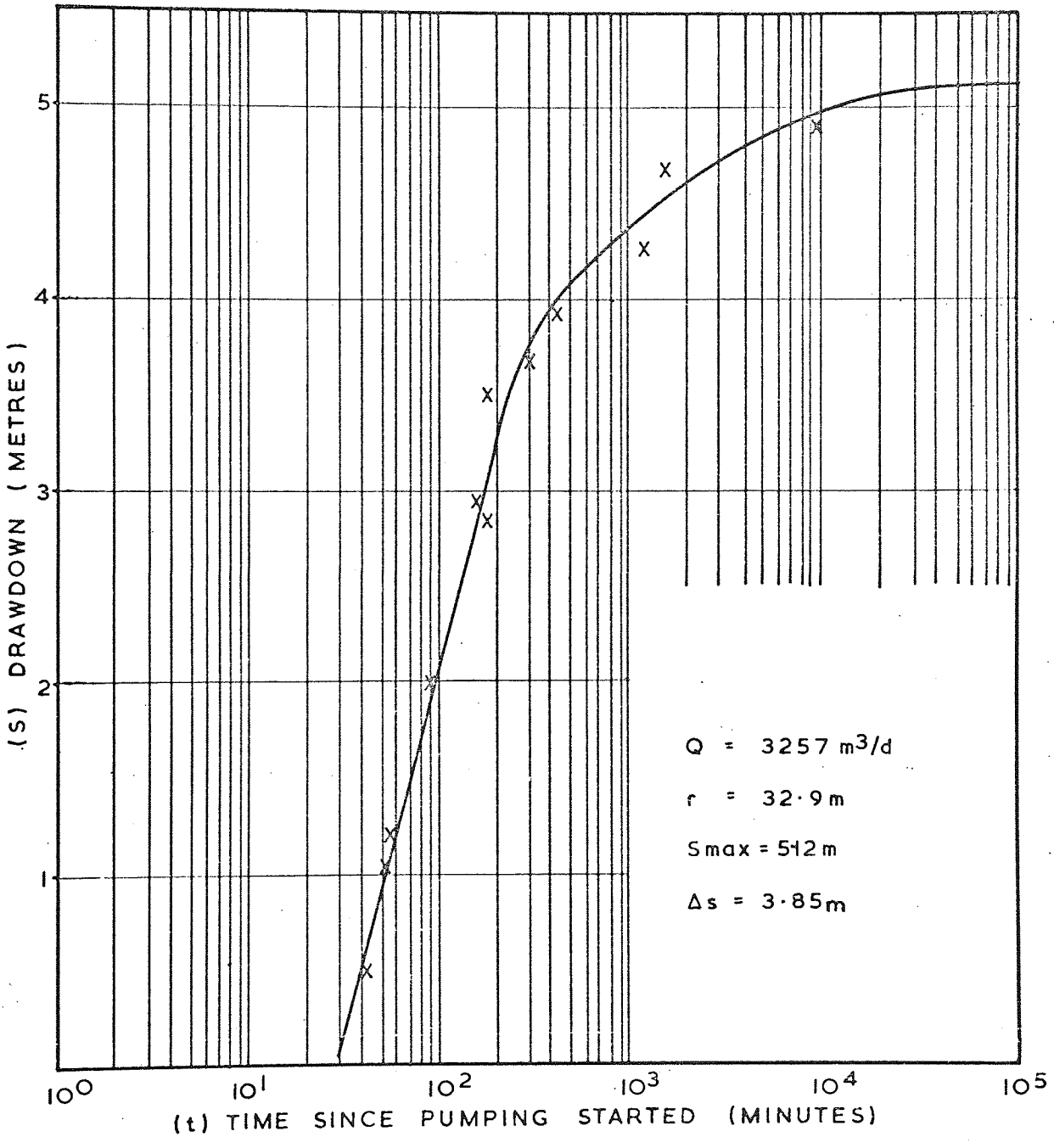

PUMP TEST ANALYSIS

TEST SITE ROUGHTON
METHOD OF ANALYSIS THEIS (1935)
TRANSMISSIBILITY 455 m^2/d
STORAGE COEFFICIENT 0·007

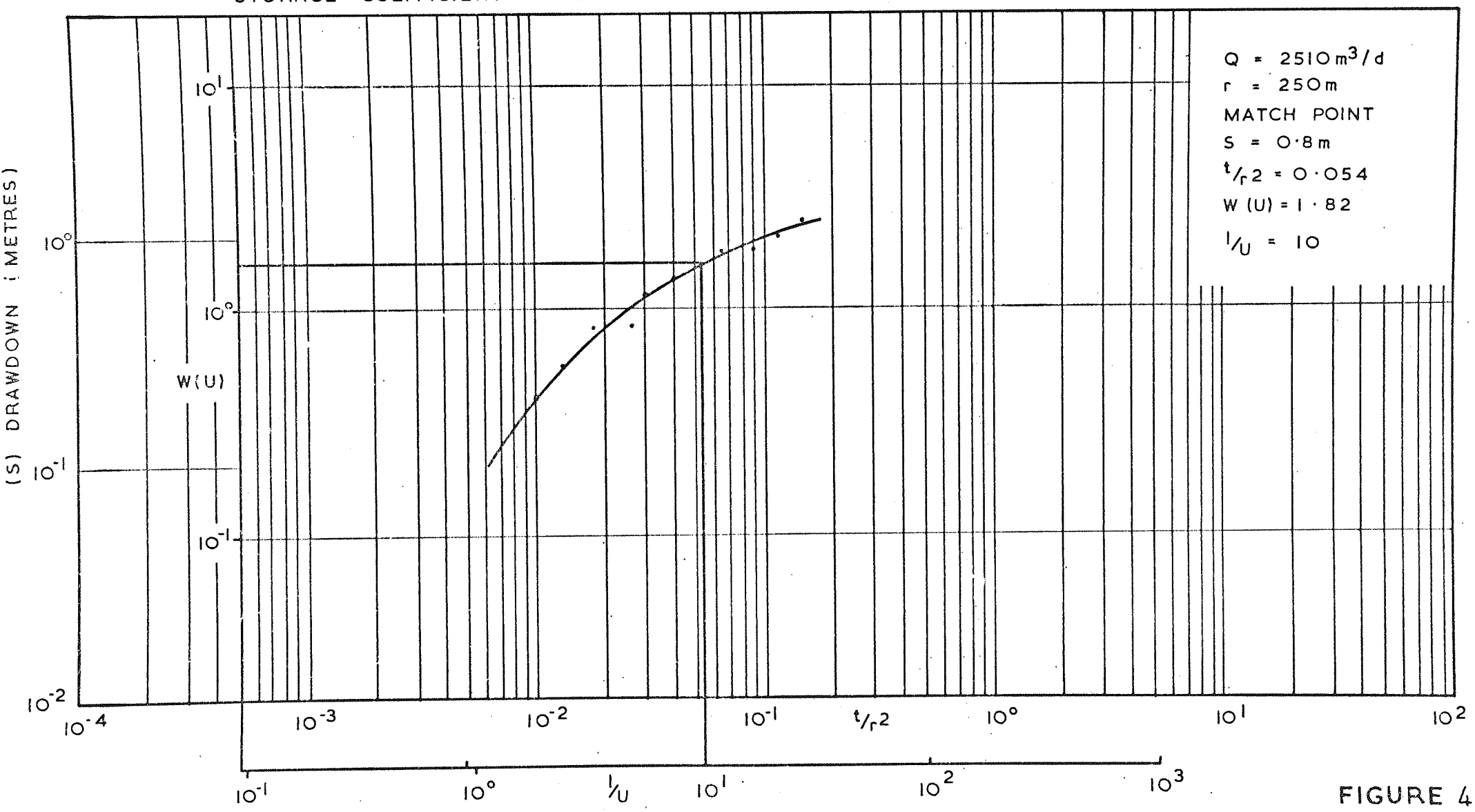

FIGURE 47

FIGURE 48

PUMP TEST ANALYSIS

TEST SITE — WESTERN JONES

METHOD OF ANALYSIS — THEIS (1935) recovery method

TRANSMISSIBILITY — 247 m^2/d

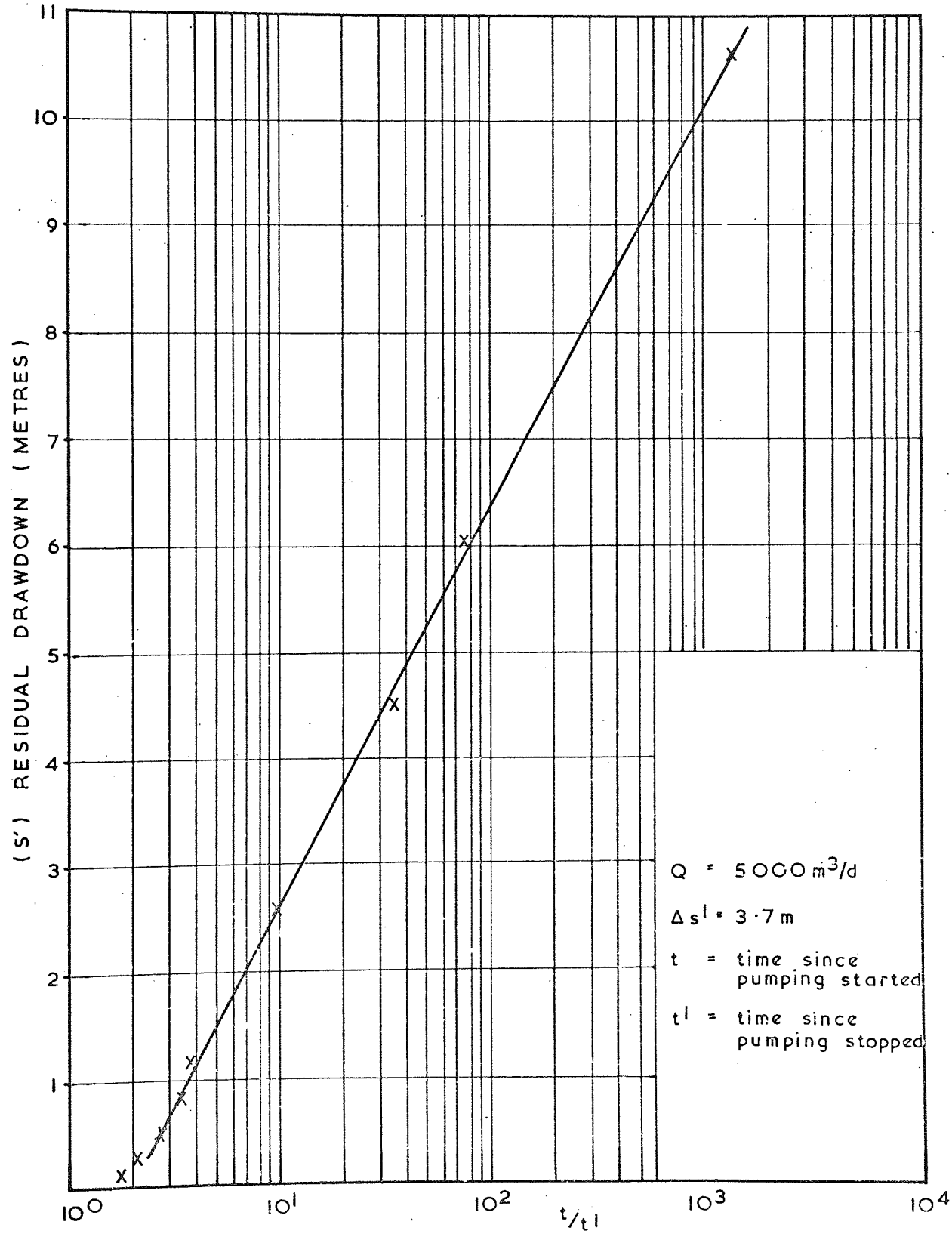

PUMP TEST ANALYSIS

TEST SITE — STABLEFORD

METHOD OF ANALYSIS — THEIS (1935) recovery method

TRANSMISSIBILITY — 695 m^2/d

FIGURE 49

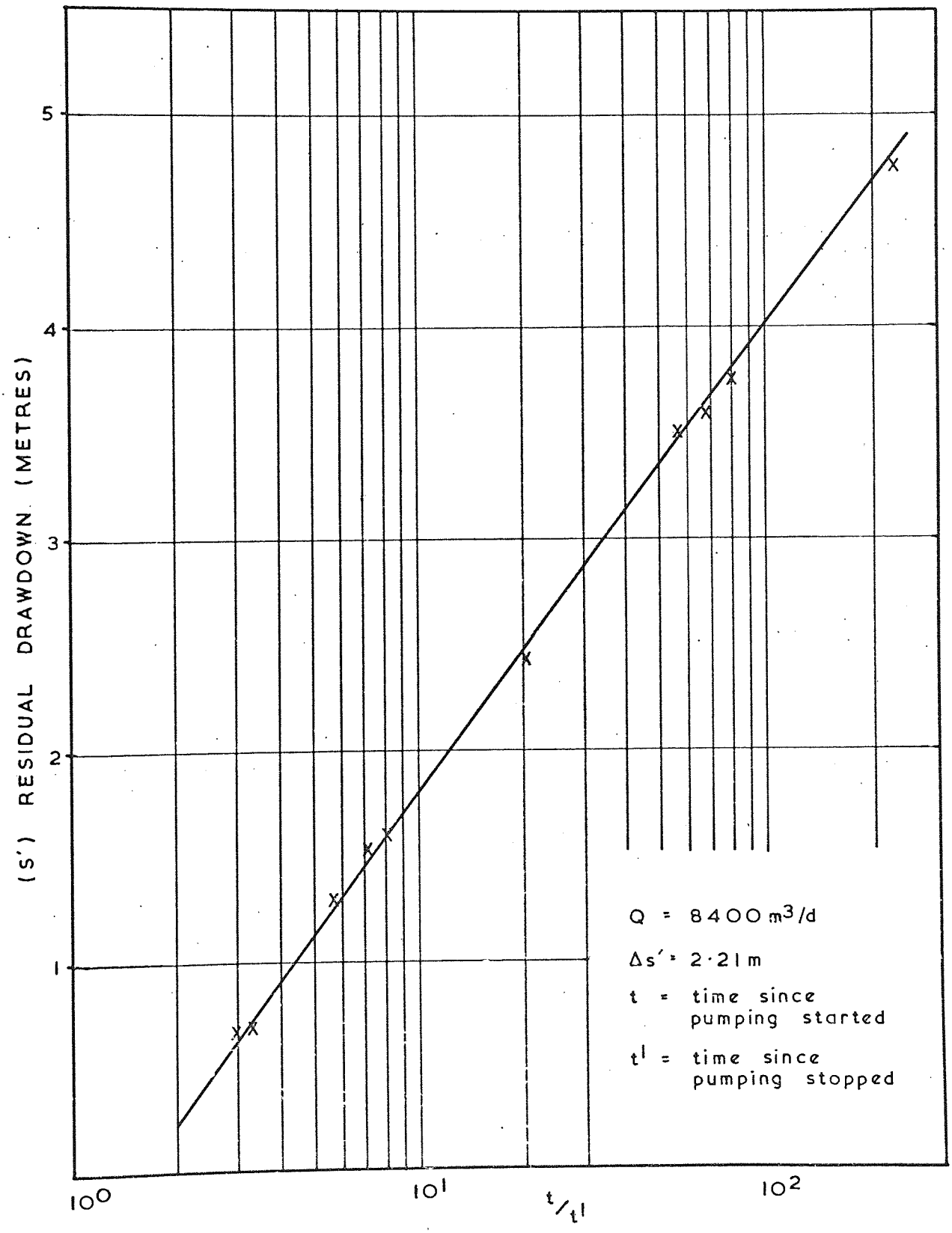

FIGURE 50

PUMP TEST ANALYSIS

TEST SITE	TOM HILL
METHOD OF ANALYSIS	THEIS (1935) recovery method
TRANSMISSIBILITY	645 m^2/d

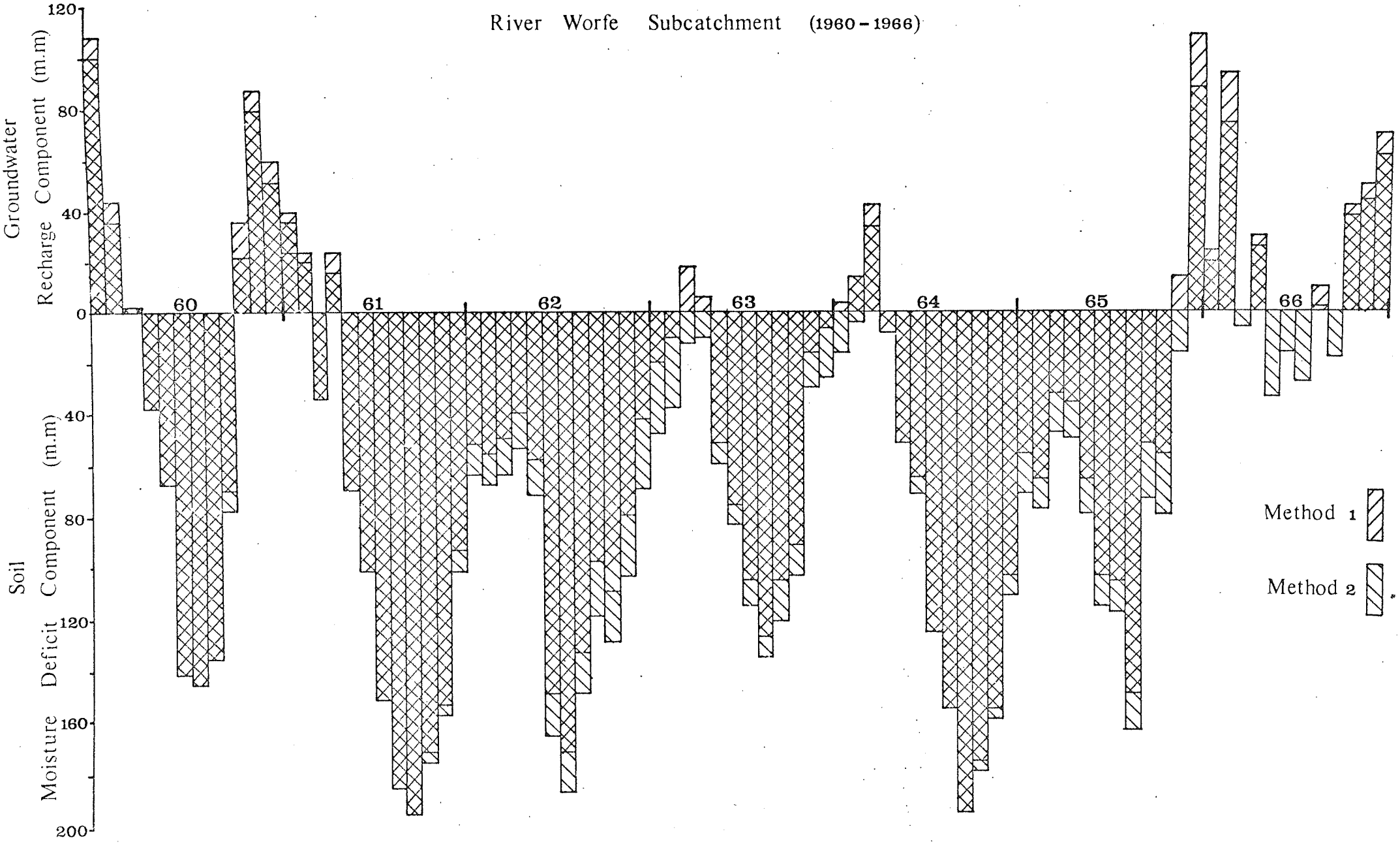

GROUNDWATER RECHARGE AND SOIL MOISTURE DEFICITS

FIGURE 51

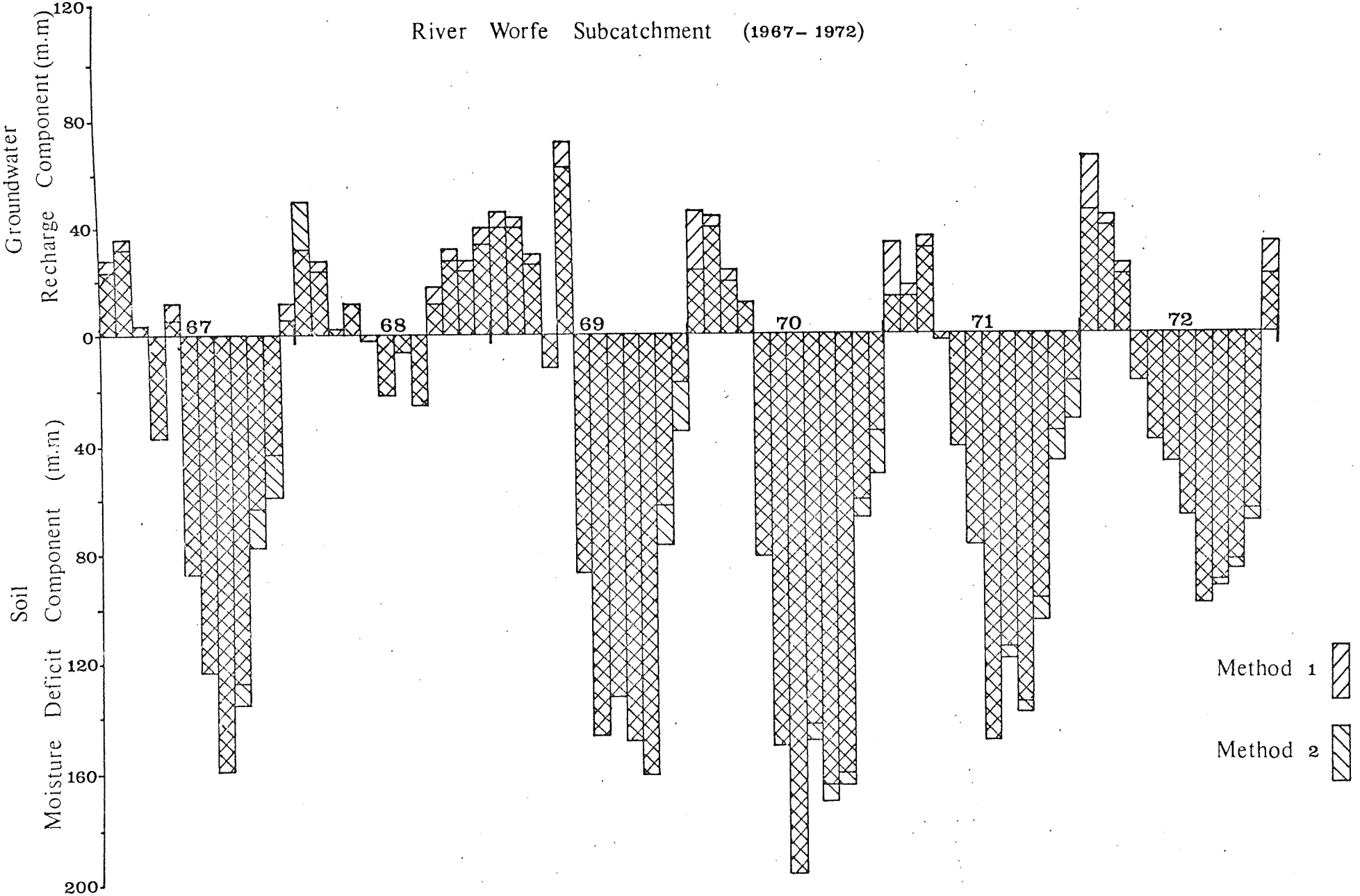

GROUNDWATER RECHARGE AND SOIL MOISTURE DEFICITS

FIGURE 51 Cont

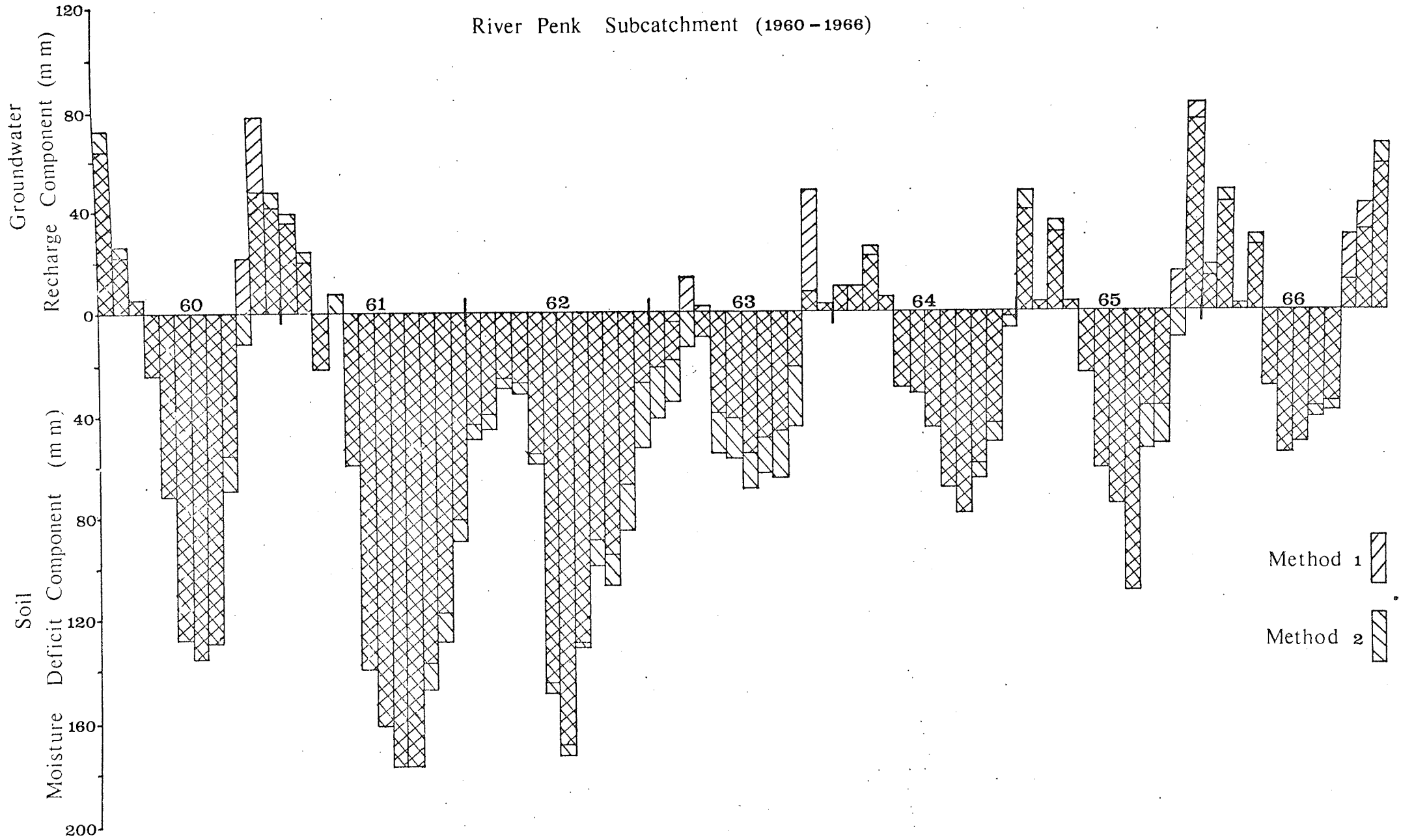

GROUNDWATER RECHARGE AND SOIL MOISTURE DEFICITS

FIGURE 52

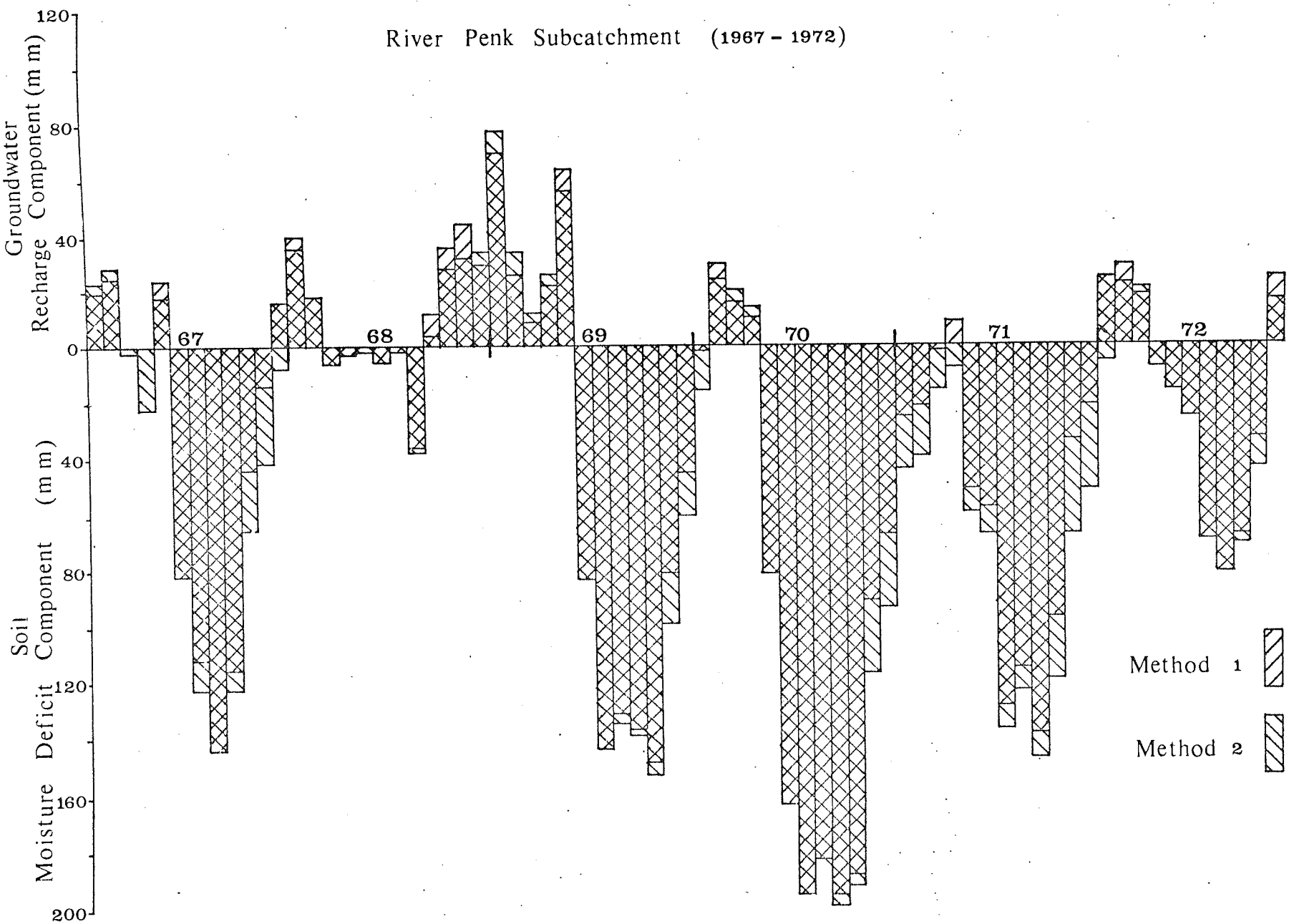

GROUNDWATER RECHARGE AND SOIL MOISTURE DEFICITS FIGURE 52 Cont

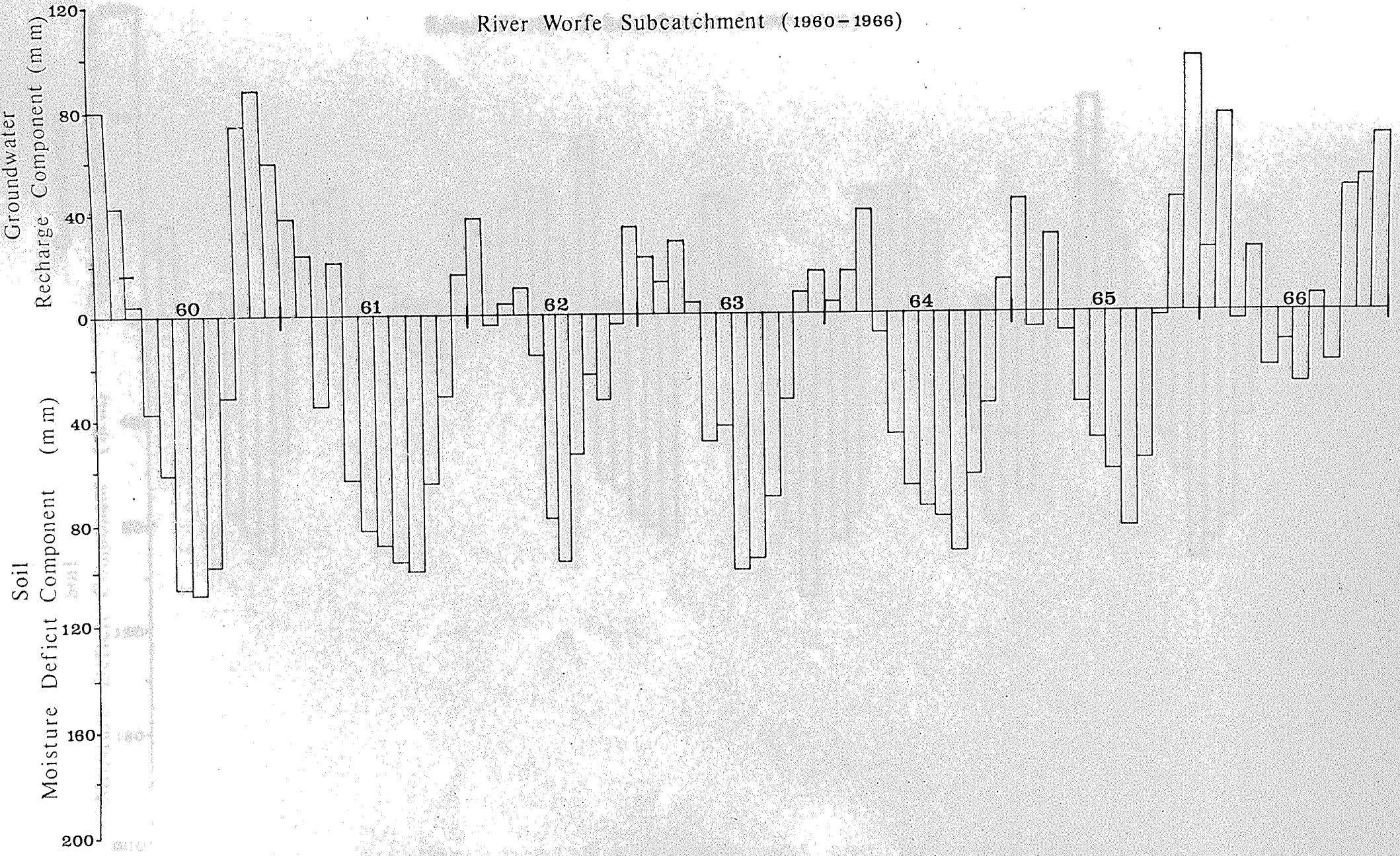

GROUNDWATER RECHARGE AND SOIL MOISTURE DEFICITS FIGURE 53

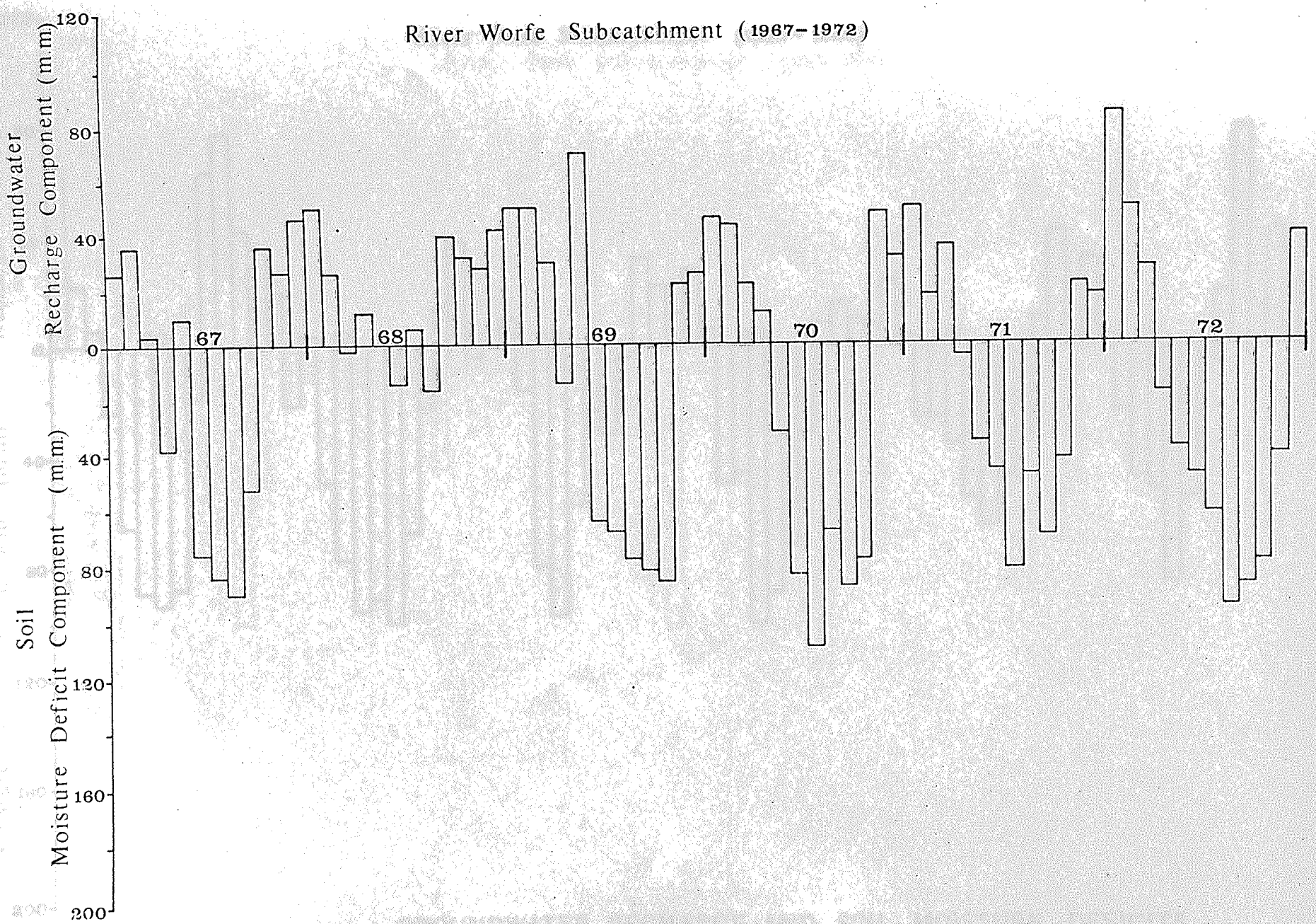

FIGURE 53 Cont

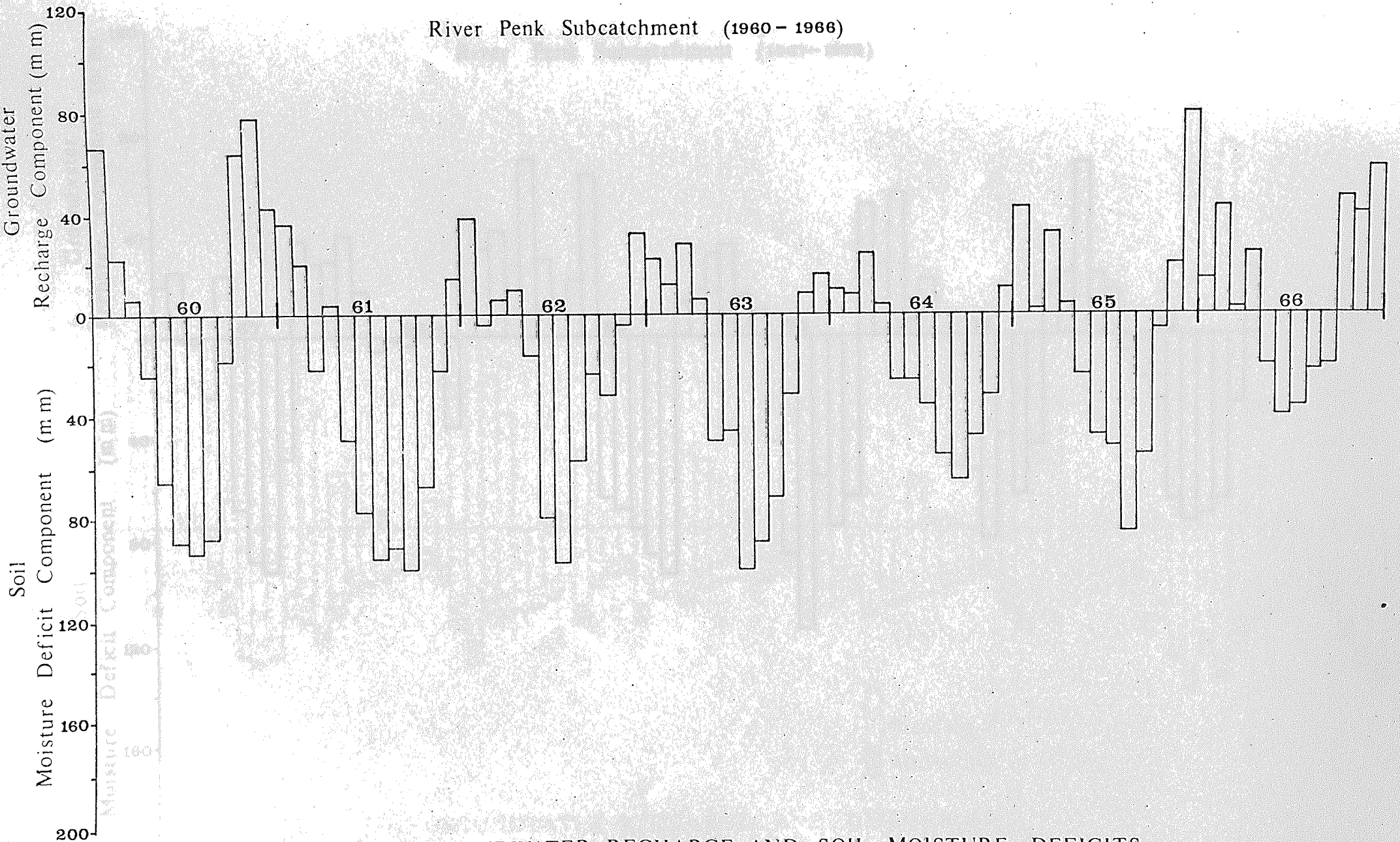

GROUNDWATER RECHARGE AND SOIL MOISTURE DEFICITS

FIGURE 54

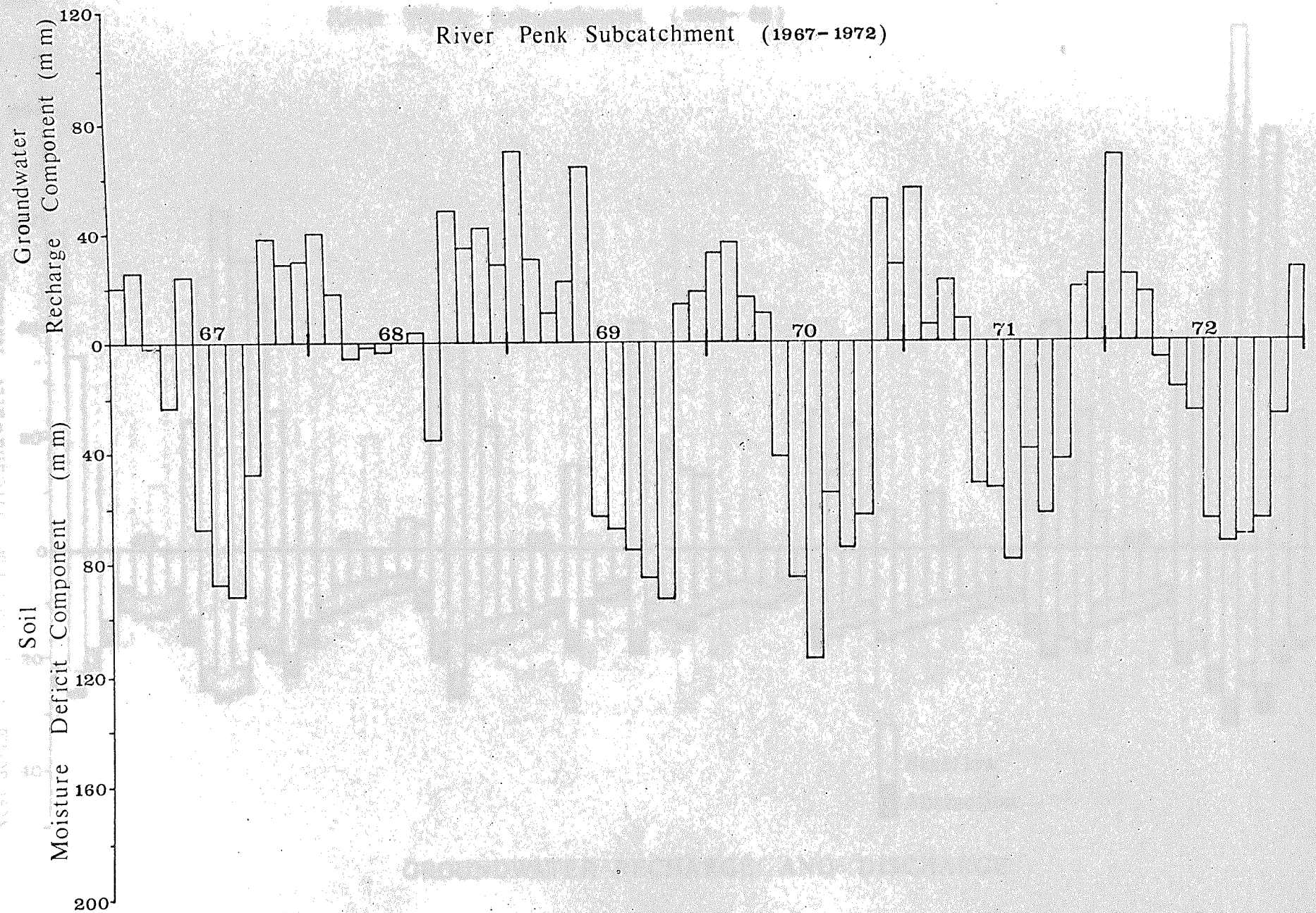

FIGURE 54Cont.

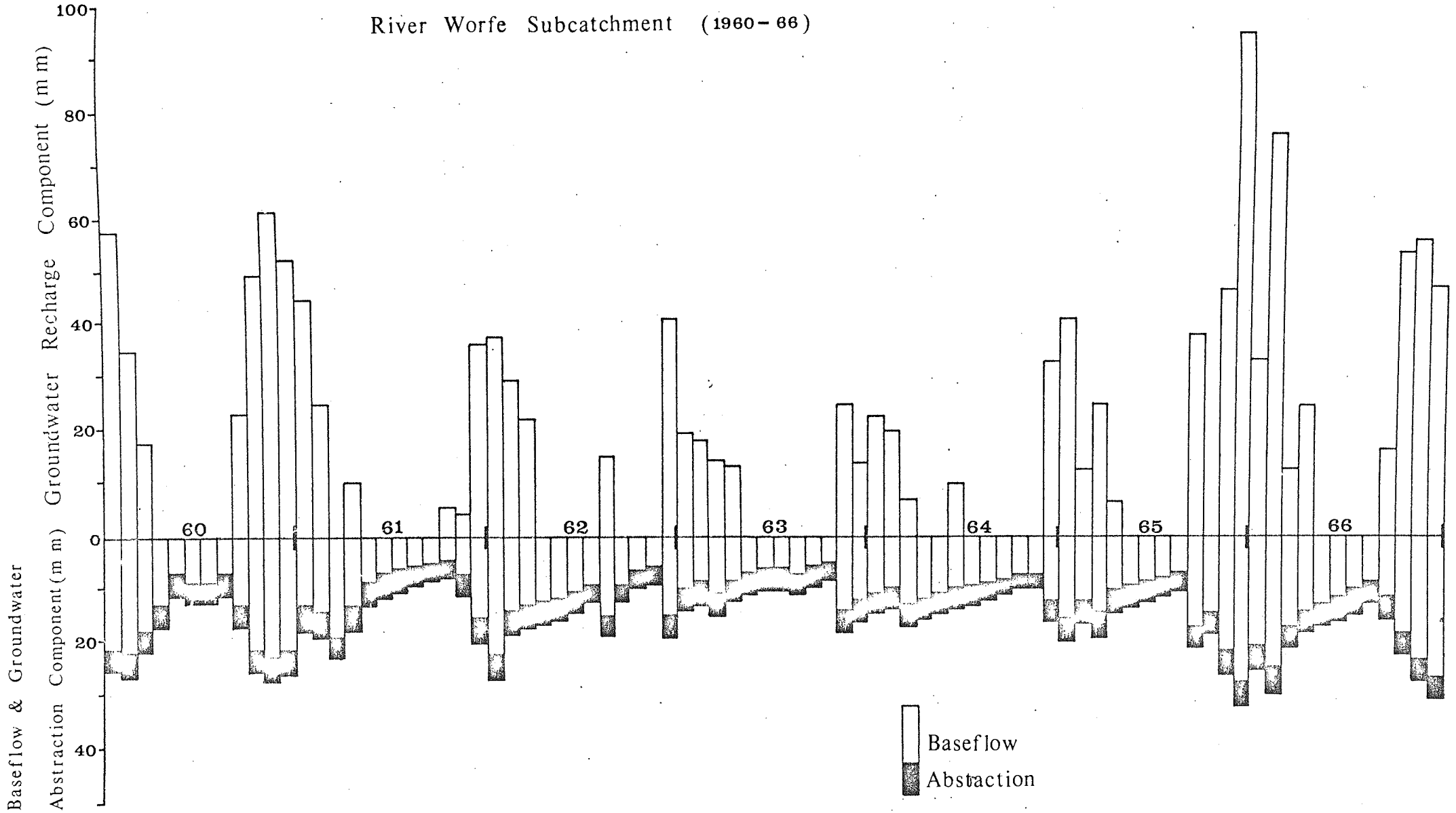

GROUNDWATER RECHARGE AND DISCHARGE

FIGURE 55

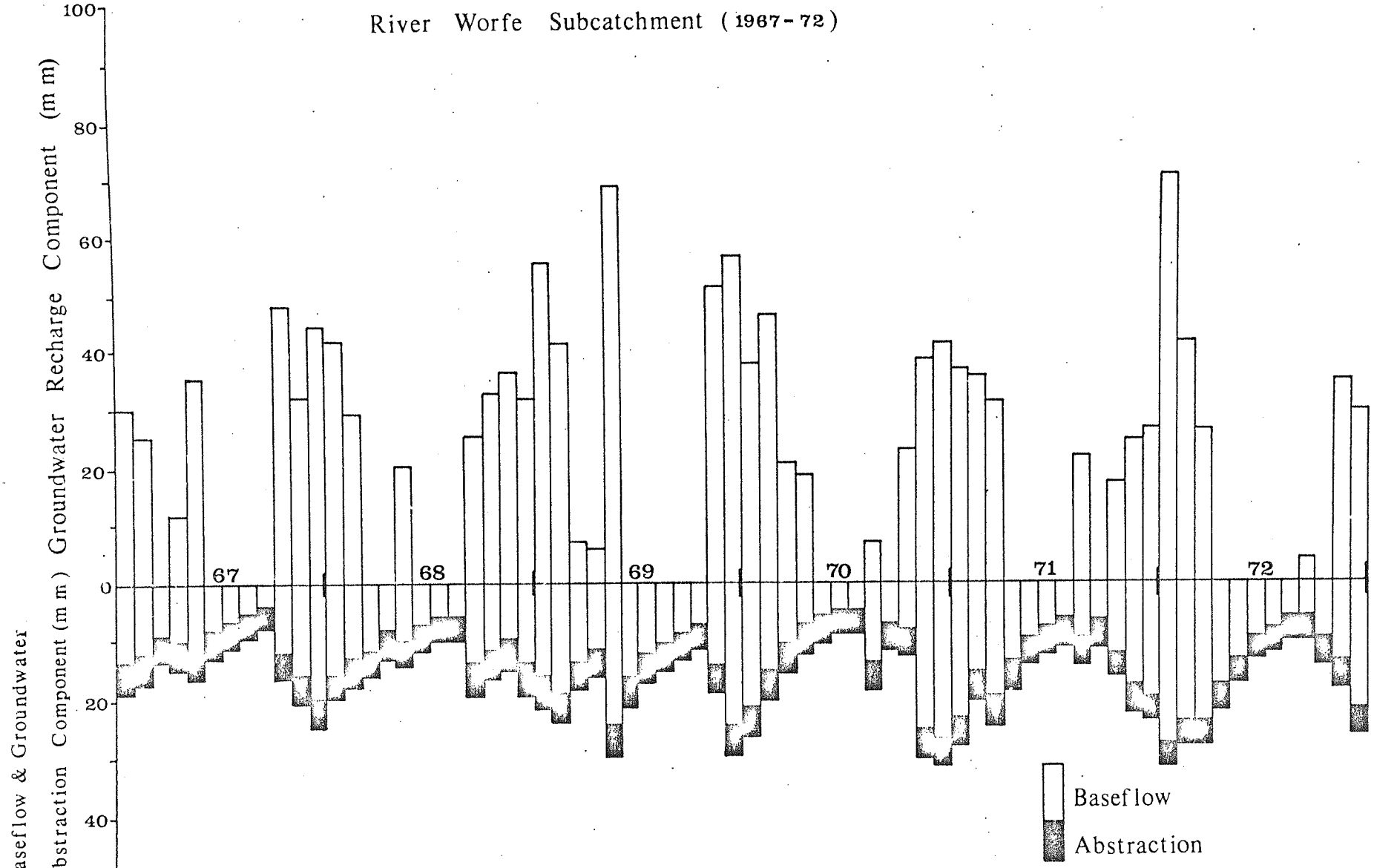

GROUNDWATER RECHARGE AND DISCHARGE

FIGURE 55Cont

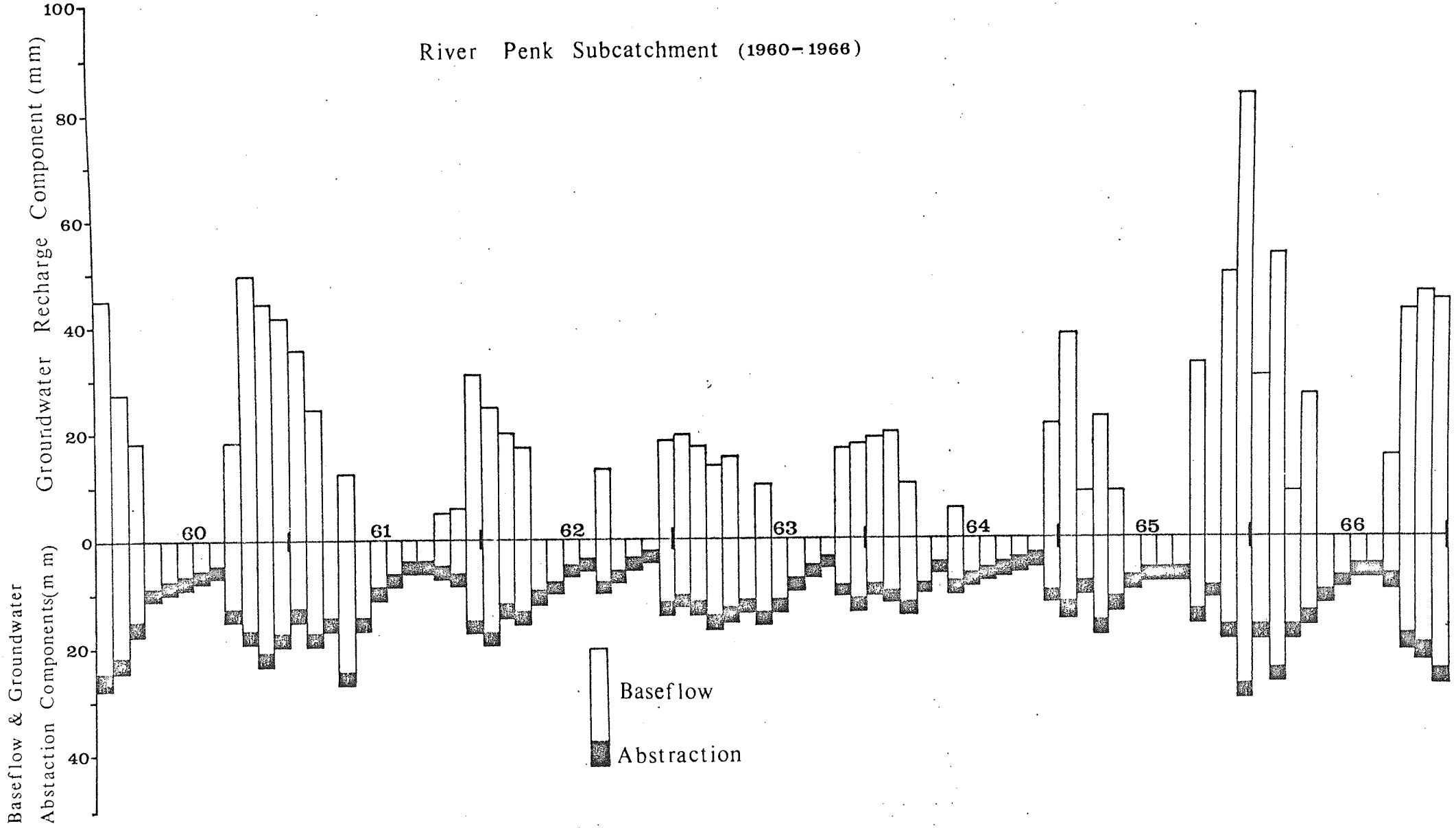

GROUNDWATER RECHARGE AND DISCHARGE

FIGURE 56

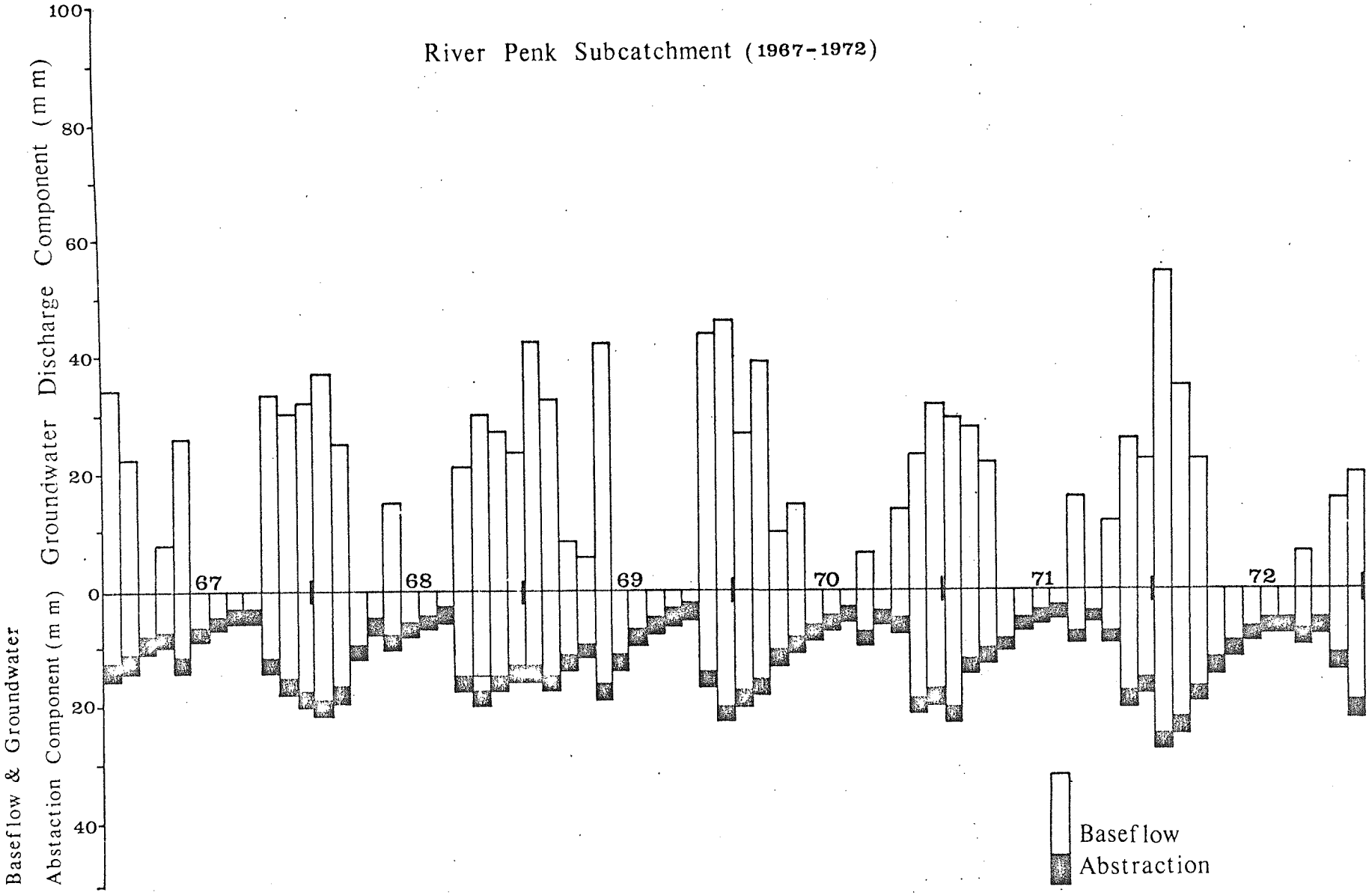

GROUNDWATER RECHARGE AND DISCHARGE

FIGURE 56 Cont

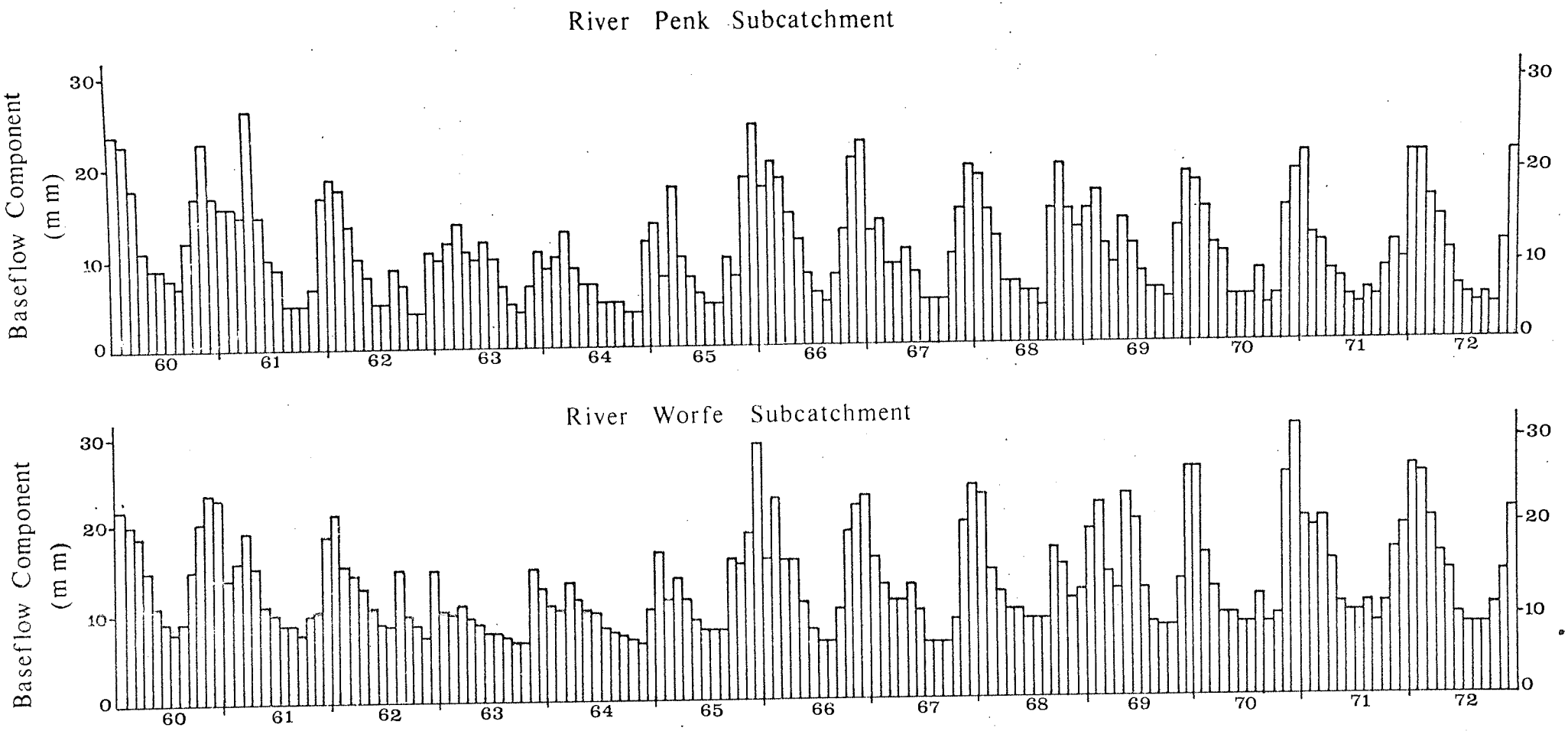

BASEFLOW COMPONENT EVALUATED FROM HISTORICAL RECORD (1960 - 72)

FIGURE 57

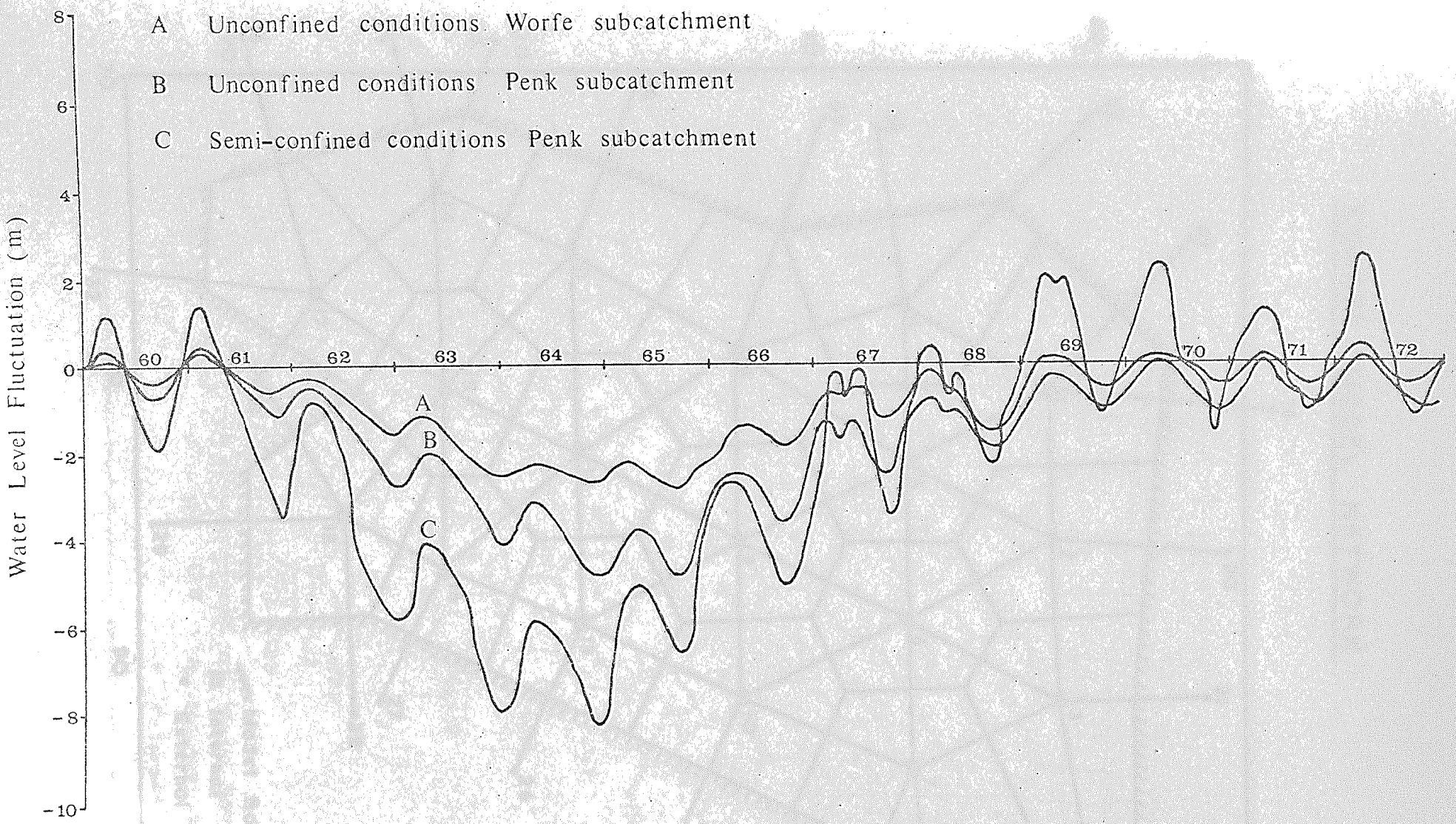

HISTORICAL GROUNDWATER LEVEL FLUCTUATIONS (1960-72)

FIGURE 58

FIGURE 59

COARSE MODEL NETWORK

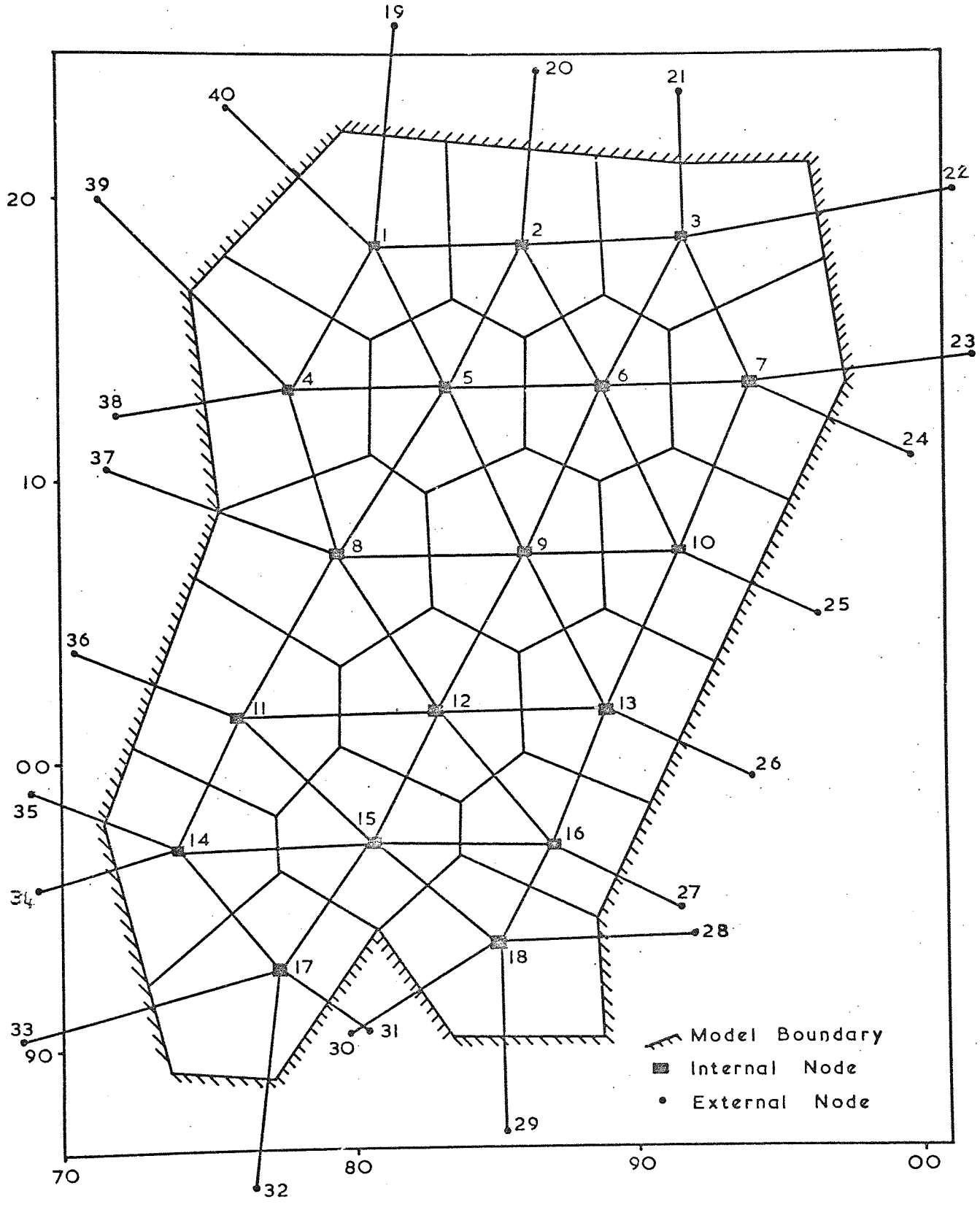

FIGURE 60

FINE MESHED NETWORK

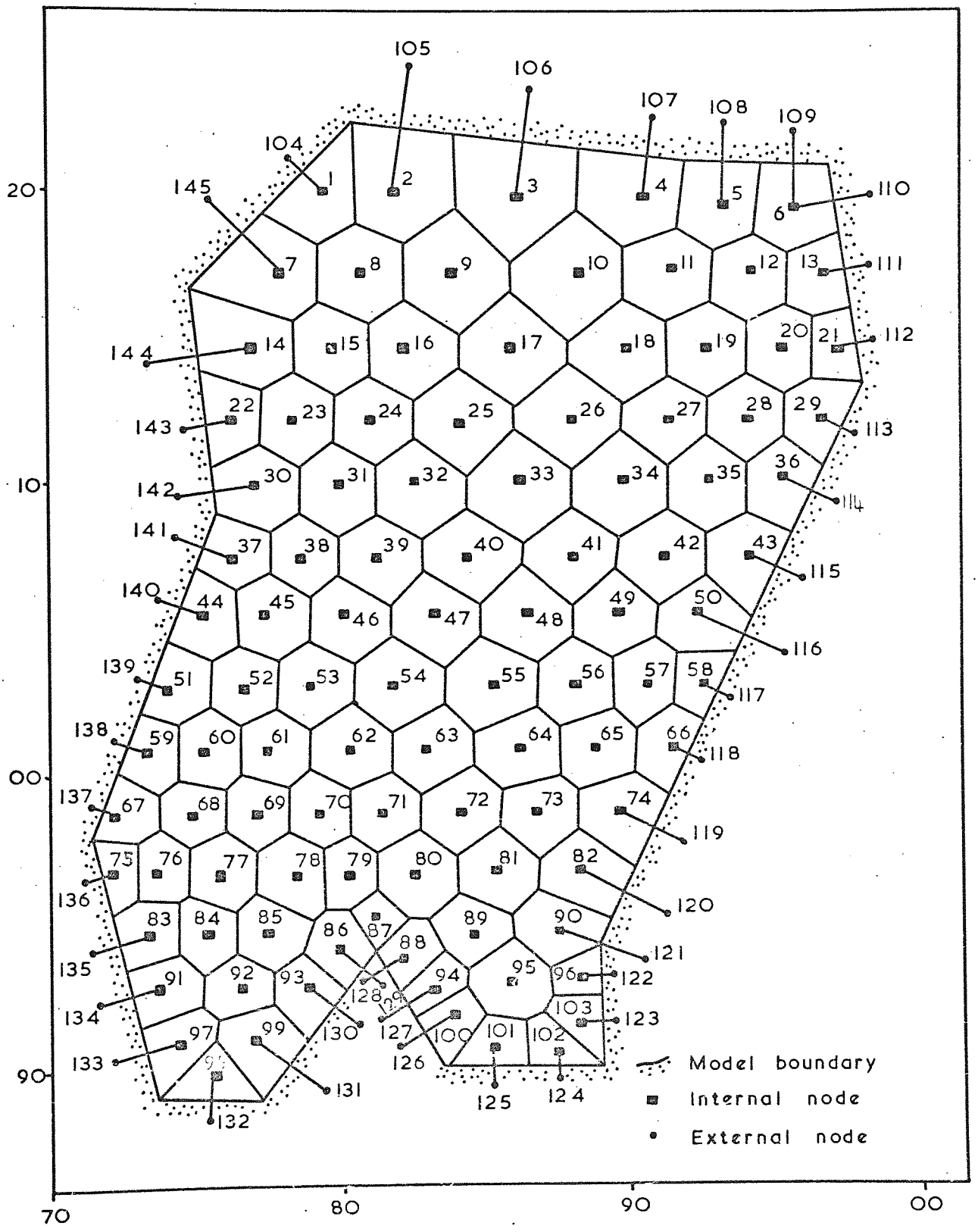

FIGURE 61

PRINCIPAL GROUNDWATER RECHARGE AREA

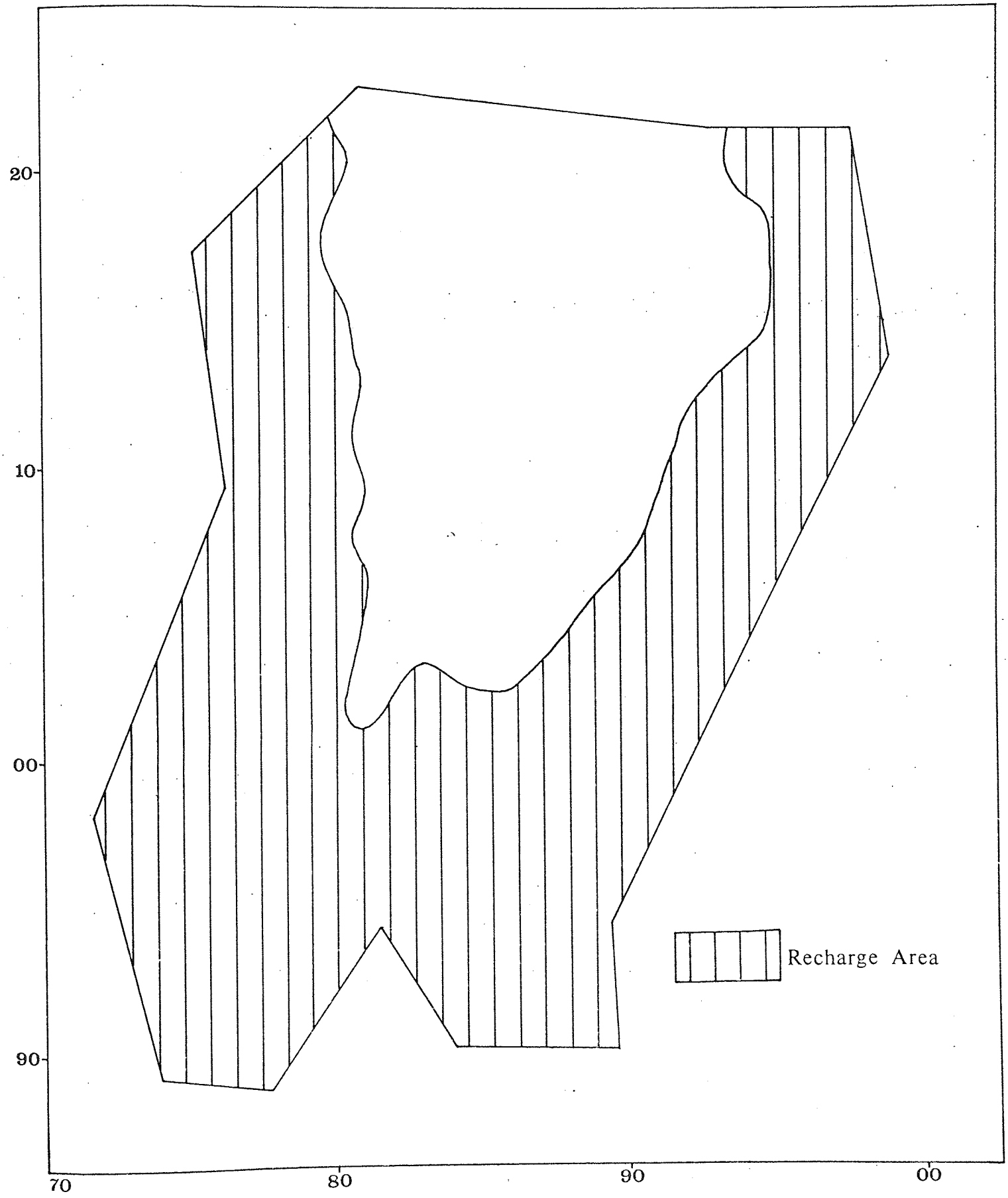

FIGURE 62

PRINCIPAL BASEFLOW CONTRIBUTARY AREAS

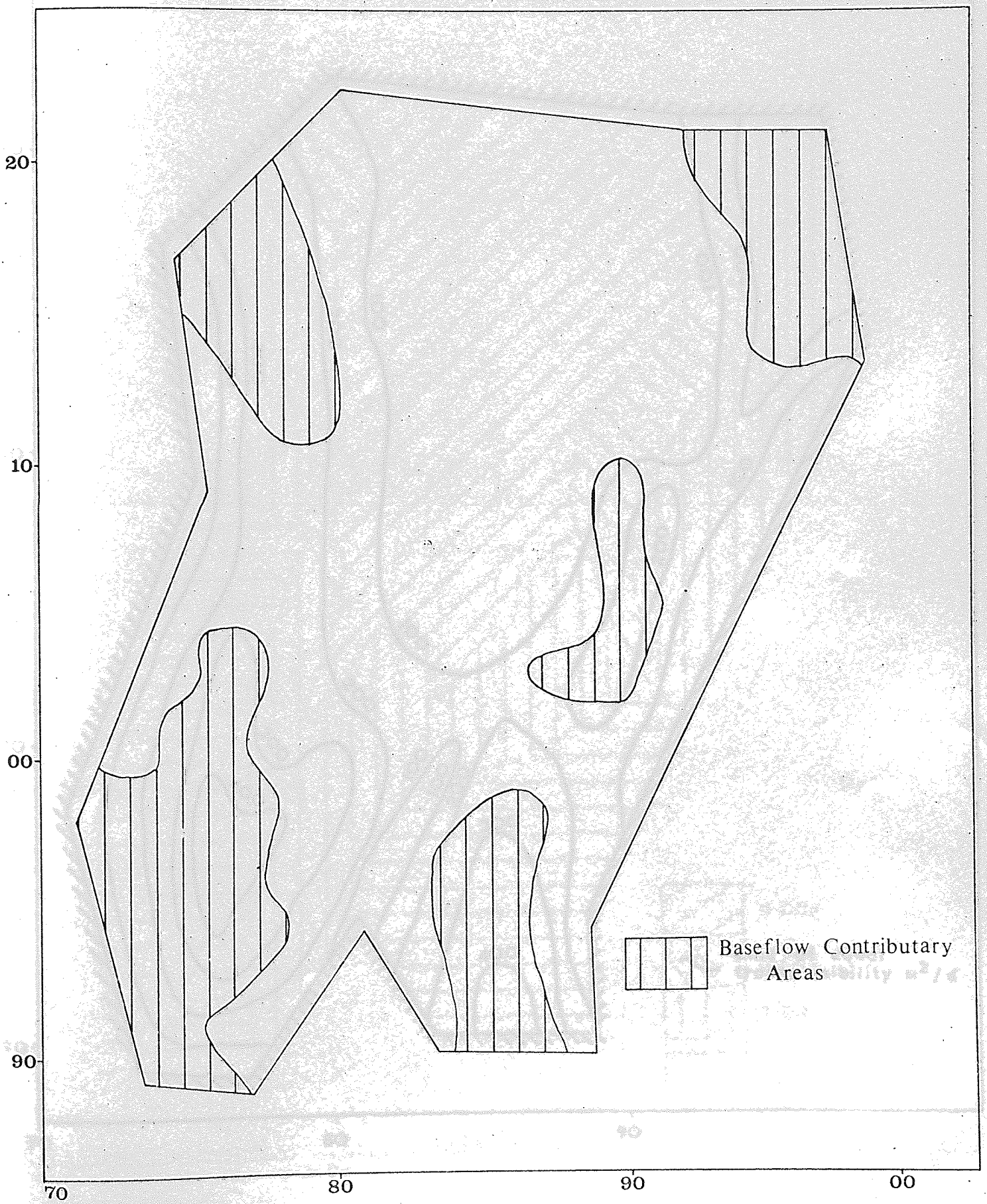

FIGURE 63

CALIBRATED TRANSMISSIBILITY NETWORK DISTRIBUTION

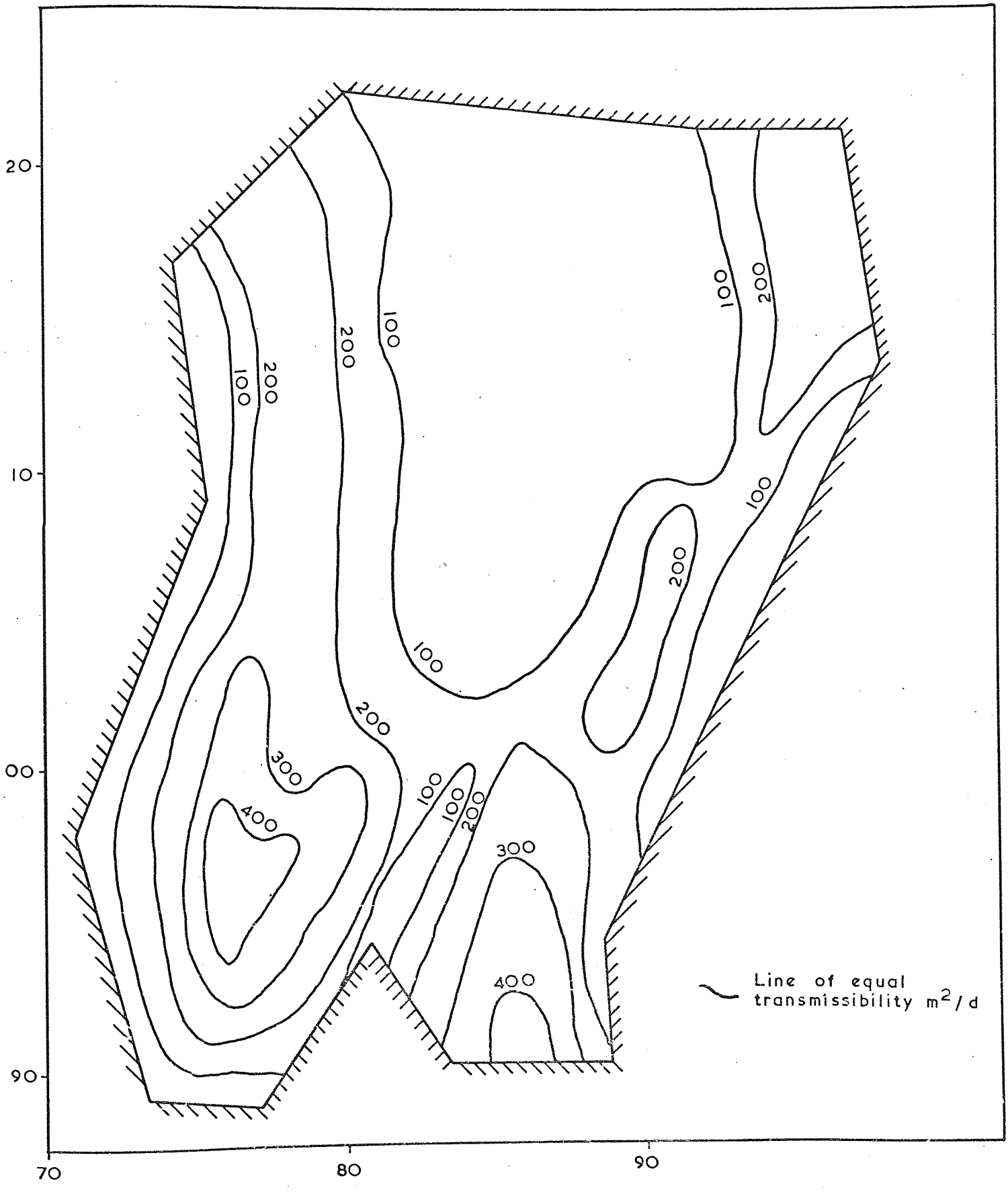

FIGURE 64

STORAGE COEFFICIENT DISTRIBUTION NETWORK

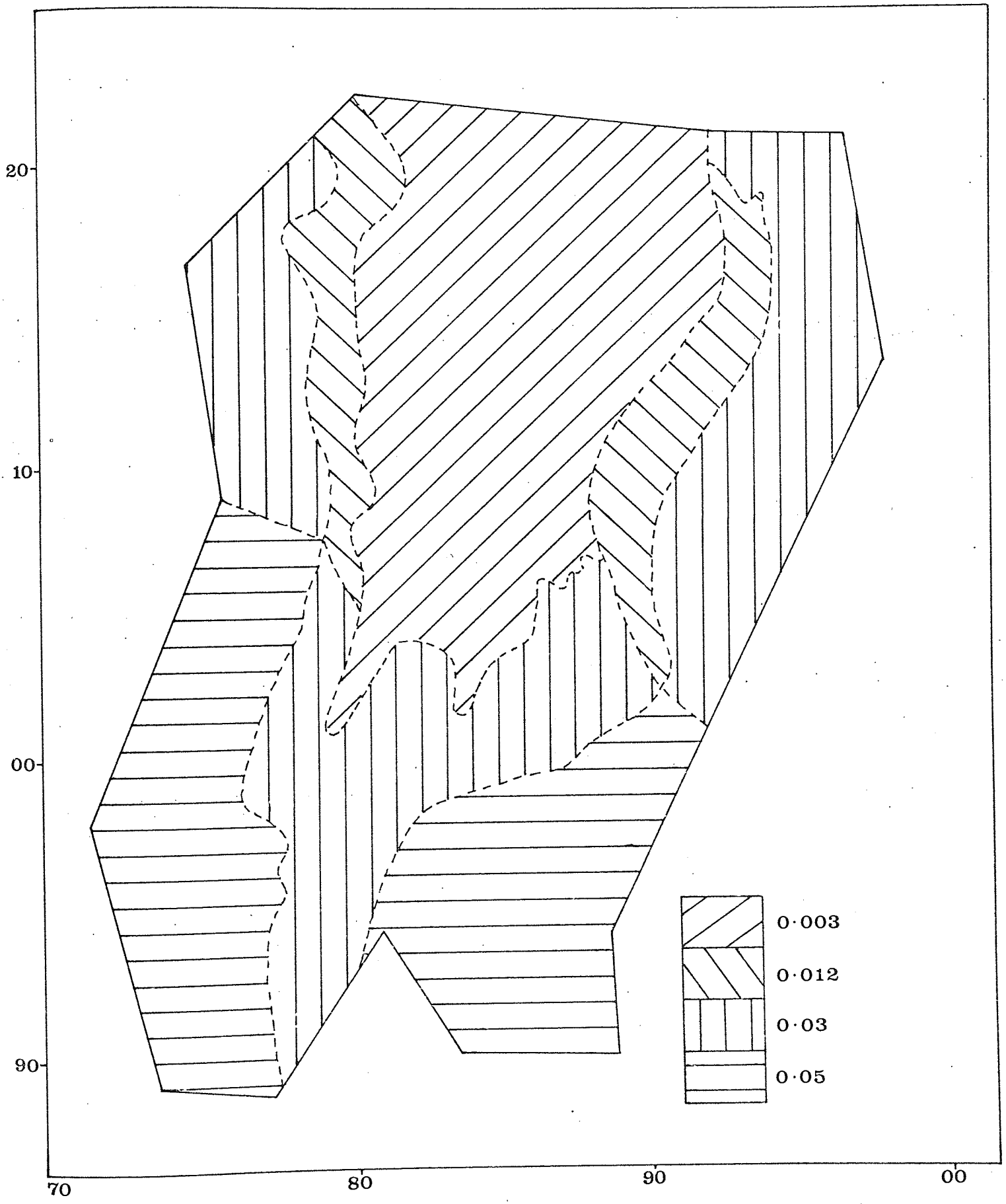

FIGURE 65

DYNAMIC EQUILIBRIUM WATER LEVEL CONDITIONS

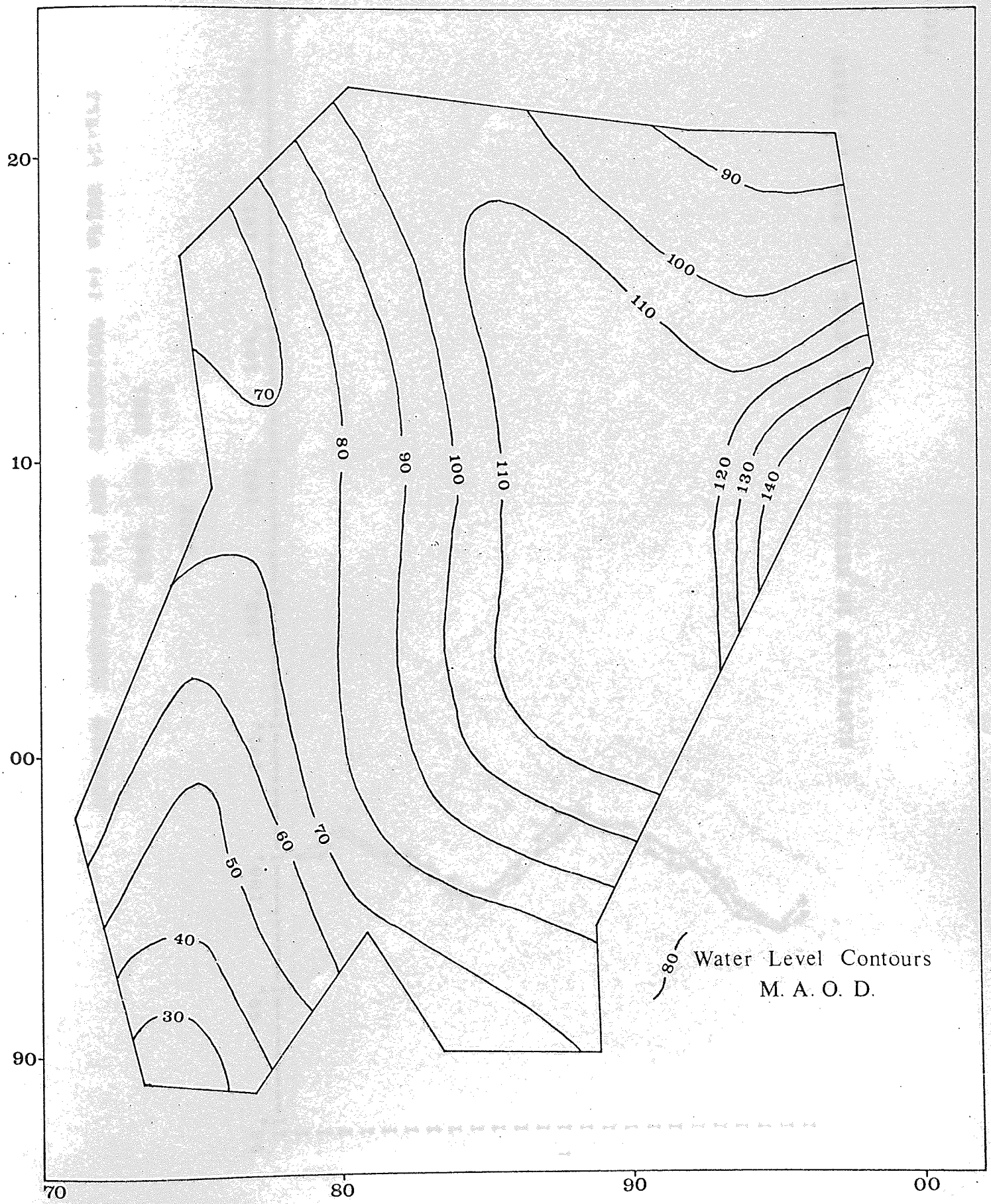

MONTHLY COMPUTED (*) AND HISTORICAL (+) WATER LEVELS

1960 AND 1961

NODE 73

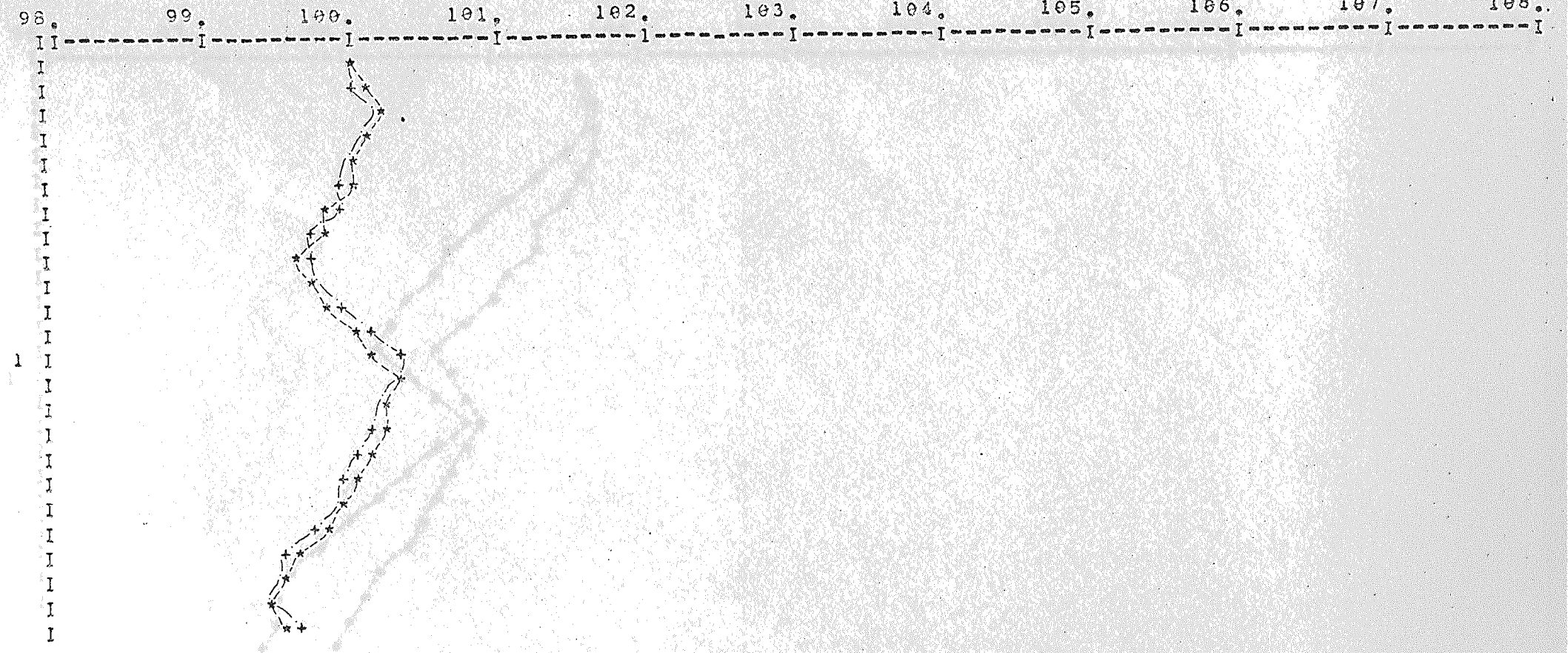

ELEVATION IN METERS ABOVE SEA LEVEL VS. TIME IN YEARS

FIGURE 66

MONTHLY COMPUTED (*) AND HISTORICAL (+) WATER LEVELS

1962 AND 1963

NODE 73

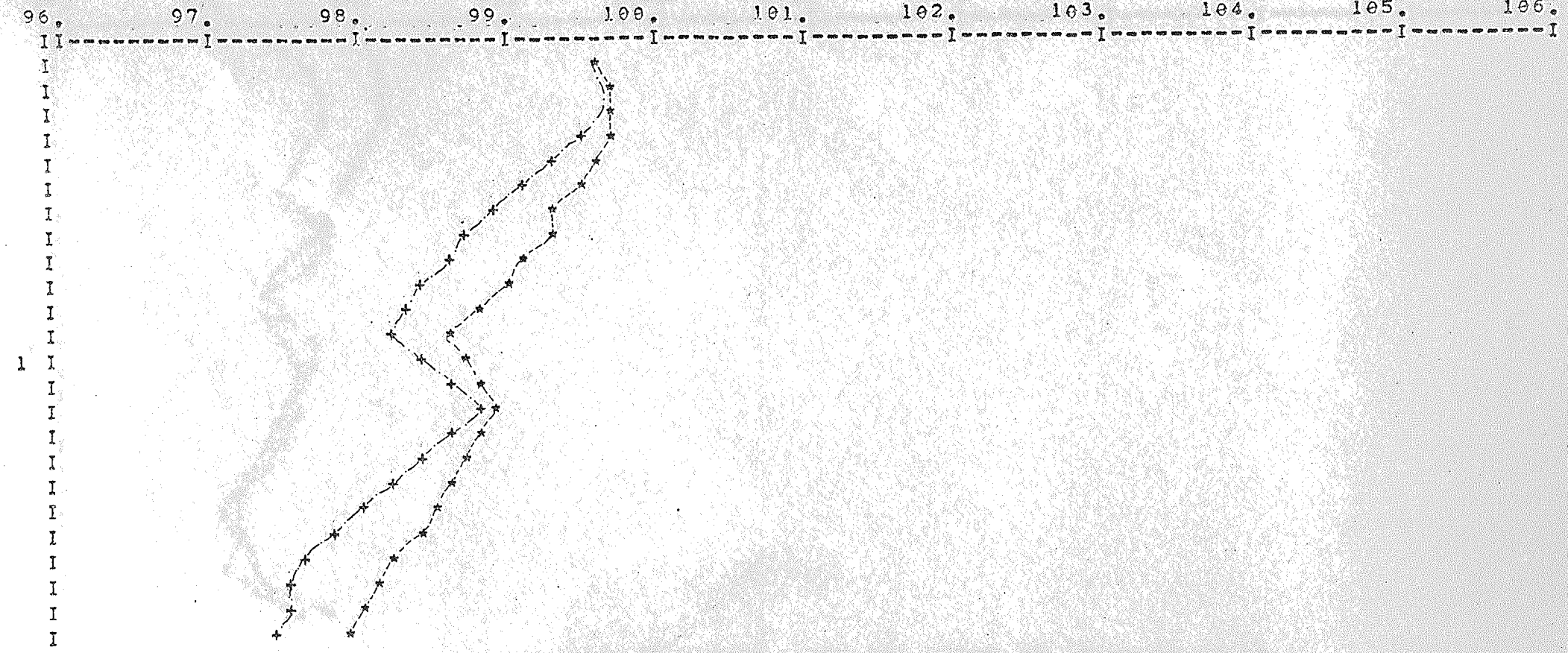

ELEVATION IN METERS ABOVE SEA LEVEL VS. TIME IN YEARS

FIGURE 66 cont.

MONTHLY COMPUTED (*) AND HISTORICAL (+) WATER LEVELS

1964 AND 1965

NODE 73

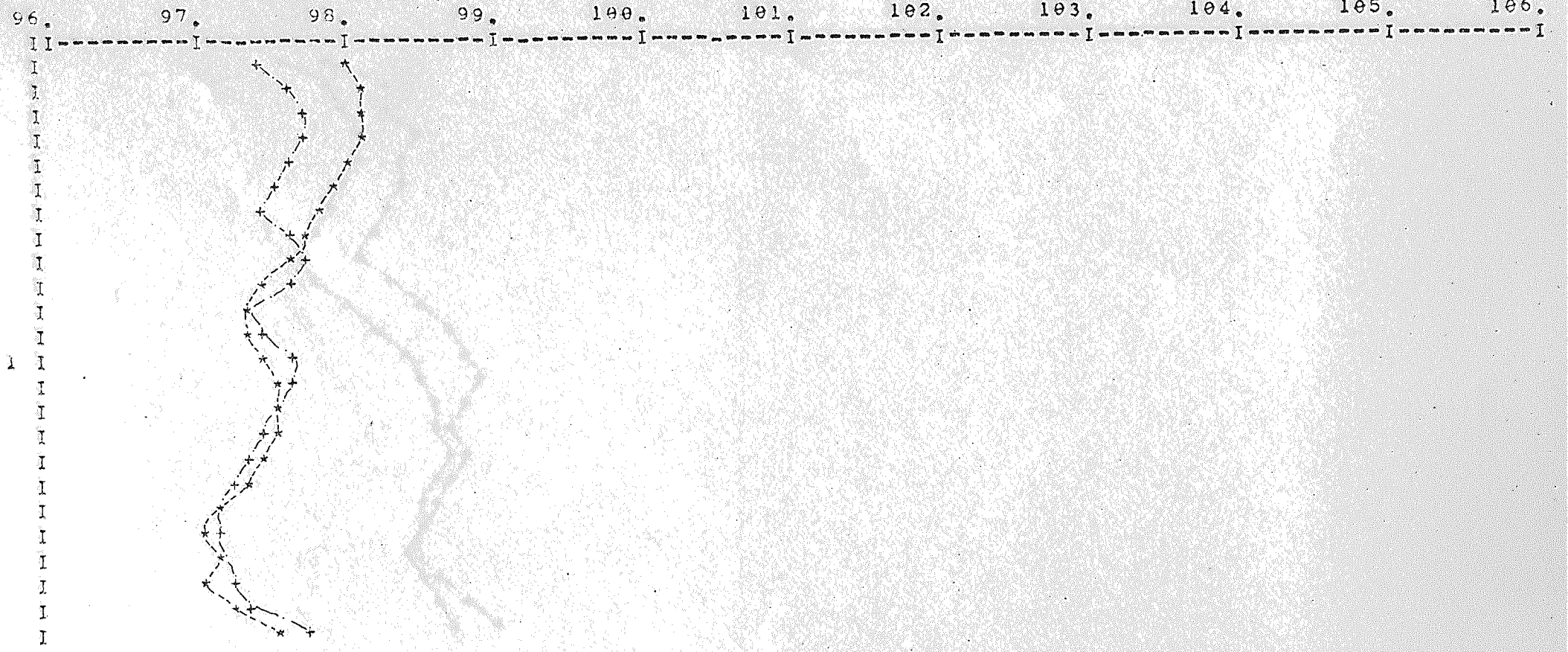

ELEVATION IN METERS ABOVE SEA LEVEL VS. TIME IN YEARS

FIGURE 66 cont.

MONTHLY COMPUTED (*) AND HISTORICAL (+) WATER LEVELS

1966 AND 1967

NODE 73

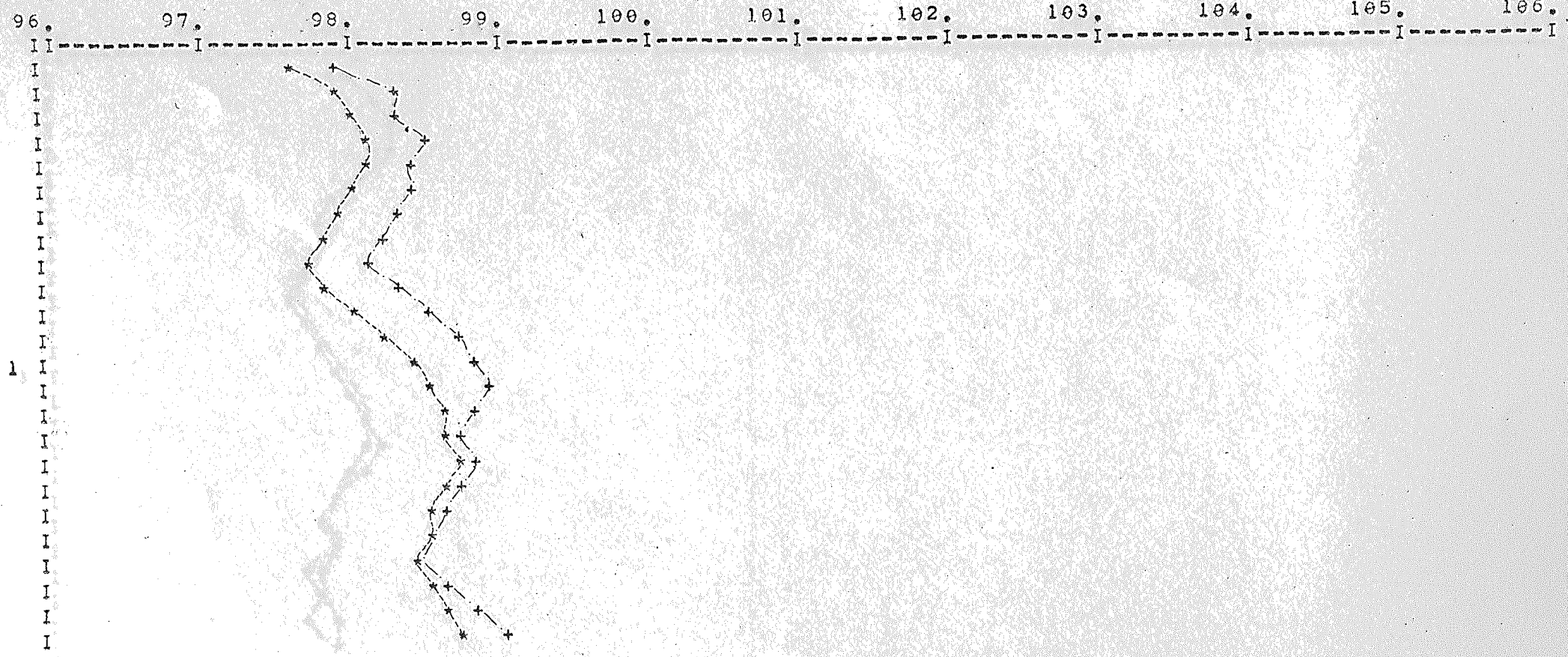

ELEVATION IN METERS ABOVE SEA LEVEL VS. TIME IN YEARS

FIGURE 66cont.

MONTHLY COMPUTED (*) AND HISTORICAL (+) WATER LEVELS

1968 AND 1969

NODE 73

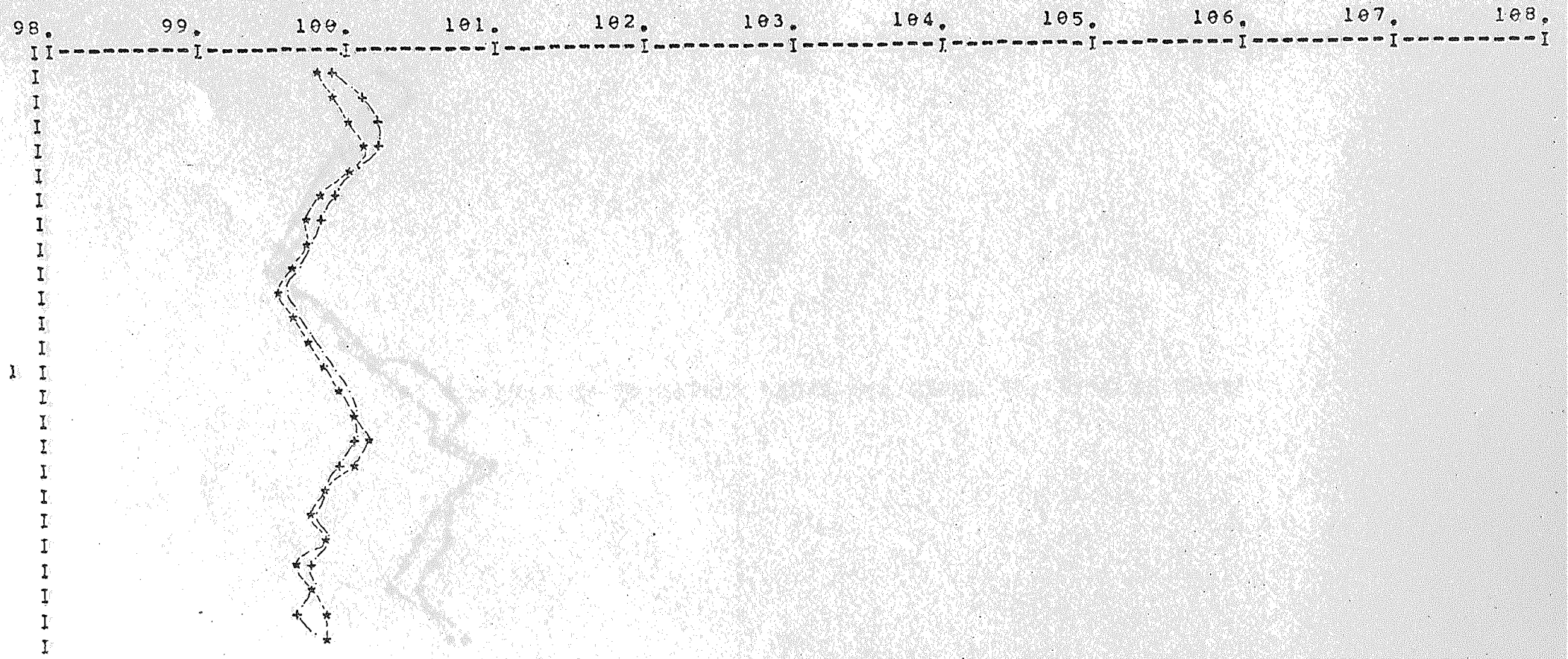

ELEVATION IN METERS ABOVE SEA LEVEL VS. TIME IN YEARS

FIGURE 66 cont.

MONTHLY COMPUTED (*) AND HISTORICAL (+) WATER LEVELS

1970 AND 1971

NODE 73

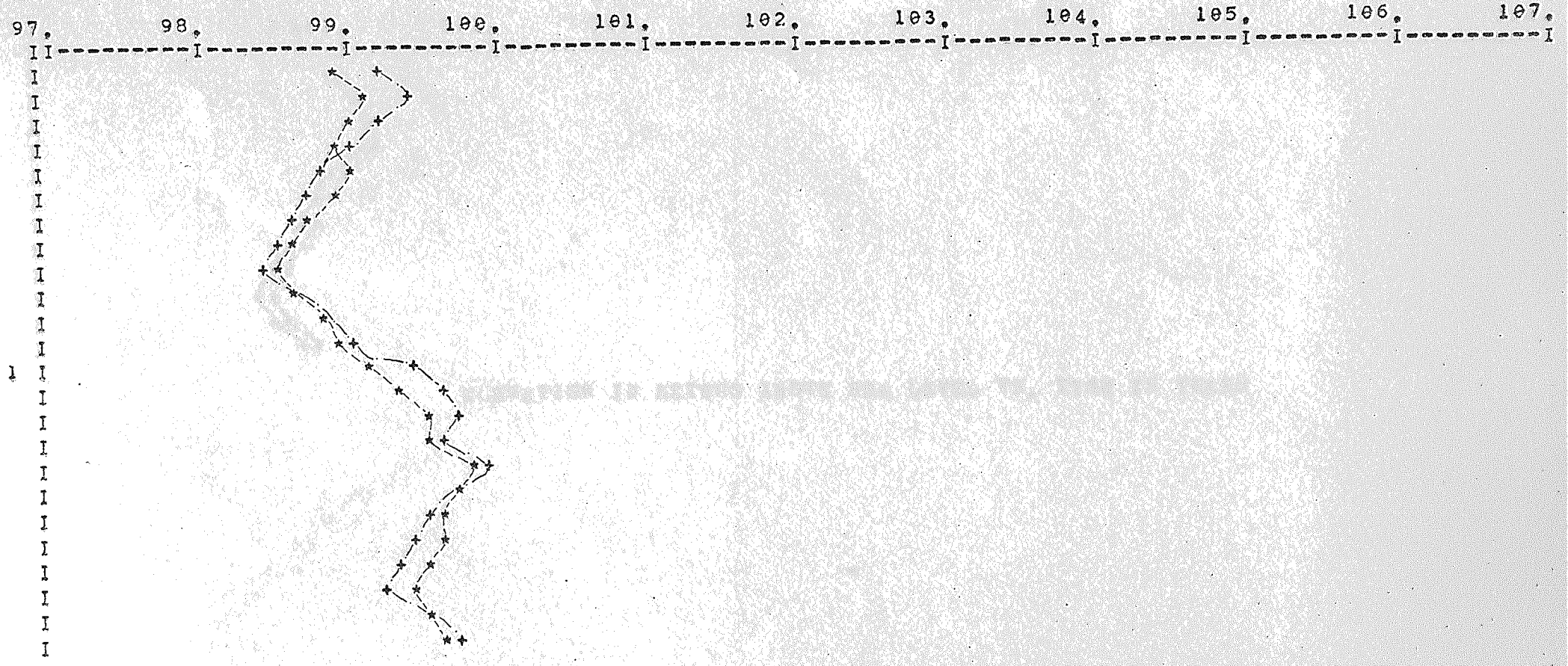

ELEVATION IN METERS ABOVE SEA LEVEL VS. TIME IN YEARS

FIGURE 66 cont.

MONTHLY COMPUTED (*) AND HISTORICAL (+) WATER LEVELS

1972

NODE 73

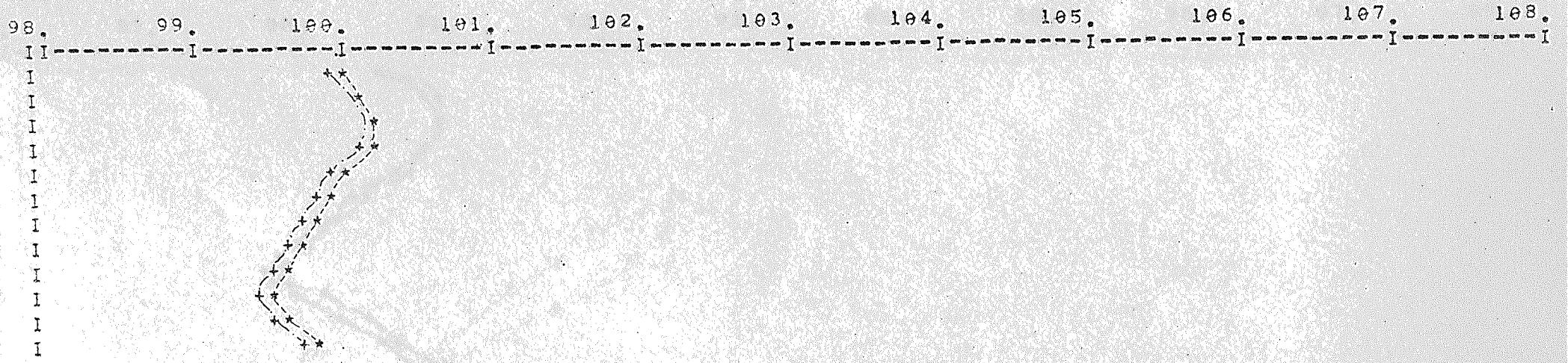

ELEVATION IN METERS ABOVE SEA LEVEL VS. TIME IN YEARS

FIGURE 66 cont.

MONTHLY COMPUTED (*) AND HISTORICAL (+) WATER LEVELS

1960 AND 1961

NODE 12

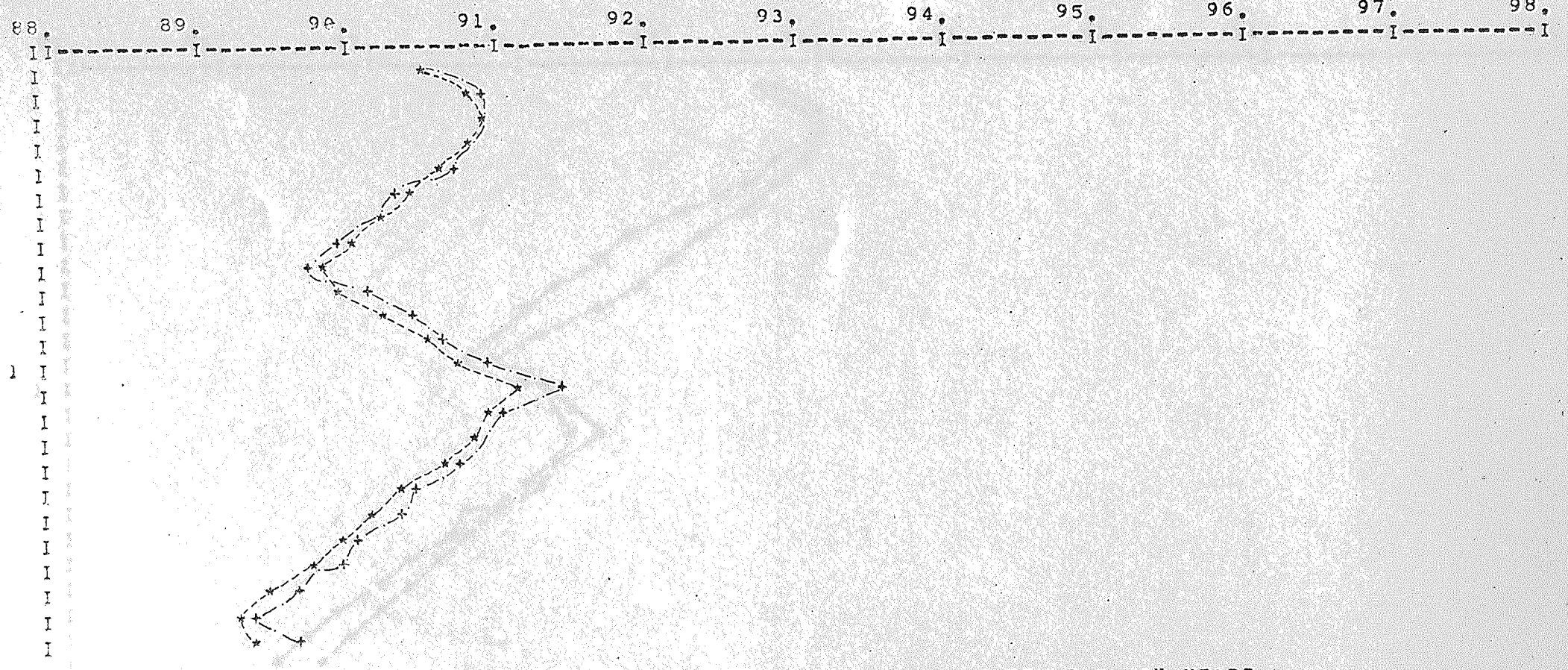

ELEVATION IN METERS ABOVE SEA LEVEL VS. TIME IN YEARS

FIGURE 67

MONTHLY COMPUTED (*) AND HISTORICAL (+) WATER LEVELS

1962 AND 1963

NODE 12

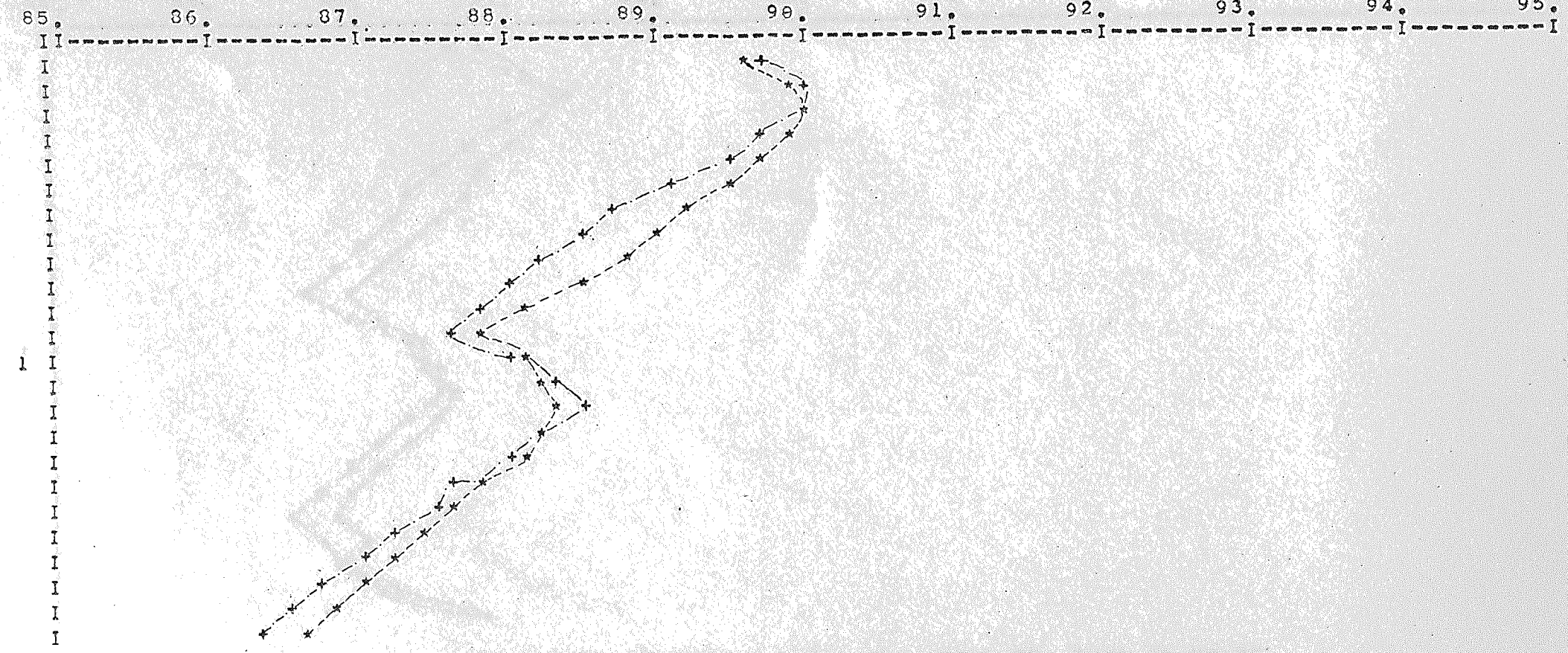

ELEVATION IN METERS ABOVE SEA LEVEL VS. TIME IN YEARS

FIGURE 67 cont.

MONTHLY COMPUTED (*) AND HISTORICAL (+) WATER LEVELS

1964 AND 1965

NODE 12

ELEVATION IN METERS ABOVE SEA LEVEL VS. TIME IN YEARS

FIGURE 67 cont.

MONTHLY COMPUTED (*) AND HISTORICAL (+) WATER LEVELS

1966 AND 1967

NODE 12

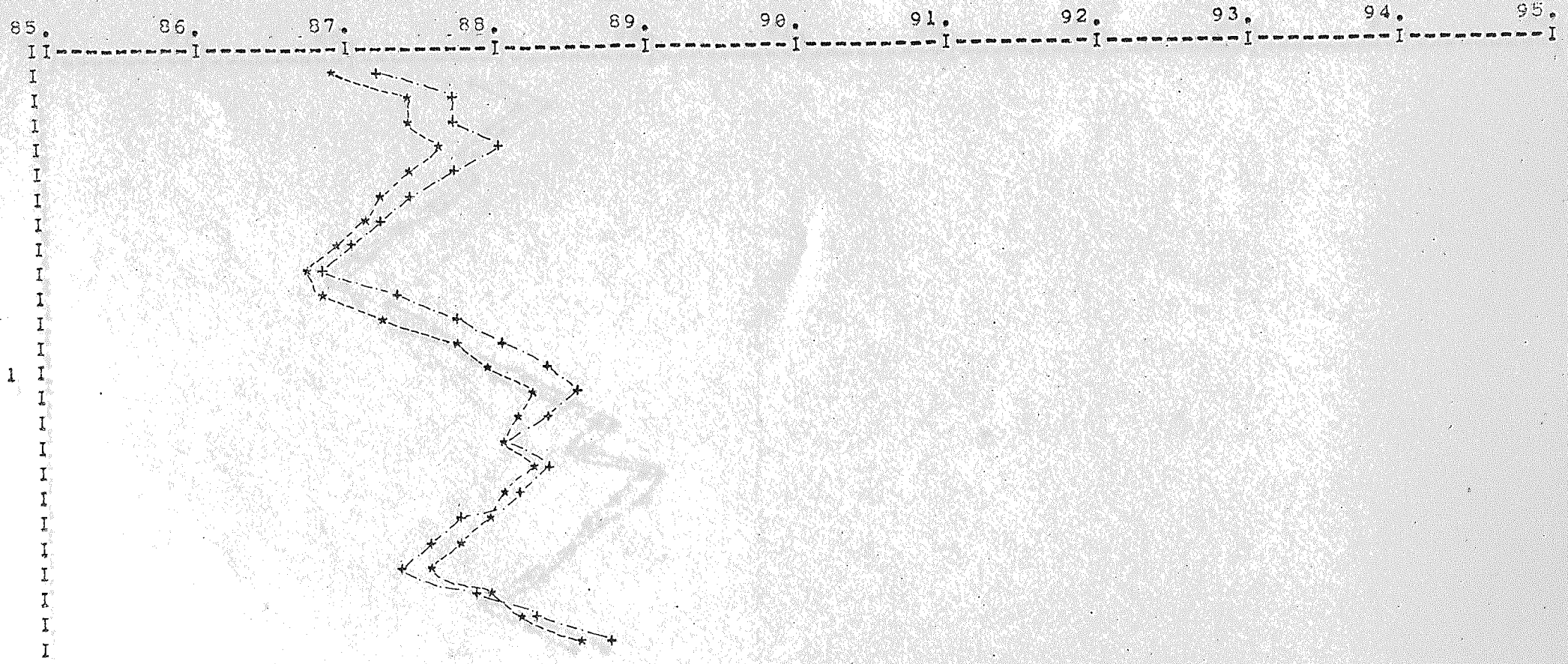

ELEVATION IN METERS ABOVE SEA LEVEL VS. TIME IN YEARS

FIGURE 67 cont.

MONTHLY COMPUTED (*) AND HISTORICAL (+) WATER LEVELS

1968 AND 1969

NODE 12

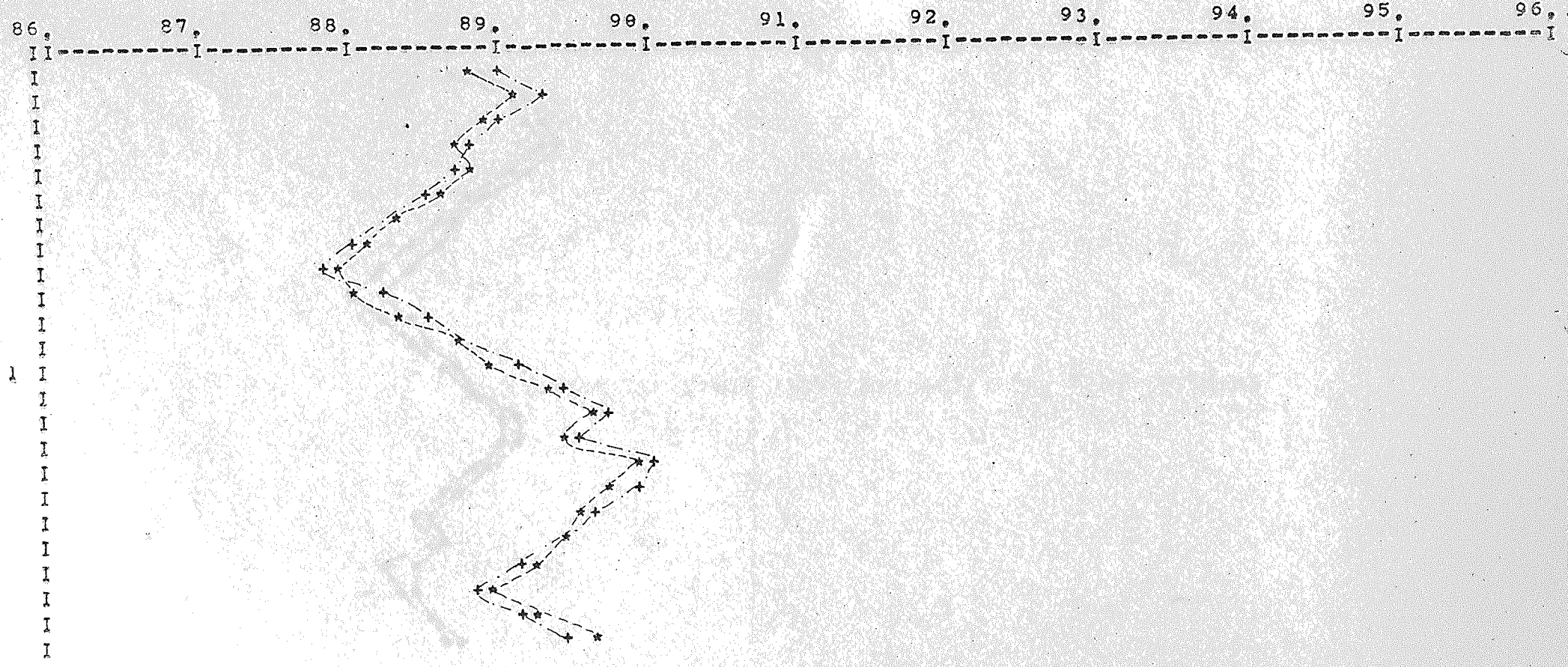

ELEVATION IN METERS ABOVE SEA LEVEL VS. TIME IN YEARS

FIGURE 67 cont.

MONTHLY COMPUTED (*) AND HISTORICAL (+) WATER LEVELS

1970 AND 1971

NODE 12

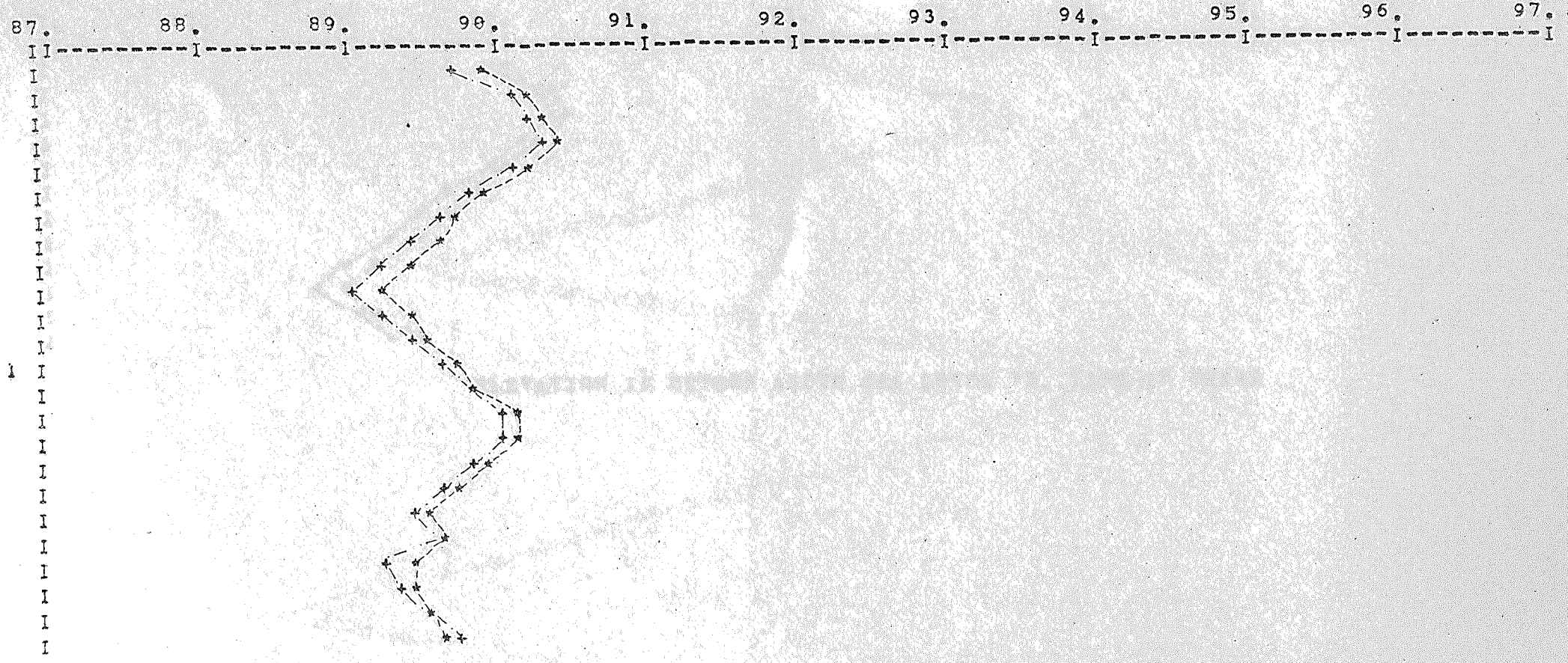

ELEVATION IN METERS ABOVE SEA LEVEL VS. TIME IN YEARS

FIGURE 67 cont.

MONTHLY COMPUTED (*) AND HISTORICAL (+) WATER LEVELS

1972

NODE 12

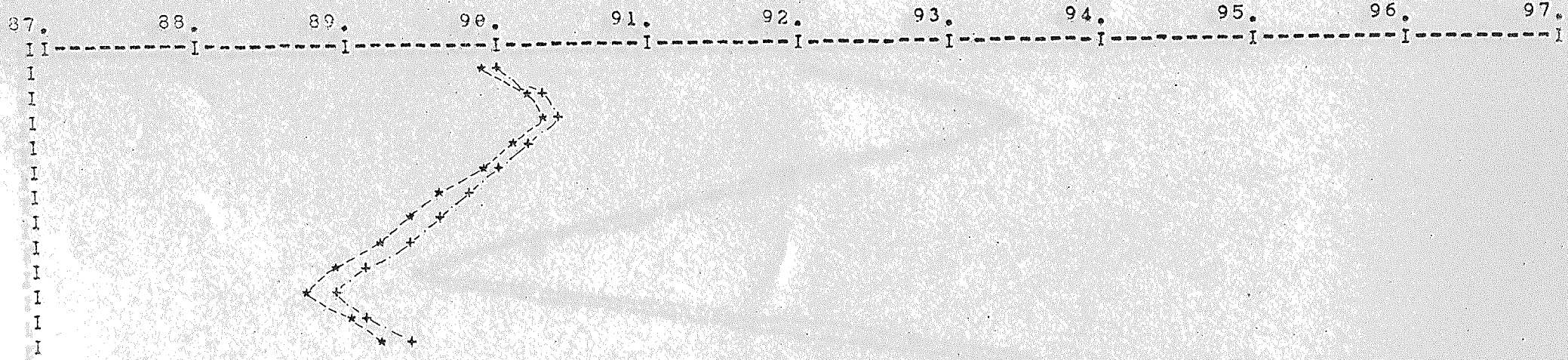

ELEVATION IN METERS ABOVE SEA LEVEL VS. TIME IN YEARS

FIGURE 67cont.

MONTHLY COMPUTED (*) AND HISTORICAL (+) WATER LEVELS

1960 AND 1961

NODE 24

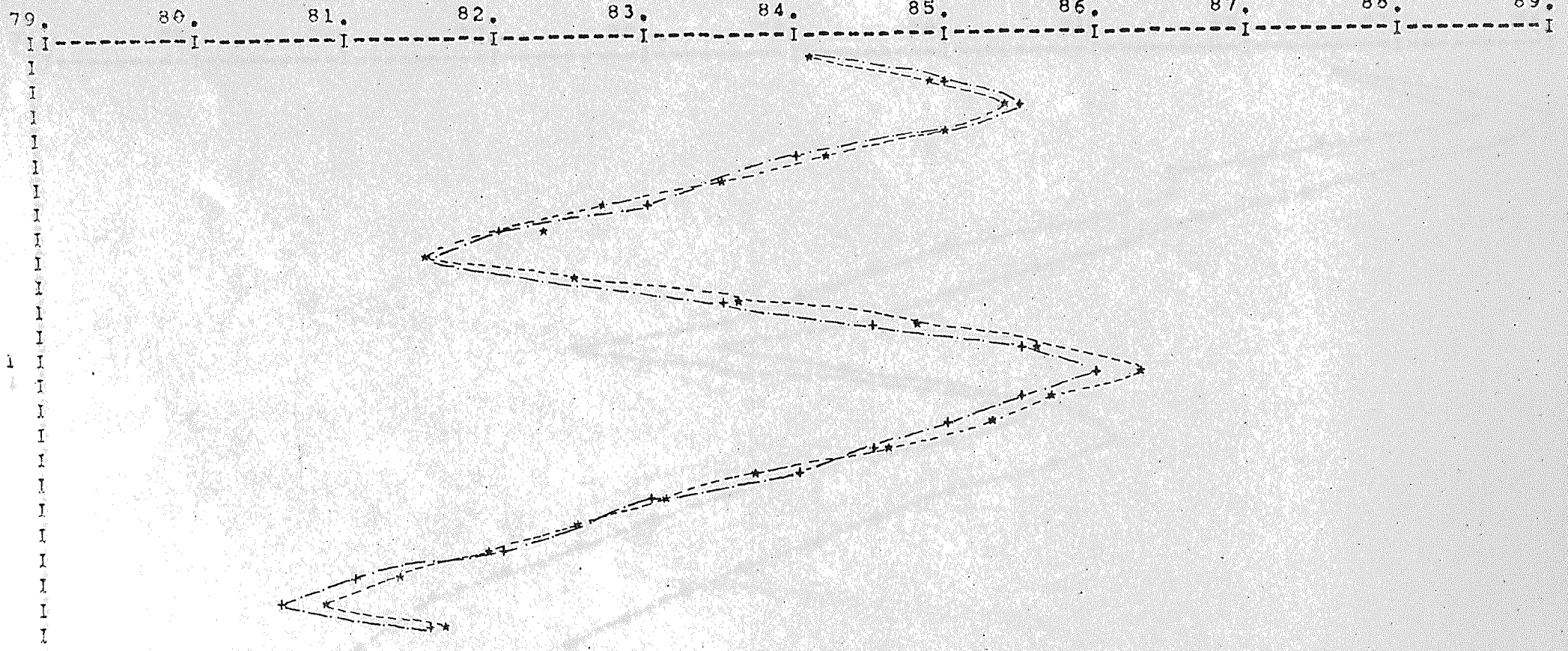

ELEVATION IN METERS ABOVE SEA LEVEL VS. TIME IN YEARS

FIGURE 68

MONTHLY COMPUTED (*) AND HISTORICAL (+) WATER LEVELS

1962 AND 1963

NODE 24

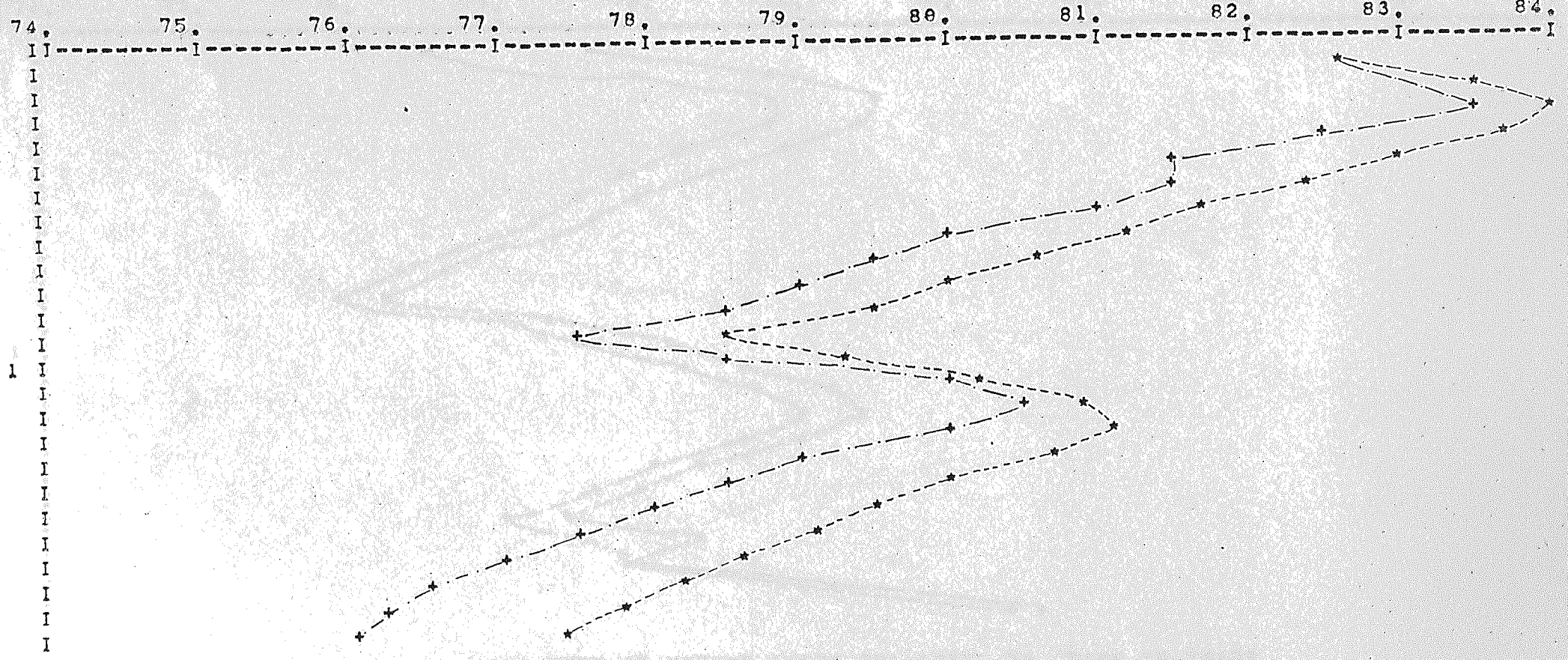

ELEVATION IN METERS ABOVE SEA LEVEL VS. TIME IN YEARS

FIGURE 68 cont.

MONTHLY COMPUTED (*) AND HISTORICAL (+) WATER LEVELS

1964 AND 1965

NODE 24

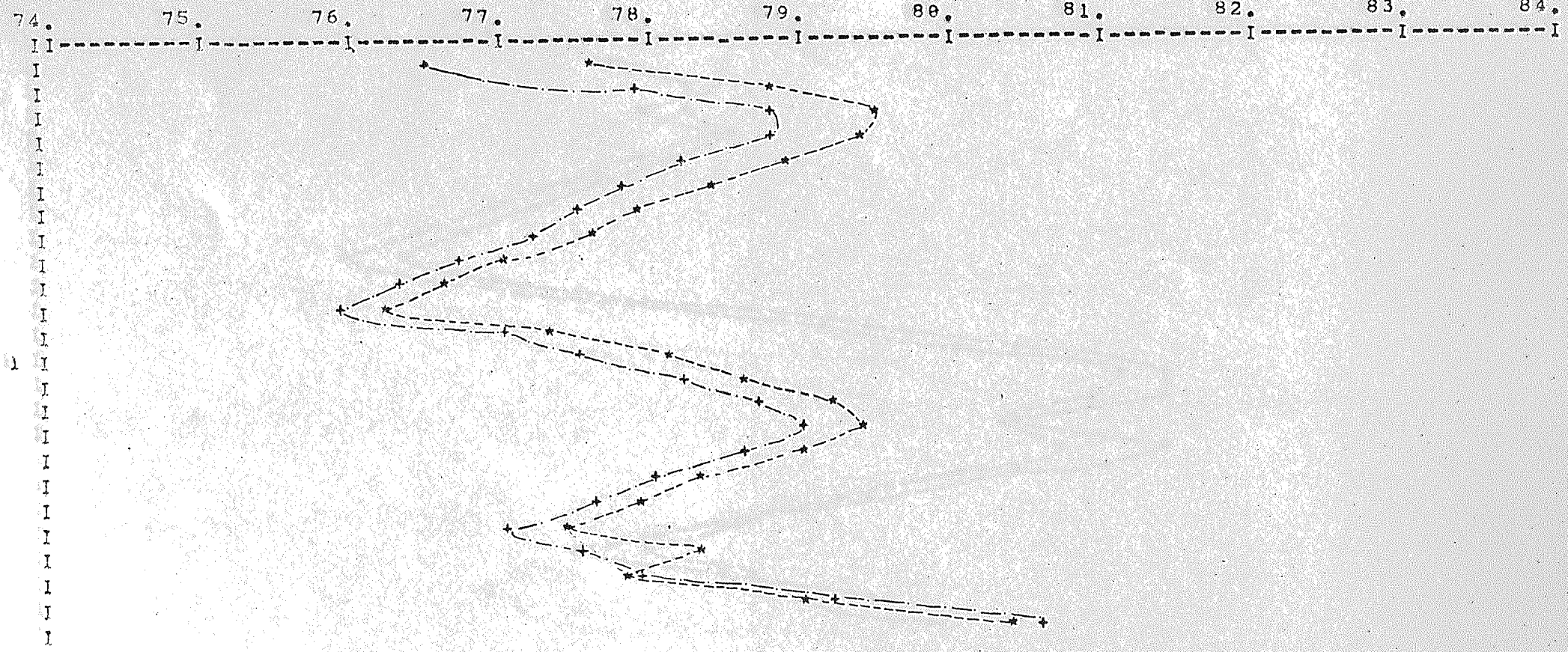

ELEVATION IN METERS ABOVE SEA LEVEL VS. TIME IN YEARS

FIGURE 68 cont.

MONTHLY COMPUTED (*) AND HISTORICAL (+) WATER LEVELS

1966 AND 1967

NODE 24

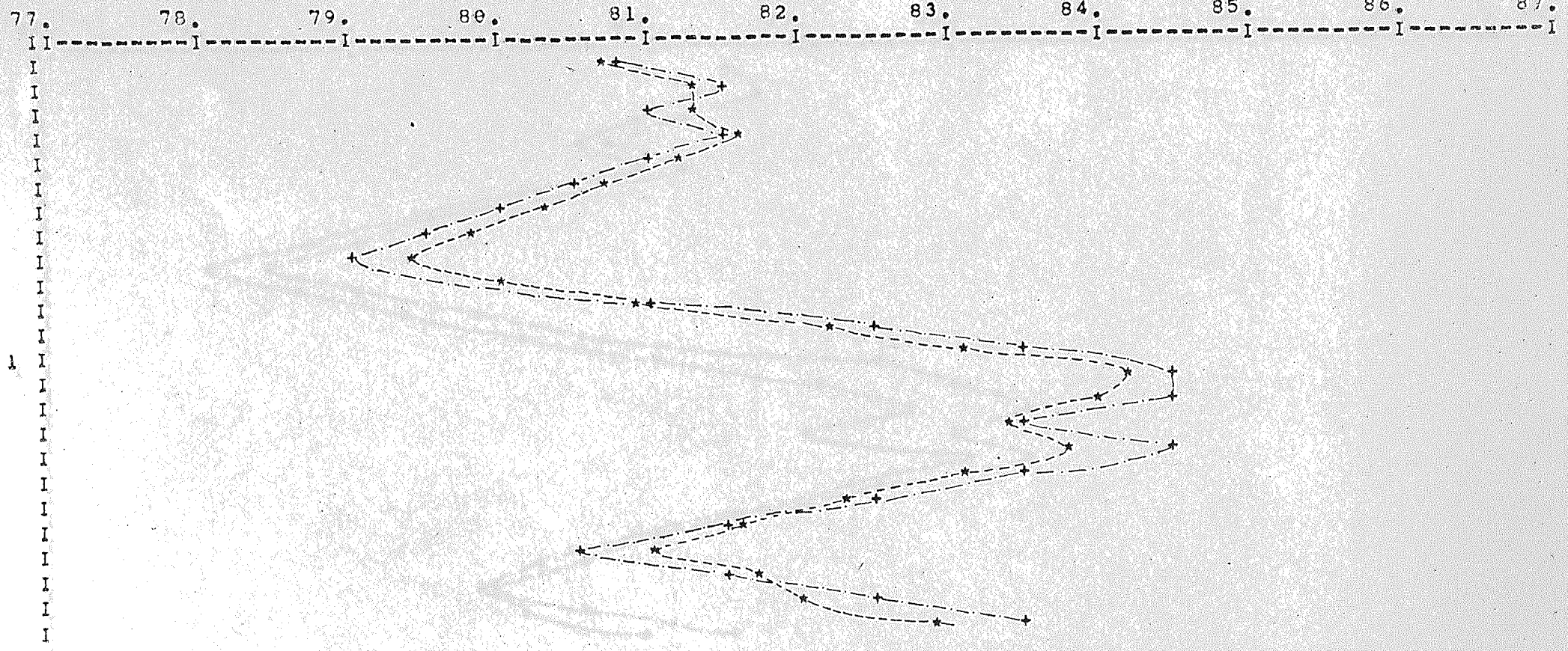

ELEVATION IN METERS ABOVE SEA LEVEL VS. TIME IN YEARS

FIGURE 68 cont.

MONTHLY COMPUTED (*) AND HISTORICAL (+) WATER LEVELS

1968 AND 1969

NODE 24

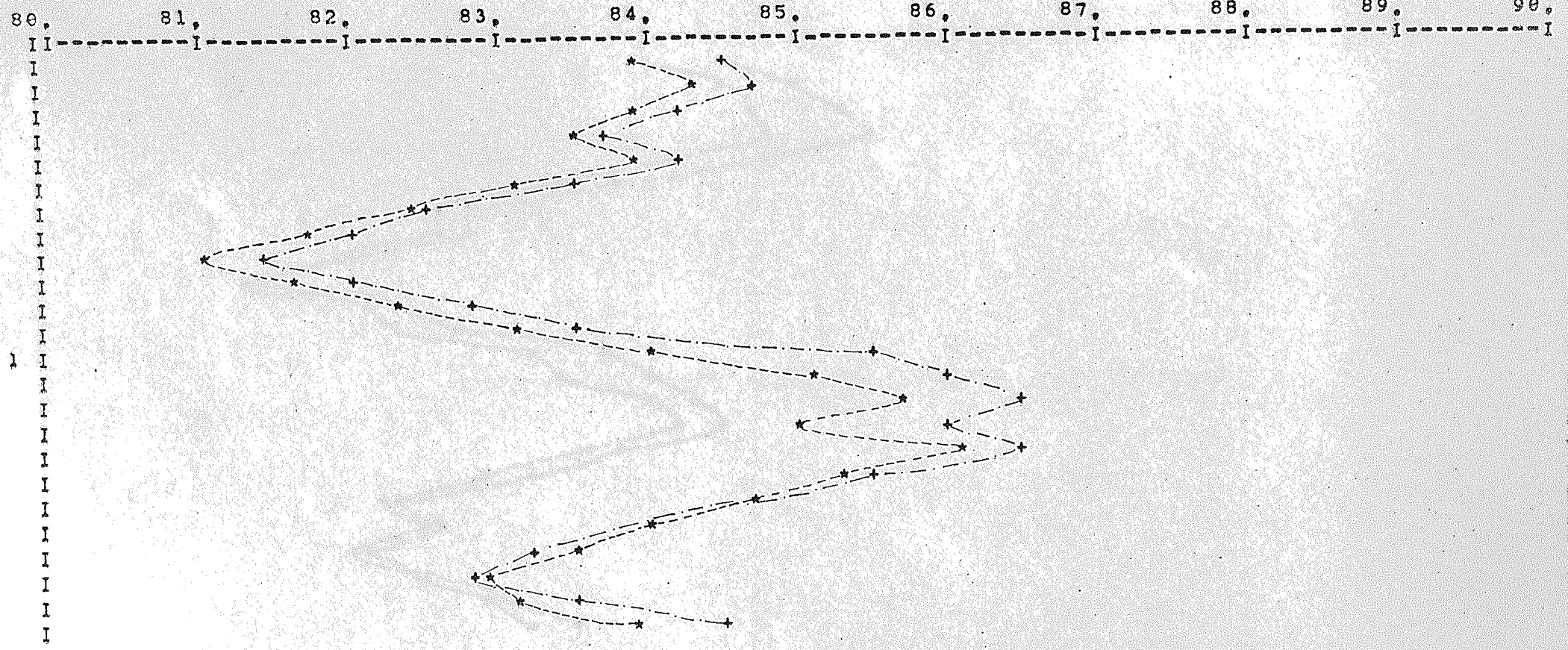

ELEVATION IN METERS ABOVE SEA LEVEL VS. TIME IN YEARS

FIGURE 68 cont.

MONTHLY COMPUTED (*) AND HISTORICAL (+) WATER LEVELS

1970 AND 1971

NODE 24

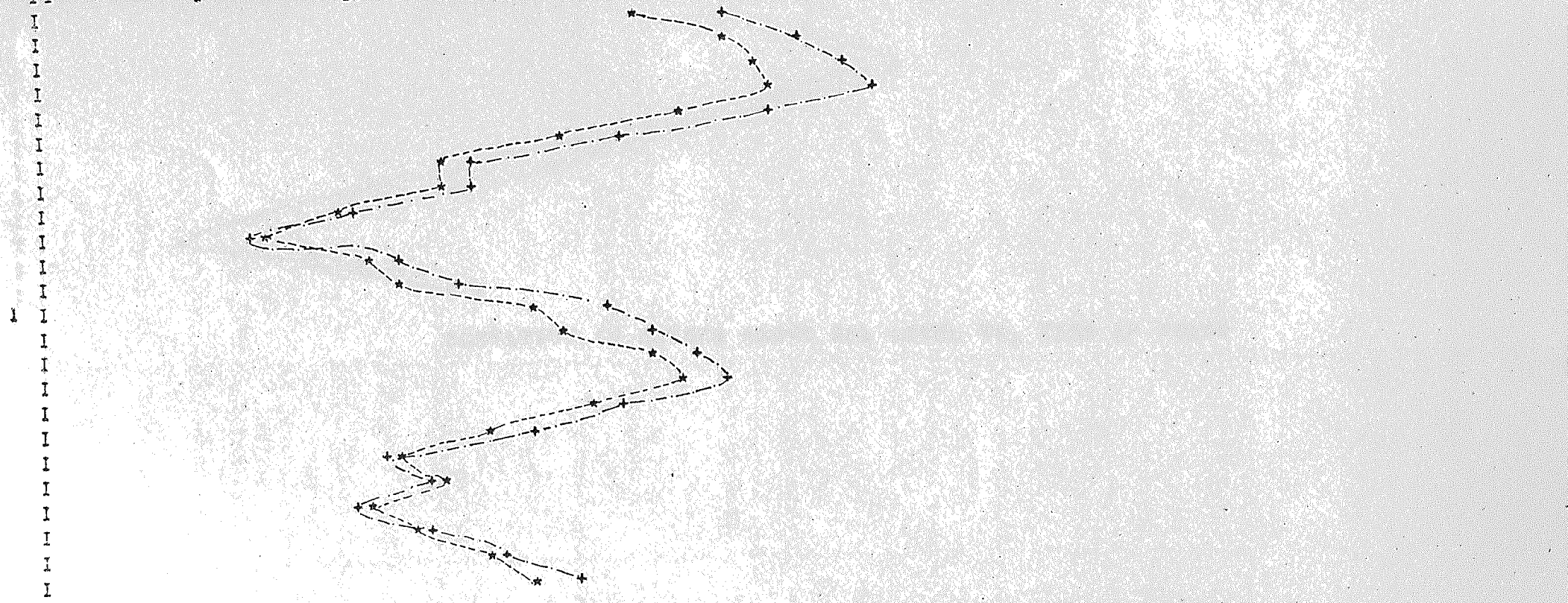

ELEVATION IN METERS ABOVE SEA LEVEL VS. TIME IN YEARS

FIGURE 68 cont.

MONTHLY COMPUTED (*) AND HISTORICAL (+) WATER LEVELS

1972

NODE 24

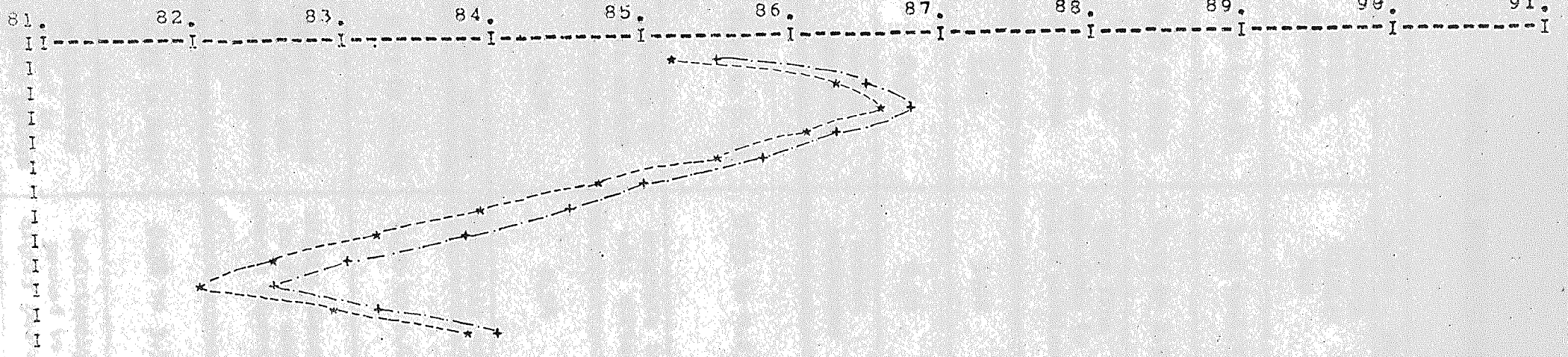

ELEVATION IN METERS ABOVE SEA LEVEL VS. TIME IN YEARS

FIGURE 68 cont.

GRAIN SIZE DISTRIBUTION STATISTICS

STATISTIC		PERMO - TRIAS FORMATIONS			
		LOWER MOTTLED SANDSTONE	BUNTER PEBBLE BED	UPPER MOTTLED SANDSTONE	LOWER KEUPER SANDSTONE
RANGE OF MEAN DIAMETER (McCAMMON)	Ø	2.02 to 0.95	3.16 to -4.57	2.75 to 1.30	2.97 to 0.35
	mm	0.25 to 0.52	0.11 to 2.38	0.15 to 0.41	0.13 to 0.78
DESCRIPTION		fine to coarse sandstone	very fine sandstone to medium pebbles	fine to medium sandstone	fine to coarse sandstone
MEAN VALUE OF MEAN DIAMETER	Ø	1.53	1-02	2.03	1.77
	mm	0.35	0.50	0.24	0.29
DESCRIPTION		medium sandstone	coarse sandstone	fine sandstone	medium sandstone
RANGE OF STANDARD DEVIATION (McCAMMON)	Ø	0.57 to 0.18	0.93 to 0.23	0.71 to 0.18	0.76 to 0.16
DESCRIPTION		moderate to well sorted	moderate to well sorted	moderate to well sorted	moderate to very well sorted
MEAN VALUE OF STANDARD DEVIATION	Ø	0.32	0.54	0.36	0.44
DESCRIPTION		well sorted	moderately sorted	well sorted	well sorted
RANGE OF SKEWNESS (Folk & Ward)	Ø	0.51 to -0.56	0.50 to 0.41	0.57 to -0.09	0.51 to -0.41
DESCRIPTION		highly skewed to fine and coarse diameters	highly skewed to fine and coarse diameters	highly skewed to fines and to normal distribution	highly skewed to fine and coarse diameters
RANGE OF KURTOSIS (FOLK & WARD)	Ø	0.73 to 2.47	0.78 to 3.34	0.85 to 2.46	0.88 to 2.47
DESCRIPTION		deficiently peaked to highly peaked	deficiently peaked to highly peaked	deficiently peaked to highly peaked	deficiently peaked to highly peaked

CATCHMENT LAND USE

LAND USE	CATCHMENT	
	SEVERN	SOW
CEREALS AND GRASSES	80	82
TREES (WOODED AREAS)	8	7
URBAN DEVELOPMENT	7	8
RIPARIAN ZONE	5	3

KEY Units expressed as a percentage of the total area.

CLASSIFICATION OF THE SUPERFICIAL COVER IN EACH SUBCATCHMENT

SUBCATCHMENTS	SUPERFICIAL COVER (expressed as a % of the total area)		
	PERMEABLE HORIZONS	SEMI-PERMEABLE HORIZONS	IMPERMEABLE HORIZONS
DOXEY BROOK	0.0	11.1	88.9
PENK	14.2	24.5	61.3
BACK BROOK	28.0	23.6	48.4
SWESTOW BROOK	81.7	8.3	8.0
WORFE	45.6	30.2	24.2

CLASSIFICATION	DERIVATION OF SOILS AND SUPERFICIAL DEPOSITS	TYPE OF SEDIMENT
PERMEABLE HORIZONS	Glacial sands and gravels, Upper Mottled Sandstone Formation. Bunter Pebble Bed Formation. Lower Mottled Sandstone Formation	Rudaceous and Arenaceous
SEMI-PERMEABLE HORIZONS	Glacial River Terraces, Lower Keuper Sandstone Formation	Arenaceous and Argillaceous
IMPERMEABLE HORIZONS	Glacial Boulder Clays. Keuper Marl Formation.	Argillaceous

CALIBRATED WATERSHED MODEL CHARACTERISTICS

	STOUR CATCHMENT		SOW CATCHMENT	
CHARACT-ERISTICS	INITIAL VALUES	CALIBRATED VALUES	INITIAL VALUES	CALIBRATED VALUES
MS	102.0	81.3	102.0	88.9
IM	22.9	55.8	17.8	48.3
IO	15.2	10.2	10.2	3.1
IE	3.0	15.0	3.0	45.0
GD	0.0066	0.0030	0.0123	0.0030
EM	3.3	3.3	3.3	3.3
SI	1.3	1.8	2.5	2.5
GI	3.0	3.5	3.8	4.4
MI	102.0	81.3	102.0	88.9
RST	1.3	1.8	2.5	2.5

KEY

MS	Maximum Soil Moisture Content	mm.
IM	Maximum Soil Infiltration Rate	mm/day.
IO	Minimum Soil Infiltration Rate	mm/day.
IE	Exponential Function of Infiltration Equation	
GD	Groundwater Depletion Factor	
EM	Maximum Evapotranspiration Rate	mm/day.
SI	Initial Surface Level Moisture Content	mm.
GI	Initial Groundwater Storage Content	mm.
MI	Initial Soil Moisture Content	mm.
RST	Interception Storage	mm.

PRINCIPAL ABSTRACTION SITES

SOURCE OF SUPPLY	WATER AUTHORITY	AVERAGE RATE OF ABSTRACTION 10^3 CU. M/DAY
BRATCH	W.W.U.	9.8
COPLEY	W.W.U.	4.1
COSFORD	W.W.U.	6.0
DIMMINGSDALE	W.W.U.	13.4
HILTON	W.W.U.	13.2
NEACHLEY	W.W.U.	8.3
RINDLEFORD	W.W.U.	1.9
ROUGHTON	W.W.U.	not operative
STABLEFORD	W.W.U.	5.3
TETTENHALL	W.W.U.	2.8
TOM HILL	W.W.U.	5.4
HINKSFORD	S.S.W.C.	6.3
HUNTINGDON	S.S.W.C.	2.0
SOMERFORD	S.S.W.C.	5.1
SLADEHEATH	S.S.W.C.	5.6
BECKBURY	E.S.W.B.	3.2
GRINDLEFORD	E.S.W.B.	4.2
NEWPORT	E.S.W.B.	2.7
SHERRIFHALES	E.S.W.B.	4.2
GNOSALL	S.C.W.U.	2.3
MILFORD	S.C.W.U.	5.4
SHUGBOROUGH	S.C.W.U.	2.3
WESTON JONES	S.C.W.U.	10.8

KEY

WATER AUTHORITY	TOTAL ABSTRACTION 10^3 CU.M/DAY
W.W.U. WOLVERHAMPTON WATER UNDERTAKING.	70.2
S.S.W.C. EAST SHROPSHIRE WATER BOARD.	19.0
E.S.W.B. STAFFORD CORPORATION WATER UNDERTAKING.	14.3
S.C.W.U. SOUTH STAFFORDSHIRE WATERWORKS COMPANY.	20.8
TOTAL	124.3

ANNUAL WATER BALANCE

JANUARY 1968 to JANUARY 1969

SOW CATCHMENT

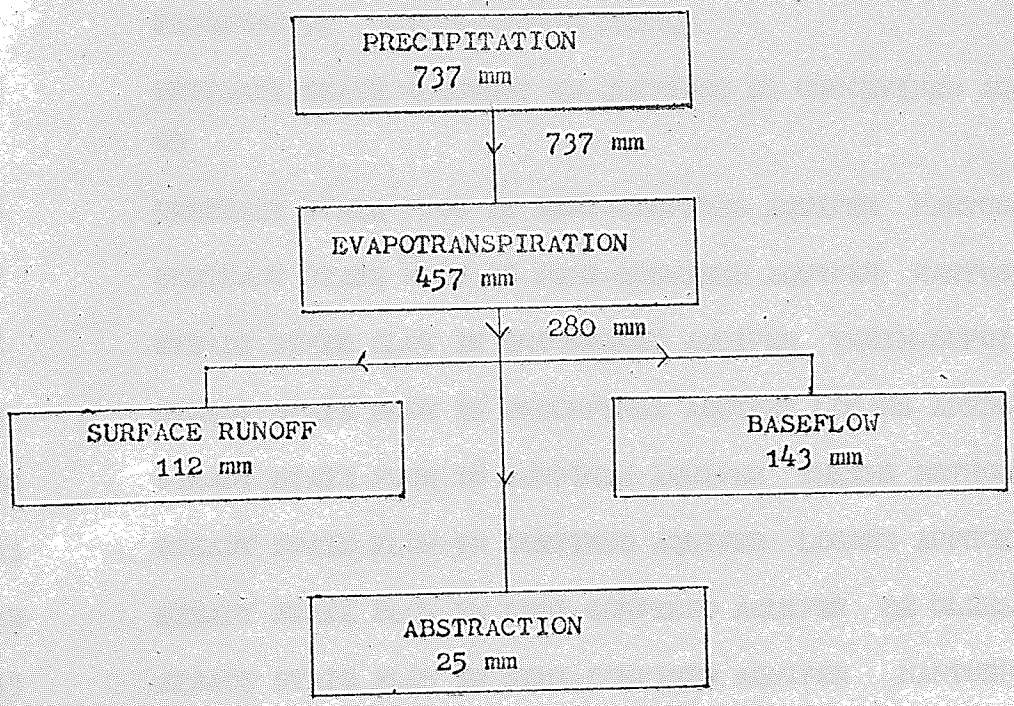

SEVERN CATCHMENT

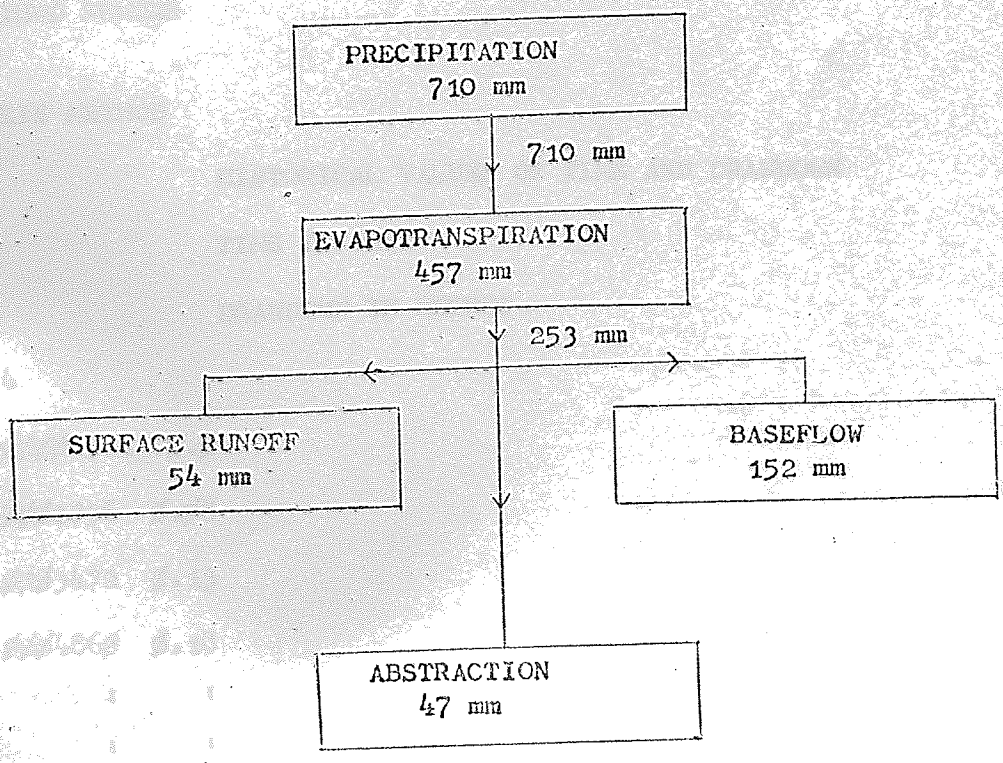

KK

1	UNSTEADY STATE FLOW IN CONFINED OR UNCONFINED/AQUIFER THEIS METHOD
2	UNSTEADY STATE FLOW IN CONFINED OR UNCONFINED AQUIFER JACOBS METHOD
3	UNSTEADY STATE FLOW IN CONFINED OR UNCONFINED AQUIFER WITH RECHARGE/ BARRIER BOUNDARIES STALLMANS METHOD
4	UNSTEADY STATE FLOW IN CONFINED OR UNCONFINED AQUIFER WITH PARTIAL PENETRATION HANTUSH-THEIS METHOD
5	UNSTEADY STATE RECOVERY IN CONFINED OR UNCONFINED AQUIFER THEIS METHOD
6	UNSTEADY STATE FLOW IN SEMI-CONFINED AQUIFER HANTUSH METHOD III
7	UNSTEADY STATE FLOW IN SEMI-CONFINED AQUIFER HANTUSH METHOD I
8	STEADY STATE FLOW IN UNCONFINED AQUIFER THEIM-DUPUIT METHOD
9	STEADY STATE FLOW IN UNCONFINED AQUIFER LOGANS APPROXIMATION METHOD
10	STEADY STATE FLOW IN CONFINED AQUIFER THEIMS METHOD
11	STEADY STATE FLOW IN CONFINED AQUIFER LOGANS APPROXIMATION METHOD
12	STEADY STATE FLOW IN SEMI-CONFINED AQUIFER DE GLEES METHOD
13	STEADY STATE FLOW IN SEMI-CONFINED AQUIFER HANTUSH-JACOB METHOD
14	STEP TYPE PUMPING COOPER-JACOB METHOD

KK
METHOD NUMBER
←1

THEIS METHOD

HISTORICAL VALUES OF TIME AND DRAWDOWN

TIME IN DAYS

DRAWDOWN IN METRES

←34

←Ø.ØØØØ6944 Ø.Ø4

←Ø.ØØØ1736 Ø.Ø8

←Ø.ØØØ3472 Ø.13

Ø.ØØØ486Ø Ø.18

: : :

: : :

: : :

←Ø.57635 1.Ø88

DATA CONTANTS REQUIRED

C(1) = INCREMENTAL STEP SIZE FOR STORAGE COEFFICIENT

C(2) = INCREMENTAL STEP SIZE FOR TRANSMISSIBILITY SQ. METRES PER DAY

C(3) = DISTANCE BETWEEN PUMPED WELL AND OBSERVATION WELL METRES

C(4) = PUMP RATE CU.M. PER DAY

←4

←Ø.ØØØ8 5ØØ.Ø 3Ø.Ø 788.Ø

X(1) = INITIAL ESTIMATE OF STORAGE COEFFICIENT

X(2) = INITIAL ESTIMATE OF TRANSMISSIBILITY SQ METRES PER DAY

← ST.COEF. Ø.ØØ8

←TRANS. 4ØØØ.Ø
Ø.Ø

INITIAL VALUES

SUM OF SQUARES = 7.Ø4

ST. COEF. Ø.8ØØØØØE-Ø2 TRANS. Ø.4ØØØØØE Ø4

OPTIMUM VALUES

SUM OF SQUARES = Ø.ØØ7Ø1

ST. COEF. Ø.132233E-Ø3 TRANS. Ø.438354E Ø3

HISTORICAL DRAWDOWN	PREDICTED DRAWDOWN
Ø.Ø4Ø	Ø.Ø35
Ø.Ø8Ø	Ø.Ø82
Ø.13Ø	Ø.122
Ø.18Ø	Ø.18Ø
: : : : : : :	
: : : : : : :	
1.Ø88	1.1Ø1

KK

METHOD NUMBER
←2

JACOB METHOD

HISTORICAL VALUES OF TIME AND DRAWDOWN

TIME IN DAYS

DRAWDOWN IN METRES

```
IF HISTORICAL DRAWDOWN DATA SAME AS PREVIOUS EXAMPLE INPUT 1;

IF NOT, INPUT Ø AND INPUT DATA

←1

DATA CONSTANTS REQUIRED

C(1) = INCREMENTAL STEP SIZE FOR STORAGE COEFFICIENT

C(2) = INCREMENTAL STEP SIZE FOR TRANSMISSIBILITY  SQ. METRES PER DAY

C(3) = DISTANCE BETWEEN PUMPED WELL AND OBSERVATION WELL  METRES

C(4) PUMP RATE  CU.M.PER DAY

←4

←Ø.ØØ4  5ØØ.Ø  3Ø.Ø  788.Ø

X (1) = INITIAL ESTIMATE OF STORAGE COEFFICIENT

X(2)  = INITIAL ESTIMATE OF TRANSMISSIBILITY  SQ. METRES PER DAY

←ST. COEF.  Ø.Ø16

←TRANS.     2ØØØ.Ø
            Ø.Ø

INITIAL VALUES

        SUM OF SQUARES = 6.79

        ST.COEF.  Ø.34ØØØØE-Ø1        TRANS.  Ø.2ØØØØØE Ø4

OPTIMUM VALUES

        SUM OF SQUARES = Ø.ØØ6118

        ST.COEF.  Ø.12132ØE-Ø3        TRANS.  Ø.45Ø442E Ø3

HISTORICAL DRAWDOWN                   PREDICTED DRAWDOWN

        Ø.Ø4Ø                         Ø.Ø45

        Ø.Ø8Ø                         Ø.Ø7Ø

        Ø.13Ø                         Ø.138

        Ø.18Ø                         Ø.184

:   :   :   :   :   :   :   :

:   :   :   :   :   :   :   :

        1.Ø88                         1.Ø78

KK
METHOD NUMBER
←15
FINISHED
```

NUMERICAL PUMP TEST

ANALYSIS ROUTINES

METHOD NUMBER	CHARACTER-ISTICS EVALUATED	TYPE OF AQUIFER	TYPE OF SOLUTION	METHOD OF ANALYSIS
1	S,T	U&C	US	JACOB, 1940
2	S,T	U&C	US	COOPER and JACOB, 1946
3	S,T	U&C	US	FERRIS et AL, 1962
4	S,T	U&C	US	HANTUSH, 1962
5	T	U&C	US	THEIS, 1935
6	S,T	SC	US	HANTUSH, 1964
7	S,T	SC	US	HANTUSH, 1956
8	T	U	SS	THIEM, 1906
9	T	U	SS	LOGAN, 1964
10	T	C	SS	THIEM, 1906
11	T	C	SS	LOGAN, 1964
12	T,P	SC	SS	DE GLEE, 1930
13	T,P	SC	SS	HANTUSH, and JACOB, 1955
14	S,T	U&C	US	COOPER and JACOB, 1946

KEY

S	Storage Coefficient or, Storage Capacity.
T	Transmissibility.
P	Permeability of semi-confining horizon.
U	Unconfined.
C	Confined.
SC	Semi-Confined.
US	Unsteady State.
SS	Steady State.

COMPARISON BETWEEN GRAPHICAL

AND NUMERICAL PUMP TEST ANALYSES

METHOD	SOURCE OF DATA	GRAPHICAL		NUMERICAL	
		S	T	S	T
1	3	0.019	125	0.012	200
1	1	0.00019	1279	0.00019	1279
1	2	0.00017	418	0.00013	438
1	3	0.001	31	0.0009	28
2	3	0.0043	90	0.0037	89
2	2	0.00017	401	0.00012	450
3	3	0.025	372	0.021	398
3	3	0.0069	89	0.0038	111
4	3	0.018	482	0.022	520
6	2	0.0019	1729	0.0016	1779
6	2	0.0023	1282	0.0018	1132
7	2	0.0019	1729	0.0017	1875
14	3	0.0012	104	0.0013	136

METHOD	SOURCE OF DATA	GRAPHICAL		NUMERICAL	
		P	T	P	T
12	2	0.0018	2114	0.0025	1829
13	2	0.0018	2114	0.0032	1768

KEY

Storage Coefficient or,

S Storage Capacity.

T Transmissibility. m^2/day.

P Permeability of semi-confining horizon.m/day.

Source of data;

1 Todd, 1959.

2 Kruseman and De Ridder, 1970.

3 Study Area. (Permo-Triassic Aquifer).

Method; See table 8 for explanation.

NUMERICAL PUMP TEST ANALYSIS:
INITIAL STARTING CONDITIONS

Example Method of Solution: Theis, 1935.

Data: U.S. Geological Survey.

	TEST EXAMPLES					
	A	B	C	D	E	F
INITIAL S	0.00024	0.0001	0.0001	0.0007	0.00022	0.00016
INITIAL T	140000	50000	200000	90000	140000	90000
INITIAL DS	0.00003	0.00001	0.00001	0.00007	0.00001	0.00001
INITIAL DT	5000	5000	10000	9000	3000	4000
INITIAL SSQ	9.93	147.51	18.22	17.81	15.22	8.19
OPTIMUM S	0.000192	0.000192	0.000188	0.000193	0.000188	0.000193
OPTIMUM T	102883	102898	102898	102885	102898	102887
FINAL SSQ	0.011	0.011	0.011	0.011	0.011	0.011

KEY

S Storage Coefficient.

T Transmissibility. (U.S. Gallons/day/foot)

DS Storage Coefficient Search Step.

DT Transmissibility Search Step.

SSQ Sum of Squares.

AQUIFER CHARACTERISTIC EVALUATION BY LEAST SQUARES METHOD

SIX NODE MODEL

NODE	TRANSMISSIBILITY LINK	HISTORICAL VALUES S	HISTORICAL VALUES T	PREDICTED VALUES S	PREDICTED VALUES T
1	2	0.05	400	-0.05	875
	4		400		1001
2	3	0.03	300	0.08	220
	5		300		889
3	6	0.01	200	-0.04	-550
4	5	0.05	400	- 0.003	144
5	6	0.03	300	0.01	-250
6		0 01		0.09	

EIGHTEEN NODE MODEL

AQUIFER TYPE	HISTORICAL VALUES S	HISTORICAL VALUES T	PREDICTED VALUES S	PREDICTED VALUES T
UNCONFINED	0.012 to 0.110	75 to 780	0.038 to 0.004	322 to 2002
SEMI-CONFINED	0.002 to 0.008	75 to 250	0.028 to 0.0008	167 to 803
CONFINED	0.0009 to 0.004	19 to 99	0.03 to 0.000006	8 to 200

KEY

S Storage Coefficient or, Storage Capacity.

T Transmissibility m^2/day.

AQUIFER CHARACTERISTIC DETERMINATION:

LINEAR PROGRAMME SOLUTION

6 NODE MODEL

NODE	LINKED NODE	HISTORICAL VALUES S	HISTORICAL VALUES T	LINEAR PROGRAMMING SOLUTIONS METHOD 1 S	METHOD 1 T	METHOD 2 S	METHOD 2 T	METHOD 3 S	METHOD 3 T
1	2	0.05	400	0.06	2204	N.E.	N.E.	0.06	3276
				B.V.	B.V.	N.E	B.V.	B.V.	B.V.
	4		400	0.06	N.E.	B.V.	N.E.	B.V.	N.E.
					B.V.		B.V.		B.V.
2	3	0.03	300	0.02	372	0.03	282	0.03	251
					415		304	B.V.	B.V.
	5		300	0.03	N.E.	0.03	N.E.	B.V.	N.E.
					B.V.		B.V.		B.V.
3	6	0.01	200	NE	N.E.	0.03	3325	0.04	3400
				B.V.	B.V.	B.V.	B.V.	B.V.	B.V.
4	5	0.05	400	N.E.	N.E.	N.E.	N.E.	N.E.	25
				B.V.	B.V.	B.V.	B.V.	B.V.	B.V.
5	6	0.03	300	0.09	N.E.	0.01	N.E.	0.2	N.E.
				B.V.	B.V.	B.V.	B.V.	B.V.	B.V.
6		0.01		N.E.		N.E.		0.03	
				B.V.		B.V.		B.V.	

KEY

S Storage Coefficient or, Storage Capacity.

T Transmissibility m^2/day.

N.E. Not evaluated.

B.V. Boundary value.

unconstrained

constrained

AQUIFER CHARACTERISTIC DETERMINATION:

LINEAR PROGRAMME SOLUTION

18 NODE MODEL

NODE	LINKED NODE	HISTORICAL VALUES S	HISTORICAL VALUES T	LINEAR PROGRAMMES PREDICTED VALUES METHOD 1 S	LINEAR PROGRAMMES PREDICTED VALUES METHOD 1 T	LINEAR PROGRAMMES PREDICTED VALUES METHOD 2 S	LINEAR PROGRAMMES PREDICTED VALUES METHOD 2 T
2	3	0.04 to 0.009	20 to 150		15		420
				0.006	B.V.	0.08	B.V.
	5			0.01	18	0.02	N.E.
					82		93
3	7	0.012 to 0.008	120 to 260		182		195
				0.01	240	0.008	224
	22			0.07	560	0.009	720
					B.V.		B.V.
9	10	0.002 to 0.009	40 to 60		N.E.		1020
					B.V.		B.V.
	12			0.005	8	0.0009	2
				BV	46	0.005	56
	13				N.E.		N.E.
					B.V.		65
10	13	0.015 to 0.002	40 to 320	N.E.	N.E.	0.03	82
				B.V.	B.V.	0.07	104
11	12	0.015 to 0.035	120 to 260		N.E.		235
					B.V.		232
	14			N.E.	757	0.07	1002
				0.03	B.V.	0.06	B.V.
	15				N.E.		303
					B.V.		252
15	14	0.015 to 0.035	110 to 260		272		880
				0.008	B.V.	0.02	B.V.
	17			0.03	80	B.V.	N.E.
					125		241
17		0.052 to 0.072		N.E.		N.E.	
				0.05		B.V.	
18		0.052 to 0.092		N.E.		N.E.	
				0.06		B.V.	

KEY

S Storage Coefficient or, Storage Capacity

T Transmissibility m^2/day

N.E. Not evaluated

B.V. Boundary value

unconstrained

constrained

AQUIFER CHARACTERISTIC EVALUATIONS:

UPPER AND LOWER BOUND VALUES

LOCALITY	NATIONAL GRID REFERENCE	AQUIFER THICKNESS (METRES)	METHOD A				METHOD B	
			S		T		T	
			L.B.	U.B.	L.B.	U.B.	L.B.	U.B.
ROUGHTON	SO 752 946	320	0.053	0.072	543	782	526	1114
STABLEFORD	SO 764 981	340	0.027	0.077	403	652	516	1348
TOM HILL	SO 837 925	220	0.092	0.052	298	470	192	443
COPLEY	SO 809 988	480	0.015	0.035	112	258	117	194
RINDLEFORD	SO 736 954	200	0.075	0.110	375	550	347	512
HILTON	SO 777 959	410	0.052	0.072	226	287	252	376
DIMMINGSDALE	SO 860 961	310	0.050	0.011	228	317	272	350
NEACHLEY	SJ 783 067	300	0.007	0.002	75	178	90	137
WESTON JONES	SJ 756 241	350	0.008	0.002	89	250	25	156
GNOSALL	SJ 815 224	390	0.004	0.0009	19	99	99	151
MILFORD	SJ 975 213	80	0.012	0.008	174	256	222	452
SOMERFORD	SJ 895 093	310	0.009	0.002	36	60	53	142
SLADEHEATH	SJ 920 067	190	0.015	0.009	112	214	171	319
BRATCH	SJ 868 937	300	-	-	-	-	300	457
HINKSFORD	SO 869 898	310	-	-	-	-	334	909
COSFORD	SJ 781 047	310	-	-	-	-	120	256
HUNTINGDON	SJ 973 123	80	-	-	-	-	124	256
ASHWOOD	SO 866 878	190	-	-	-	-	276	401

KEY

S Storage Coefficient or,
Storage Capacity.

T Transmissibility. M^2/day

L.B. Lower Bound Value.

U.B. Upper Bound Value.

Method A : Numerical Pump Test Analysis Solution.

Method B : Steady State and Recovery Methods of Solution.

GRAIN SIZE ANALYSIS PROGRAM:

FLOW DIAGRAM

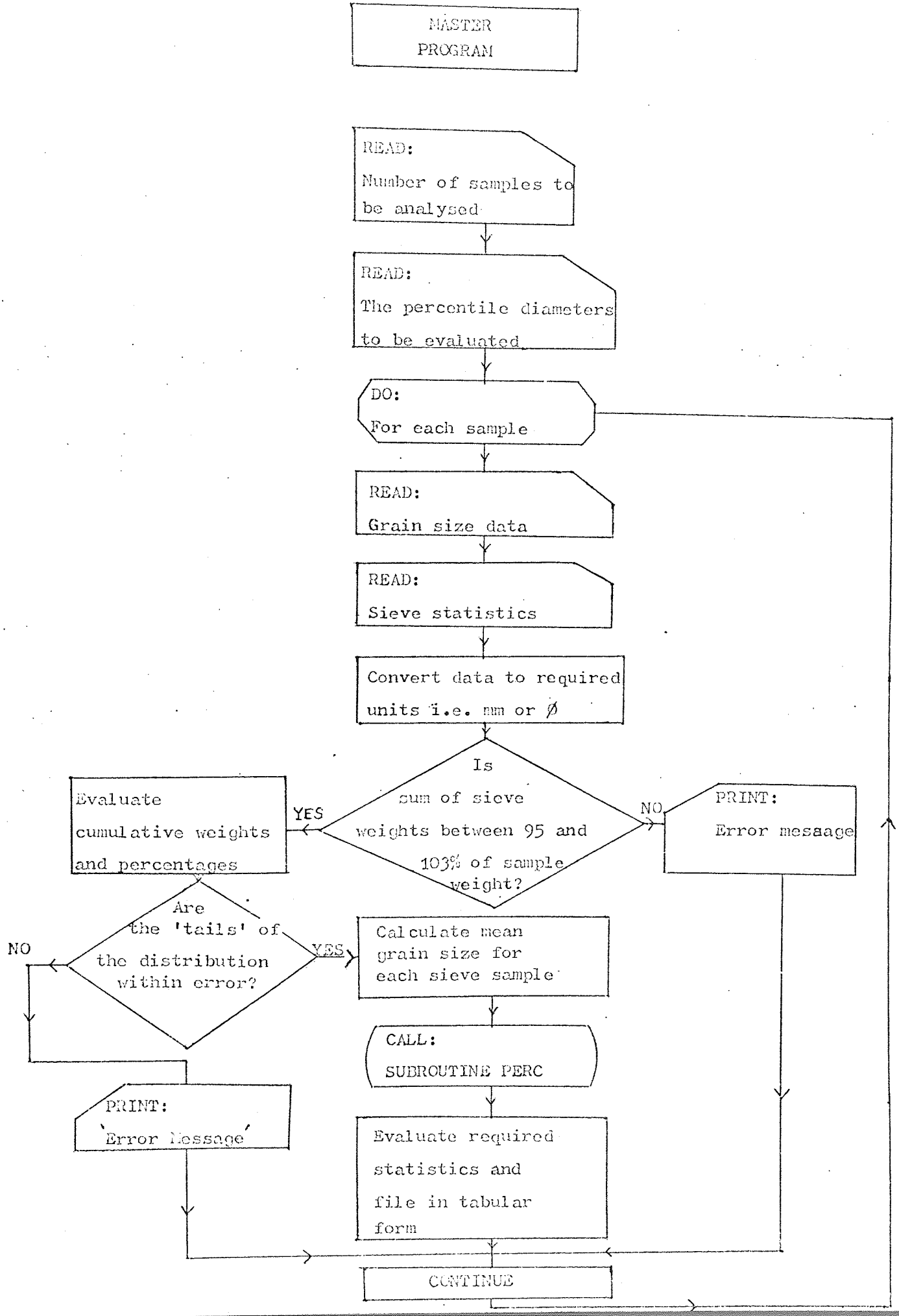

GRAIN SIZE ANALYSIS PROGRAM:

FLOW DIAGRAM

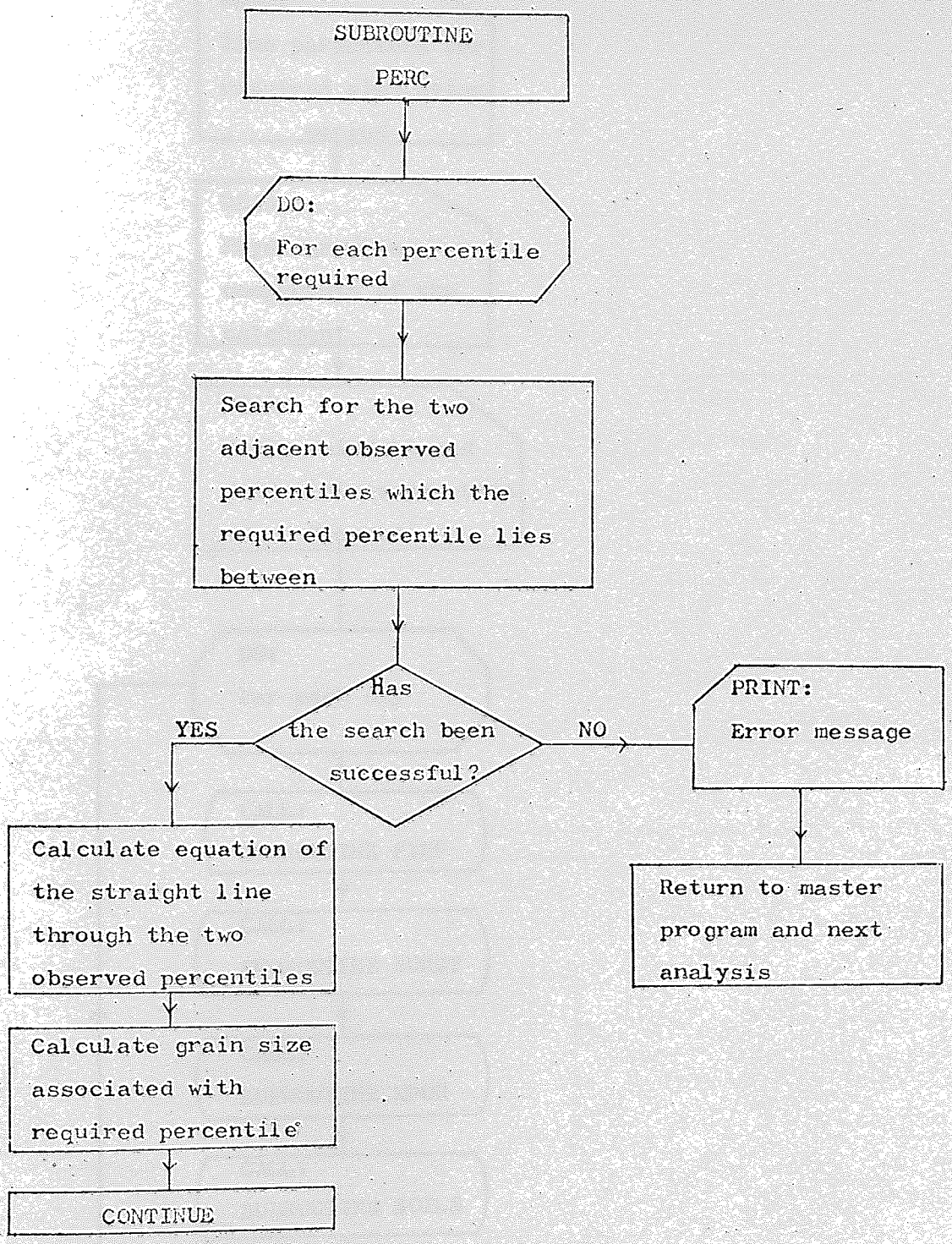

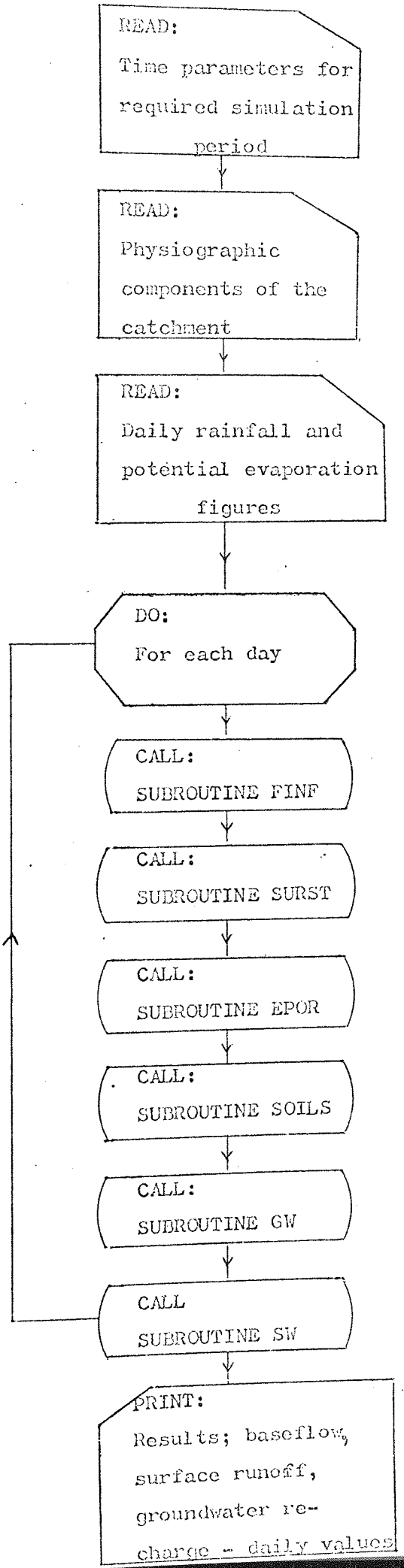
READ:
Time parameters for required simulation period
READ:
Physiographic components of the catchment
READ:
Daily rainfall and potential evaporation figures
DO:
For each day
CALL:
SUBROUTINE FINF
CALL:
SUBROUTINE SURST
CALL:
SUBROUTINE EPOR
CALL:
SUBROUTINE SOILS
CALL:
SUBROUTINE GW
CALL
SUBROUTINE SW
PRINT:
Results; baseflow, surface runoff, groundwater re-charge - daily values

DIGITAL GROUNDWATER PROGRAM

FLOW DIAGRAM OF SUBROUTINE KRGWM

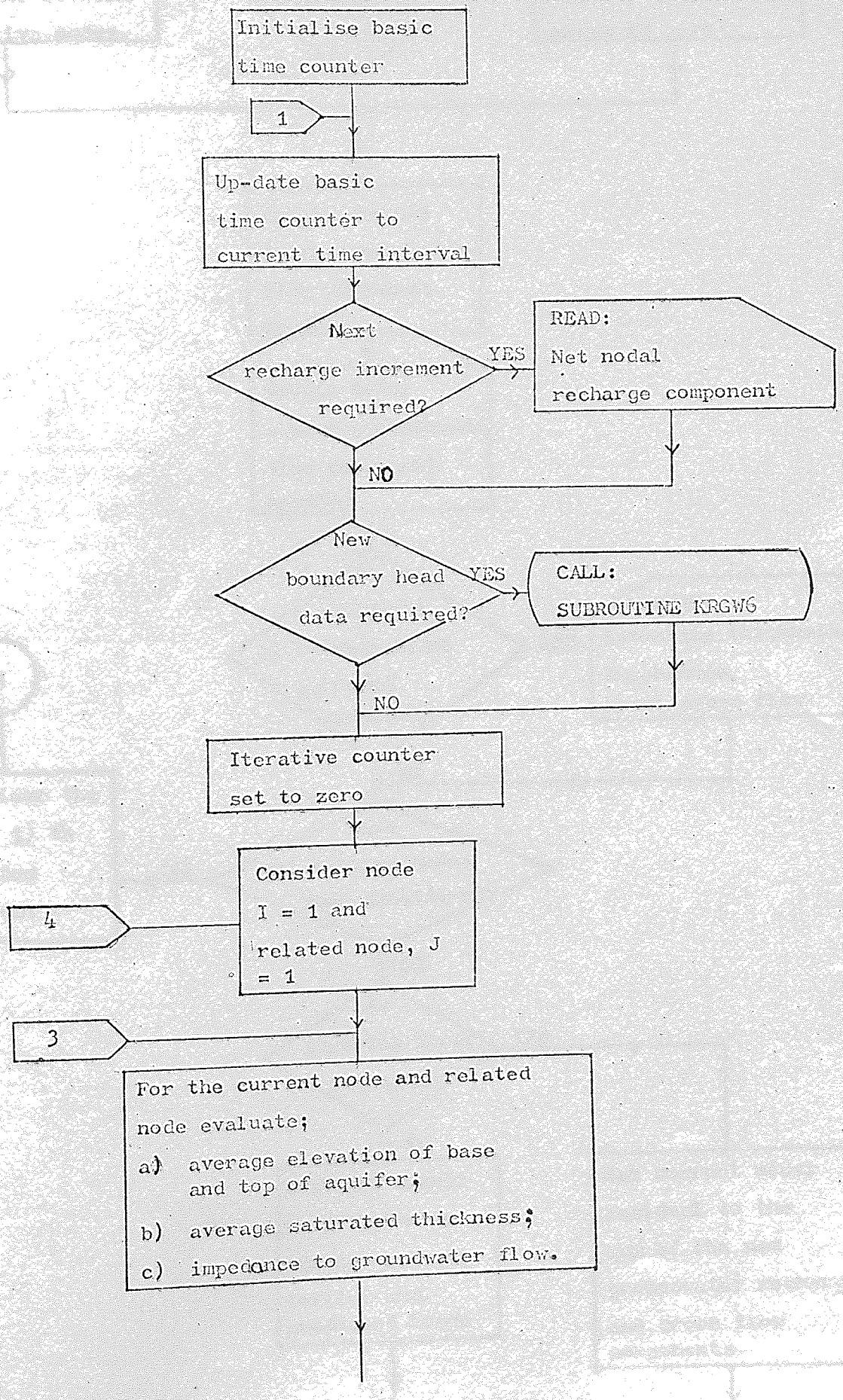

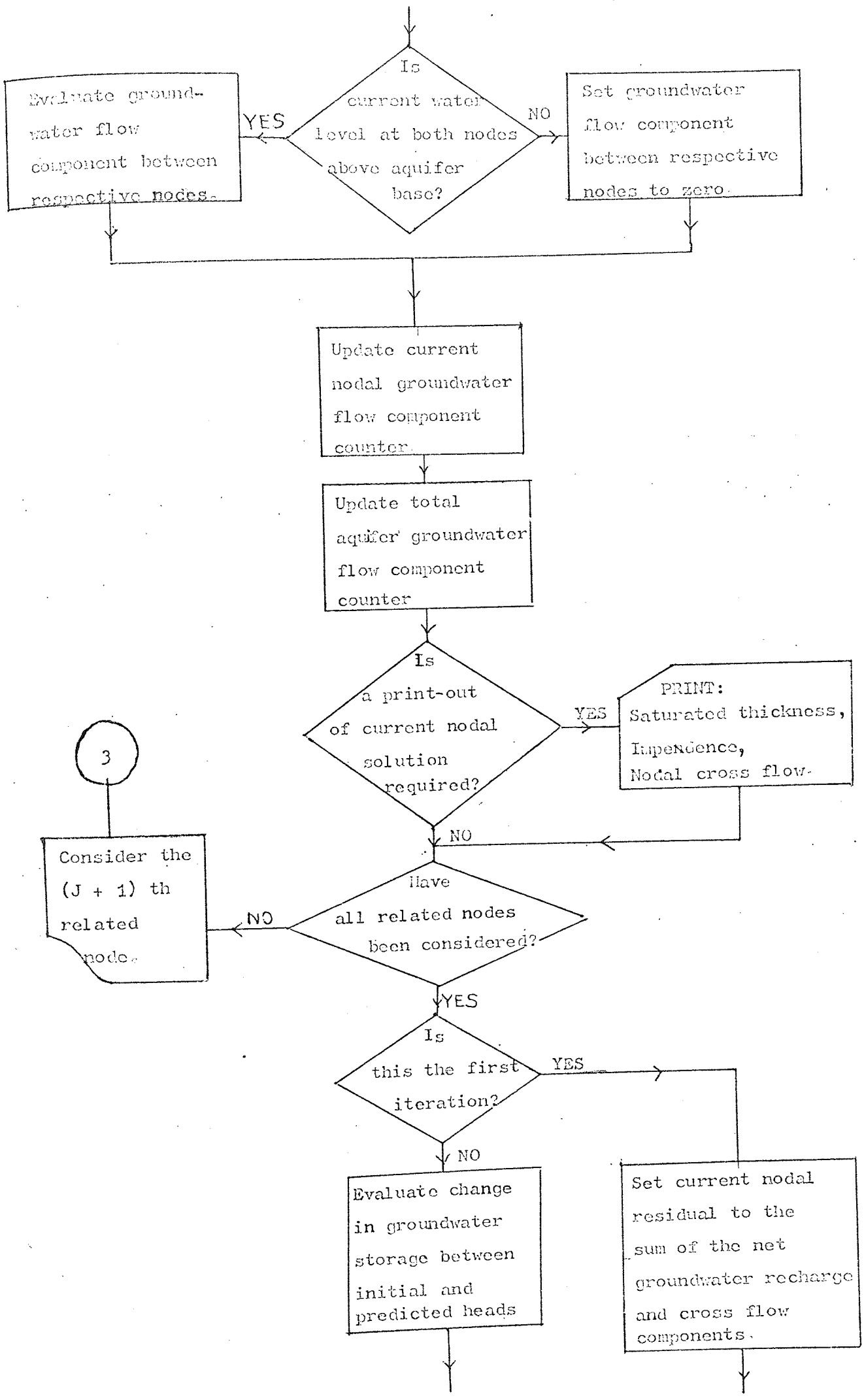
Is current water level at both nodes above aquifer base?
YES
NO
Evaluate groundwater flow component between respective nodes.
Set groundwater flow component between respective nodes to zero.
Update current nodal groundwater flow component counter.
Update total aquifer groundwater flow component counter
Is a print-out of current nodal solution required?
YES
PRINT: Saturated thickness, Impedence, Nodal cross flow.
NO
3
Consider the (J + 1) th related node.
NO
Have all related nodes been considered?
YES
Is this the first iteration?
YES
NO
Evaluate change in groundwater storage between initial and predicted heads
Set current nodal residual to the sum of the net groundwater recharge and cross flow components.

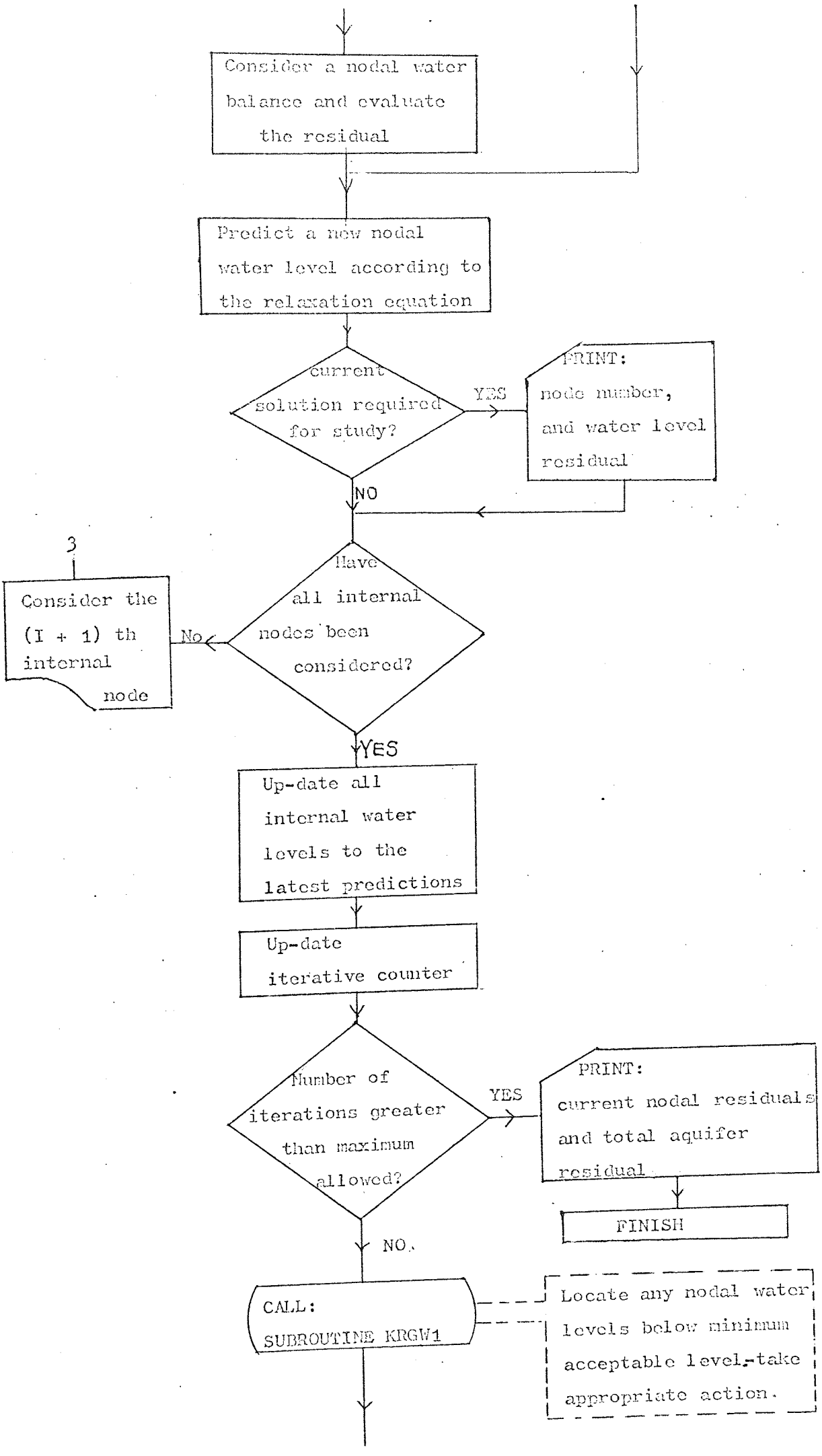
Consider a nodal water balance and evaluate the residual
Predict a new nodal water level according to the relaxation equation
current solution required for study?
YES
PRINT: node number, and water level residual
NO
3
Consider the (I + 1) th internal node
No
Have all internal nodes been considered?
YES
Up-date all internal water levels to the latest predictions
Up-date iterative counter
Number of iterations greater than maximum allowed?
YES
PRINT: current nodal residuals and total aquifer residual
FINISH
NO.
CALL: SUBROUTINE KRGW1
Locate any nodal water levels below minimum acceptable level-take appropriate action.

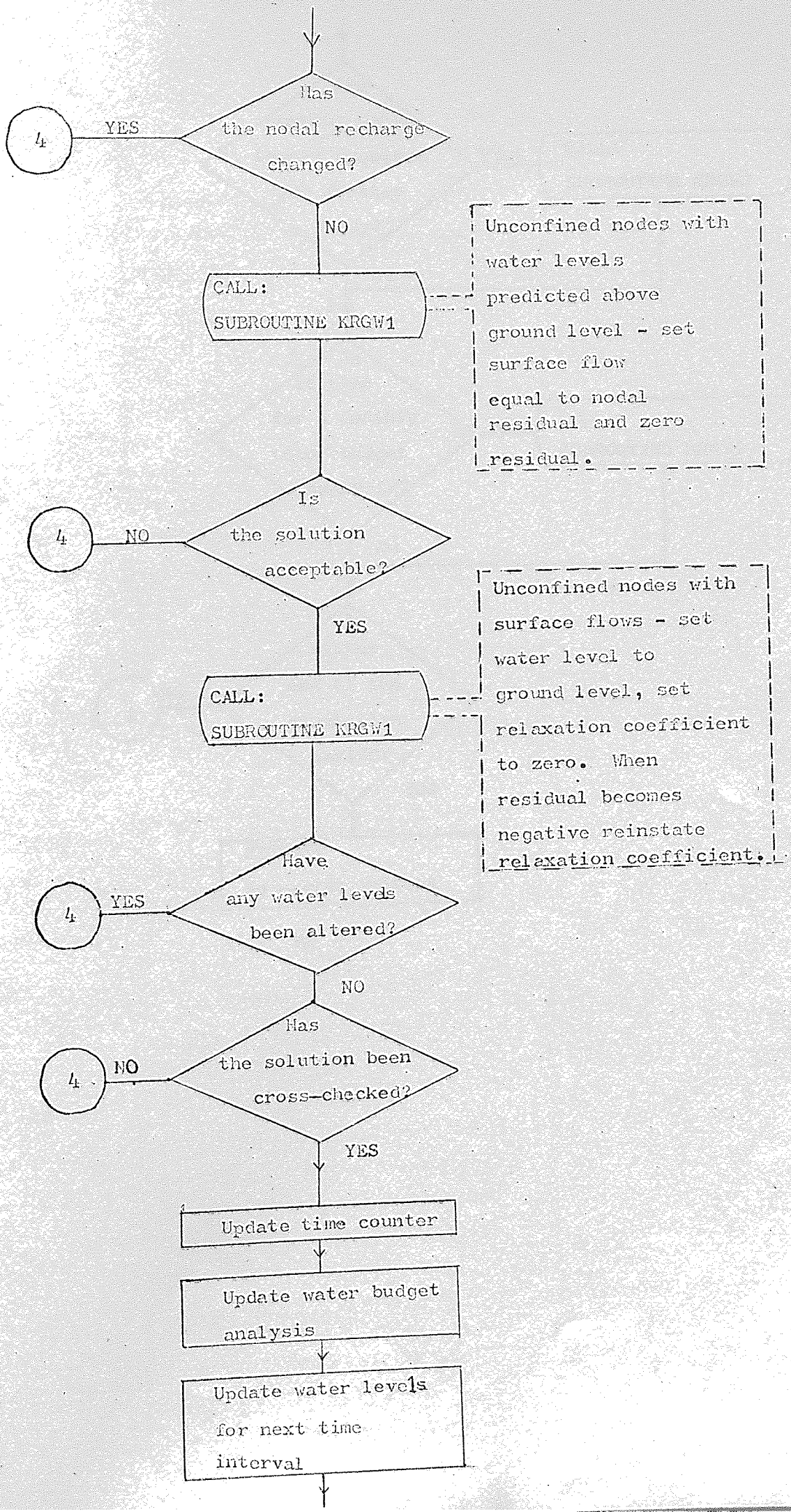
4
YES
Has the nodal recharge changed?
NO
CALL: SUBROUTINE KRGW1
Unconfined nodes with water levels predicted above ground level - set surface flow equal to nodal residual and zero residual.
4
NO
Is the solution acceptable?
YES
CALL: SUBROUTINE KRGW1
Unconfined nodes with surface flows - set water level to ground level, set relaxation coefficient to zero. When residual becomes negative reinstate relaxation coefficient.
4
YES
Have any water levels been altered?
NO
4
NO
Has the solution been cross-checked?
YES
Update time counter
Update water budget analysis
Update water levels for next time interval

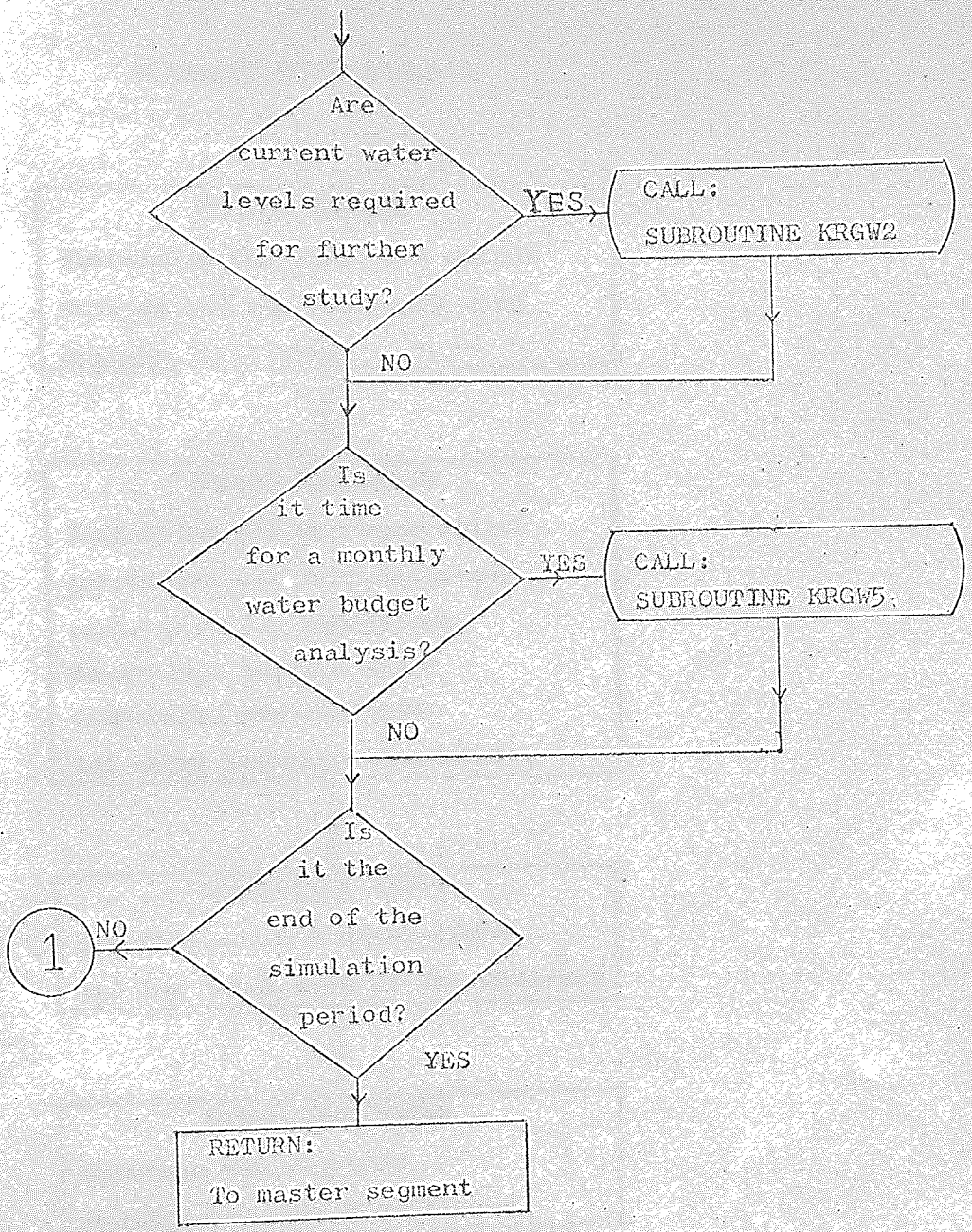
Are current water levels required for further study?
YES
CALL: SUBROUTINE KRGW2
NO
Is it time for a monthly water budget analysis?
YES
CALL: SUBROUTINE KRGW5
NO
Is it the end of the simulation period?
NO
1
YES
RETURN: To master segment

DIGITAL GROUNDWATER PROGRAM

SCHEMATIC FLOW DIAGRAM

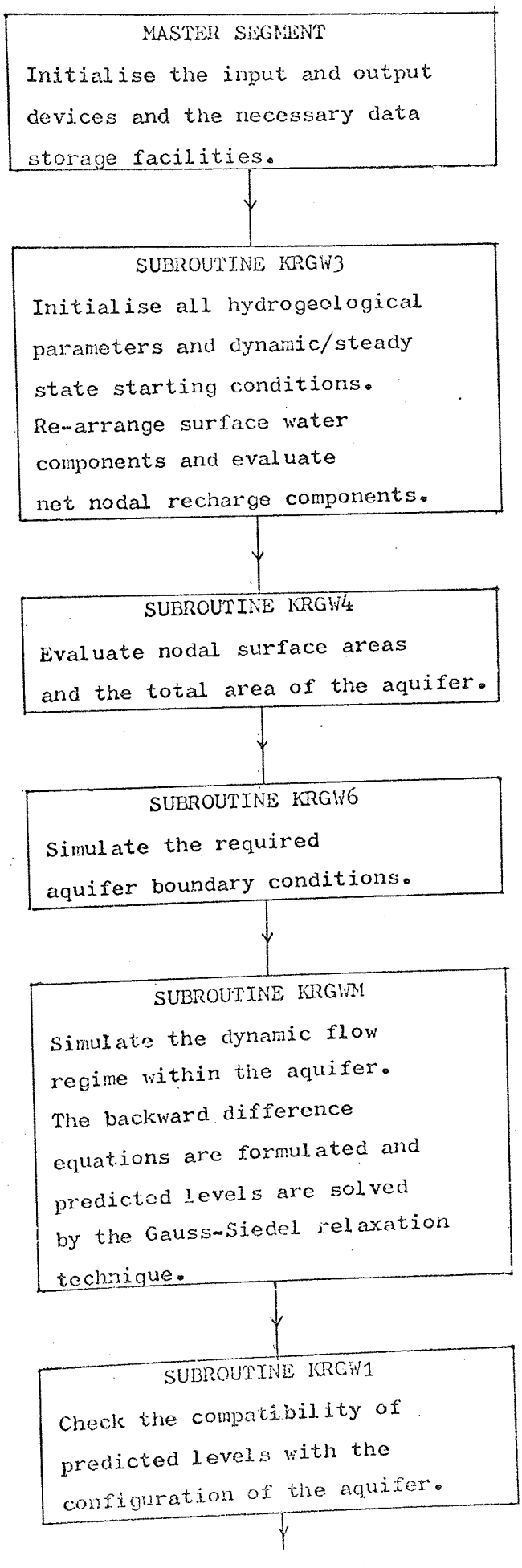

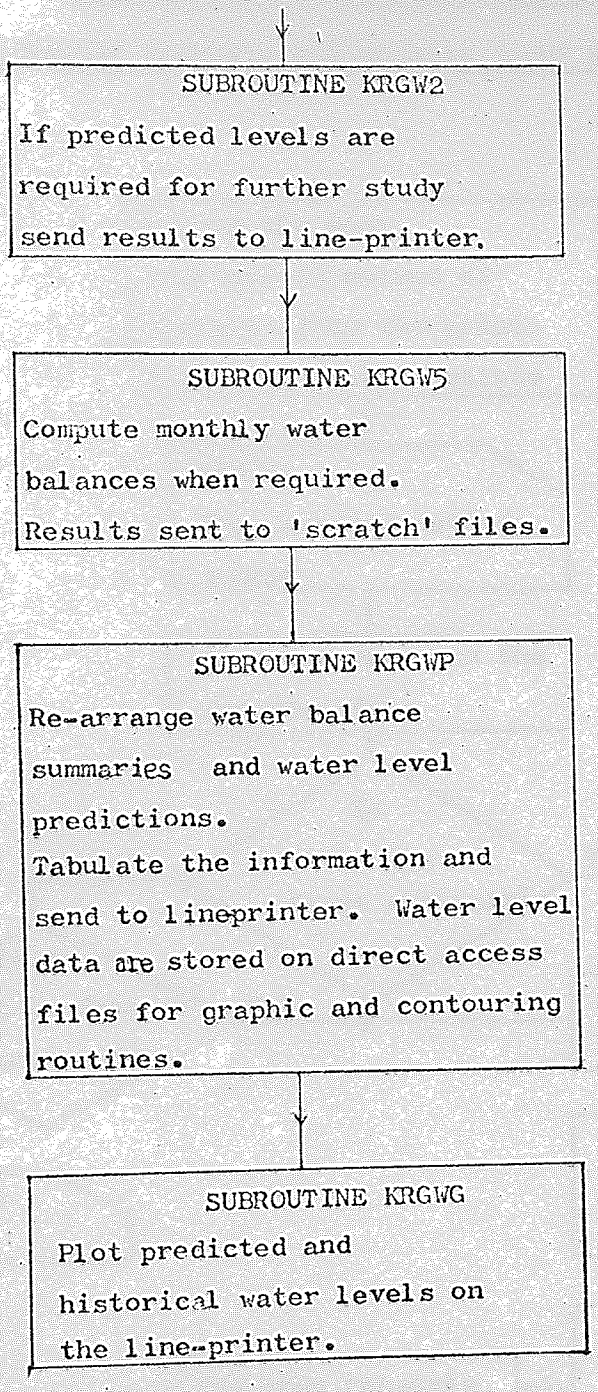
SUBROUTINE KRGW2
If predicted levels are required for further study send results to line-printer.
SUBROUTINE KRGW5
Compute monthly water balances when required.
Results sent to 'scratch' files.
SUBROUTINE KRGWP
Re-arrange water balance summaries and water level predictions.
Tabulate the information and send to lineprinter. Water level data are stored on direct access files for graphic and contouring routines.
SUBROUTINE KRGWG
Plot predicted and historical water levels on the line-printer.

NUMERICAL PUMP TEST ANALYSIS PROGRAM:

SCHEMATIC FLOW DIAGRAM OF DATA INPUT PROCEDURE

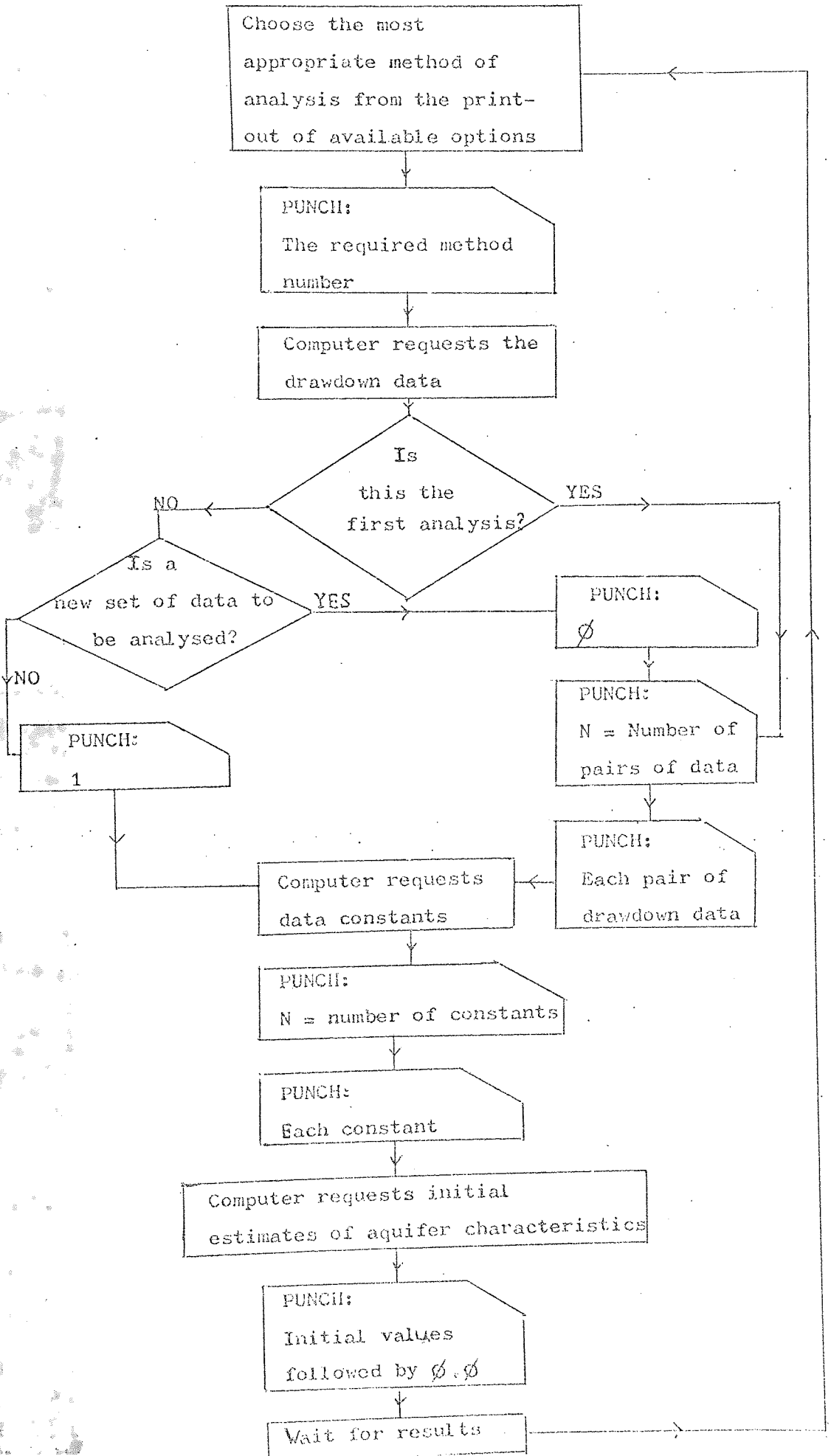

BIBLIOGRAPHY

Anonymous, 1964 — Steady state flow of groundwater towards wells. The Hague, P.179 Proc. Comm. Hydrol. Res. T.N.O., nr. 10.

Audley-Charles, M.G. 1970a — Stratigraphical correlation of the Triassic Rocks of the British Isles. Quart. Jour. Geol. Soc. 126, 19 - 46.

Audley-Charles, M.G. 1970b — Triassic palaeography of the British Isles. Quart. Jour. Geol. Soc. 126, 49 - 91.

Bittenger, M.W. 1967 et al. — Mathematical simulations for better aquifer management. Extract publication No. 72 (I.A.S.H.), 509-519.

Bosworth, T.O. 1912 — The Keuper Marl around Charnwood Forest. Quart. Jour. Geol. Soc. 68, 251.

Boulton, W.S. 1916 — An Esker near Kingwinford, S. Staffs. Proc. B'Ham Nat. Hist. & Phil. Soc. XIV, 1.

Boulton, N.S. 1963 — Analysis of data from non-equilibrium pumping tests allowing for delayed yield from storage. Proc. Inst. Civ. Eng. 26, 469-482.

Bruce, G.H. 1953 et al. — Calculations of unsteady state gas flow through porous media. Trans. Am. Inst. Mech. Eng. 198, 79-92.

Brunstrom, R.G.W. 1967 — Origin of the Keuper Salt in Britain. Nature, London. 215, 1474.

Kent, P.E.

Buller, A.T. 1971 McManus, J. — Simple metric sedimentary statistics used to recognise different environments. Sedimentology. 18, 1-21.

Carre, B.A. 1961 — The determination of the optimum accelerating factor for successive over-relaxation. Comp. Jour. 4, 243-254.

Chidley, T.R.E. 1971 "Report on computer procedures and programs the analysis of project data", Raikes and Part. Report to the Sandstone Aquifers Project of East Jordan, U.N.D.P./F.A.O. Project No. 212.

Chidley, T.R.E. 1970
Pike, J.G. A generalised computer program for the solution of the Penman Equation for evapotranspiration. Jour. Hydrol. 10, 75-89.

Cloud, F.W. 1941 Effects of sand grain size distribution upon porosity and permeability. Oil Weekly. 103, 25-32.

Cole, J.A. 1973
et al. Calculating aquifer properties and baseflow compensation. Water Res. Ass. T.P. 96.

Cook, A.H. 1952
et al. A gravity survey of the country between the Clee Hills and Nuneaton. Quart. Jour. Geol. Soc. 107, 287-302.

Cook, A.H. 1955
Thirlaway, H.I.S. The geological results of measurements of gravity in the Welsh Borders. Quart. Jour. Geol. Soc. 111, 47-70.

Cook, J.M. 1970
Howell, F.T. Three new simple tests for measuring the permeability of the Permo-Triassic sandstones of N.W. England. Geotechnique. 20, 446-451.

Cooper, H.H. 1946
Jacob, C.E. A generalised graphical method for evaluating formation constants and summarising well field history. Am. Geophys. Union Trans. 27, 526-534.

Crook, J.M. 1971 et al. Permeation properties of unfissured Bunter Sandstones of Lancashire and Yorkshire. Geotechnique. 21, 256-259.

Curle, N. 1968
Davies, H.J. Modern fluid dynamics. The New University Mathematics Series. D. Van Nostrand, London.

Darcy, H.P.G. 1856 Les Fontaines publiques de la ville Diijon, Victor Dalmont, Paris.

Dawdy, D.R. 1965
O'Donnell, T. Models of catchment behaviour. Jour. Proc. Am. Soc. Civ. Eng. 91, 123 - 137.

De Glee, G.J. 1930 Over groundwaterstomingen bij water onttrekking door middel van pultern. Thesis, J. Waltman, Delft (The Netherlands) P.175.

De Glee, G.J. 1951 Berekenings methoden voor de winnings of groundwater. In: Drinkwatervoorzeining, ze vacantie cursus: 38-80 Moorman's periodieke pers, The Hague (The Netherlands).

De Ridder, N.A. 1965
Wit, K.E. A comparative study of the hydraulic conductivity of unconsolidated sediments. Jour. Hydrol. 3, 180-206.

Dracup, J. 1966 The optimum use of groundwater and surface water systems - a parametric linear programming approach. Water Res. Contrib. No. 107.

Dupuit, J. 1863 Etudes theoriques et pratiques sur le mouvement des eaux dans les canaux decouvert et a travers les terrains permeables. 2eme edition, Dunot, Paris P.304.

Falcon, N.L. 1951
Tarrant, L.H.
The gravitational and magnetic exploration of parts of the Mesozoic-covered areas of South-Central England. Quart. Jour, Geol. Soc. 106, 141-70.

Fayers, F.J. 1962
Sheldon, J.W.
The use of a high speed digital computer in the study of the hydrodynamics of a geologic basin. Jour. Geophys. Res. 67, 2421-2431.

Ferris, J.G. et. al. 1962
Theory of aquifer tests. U.S. Geol. Surv. Water Supply Paper. 1536 - E.

Flood, M.M. 1964
Leon, A.
A generalised direct search code for optimisation. Mental Health Research Institute. Univ. Michigan. Ann Abor. Michigan reprint 129.

Folk, R.L. 1957
Ward, W.C.
Brazos River Bar : A study in the significance of grain size parameters. Jour. Sed. Pet. 27, 8-26.

Fraser, H.J. 1935
Experimental study of porosity and permeability of clastic sediments. Jour. Geol. 43, 910-1010.

Friedman, G.M. 1961
On sorting, sorting coefficients, and the lognormality of the grain size distribution of sandstones. Jour, Geol. 69, 737-756.

Glasspoole, J. 1949
Seasonal weather sequences over England and Wales. Met. Mag. 78, 193-198.

Goodwill, I.M. 1971
Study of the water resources and their exploitation for irrigation in Eastern Crete, Greece. Raikes and Part. F.A.O. of the United Nations. FAO/SF 166/GRE.

Graton, L.C. 1935
Fraser, H.J.
Systematic packing of spheres with particular relation to porosity and permeability. Jour. Geol. 43, 785-909.

Green, F.H.W. 1964
A map of annual average potential water deficit in the British Isles. Jour. Appl. Ecol. 1, 151-58.

Griffiths, J.C. 1952
Grain size distribution and reservoir-rock characteristics. Bull. Am. Assoc. Petrol. Geol. 36, 205-229.

Grindley, J. 1969
The calculation of actual evaporation and soil moisture deficit over specified catchment areas. Hydrological Memorandum No. 38. Meteorological Office, Bracknell, Berkshire.

Hantush, M.S. 1955
Jacob, C.E.
Non-steady radial flow in an infinite leaky aquifer. Am. Geophys. Union Trans. 36, 95-100.

Hantush, M.S. 1956
Analysis of data from pumping tests in leaky aquifers. Am. Geophys. Union Trans. 137, 702-714.

Hantush, M.S. 1962a
Aquifer tests on partially penetrating wells. Am. Soc. Civ. Eng. Trans. 127, 284-308.

Hantush, M.S. 1962b
Drawdown around a partially penetrating well. Am. Soc. Civ. Eng. Trans. 127, 268-283.

Hantush, M.S. 1964
Hydraulics of wells. In : Chow V.T. Advances in Hydroscience, 1. Academic Press, New York & London.

Heath, R.C. 1968
Trainer, W.T.
Introduction to groundwater hydrology. John Wiley & Sons. Inc.

Horton, R.E. 1933 — The role of infiltration in the hydrological cycle. Trans. Am. Geophys. Un. 14, 446-460.

Horton, R.E. 1940 — An approach towards a physical interpretation of infiltration capacity. Proc. Soil Sci. 5, 399-417.

Hubert, M.K. 1940 — The theory of groundwater motion. Jour. Geol. 48, 785-944.

Hubert, M.K. 1956 — Darcy's Law and the field equations of the flow of underground fluids. Trans. Am. Inst. Mech. Eng. 207, 222-239.

Ineson, J. 1964
Downing, R.A. — The groundwater components of river discharge and its relationship to hydrology. Jour. Inst. Water Eng. 18, 519-541.

Inman, D.L. 1952 — Measures for describing the size distribution of sediments. Jour. Sed. Pet. 22, 125-145.

Jacob, C.E. 1940 — On the flow of water in an elastic artesian aquifer. Am. Geophys. Union Trans. 72, 574-586.

Jacob, C.E. 1963a — Determining the permeability of water-table aquifers. U.S. Geol. Survey Water Supply Paper. 1536-I, 245-271.

Jacob, C.E. 1963b — Correction of drawdowns caused by a pumped well tapping less than the full thickness of an aquifer. In. Bentall. R. Methods of determining permeability, transmissibility and drawdown. U.S. Geol. Surv. Water Supply Paper. 1536, 272-282.

Johnson, W.E. 1951
Breston, JN. — Directional permeability measurements of oil-sandstones from various states. Producers Monthly. 15, 10-19.

Kendrew, W.G. 1953 — The climates of the continents. Claredon Press, Oxford.

Kent, P.E. 1949 — A structure contour map of the surface of the buried pre-Permian rock of England and Wales. Proc. Geol. Ass. 60, 87-104.

Kleindeke, D. 1971 — Use of linear programming for estimating geohydrologic parameters of groundwater basins. Water Resources Res. 7, 367-376.

Krumbein, W.C. 1958
Sloss, L.L. — High-speed digital computers in stratigraphic and facies analysis. Bull. Am. Assoc. Petrol. Geol. 42, 2650-2669.

Kruseman, G.P. 1970
De Ridder, N.A. — Analysis and evaluation of pumping test data. Int. Inst. for Land Reclamation and Improvement. Wageningen (The Netherlands).

Lamb, H.H. 1964 — The English climate. English Universities Press, London.

Land, D.H. 1966 — Hydrogeology of the Triassic sandstones in the Birmingham - Lichfield district. Water Supply Papers, Geol. Surv. U.K.

Landsberg, H. 1963 — Physical climatology. Gray Printing Co. Inc., London.

Law, F. 1953 — The estimation of the reliable yield of a catchment by correlation of rainfall and runoff. Jour. Inst. Water Eng. 7, 273-292.

Logan, J. 1964 — Estimating transmissibility from routine production tests of water wells. Groundwater, 2, 35-37.

Lovell, R.E. 1972 — Use of subjective information in Estimation of aquifer parameters. Water Resources Res. 8, 680-690.

Manley, G. 1962 — Climate and the British scene. Collins Press, London.

Martin, D.W. 1961
Tee, G.J.
Iterative methods for linear equations with symmetric positive definite matrix. Comp. Jour. 4, 243-254.

Mash, F.D. 1966
Grain size distribution and its effects on the permeability of unconsolidated sands. Water Resources Res. 2, 665-667.

McCammon, R.B. 1962
Moment measures and the shape of the size frequency distributions. Jour. Geol. 70, 80-92.

Papadakis, J. 1966
Climates of the world and their agricultural potentialities. University Press, London.

Penman, H.L. 1948
Natural evaporation from open water, bare soil and grass. Proc. Roy. Soc. 193, 125-145.

Penman, H.L. 1949
The dependence of transpiration on weather and soil conditions. Jour. Soil. Sci. 1, 74-89.

Pinder, G.F. 1968
Bredehoft, J.D.
Application of the digital computer for aquifer evaluation. Water Resources Res. 14, No. 5.

Raw, F. 1934
On the Triassic and Pleistocene surfaces developed on some Leicestershire igneous rocks. Geol. Mag. 71, 23.

Richardson, L. 1929
In J.W. Evans & G.J. Stubblefield's Trias, handbook of the geology of Gt. Britain. Murphy, London.

Rubin, J. 1968
Theoretical analysis of two dimensional transient flow of water in unsaturated and partly unsaturated soils. Proc. Soil. Sci. Am. 31, 222-235.

Rushton, K.R. 1970
Bannister, R.G.
Aquifer simulation on slow time resistance capacitance networks. Groundwater. 8, 15-24.

Rushton, K.R. 1971
Tomlinson, L.M.
Digital computer solutions of groundwater flow. Jour. Hydrol. 12, 339-362.

Rushton, K.R. 1973
Discrete time steps in digital computer analysis of aquifers containing pumped wells. Jour. Hydrol. 18, 1-19.

Rushton, K.R. 1973.
Wedderburn, L.A.
Starting conditions for aquifer analysis. Groundwater. 11, 37-42.

Rushton, K.R. 1974
Critical analysis of the alternating direction implicit method of aquifer analysis. Jour. Hydrol. 21, 153-172.

Ryder, H.M. 1948
Permeability, absolute, effective measured. World Oil. 125, 173-177.

Schlee, J. 1967
Webster, J.
A computer program for grain size data. Sedimentology. 8, 45-53.

Shearman, D.J. 1966
Origin of marine evaporites by diagenesis. Trans. Inst. Min. Metall. 75,208-15.

Shotton, F.W. 1937
The Lower Bunter Sandstone of North Worcestershire and East Shropshire. Geol. Mag. 74, 534-53.

Slichter, C.S. 1899
Theoretical investigation of the motion of groundwaters. U.S. Geol. Surv. 295-384.

Smith K. 1964
Some aspects of the hydrology and water use of the Nidd Valley, Yorkshire. Unpublished Ph. D. thesis, Univ. of Hull.

Smith, K. 1966
Percolation, groundwater discharge and stream flow in the Nidd Valley. Jour. Inst. Water Eng. 20, 459-471.

Stallman, R.W. 1956
Numerical analysis of regional water levels to define aquifer hydrology. Trans. Am.Geophys. Union. 37, 451-460.

Takar, H.S. 1970
Rudge, A.J.
Evaporation studies in standard catchments. Jour. Hydrol. 11, 329-359.

Taylor, J.A. 1967
Yates, R.A.
British weather in maps. St. Martins Press, London.

Taylor. J.M. 1950
Pore-space reduction in sandstones. Bull. Am. Assoc. Petrol. Geol. 34, 701-716.

Theis, C.V. 1935
The relation between the lowering of the piezometric surface and the rate and duration of a discharge of a well using groundwater storage. Am. Geophys. Union Trans. 16, 519-524.

Theissen, A.H. 1911
Precipitation averages for large areas. Mon. Wea. Rev. 39, 1082-1084.

Thiem, G. 1906
Hydrologische Methoden. Geb. Hardt. Leipzig.

Todd, K. 1959.
Groundwater Hydrology. John Wiley & Sons, New York.

Trask, P.D. 1931
Compaction of sediments. Bull, Am. Assoc. Petrol. Geol. 22, 1272-79.

Tyson, H.N. 1963
Weber, E.M.
Use of electronic computers in the simulation of the dynamic behaviour of groundwater basins. Am. Soc. Civ. Eng. Water Resources Engineering Conference, Milwaukee, Winconsin.

Warrington, G. 1970
The stratigraphy and palaeontology of the Keuper Series.
Quart. Jour. Geol. Soc. 126, 183-223.

Wells, A.K. 1966
Kirkalady, J.F.
Outline of historical geology (5th Ed.). George Allen & Unwin Ltd., London.

Whitehead, T.H. 1927
et al.
The country between Stafford and Market Drayton, Mem. Geol. Surv. U.K. Sheet Memoir No. 139.

Whitehead, T.H. 1928 et al. The country between Wolverhampton and Oakengates. Mem. Geol. Surv. U.K. Sheet Memoir No. 153.

Whitehead, T.H. 1947 et al. Dudley and Bridgnorth. Mem. Geol. Surv. U.K. Sheet Memoir No. 167.

Wills, L.J. 1948. The palaeography of the Midlands. Univ. Press Liverpool, London.

Wills, L.J. 1970 The Triassic succession in the Central Midlands in its regional setting. Quart. Jour. Geol. Soc. 126, 225-287.

Yuster, S.T. 1937 Determining the porosity of oil sands. The Producers Monthly, October.